

CHEMICAL CONSTITUENTS OF FAN-SI *Abutilon indicum* STEMS



A Thesis Submitted in Partial Fulfillment of the Requirements
for the Degree of Master of Science in Chemistry

Department of Chemistry

FACULTY OF SCIENCE

Chulalongkorn University

Academic Year 2021

Copyright of Chulalongkorn University

องค์ประกอบทางเคมีของลำต้นฝิ่นสี *Abutilon indicum*



วิทยานิพนธ์นี้เป็นส่วนหนึ่งของการศึกษาตามหลักสูตรปริญญาวิทยาศาสตรมหาบัณฑิต

สาขาวิชาเคมี ภาควิชาเคมี

คณะวิทยาศาสตร์ จุฬาลงกรณ์มหาวิทยาลัย

ปีการศึกษา 2564

ลิขสิทธิ์ของจุฬาลงกรณ์มหาวิทยาลัย

อาร์ม เรสตู วิทยาศาสตร์ : องค์ประกอบทางเคมีของลำต้นพืชน้ำ *Abutilon indicum*. (

CHEMICAL CONSTITUENTS OF FAN-SI *Abutilon indicum* STEMS)

อ.ที่ปรึกษาหลัก : รศ. ดร.สุรัชย์ พรหมกุล

การศึกษานี้มีวัตถุประสงค์เพื่อแยกสารทุติยภูมิจากส่วนลำต้นของต้นครอบพืชน้ำ (*Abutilon indicum*) และเพื่อประเมินฤทธิ์ยับยั้งการทำงานของเอนไซม์แอลฟาไกลูโคซิเดสไลเปสจากตับอ่อน และแอลฟาโคโมทริปซิน การแยกสารสกัดหยาบเฮกเซนด้วยเทคนิคโครมาโทกราฟี นำไปสู่การแยกสารเมตาโบไลต์ที่รู้จัก 3 ชนิด (1-3) โดยสารสกัดหยาบจากทุกส่วนของต้นครอบพืชน้ำได้รับการประเมินฤทธิ์ยับยั้งการทำงานของเอนไซม์แอลฟาไกลูโคซิเดส พบว่าสารสกัดไดคลอโรมีเทนจากส่วนรากมีฤทธิ์ยับยั้งการทำงานของเอนไซม์ร้อยละ 10.2 ที่ความเข้มข้น 25 ไมโครกรัม/มิลลิลิตร สารสกัดเฮกเซนและเมทานอลจากส่วนก้านมีฤทธิ์ยับยั้งร้อยละ 11.0 ที่ 25 ไมโครกรัม/มิลลิลิตร และร้อยละ 8.0 ที่ 0.25 ไมโครกรัม/มิลลิลิตร สารสกัดเฮกเซน ไดคลอโรมีเทน และเมทานอลจากส่วนใบมีฤทธิ์ยับยั้งร้อยละ 20.2 ที่ 0.025 ไมโครกรัม/มิลลิลิตร ร้อยละ 20.0 ที่ 0.025 ไมโครกรัม/มิลลิลิตร และร้อยละ 14.6 ที่ 2.5 ไมโครกรัม/มิลลิลิตร ตามลำดับ นอกจากนี้ไฟโตเคมีคอลของต้นครอบพืชน้ำยังได้รับการศึกษาเกี่ยวกับปฏิกิริยายับยั้งการทำงานของเอนไซม์แอลฟาไกลูโคซิเดสไลเปสจากตับอ่อน และแอลฟาโคโมทริปซินด้วยวิธี Molecular docking จากการศึกษาทาง *In silico* การตรวจสอบ ADMET และการทำนายความเป็นพิษของสารประกอบ 66 ชนิดพบว่าสารประกอบ 9 ชนิด (2811, 3121, 3131, 3151, 3171, 3181 และ 3191) มีโอกาสที่จะพัฒนาเป็นตัวยับยั้งแบบใหม่ในการยับยั้งเอนไซม์แอลฟาไกลูโคซิเดสไลเปสจากตับอ่อน และแอลฟาโคโมทริปซิน ผลการศึกษานี้พบว่าสารประกอบที่แยกได้จากต้นครอบพืชน้ำมีฤทธิ์ต้านเบาหวาน ลดความอ้วน

สาขาวิชา เคมี
ปีการศึกษา 2564

ลายมือชื่อนิสิต
ลายมือชื่อ อ.ที่ปรึกษาหลัก

6272027823 : MAJOR CHEMISTRY

KEYWORD: Abutilon indicum; steroids; fatty acids; percent inhibition; α -glucosidase; human pancreatic lipase; α -chymotrypsin; molecular docking

Arum Restu Widyasti : CHEMICAL CONSTITUENTS OF FAN-SI *Abutilon indicum* STEMS. Advisor: Assoc. Prof. SURACHAI PORNPAKAKUL, Ph.D.

This study aimed to isolate secondary metabolites from the stems of *Abutilon indicum* and to evaluate their α -glucosidase, pancreatic lipase, α -chymotrypsin inhibitory activity. Chromatographic fractionation of the *n*-hexane crude extracts led to the isolation of three known metabolite (1-3). The crude extract from all parts of the plant were evaluated for inhibitory activity on the alpha-glucosidase enzyme. The DCM-soluble roots were active with 10.2% at 25 $\mu\text{g/mL}$. The hexane and MeOH-soluble stems were active with 11.0% at 25 $\mu\text{g/mL}$ and 8.0% at 0.25 $\mu\text{g/mL}$. The hexane, DCM, and MeOH-soluble leaves are active with 20.2% at 0.025 $\mu\text{g/mL}$; 20.0% at 0.025 $\mu\text{g/mL}$; and 14.6% at 2.5 $\mu\text{g/mL}$, respectively. Furthermore, the phytochemicals of *A. indicum* were studied for its interaction against α -glucosidase, pancreatic lipase, α -chymotrypsin through molecular docking. Based on the *in silico* study, ADME investigation, and toxicity prediction, nine compounds (2, 8, 11, 12, 13, 15, 17, 18, and 19) out of 66 compounds were potential to be developed as novel inhibitor for α -glucosidase, human pancreatic lipase, and α -chymotrypsin. The result demonstrated that isolated compounds from *A. indicum* potential to be anti-diabetes, anti-obesity, and anti-ulcer.

Field of Study: Chemistry

Student's Signature

Academic Year: 2021

Advisor's Signature

ACKNOWLEDGEMENTS

Praise God the Almighty, the most merciful who has blessed me with the biggest things in my life, including the blessing that empowered me to accomplish this thesis. Peace be upon God's Messenger.

This thesis is my journey to obtain the degree of Master of Science, representing a milestone in studying at the Department of Chemistry of Chulalongkorn University. Though this thesis is an individual work, I could never have reached the heights or explored the depths without their help, support, and guidance. It is a pleasure to convey my gratitude to them all in my acknowledgment.

First of all, I would like to express my deepest gratitude to my supervisor, Associate Professor Dr. Surachai Pornpakakul, Department of Chemistry, Faculty of Science, Chulalongkorn University, for his motivation, enthusiasm, and immense knowledge. I thank him for guiding me during the process of research and thesis writing.

Moreover, many thanks to the chairperson: Professor Dr. Preecha Phuwapraisirisan, Department of Chemistry, Faculty of Science, Chulalongkorn University; the thesis examiners: Associate Professor Dr. Pattara Thiraphibundet, Department of Chemistry, Faculty of Science, Chulalongkorn University, and the external examiner: Assistant Professor Dr. Jirapast Sichaem, Faculty of Science and Technology, Thammasat University Lampang Campus.

I am extremely grateful to my parent for their love, never stop prayer and support, sacrifices, and understanding to complete this study phase. Special thanks to my fellow labmates in Research Centre for Bioorganic Chemistry for supporting each other and for all the fun we have had. Last but not least, thanks to everyone for all the good memories and experiences.

Arum Restu Widyasti

TABLE OF CONTENTS

	Page
ABSTRACT (THAI).....	iii
ABSTRACT (ENGLISH).....	iv
ACKNOWLEDGEMENTS.....	v
TABLE OF CONTENTS.....	vi
LIST OF TABLES.....	x
LIST OF FIGURES.....	xi
LIST OF ABBREVIATIONS.....	xiii
CHAPTER I INTRODUCTION.....	1
CHAPTER II LITERATURE REVIEW.....	4
2.1 <i>Abutilon indicum</i> (L.) Sweet.....	4
2.1.1 Description of <i>Abutilon indicum</i> (L.) Sweet.....	4
2.2.2 Taxonomy of <i>A. indicum</i> (L.) Sweet.....	6
2.2.3 Botany of <i>A. indicum</i> (L.) Sweet.....	7
2.2.4 Phytochemicals from <i>A. indicum</i>	9
2.2.5 Biologically active metabolites from <i>A. indicum</i> (L.) Sweet.....	1
2.2.4.1 Antidiabetic activity.....	1
2.2.4.2 Antiulcer activity (Wound healing activity).....	1
2.2.4.3 Anticancer activity.....	1
2.2.4.4 Anti-inflammatory and antiproliferative activity.....	1
2.2.4.5 Larvacidal activity.....	2
2.2.4.6 Acetylcholinesterase inhibitory activity.....	2

2.2.4.7 Antimicrobial activity	2
2.2.4.8 Anti-diarrhoeal.....	2
2.2.4.9 Immunomodulatory activity.....	3
2.2.4.10 Anti-estrogenic activity	3
2.2.4.11 In vitro anti-arthritic activity	3
2.2.4.12 Hepatoprotective activity	4
2.2 Diabetes.....	4
2.3 Obesity.....	6
2.4 Diabetic Foot Ulcer (DFU).....	10
CHAPTER III EXPERIMENTAL.....	15
3.1 <i>In silico</i> approach (α -glucosidase, pancreatic lipase, and α -chymotrypsin inhibition assays).....	15
3.1.1 Ligand preparation	15
3.1.2 Protein preparation.....	15
3.1.3 Molecular docking.....	15
3.1.4 Drug-likeness prediction.....	16
3.1.5 Toxicity, carcinogenicity, and mutagenicity prediction.....	16
3.2 Plant Materials.....	16
3.3 General Experimental Procedures.....	16
3.3.1 Thin-layer chromatography (TLC).....	16
3.3.2 Column chromatography.....	16
3.3.3 Nuclear magnetic resonance spectroscopy (NMR).....	17
3.3.4 Mass spectrometry (MS).....	17
3.3.5 Fourier transforms infrared spectrophotometry (FT-IR).....	17

3.3.6	Ultraviolet-visible spectrophotometry (UV-Vis).....	17
3.3.7	High-performance liquid chromatography (HPLC)	18
3.3.8	Microplate spectrophotometer	18
3.4	Chemicals	18
3.5	<i>In vitro</i> α -Glucosidase inhibition assay	18
3.6	Extraction and isolation.....	19
3.6.1	Extraction of stems	19
3.6.2	Extraction of roots.....	20
3.6.3	Extraction of leaves.....	21
3.6.4	Extraction of dry-fruits	22
3.6.5	Extraction of green-fruits.....	23
3.6.6	Extraction of flowers.....	24
3.6.7	Isolation of metabolite from <i>n</i> -hexane-soluble stems extract.....	25
CHAPTER IV RESULTS AND DISCUSSION		27
4.1	<i>In vitro</i> α -glucosidase inhibition assay	27
4.2	<i>In silico</i> approach (α -glucosidase, pancreatic lipase and α -chymotrypsin inhibition assay).....	30
4.2.1	<i>In silico</i> study of phytochemicals of <i>A. indicum</i> as α -glucosidase inhibitors.....	30
4.2.2	<i>In silico</i> study of phytochemicals of <i>A. indicum</i> as human pancreatic lipase (HPL) inhibitors	51
4.2.3	<i>In silico</i> study of phytochemicals of <i>A. indicum</i> as α -chymotrypsin inhibitors.....	91
4.2.4	The physicochemical properties of the phytochemicals from <i>A. indicum</i> based in Lipinski's rule of five	110

4.2.5 Toxicity of the phytochemicals of <i>A. indicum</i>	113
4.3 Structure elucidation of isolated metabolites.....	118
4.3.1 Structure elucidation of metabolite 1	118
4.3.2 Structure elucidation of metabolites 2.....	121
4.3.3 Structure elucidation of metabolites 3.....	124
CHAPTER V CONCLUSIONS.....	125
REFERENCES	126
APPENDIX.....	149
VITA.....	230



LIST OF TABLES

	Page
Table 1 Phytochemicals from <i>Abutilon indicum</i> (L.) Sweet	9
Table 10 The percent inhibition of the crude extract of <i>A. indicum</i> against α -glucosidase enzyme	28
Table 2 Calculated free binding energy (kcal/mol) of the phytochemicals (1-66) from <i>A. indicum</i> against processing α -glucosidase I (PDB code: 4J5T)	30
Table 3 The type of molecular interactions of the phytochemicals (1-66) within the active site of the α -glucosidase (PDB ID: 4J5T)	41
Table 4 Calculated free binding energy (kcal/mol) of the phytochemicals (1-66) from <i>A. indicum</i> against HPL (PDB ID: 1LPB)	51
Table 5 The type of molecular interactions of the phytochemicals (1-66) within the active site of the HPL (PDB ID: 1LPB)	80
Table 6 Calculated free binding energy (kcal/mol) of the phytochemicals (1-66) from <i>A. indicum</i> against α -chymotrypsin (PDB ID: 5J4S)	91
Table 7 The type of molecular interactions of the phytochemicals (1-66) within the active site of the α -chymotrypsin (PDB ID: 5J4S)	100
Table 8 The physicochemical properties of the phytochemicals from <i>A. indicum</i> based on Lipinski's rule of five	110
Table 9 Toxicity of the phytochemicals of <i>A. indicum</i>	114
Table 11 ^1H NMR data of β -sitosterol (chloroform-d, 500 MHz) (500 MHz, CDCl_3)	119
Table 12 ^{13}C -NMR data of metabolites 1 (500 MHz, CDCl_3)	119
Table 13 ^1H NMR data of metabolite 2 (500 MHz, CDCl_3)	121
Table 14 ^{13}C NMR data of metabolites 2 (500 MHz, CDCl_3)	122

LIST OF FIGURES

	Page
Figure 1 Major classes metabolites of <i>A. indicum</i>	6
Figure 2 Various parts of <i>A. indicum</i> : Flower and leaves (1); ripening fruit (2); mature seed capsules (3); and flower (4).	8
Figure 3 Healthy pancreas, pancreas in type 1 and type 2 diabetes mellitus	5
Figure 4 Lipid metabolic pathways in the human body [87-89].....	6
Figure 5 Mechanism of hydrolysis of p-nitrophenyl α -D-glucopyranoside (p-NPG) by α -glucosidase [158].....	19
Figure 17 The deprotonation of 4-nitrophenol to 4-nitrophenoxide happened after the addition of base.....	27
Figure 8 3D presentation of the phytochemicals from <i>A. indicum</i> in the active site of α -glucosidase (PDB code: 4J5T)	36
Figure 9 3D molecular amino interaction of the phytochemicals of <i>A. indicum</i> in the binding site of α -glucosidase (PDB code: 4J5T)	38
Figure 10 Amino acids residual interactions of the interacting pocket between α -glucosidase (PDB ID: 4J5T) and ligands	41
Figure 11 3D presentation of the phytochemicals from <i>A. indicum</i> in the active site of HPL (PDB code: 1LPB).....	67
Figure 12 3D molecular amino interaction of the phytochemicals of <i>A. indicum</i> in the binding site of HPL (PDB code: 1LPB).....	72
Figure 13 Amino acids residual interactions of the interacting pocket between HPL (PDB ID: 1LPB) and ligands	80
Figure 14 3D presentation of the phytochemicals from <i>A. indicum</i> in the active site of α -chymotrypsin (PDB code: 5J4S).....	96

Figure 15 3D molecular amino interaction of the phytochemicals of <i>A. indicum</i> in the binding site of α -chymotrypsin (PDB code: 5J4S).....	98
Figure 16 Amino acids residual interactions of the interacting pocket between α -chymotrypsin (PDB ID: 5J4S) and ligands.....	100
Figure 18 Structure of metabolite 1	118
Figure 19 Structure of metabolite 2	121



LIST OF ABBREVIATIONS

$[\alpha]_D^{25}$	Specific rotation at 25°C and using the wavelength of light at 589 m (sodium D line) for the observation
δ	Chemical shift (NMR)
δ_C	Chemical shift of carbon (NMR)
δ_H	Chemical shift of proton (NMR)
λ_{\max}	Wavelength of maximum absorption (UV)
μL	Microliter (s)
μg	Microgram (s)
μM	Micromolar
μm	Micrometer (s)
ν_{\max}	Reciprocal wavelength at the highest signal in IR spectroscopy
°C	Degree Celsius
^1H NMR	Proton nuclear magnetic resonance spectroscopy
^{13}C NMR	Carbon-13 nuclear magnetic resonance spectroscopy
2D NMR	Two-dimensional nuclear magnetic resonance spectroscopy
Ac	Acetyl
amu	Atomic mass unit
A_0	Absorbance of the control
A_1	Absorbance of the test sample
ATR-FTIR	Attenuated total reflectance-Fourier transformed infrared
$\text{Ba}(\text{OH})_2$	Barium hydroxide
br	Broad (NMR)
Bz	Benzyl
c	Concentration
calcd	Calculated
cat.	Catalyst
CC	Column chromatography
CDCl_3	Deuterated chloroform
CD_3OD	Deuterated methanol

$\text{Ce}(\text{SO}_4)_2$	Cerium (IV) sulfate
CH_2Cl_2	Dichloromethane
cm	Centimeter
cm^{-1}	Unit of reciprocal wavelength (or wavenumber) in IR
COSY	Correlation spectroscopy (NMR)
d	Doublet
D	Dextrorotatory rotation (turned clockwise of the plane of polarization)
D_2O	Deuterium oxide
dd	Doublet of doublet (NMR)
ddd	Doublet of doublet of doublet (NMR)
Dig	Digitoxose
DMF	<i>N,N</i> -dimethylformamide
DMSO	Dimethyl sulfoxide
dq	Doublet of quartet (NMR)
dt	Doublet of triplet (NMR)
EtOH	Ethanol
EtOAc	Ethyl acetate
v/v	Volume per volume
g	Gram (s)
h	Hour (s)
H_2SO_4	Sulfuric acid
H_2O	Water
Hz	Hertz (s)
HMBC	Heteronuclear multiple-bond correlation spectroscopy
HRESIMS	High-resolution electrospray ionization mass spectrometry
HPLC	High-performance liquid chromatography
HSQC	Heteronuclear single quantum correlation spectroscopy
sp.	Species
sp^3	sp^3 hybridisation
MTPA	α -methoxy- α -trifluoromethylphenylacetic acid
MTPACl	α -methoxy- α -trifluoromethylphenylacetyl chloride

MTT	3-(4,5-Dimethylthiazol-2-yl)-2,5-diphenyltetrazolium bromide
IC ₅₀	Half maximal inhibitory concentration
<i>J</i>	Coupling constant
L	Liter (s)
L-	Levorotatory rotation
lit.	Literature
m	Multiplet (NMR)
m	Meter (s)
M	Molar
MeOH	Methanol
mg	Milligram (s)
MHz	Megahertz (s)
mm	Millimeter (s)
mM	Millimolar
mmol	Millimole (s)
mp.	Melting point
<i>m/z</i>	Mass per charge ratio
[M+H] ⁺	Protonated molecule ion
[M+Na] ⁺	Pseudo-molecule ion
nm	Nanometer (s)
(NH ₄) ₆ Mo ₇ O ₂₄	Ammonium molybdate
NOESY	Nuclear Overhauser effect spectroscopy
Ole	Oleandrose
PNPG	<i>p</i> -nitrophenyl- α -D-glucopyranoside
ppm	Parts per million
q	Quartet (NMR)
qd	Quartet of doublet (NMR)
RP-18	Reverse phase C18 column
<i>R</i>	Rectus for right (configuration)
rt	Room temperature
s	Singlet (NMR)

S	Sinister for left (configuration)
t	Triplet (NMR)
td	Triplet of doublet (NMR)
Thv	Thevetose
Tig	Tigloyl
TLC	Thin layer chromatography
t_R	Retention time
U	Unit



CHAPTER I

INTRODUCTION

Chemical molecules generated by plants, animals, or microorganisms are known as natural products. Cosmetics, drugs, dyes, nutritional supplements, and foodstuffs made from natural sources that are minimally processed or do not include artificial chemicals are example of natural goods in commercial usage. Natural products are organic molecules obtained and isolated from natural sources and created by the metabolic pathways or primary or secondary metabolism in organic chemistry. Within the discipline of medicinal chemistry, the term is usually narrowed to secondary metabolites, which are tiny molecules (mol wt <2000 amu) that are not required for the organism's existence [1].

Organic substances important for growth, development, reproduction, and survival, including as nucleic acids, amino acids, proteins, carbohydrates, and different energy components involved in all living organisms' fundamental metabolic pathways, are known as primary metabolites. Secondary metabolites, unlike primary metabolites, are found exclusively in certain organisms and are expressions of species identity. Organic substances that are not required for metabolism are known as secondary metabolites. Secondary metabolites rather play a role in circumstantial adjustment or as a feasible defensive technique for the organism's self-protection [2]. Ecological pressures such as food and space contests, as well as predator and surface fouling, have resulted in the creation of secondary metabolites with a variety of biological functions. Several secondary metabolites, in particular, are poisonous to predators, stimulating allure to the identical or the different species, or colorant to entice or to threat distinct species. Most natural compounds, by definition, have pharmacological or biological activity that can aid the treatment of disorders [3].

Natural products, particularly those derived from higher plants, have served humanity as a vital origin of curative manner to treat or prevent disease and enhance quality of life for thousands of years through traditional medicines. According to a

report published by the World Health Organization (WHO), 80 percent of the world's occupants still administer plant-based herbal remedies for basic health care [4]. Photosynthesis is the process by which higher plants transform carbon dioxide and water into simple sugars using light energy from sun. Plants are key sources of complex and extremely structurally varied secondary metabolites with ethnomedicinal qualities that have been recognized as leading sources of remedy for ancient drug establishment, apart from synthesizing oxygen and serving as a foodstuff supply. Many natural compounds that have become well-known medications, such as aspirin, digitoxin, morphine, pilocarpine, and quinine, have been isolated via clinical pharmacological, and chemical research or medicinal plants [5]. Natural goods are the source of inspiration for over half of all FDA-approved medications in the United States [6]. Natural products and artificially modified natural product derivatives have influenced a significant behaviour in the medicament of human disease, with anti-cancer agents [4, 7], anti-fungal agents [8], anti-bacterial [9], anti-viral agents [10], and anti-diabetic agents [11].

During the last 30 years, there has been a noteworthy escalation in the sum total of natural product studies focused on plant-derived foremost compounds [12]. Despite a renewed interest in studying plants as a source of natural products, the number of secondary products obtained from plants is far from the finish line. Only 15% of the approximately 250,000 higher plant species accessible on Earth have been examined for their active chemicals, and only 6% have been evaluated for their biological features [12, 13]. As a result, there are many more potential candidates for novel active chemicals that have yet been found.

Abutilon is an enormous genus belonging to the family Malvaceae, sub-family Malvoideae, with over 150 species found in India, Malays, Philippine Islands, and Indochina, consisting of more than 150 species. This genus includes annual and perennial herbs, shrubs, and small trees that are endemic to tropical and subtropical climates [14]. Six *Abutilon* species are identified as indigenous in Thailand. Several introduced species can be found for ornamental such as *A. megapotamicum* (Spreng.) and *A. pictum* (Gillies ex Hook) Walp. from South America [15]. Traditional medicine makes extensive use of plants in this genus. Carbohydrates, steroids,

glycosides, flavonoids, tannins, and phenolic compounds are only a few of the chemical ingredients found in *Abutilon* [16].

A. indicum is a gently tomentose evergreen perennial shrub that grows up to 3 meters tall [17]. A Northeastern Thai folk tradition recipe consisting *Abutilon indicum* and *Mimosa pudica* have been reported as being effective for diabetic treatment [18]. Furthermore, traditional medicinal use of *A. indicum* as antimicrobial [19], antidiarrheal [20], wound healing [21], antidiabetic/hypoglycemic & anti-obesity [22], anti-ulcer [22], and female fertility control [23]. Phytochemical investigation of *A. indicum* reported that alkaloids, amides, coumarins, benzoids, ionones, nucleosides, and steroids were isolated from its flowers, leaves, aerial parts, roots, and whole plants [11, 24-30]. In addition, biological activities of extracts and isolated compounds were studied as antidiabetic [11, 24, 26, 31] and antimicrobial [30] activities.

Although many researches of phytochemical, pharmacological tests, and isolation work on *A. indicum* have been published, there were only a few reports from the stems. The change of nutritional elements from diverse geographical characteristics has a significant impact on metabolites in stem sections. Therefore, this thesis focused on seeking new pharmaceutical candidates from *Abutilon indicum* (L.) Sweet. According to the main objective of this research, the bioactive compounds of *Abutilon indicum* stems were isolated by column chromatographic techniques and screened for the active extracts possessing a particular biological effect, followed by the identification of the active substance responsible for the activity.

CHAPTER II

LITERATURE REVIEW

2.1 *Abutilon indicum* (L.) Sweet

2.1.1 Description of *Abutilon indicum* (L.) Sweet

There are roughly 150 species in the genus *Abutilon*, which is a part of the Malvaceae family, including some species found in Thailand. The secondary metabolites produced from the genus *Abutilon* have been a global interest for its pharmacological actions, including antidiabetic activity. A methanolic extract from the leaves of *A. pannosum* (Frost.f.) Schlecht had bactericidal activity proportional to penicillin potassium and streptomycin sulphate towards Gram positive (*Bacillus subtilis*, *Staphylococcus aureus*, *Sarcina leuka*, and *Bacillus megaterium*) and Gram negative (*Escherichia coli*, *Pseudomonas aeruginosa*, *Proteus vulgaris*, and *Shigella sonnie*) bacteria [32]. In 2004, Beha and colleagues found that an ethyl acetate extract from the roots or root bark of *A. grandiflorum* G. Don had significant *in vivo* activity versus *Plasmodium vinckei* in mice and *in vitro* versus *Plasmodium falciparum* strains HB3 and FCB. The extract showed significant cytotoxicity when examined *in vitro* on the colon cell line HT29 [33]. Further, an ethanolic extract from the leaves of *A. mauritianum* exhibited antibacterial activity over *Klebsiella pneumonia*, *P. aeruginosa*, and *E. coli* at minimum inhibitory concentration of 15%, 20%, and 25% w/v, respectively [34]. When compared to the positive control, abutilins C-D from *A. pakistanicum* demonstrated good activity against enzyme α -glucosidase with IC_{50} values 8.27 and 52.43 $\mu\text{g}/\text{mL}$ compared with positive control acarbose (IC_{50} , 5.92 $\mu\text{g}/\text{mL}$) [35].

Abutilon indicum is one of the species in the genus *Abutilon*. The distribution of this plant is all over Asia in a tropical and subtropical areas, including Bhutan, Cambodia, China, India, Indonesia, Laos, Myanmar, Nepal, Sri Lanka, Taiwan, Thailand, and Vietnam. *A. indicum* is used in many countries for different purposes. Ethnobotanist have found almost all portions of *A. indicum* plant to be valuable in

ethnobotanical surveys. Indians, Malayans, Filipinos, and Indochina residents have been recorded to use its components for medical and other uses. A strong white fiber is produced from the stem barks. Furthermore, mature stem fiber may be used to make cordage, twine, and rope, but younger stem fiber can be used to weave textiles [36]. Syphilis is treated by chopping up the leaves and seeds and mixing them with water to produce a paste that are administered to the penis [37-39]. Eyewash, mouth wash, in catarrh, and bilious diarrhoea are among remedies that employ leaves. To cure hemorrhoid and to soothe leg soreness, a leaf paste is given orally [40]. To treat uterus displacement, a bread made from a blend of leaf powder and wheat flour is consumed daily at night for about a month [41]. Snakebite is treated with the leaf juice combined with coarse dark brown sugar as an antidote [42]. The fruit is used to treat piles, gonorrhoea and cough [43, 44]. To treat haemorrhagic septicemia, a fruit decoction combined with ammonium chloride is administered orally [45]. Seed powder is utilized as an aphrodisiac and laxative when taken orally with water [46].

Eleven species of the genus *Abutilon* were found naturally in Thailand, *Abutilon x hybridum* hort., *A. graveolens* (Roxb. ex Hornem.) Wight & Arn., *A. hirtum* (Lam.) Sweet, *A. indicum* (L.) Sweet, *A. indicum* (L.) Sweet subsp. *guineense* (Schumach.) Borss. Waalk., *A. megapotamicum* (Spreng.) A.St.-Hil. & Naudin, *A. persicum* (Burm.f.) Merr., *A. pictum* (Gillies ex Hook.) Walp., *A. sinense* Oliv., *A. substellatum* Phuph. & Poopath, *A. theophrasti* Medik [47]. *Abutilon indicum* (L.) Sweet is locally known as Top taep (ตออบแตบ) (Ratchaburi), Pop paep (ปออบแปบ) (Northern), Phong phang (โพงพาง) (Nakhon Ratchasima), Fan si (ฟันสี) (Central), and Ma kong khao (มะก่องข้าว) (Northern). *A. indicum* is also known as “Indian Mallow” [48]. Several metabolites have been isolated from the genus *Abutilon*. Those metabolites showed potential sources for a wide range of drug discovery and development. A phytochemical study of *A. indicum* reported that phenolic acid and derivatives, flavonoids, sterols, and terpenoids are the significant metabolites (**Figure 1**). Those chemical constituents were obtained from their whole plant, aerial parts, roots,

stems, leaves, fruits, and flowers. Phenolic acid and derivatives are primarily found in the whole plant and aerial parts. The previous report showed their antibacterial and anti-radical activities. Flavonoids are a group of natural substances with variable phenolic. Flavonoids can be classified as flavonols, flavones, flavanols, and anthocyanins. Flavonoids showed promising α -glucosidase activity. Sterols comprise a typical steroid core of an attached four-ring structure with a hydrocarbon side chain and alcohol group. Its medicinal chemistry roles have been well-known due to broad-spectrum pharmacological agents, such as anticancer, antidepressant, anti-obesity, antihyperlipidemic, and mosquito larvicidal activities. Triterpenoids are metabolites that contain six isoprenes and exhibited a broad spectrum of bioactivities, including bactericidal, cardiovascular, analgesic, and anti-allergic properties.

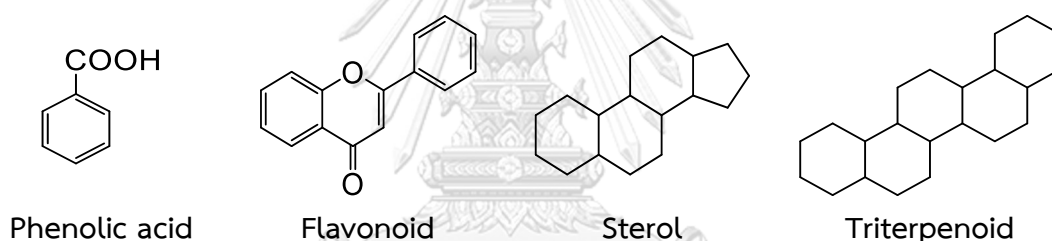


Figure 1 Major classes metabolites of *A. indicum*

2.2.2 Taxonomy of *A. indicum* (L.) Sweet

The genus *Abutilon* is placed in the Malvaceae family. Based on the Integrated Taxonomical Information System (ITIS), the taxonomy of *A. indicum* (L.) Sweet is classified as:

Kingdom: Plantae

Division: Tracheophyta

Class: Magnoliopsida

Order: Malvales

Family: Malvaceae

Genus: *Abutilon* Mill.

Species: *Abutilon indicum* (L.) Sweet

2.2.3 Botany of *A. indicum* (L.) Sweet

Abutilon indicum (L.) Sweet (Malvaceae), predominately under the name of “country mallow”, is a multi-branched, erect velvety-pubescent subshrub with a round stem, often tinged with purple, up to 2.5 m in height. Furthermore, this plant is grey puberulent entirely. The stems are sturdy, branched, 1-2 m tall, pubescent. The leaves are a green and thin flattened lateral outgrowth of the stem. The leaves are ovate, acuminate, toothed, rarely subtrilobate, and 1,9-2,5 cm long. It is slightly hairy and velvety on both sides. The petioles 3.8-7.5 cm long, stipules 9 mm long; pedicels often 2.5-5 mm long, axillary solitary, jointed very near the top; calyx 12.8 mm long, divided into the middle, lobes ovate, apiculate, and corolla 2.5 cm diameter, yellow, opening in the evening. The flowers are bright yellow, opening in the evening, bracteates, pedicellate, complete, actinomorphic, hermaphrodite, pentamerous, hypogynous, and cyclic. The flowers are epicalyx absent. Moreover, the flowers are about 3 cm in diameter, made up of 5 petals (polypetalous), slightly connate twisted, and peduncle jointed above the middle. The fruits are multi ridged capsules (carserule), substantially pubescent, with prominent and horizontally spreading beaks. The seeds are 3-5 mm, black or dark brown, reniform, tubercled or minutely stellate-hairy, and minutely pitted [16, 49, 50]. The picture of *A. indicum* (L.) Sweet and its various parts are shown in **Figure 2** [36].



(1)



(2)



(3)



(4)

Figure 2 Various parts of *A. indicum*: Flower and leaves (1); ripening fruit (2); mature seed capsules (3); and flower (4).



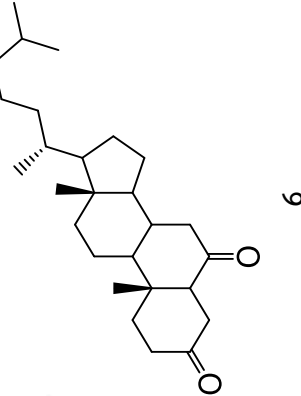
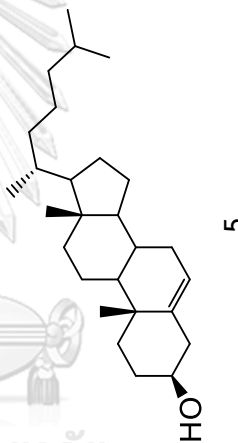
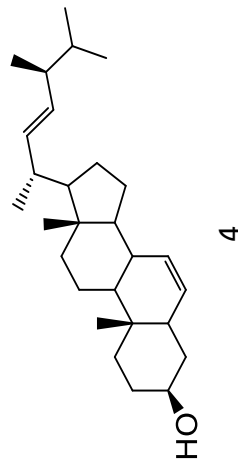
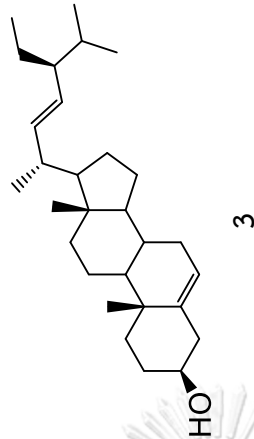
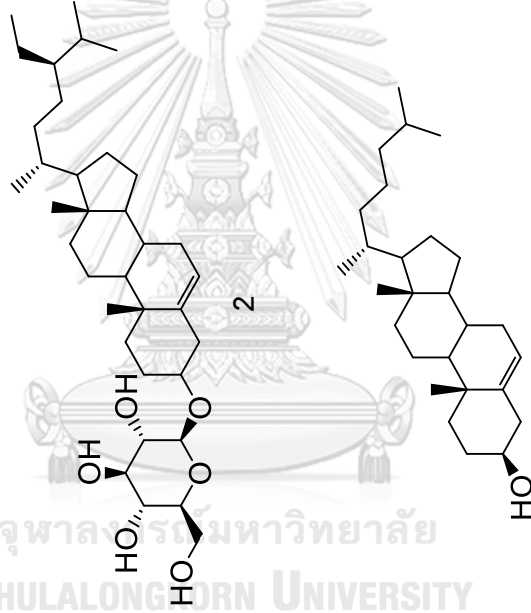
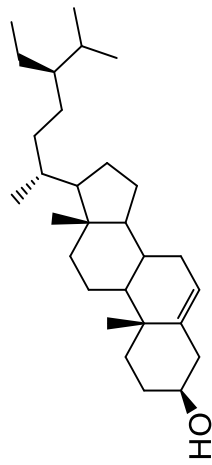
Classification	No	Compound name	Part used	Reference
			Whole plant	[54]
	10	Quercetin-3-O- β -D-glucopyranoside	Flowers	[59]
			Leaves	[60]
	11	Quercetin-3-O- α -rhamnopyranosyl (1 \rightarrow 6)- β -glucopyranoside	Flowers	[59]
	12	Gossypetin-7-O- β -glucoside	Flower petals	[61]
	13	Gossypetin-8-O- β -glucoside	Flower petals	[61]
Flavones	14	Luteolin	Flowers	[59]
			Leaves	[60]
	15	Luteolin-7-O- β -glucopyranoside	Flowers	[59]
			Leaves	[60]
	16	Chrysoeriol	Flowers	[59]
			Leaves	[60]
	17	Chrysoeriol-7-O- β -glucopyranoside	Flowers	[59]
			Leaves	[60]
	18	Apigenin-7-O- β -glucopyranoside	Flowers	[59]
Anthocyanin	19	Cyanidin-3-O-rutinoside	Flowers petals	[61]
Phenolic acid and	20	Benzoic acid	Whole plant	[27]

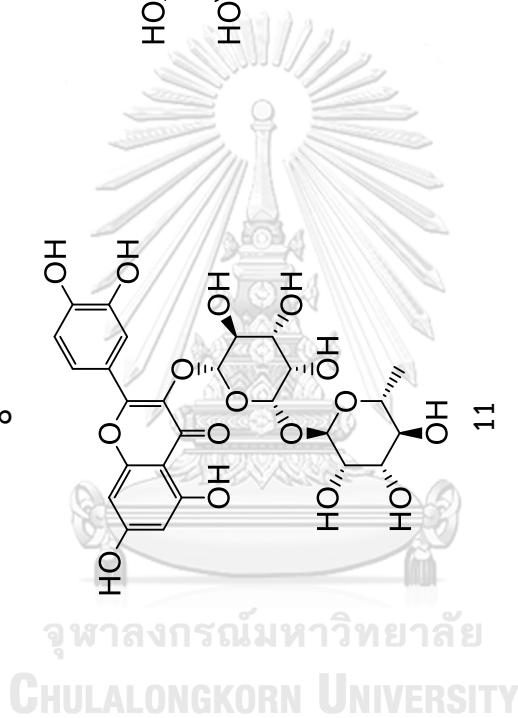
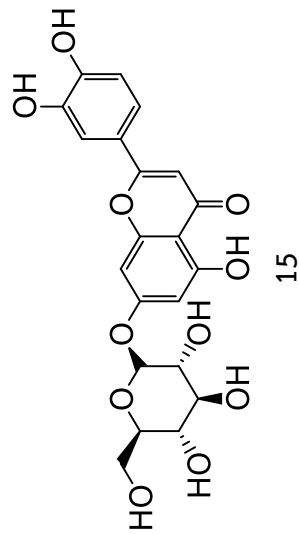
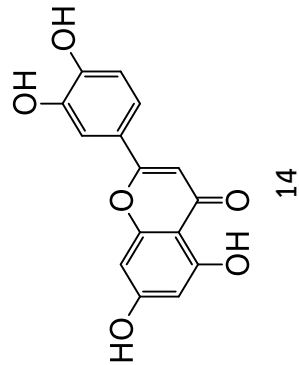
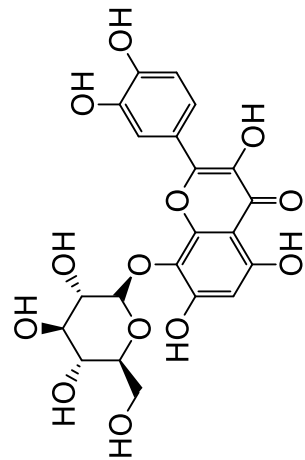
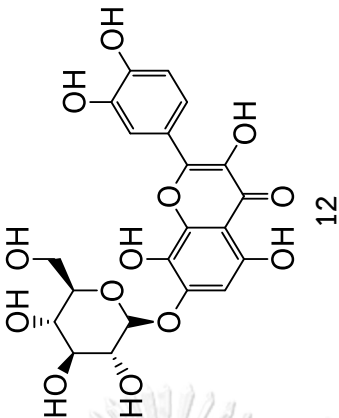
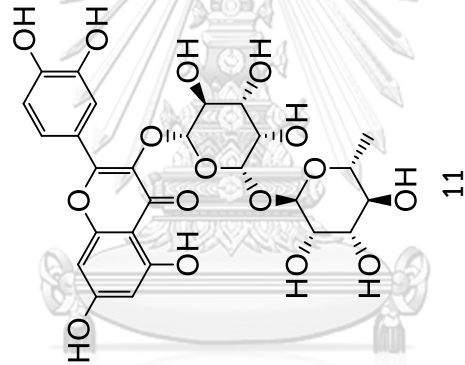
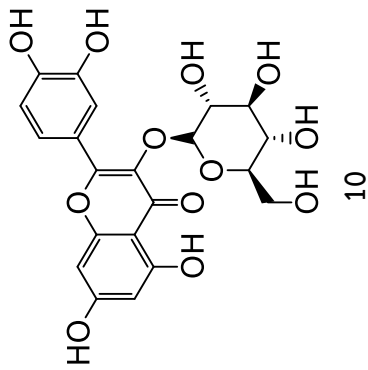
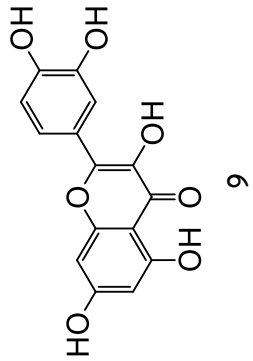
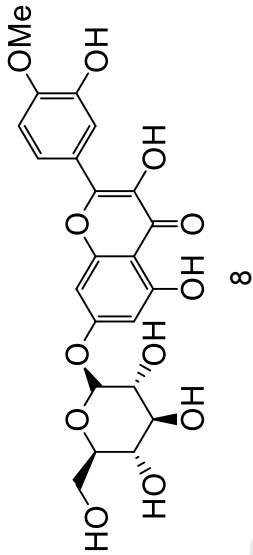
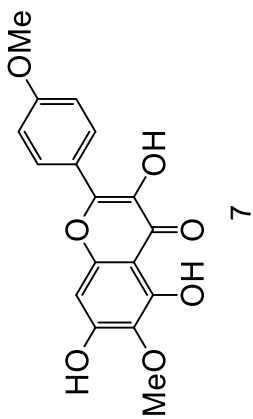
Classification	No	Compound name	Part used	Reference
derivatives	21	p-Hydroxybenzoic acid	Whole plant	[27, 52, 62, 63]
			Aerial parts	[54]
	22	Vanillic acid	Whole plant	[27, 53]
			Aerial parts	[62]
	23	Glucovanilloylglucose	Aerial parts	[62]
	24	4-Hydroxyacetophenone	Whole plants	[27]
	25	4-Hydroxybenzaldehyde	Whole plants	[27]
	26	Vanillin	Whole plants	[27]
	27	Syringaldehyde	Whole plants	[27]
	28	Methyl-4-hydroxybenzoate	Whole plants	[27, 52]
	29	Eudesmic acid	Leaves	[64]
	30	Gallic acid	Roots	[54, 55]
			Aerial parts	[55]
	31	2,6-Dihydroxy-4-methoxyacetophenone	Whole plants	[52]
	32	4-O- β -Glucosylbenzoic acid	Whole plants	[55, 63]
		Aerial parts	[62]	
33	2,6-Dihydroxy-5-methoxy-(3-C-glucopyranosyl) benzoic acid	Whole plant	[52]	

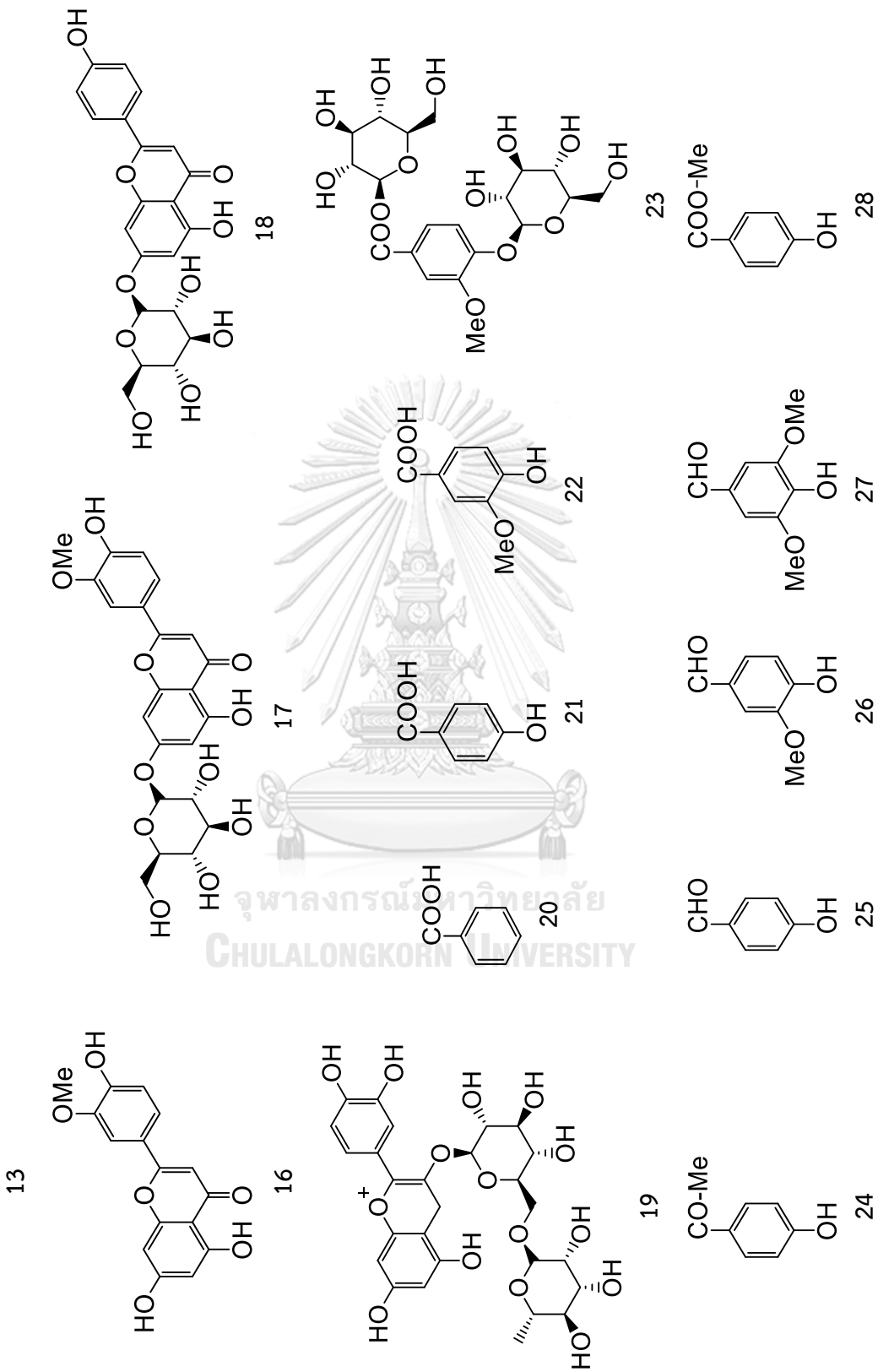
Classification	No	Compound name	Part used	Reference
	34	<i>p</i> -Coumaric acid	Whole plant	[27]
			Aerial parts	[62]
	35	Caffeic acid	Whole plant	[52, 63]
			Leaves	[63]
			Aerial parts	[62]
			Leaves	[64]
Triterpenes	36	Ferulic acid	Whole plant	[27]
	37	4-Hydroxy-3-methoxy- <i>E</i> -cinnamic acid methyl ester	Whole plant	[27]
	38	Methyl 4-hydroxyphenylacetate	Whole plant	[27]
	39	Methylcoumarate	Whole plant	[27]
	40	Abutilin A	Whole plant	[27]
	41	Fumaric acid	Aerial parts	[62]
	42	β -Amyrin	Aerial parts	[54]
	43	Oleanic acid	Whole plant	[53]
	44	β -Amyrin-3-palmitate	Leaves	[28]
	45	Lupeol	Aerial parts	[54]
	46	Squalene	Leaves	[28]
Quinone	47	2,6-Dimethoxy-4-benzoquinone	Whole plant	[53]
Coumarins	48	Scoparone	Whole plant	[27]

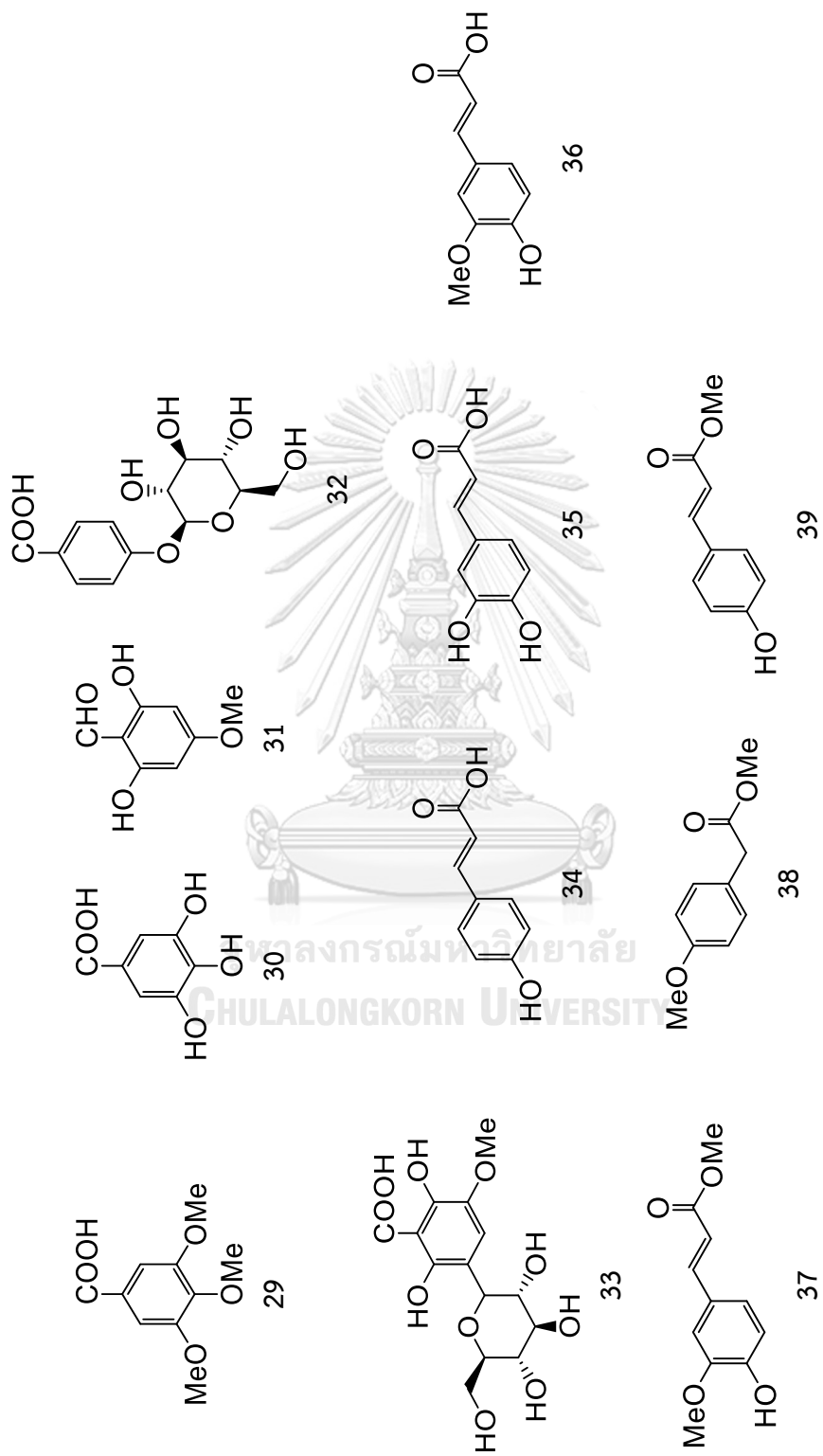
Classification	No	Compound name	Part used	Reference
	49	Scopoletin	Whole plant	[27]
	50	3,7-Dihydroxychromen-2-one	Whole plant	[27]
Alkaloids and amides	51	Aurantiamide acetate	Whole plant	[27]
	52	(<i>R</i>)- <i>N</i> -(1'-Methoxycarbonyl-2'phenylethyl)-4-hydroxybenzamide	Whole plant	[27]
	53	<i>N</i> -Feruloyl tyrosine	Whole plant	[27]
	54	1-Lycoperodine	Whole plant	[27]
	55	1-Methoxycarbonyl- β -carboline	Whole plant	[27]
	56	Methyl indole-3-carboxylate	Whole plant	[27]
	57	Vasicine	Aerial parts	[54]
Lactones	58	Alantolactone	-	[65]
	59	Isoalantolactone	-	[65]
Ionones	60	3-Hydroxy- β -damascone	Whole plant	[27]
	61	3-Hydroxy- β -ionol	Whole plant	[27]
Nitrogenous bases	62	Riboflavin	Whole plant	[27]
	63	Adenosine	Whole plant	[27]
	64	Adenine	Whole plant	[27]

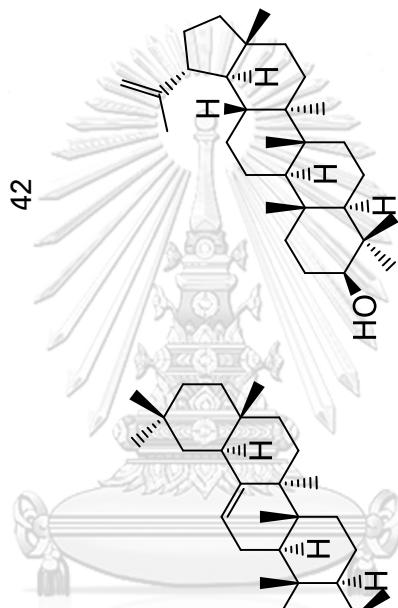
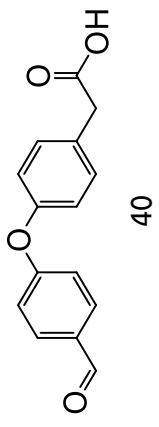
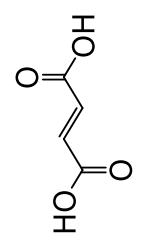
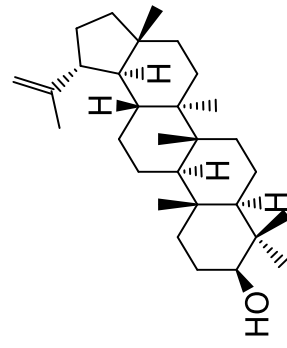
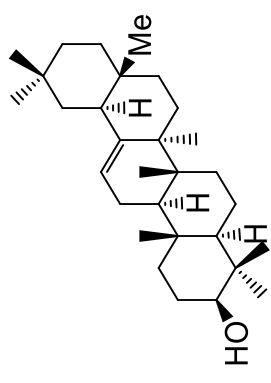
Classification	No	Compound name	Part used	Reference
	65	Thymine	Whole plant	[27]
	66	Methyl triacontanoate	Aerial parts	[54]



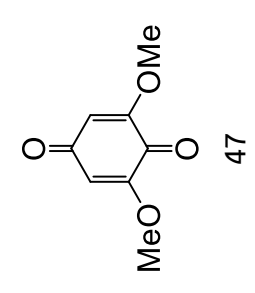
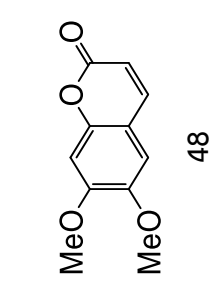
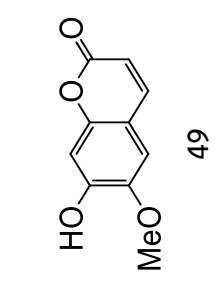
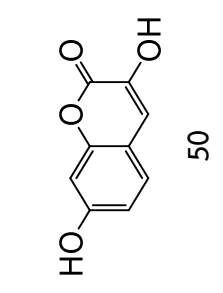
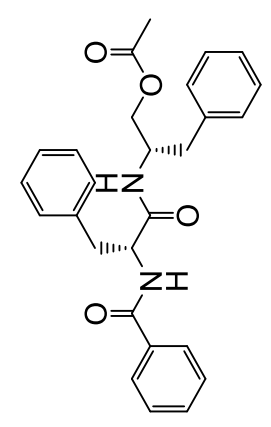
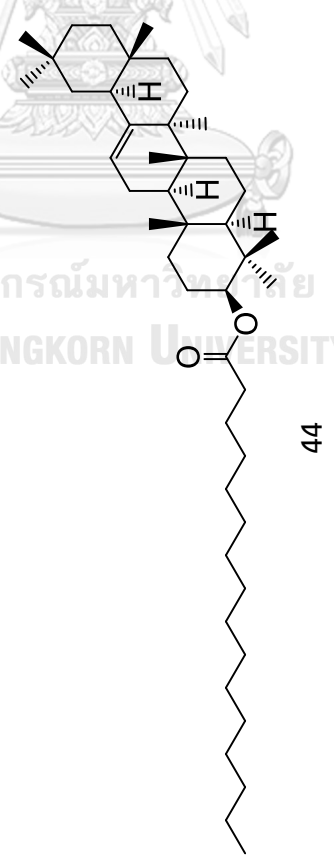
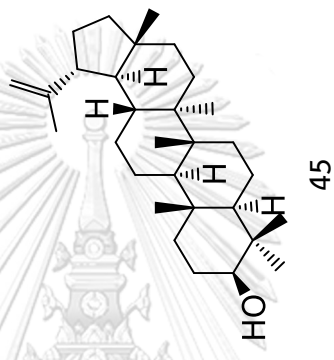
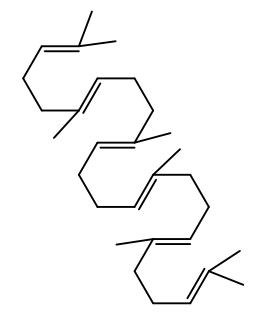




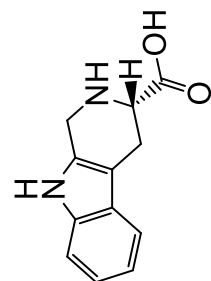




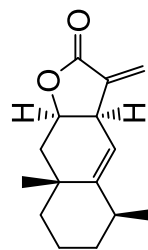
จุฬาลงกรณ์มหาวิทยาลัย
CHULALONGKORN UNIVERSITY



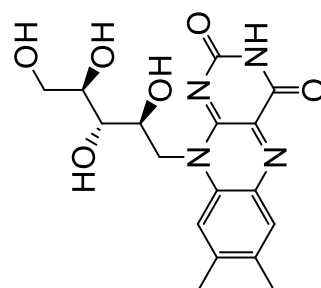
51



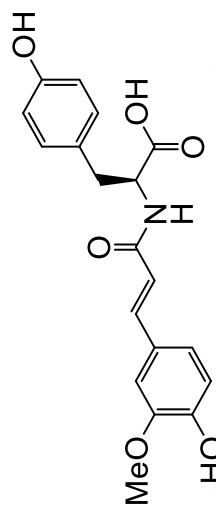
55



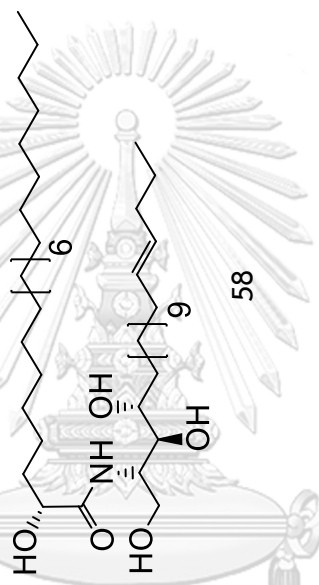
59



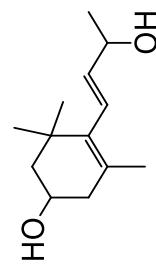
63



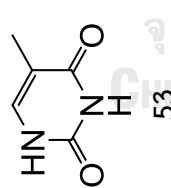
54



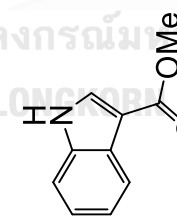
58



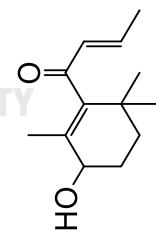
62



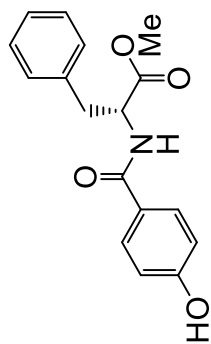
53



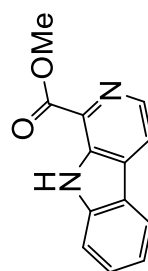
57



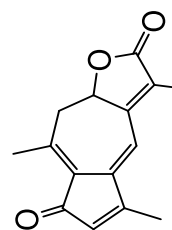
61



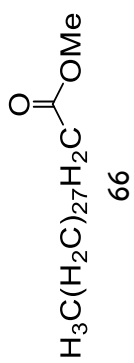
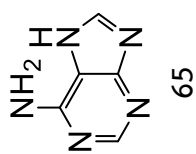
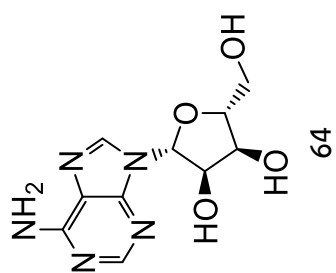
52



56



60



จุฬาลงกรณ์มหาวิทยาลัย
CHULALONGKORN UNIVERSITY

2.2.5 Biologically active metabolites from *A. indicum* (L.) Sweet

2.2.4.1 Antidiabetic activity

Polar extracts (alcoholic and aqueous) of *A. indicum* leaves (400 mg/kg, p.o.) had remarkable hypoglycemic impact in healthy rats 4 hours subsequent to application (23.10 % and 26.95 % severally) [11]. The aqueous extract was found quite effective in lowering blood glucose levels [66]. It was also explained to enhance insulin sensitivity. The aqueous extract of the entirety plant, including leaves, twigs, and roots of *A. indicum* (L.) Sweet could activate glucose transporters 1 (GLUT1) promoter activity. It has been suggested that the extract from *A. indicum* (L.) Sweet might help to reduce insulin resistance by adjusting adipocyte distinction via PPAR- γ agonist action and reviving glucose consumption via GLUT1 [26].

2.2.4.2 Antiulcer activity (Wound healing activity)

slices, pieces, and dead wound simulations in albino rats were used to test wound healing efficacy of an ethanolic extract of *A. indicum*. The ethanolic extract was examined at a dosage of 400 mg/kg body weight. The rate of wound shrinkage, skin breaking strength, granuloma strength, and dried granuloma weight were elevated enormously [8].

2.2.4.3 Anticancer activity

The potential antioxidant properties of *A. indicum* extract was screened using FRAP, 1,1-diphenyl-2-picrylhydrazyl (DPPH) radical scavenging activity and Nitric Oxide radical inhibition estimated using Griess Illosvoy reaction. The extract shows antioxidant capabilities as well as inhibitory effects on cancer cells with increased dosage and time [67]. The present study reports the synergistic effect between gallic acid and the phytoconstituents of the medicinal plant *A. indicum* stem to induce apoptosis in Human U87 glioblastoma cells [68].

2.2.4.4 Anti-inflammatory and antiproliferative activity

The ethanolic leaf extract of *A. indicum* (L.) for plausible chemopreventive agent revealed valuable anti-inflammatory activity (IC_{50} =8.89 μ g/mL) based on 5-lipoxygenase (5-LOX) inhibition assay. It has also shown a satisfying response on

human Caucasian lung carcinoma of A549 cell line ($IC_{50}=85.2 \mu\text{g/mL}$) for antiproliferative activity. Bioactive components present in the ethanolic leaf extract of *A. indicum* showed stunning anti-inflammatory and antiproliferative activities by inducing Apaf-1 through CASP9, CASP3, CYCS, BCL2L1, TP53, BCL2, CASP8, HSPA4, DIABLO, and CASP7 network [69].

2.2.4.5 Larvicidal activity

The crude hexane, ethyl acetate, petroleum ether, acetone, and methanolic extracts of *A. indicum* were assayed for their toxicity. All extracts showed moderate larvicidal effects against mosquito (*C. quinquefasciatus*) with the highest larval mortality was found in petroleum ether extract ($LC_{50} = 26.67 \text{ ppm}$) and further identified as β -sitosterol [51].

2.2.4.6 Acetylcholinesterase inhibitory activity

A methanolic extract of *A. indicum* L. inhibited the activity of acetylcholinesterase (AChE), major enzyme in the breakdown of acetylcholine, by $30.66 \pm 1.06\%$ at 0.1 mg/mL [70]. The inhibition of this enzyme is suspected to be a potential therapy for neurological diseases such as Alzheimer's disease, senile dementia, ataxia, and myasthenia gravis.

2.2.4.7 Antimicrobial activity

A. indicum extracts (fruits, roots, and leaf) showed no inhibition against microorganisms *Bacillus cereus* var *mycoides*, *Bacillus pumilus*, *Bacillus subtilis*, *Bordetella bronchiseptica*, *Micrococcus luteus*, *Staphylococcus aureus*, *Staphylococcus epidermis*, *Escherichia coli*, *Klebsiella pneumonia*, *Pseudomonas aeruginosa*, *Streptococcus faecalis*, *Candida albicans*, *Aspergillus niger*, and *Saccharomyces cerevisiae* [40]. The screening of the seeds of *A. indicum* (L.) showed mycelial inhibition (%) against *Absidia ramose* and *Aspergillus niger* by 6.97 and 37.25, respectively [71].

2.2.4.8 Anti-diarrhoeal

The anti-diarrhoeal action of the leaf extracts of *A. indicum* was investigated by gastrointestinal motility, castor oil-induced diarrhoea, and prostaglandin E2-

induced entero-pooling. The methanolic and aqueous extracts had substantial anti-diarrhoea efficacy in castor oil-induced diarrhoea and prostaglandin E2-induced diarrhoea [20].

2.2.4.9 Immunomodulatory activity

The ethanol extract of *A. indicum* leaves was evaluated for the modulatory influence on hepatic antioxidant status and lipid peroxidation in contra with alcohol-induced liver injury in rats. Peroxidative damage was low in both liver and serum of alcohol-treated rats at dosages of 100 and 200 mg/kg body weight/day for 21 days. This was owing in part to the flavonoids and micronutrients ability to efficiently induce the antioxidant potential through free radical scavenging [60].

The immunomodulatory activity of ethanolic and aqueous extract of leaves of *A. indicum* in the doses of 200 and 400 mg/kg by haemagglutination antibody (HA) titre, delayed-type hypersensitivity (DTH), neutrophil adhesion test, and carbon clearance test showed a notably potentiated DTH reaction and rise in percentage neutrophil adhesion test. The extracts were found to have a considerable immunostimulatory potency [72].

2.2.4.10 Anti-estrogenic activity

The methanolic extracts of *A. indicum* possessed anti-estrogenic effect on uterotrophic and uterine peroxidase activities in ovariectomized rats and caused significant suppression of enzyme activity as well as uterotrophic reaction induced by estradiol [73].

2.2.4.11 In vitro anti-arthritis activity

The water-soluble extract of *A. indicum* (L.) was tested on three *in vitro* parameters: inhibition of protein denaturation, membrane stabilization, and proteinase inhibition. *A. indicum* at doses of 100 and 250 mcg/mL defend opposing the denaturation of proteins and hypotonic saline induced RBC membrane destruction. It also revealed considerable anti-proteinase activity [74].

2.2.4.12 Hepatoprotective activity

The aqueous extract of the leaves of *A. indicum* disclosed prominent hepatoprotective activity at 100 and 200 mg/kg dose levels in CCl₄-treated rats [75]. The aqueous extract of *A. indicum* exhibited significant hepatoprotective activity by reducing carbon tetrachloride- and paracetamol-induced change in biochemical variables proven by enzymatic examination. The extract inhibits the production of free radicals, which resulted in hepatoprotective effects. However, the LD₅₀ value greater than 4 g/kg body weight displayed acute toxicity [76].

2.2 Diabetes

Diabetes mellitus (DM) is a severe multifactorial disorder represented by hyperglycemia (very high blood glucose level) and glucose intolerance. It is either in consequence of the deficiency in insulin secretion or the ineffectiveness of insulin to promote glucose uptake. Nowadays, DM is categorized based on the etiology and clinical manifestations into four categories [77]:

- (1.) Type 1 DM (T1D) is classified by gradual loss of insulin-producing β -cell (in pancreas) caused by autoimmune destruction (**Figure 3**) [78];
- (2.) Type 2 DM (T2D) is accounted predominantly by severe insulin resistance and subsequent β -cell failure (leading to insufficient compensatory insulin secretory response) (**Figure 3**) [78];
- (3.) Gestational DM is implied as hyperglycemia that begins or is first recognized throughout pregnancy; and
- (4.) Other distinctive types include monogenic forms of DM (neonatal DM and maturity onset diabetes of the young) and DM attributable to the disease of the exocrine pancreas, other endocrinopathies, and drug-induced DM.

DIABETES MELLITUS

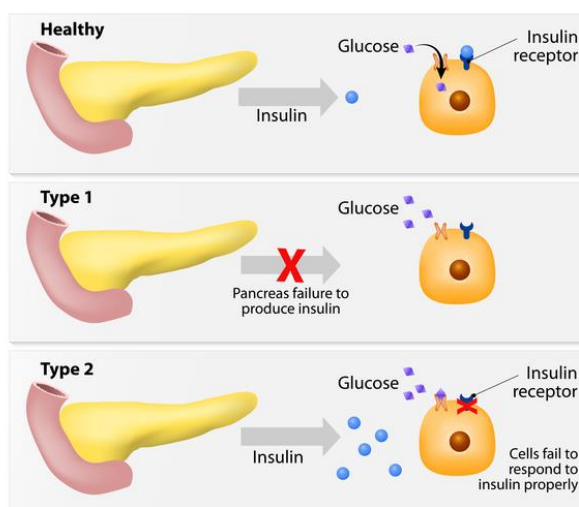


Figure 3 Healthy pancreas, pancreas in type 1 and type 2 diabetes mellitus

DM affects more than 422 million individuals globally, with the majority living in low- and middle-income nations based on the World Health Organization (WHO). Furthermore, diabetes is directly accountable for 1.6 million fatality per year [79]. Type 2 diabetes mellitus, found in the majority of those DM patients, is a condition in which the ability of the body to manage and utilize sugar (glucose) as an energy source is impaired. It regards for nearly 90-95% of with diabetes, type 2 diabetes, that prior to this introduced as non-insulin-dependent diabetes or adult-onset diabetes. It covers to those who suffers from insulin resistance as well as insulin insufficiency. Autoimmune destruction of β -cells does not happen to these people, so that they do not require insulin therapy to outlive, at least at the beginning and often during their lifetime [77]. However, it may drive to serious complications, including hyperlipidemia (an abnormally vast amount of lipid in the blood vessel), oxidative stress, and protein enzymatic glycation [80].

Besides, the chronic hyperglycemia of diabetes is correlated with long-lasting harm, dysfunction, and collapse of different organs, particularly kidneys, nerves, heart, blood vessels, and the eyes. Acarbose is one of the commercially available drugs for controlling hyperglycemia as the most effective way in diabetic patients [81, 82]. α -glucosidase inhibitors (AGIs) can hold the α -glucosidase activity back that leads

to the lowering of the hydrolytic cleavage of non-reducing ends of dietary oligosaccharides and diminishing liberate of α -glucose [83]. Due to AGIs, carbohydrate metabolism and intake of glucose in the small intestine are delayed to uphold the postprandial blood glucose at normal levels [84]. Notwithstanding the advantages, regular consumption of inhibitor leads to numerous side secondary responses, for instance diarrhoea, vomiting, flatulence, severe stomach ache, and allergic reactions [85, 86]. Despite these commercially available AGIs, researchers have been discovering novel biologically active AGIs with high inhibitive prospects and minor aftereffects.

2.3 Obesity

The autoimmune destruction of the β -cells of the pancreas results in insulin shortage to abnormalities, such as anomaly in carbohydrate, fat, and protein uptake. It is due to ineffective action on the target tissue and further causes resistance to insulin action. People with diabetes are more likely to have hypertension and impaired lipoprotein metabolism which leads to obesity [77].

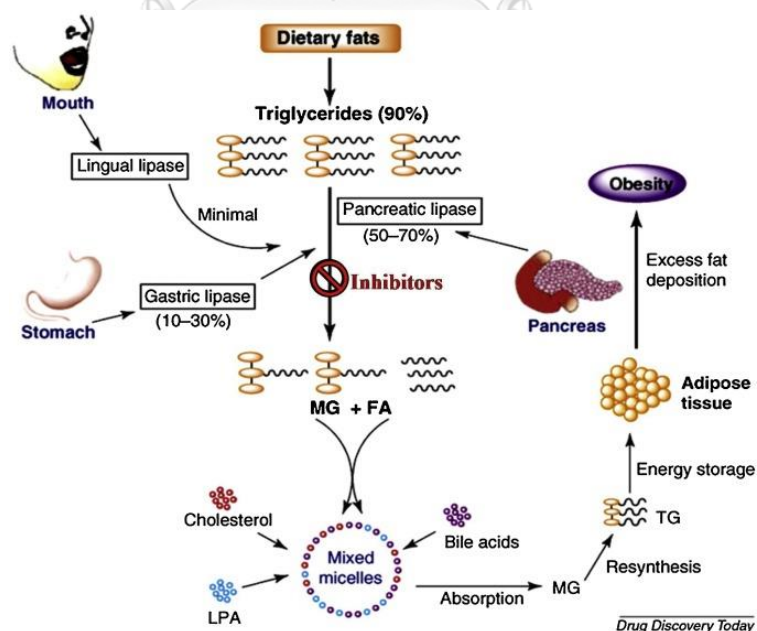


Figure 4 Lipid metabolic pathways in the human body [87-89]

The metabolism, transmission, and storage of lipids include a wide range of metabolic activities as shown in **Figure 4**. Following ingestion of a fat-rich meal in,

triglycerides (TG) is lipolyzed in the intestinal lumen to form free fatty acid (FFA) and 2-monoacylglycerols (MAG), which are subsequently taken up by enterocytes via passive diffusion and specialized transporters such as CD36 [89]. Cholesterol is taken up by enterocytes via the cholesterol transporter Nieman-Pick C1 Like 1 protein [87, 88]. Cholesterol is converted to cholesterol-esters in the enterocyte, whilst FFA and MAG are reassembled into TG. Lastly, chylomicrons are formed when cholesterol-esters and TG are packed together with phospholipids and apolipoprotein (apo) B48 [89, 90]. The chylomicrons are assembled and then secreted into the lymphatics before entering the circulation via the thoracic duct. When food-derived TG and FFA enter the liver, the liver synthesizes TG-rich lipoproteins known as very low-density lipoproteins (VLDL), which rise postprandially. VLDL (and its remnants, i.e., intermediate density lipoproteins (IDL) and low-density lipoproteins (LDL)) are assembled in a similar manner to chylomicrons, but apo B100 is the structural protein of VLDL [90].

Chylomicrons and VLDL transmit FFA to the heart, skeletal muscle and adipose tissue for energy expense and deposit. Enough lipolysis of TG-rich lipoproteins is required for the release of FFA in the circulation. The major enzyme for TG lipolysis in the blood, lipoprotein lipase (LPL), is highly expressed in tissue that require significant quantities of FFA, such as the heart, skeletal muscle, and adipose tissue [91]. The quantity of FFA released from chylomicrons and VLDL is determined by LPL activity, which is enhanced by insulin [92, 93]. Apo C-III, on the other hand, inhibits both LPL and hepatic lipase, so that the concentration of plasma C-III and plasma TG are positively correlated [94]. Furthermore, chylomicrons compete for LPL activity with endogenous VLDL [95]. Adipocytes readily absorb the released FFA and re-synthesize it into TG in the cytoplasm, where the acylation-stimulating protein (ASP)/C3adesArg pathway play a key role [96, 97]. The scavenger receptor CD36 is the best characterized FFA transporter and it is found in muscle, adipose tissue and the endothelium of capillaries [98]. CD36 expression is increased by insulin and muscular contractions, making FFA absorption easier [91].

One of the most significant regulating mechanisms for fuel storage is the postprandial surge in insulin. The efficient inhibition of hormone sensitive lipase, which is the primary enzyme for the breakdown of intracellular lipids, occurs as a result of the postprandial rise in insulin. In spite of the absorption of FFA by adipocytes and myocytes, some FFA spills over into the plasma compartment, where it is bound by albumin and delivered to the liver [99]. While FFA supply is inadequate for energy expenditure, such as when fasting, FFA can be mobilized by adipose tissue for oxidation in energy-demanding tissues such as cardiomyocytes. Insulin has a role in FFA mobilization from adipose tissue as well [93]. Insulin resistance, as a result, has a significant influence on the metabolism of TG-rich lipoproteins and FFA.

During lipolysis, chylomicrons and VLDL decrease in diameter, resulting in chylomicron remnants and bulky LDL are progressively produced as a result of the slow diameter reduction of chylomicrons and VLDL during lipolysis. Multiple mechanisms, including apo E, hepatic lipase, the LDL receptor, the LDL receptor-related protein, and heparan sulphate proteoglycans, are used by the liver to absorb chylomicron remnants [100-105]. LDL, on the other hand, is largely absorbed by the liver through the LDL receptor [106, 107]. The LDL receptor is re-shuttled back to the cell surface after being recycled. Many research in the recent decade have added to our understanding of the LDL receptor recycling mechanism, which is controlled by the proprotein convertase subtilisin/kexin type 9 (PCSK9) [107, 108]. When PCSK9 is attached to the LDL receptor, it encounters lysosomal derivation throughout the shuttling process, but it is recycled back to the hepatocytes' surface in the absence of PCSK9 [108]. PCSK9 neutralization enhances hepatocytes' overall LDL binding capacity, resulting in lower LDL-C concentrations [108].

Obesity is common in T2D patients and contributes to insulin resistance. Obesity is an imbalance in the intake of calories and their utilization by the body caused a disproportionate fat accumulation in the body. As mentioned on the recent reports of the World Health Organization, the number of obese people has closely

tripled globally since 1975. It should be noted that obesity is estimated to be in charge of 80-85% of the risk of getting T2D, and the new study shows that obese persons are up to 80 times greater risk to acquire T2D than those with a Body Mass Index (BMI) less than 22 [109]. As a result, BMI is closely associated to diabetes and insulin resistance. In obese persons, impairment of β -cell and increase amount of glycerol, hormones, cytokines, pro-inflammatory chemicals, and other compounds are linked to the case of insulin resistance [110].

Chylomicron remnants and LDL may move into the sub-endothelium and become stranded in the sub-endothelial space, where monocytes and macrophages can pick them up [111-113]. Small dense LDL has a higher affinity for arterial proteoglycans, resulting in greater lipoprotein retention in the sub-endothelial space [114]. In contrast to native LDL, subendothelial remains of chylomicrons and VLDL do not need to be changed to facilitate absorption by macrophage scavenger receptors [115]. Small dense LDLs have been shown to be more vulnerable to oxidation, in part due to their lower free cholesterol and anti-oxidative content [116]. Alternatively, LPL-enriched chylomicron and VLDL remnants could be delivered to tissues, where they engage with proteoglycans and lipoprotein receptors to remove particles. This process occurs in the liver and works as an anti-atherogenic mechanism, but it may also occur in other tissues where cholesterol is not eliminated successfully, resulting in cholesterol build up and hence the formation of atherosclerotic plaque [111, 112, 117, 118].

The waist/hip ratio was the greatest predictor for the fractional catabolic rate in studies utilizing stable isotopes, with the waist/hip ratio being the best predictor for the fractional catabolic rate [119]. In the case of obesity, higher levels of apo C-III can explain the poor clearance of residual lipoproteins [120]. Increased apo C-III levels in obesity can be described by glucose-stimulated apo C-III transcription, and plasma apo C-III levels have been shown to associate with fasting glucose and glucose excursion following an oral glucose test in obese adults [121]. Lastly, obesity lowers the expression of LDL receptors.

Orlistat, scientifically known as [(2S)-1-[(2S,3S)-3-hexyl-4-oxooxetan-2-yl]tridecan-2-yl] (2S)-2-formamido-4-methylpentanoate, is the extremely wide used prescription in the therapy of obesity [122]. Orlistat hinders of pancreatic, gastric, and carboxylic ester lipases, as well as phospholipase A₂, which are involved in the hydrolysis of dietary fats into fatty acids and monoglycerides in the gastrointestinal (GI) tract, thus reducing absorption of dietary fat [123]. However, the medication administration stirs up gastrointestinal adverse consequences, such as fatty/oily faeces, faecal incontinence, increased defecation, and faecal urgency. These constitute the main reason for discontinuation of the therapy by most patients [124]. Consequently, the finding of novel pancreatic lipase inhibitor candidates carries on essential issues. Along with that, natural products have been a prospective source of lead metabolites for drug discovery and development.

2.4 Diabetic Foot Ulcer (DFU)

Normal physiologic process of tissue repair. All conditions of tissue wound undergo physiological mechanisms of recuperation, which induce to structural and functional recovery of the broken tissues. The wound healing can be splitted into four continuous and overlapping stages, which are hemostasis and coagulation, inflammation, proliferation, and remodelling [125-127].

Phase I: Hemostasis and coagulation. Injured blood arteries shrink, platelets get active, the congealment cascade begins, a fibrin clot forms, and numerous chemicals liberated from platelets and damage cells throughout this period. The chemicals provoke secondary dilatation of blood vessels, enhance vascular permeability, and function as chemotactic triggers for various cells, preparing forthcoming restore processes easier [7]. Plasmin, a serine protease constituted from plasminogen activators, eventually seizes and deteriorates the temporary fibrin matrix, allowing circulation to re-establish [128, 129].

Phase II: Inflammation. It begins around 24 hours after the injury and persist up to 2 weeks indicated by the deliverance of growth factors and inflammatory

cytokines from the activated platelets and the injured cells, which pull inflammatory cells (leukocytes) from circulation to the injury site [130]. Neutrophils are the first leukocytes to arrive at the site of the injury, they adhere to vascular endothelial cells before migrating to the extravascular area [130]. Elastase, which helps in the cleaning process by breaking down and removing cellular debris, is one of the proteases that generated by neutrophils; while macrophages produce α -1 protease inhibitor which regulate the action of elastase. Proteases also helps neutrophils to migrate into the extracellular space where they undertake phagocytosis to protect against contamination and infection [130, 131]. Reactive oxygen species (ROSs), which have anti-infective characteristics, are also released by neutrophils [132, 133]. Fibroblasts and epithelial cells, which are involved in tissue healing and remodelling, are attracted to the site of injury by the proinflammatory cytokines that neutrophils release [130]. Blood monocytes start to infiltrate the wound within 2 days following the damage [129, 134]. The decrease in neutrophil infiltration occurs concurrently with their arrival. When they penetrate the wound, they transform into macrophages, which play a crucial role in regulating the healing process in addition to phagocytosing bacteria and muscle debris [132]. The production of extracellular matrix (ECM), angiogenesis, fibrosis, and the recruitment of fibroblasts, endothelial cells, and keratinocytes to the site of damage are all regulated by the various cytokines, growth factors, and free radicals released by macrophages [130, 132, 133]. Inflammatory cells undergo apoptosis, which ends the inflammatory phase but whose causes are mostly unclear [125, 133].

Phase III: Proliferation. The proliferative phase starts once the inflammatory phase has passed [125]. Re-epithelialization, angiogenesis, and degradation and remodelling of ECM by proteases, particularly matrix metalloproteinases and their inhibitors, occur during this period, and the wound close as a result [126, 132, 133].

Phase IV: Remodelling. After the wound has healed, the remodelling phase starts, which results in the development of collagenous scar whose tensile strength is around 80% that of the healthy, uninjured tissue [129, 130, 133].

The levels of the protease inhibitors α 1-antitrypsin and α 2-macroglobulin spike sharply after an acute injury. Several proteolytic enzymes are inhibited by these acute phase reactants, which is unchecked might result in uncontrolled inflammation and impede recovery. The order of affinity of α 1-antitrypsin with proteolytic enzymes is as follows: elastase > chymotrypsin > cathepsin > trypsin > plasmin. Similar to this, α 2-macroglobulin and cathepsin G have strongest affinity. It must be emphasized once more at this point that plasmin promotes fibrinolysis. Therefore, following acute injury, a sharp increase in α 1-antitrypsin and α 2-macroglobulin induces a period of fibrinolytic shutdown, which in turn causes a delay in healing and the maintenance of the inflammatory response and edema. This initial stage of inflammation is targeted by the oral mixture of trypsin:chymotrypsin. Oral supplementation of the enzyme complex guarantees that plasmin is kept accessible for fibrinolysis and reduces the length of the fibrinolytic shutdown phase since α 1-antitrypsin has stronger affinity for trypsin and chymotrypsin than plasmin does. As a result, local microcirculation is restored, inflammatory edema is cleaned out, and tissue healing is aided [128]. Overall, trypsin:chymotrypsin therapy minimizes tissue damage and inflammatory edema in individuals promoting quick recovery [135, 136].

Diabetes-case tissue repair

When a person has diabetes, the high levels of glucose in their blood vessel affect how well their blood cell work. In order for the immune system to function, white blood cells are essential. The body's capacity to combat infections and heal wounds is decreased when white blood cells are unable to operate properly. Uncontrolled diabetic patients may experience impaired circulation. Blood travels slowly when circulation declines, making it harder for the body to nourish wounds. As a result, the wounds might not heal at all or they might heal slowly [137].

Macrovascular impairment (such as coronary artery disease, peripheral arterial disease, and stroke) and microvascular disability (such as diabetic nephropathy, neuropathy, and retinopathy) complications are just a few of the life-threatening

band together with DM [138]. Foot/lower limb ulcerations are common DM consequence, with a lifetime risk of up to 25% [139], culminating in 40%–60% non-traumatic lower limb amputations in these person [140]. Diabetic foot ulcer (DFU) become serious global health, social, and economic concern [141] with a global predominance of 6.3% [142]. North America had the greatest incidence of 13%, while Oceania had the lowest prevalence of 3% [142]. It varied from 1.5% to 16.6%: with Australia having the lowest frequency at 1.5% , and Belgium having the topmost prevalence at 16.6% [142]. The prevalence was observed to range from 4.6% to 19.1% in another research [143, 144]. DFU is linked to a multifaceted and complicated etiology [145]. Peripheral vascular disease (PVD) and nerve fibre loss with concomitant loss of pain perception are among the primary causes of foot ulcers and slowed wound healing in persons with DM [146, 147].

Since the 1960s, chymotrypsin has been used as an oral proteolytic enzyme preparation. It is more effective than other enzyme formulations at resolving inflammatory marker and promoting faster return to health from severe tissue damage [148]. The creation and remodelling of the extracellular matrix during a wound healing involve various processes that occur in a sequential order. Fibronectin and fibrin composed the majority of the clot that forms throughout the healing process [149]. Plasmin then breaks down the fibrin barrier to allow blood to flow again. In reaction to traumatization, the liver produces acute-phase proteins including α 1-antitrypsin and α 2-macroglobulin which bind to plasmin and stop fibrinolysis. Chymotrypsin reduces fibrinolytic shutdown and the intensity of the inflammatory [134, 148].

Chymostatin is the upmost frequently available medication used for the therapy of α -chymotrypsin enzyme. Muscle proteins, like those in other tissues, are constantly degraded and replaced. Changes in protein breakdown rate may contribute in normal muscular buildout in parallel with atrophy caused by denervation, dystrophy, and thyrotoxicosis. Libby and Goldberg revealed that chymostatin dropped off the pace of protein decomposition in the red soleus

muscle, the white extensor digitorum-longus muscle, and the diaphragm. Over the concentration range of 0-20 μM , the degree of proteolysis inhibition in the soleus muscle escalate [150]. One of the objectives of this research is to obtain new agent that may block protein decomposition in viable cells without causing toxicity, which could be valuable in maintaining tissue in culture.

Some plant-derived natural products showed good inhibition activity towards α -glucosidase. 3β -Hydroxy- 11α -hydroperoxyolean-12-en-28-oic acid and 3β -hydroxy- 11α -hydroperoxyursan-12-en-28-oic acid were isolated from the methanolic extract of the fresh seedpods of *Holarrhena curtisii*. The isolated metabolites demonstrated their *in vitro* α -glucosidase inhibitory activity with IC_{50} values of 79.3 and 49.7 μM , respectively. They were comparable with the acarbose with IC_{50} values of 884.6 μM [31]. Guttiferone I [151] was isolated from ethyl acetate extract of the leaves of *Garcinia cowa* Roxb. ex Choisy (Clusiaceae), a Thai edible plant. It showed high efficacy in inhibiting α -glucosidase enzyme and promoting glucose consumption activity by 3T3-L1 cells, with IC_{50} values of 0.5 μM and 13.1 μM , without causing toxicity to the cells [152]. Five resveratrol oligomers, namely *E*-resveratrol [141, 153], (-)- ϵ -viniferin [154], (-)- α -viniferin [154], trihydroxyphenanthrene glucoside (THPG) [155], and vaticaphenol A [156], were isolated from the acetone and ethanol of the stem bark of *Hopea ponga* (Dennst.) Mabb. They showed prominent α -glucosidase inhibition with IC_{50} values, 12.56 ± 1.00 , 23.98 ± 1.11 , 7.17 ± 1.10 , 31.74 ± 0.42 and 16.95 ± 0.39 μM , respectively [157]. Those studies prove that plants are well recognized as an important source of providing antidiabetic agents. It further leads to isolate the metabolites from the plant species *A. indicum* (L.) Sweet and evaluate their inhibition towards α -glucosidase, pancreatic lipase, and α -chymotrypsin enzymes.

CHAPTER III

EXPERIMENTAL

3.1 *In silico* approach (α -glucosidase, pancreatic lipase, and α -chymotrypsin inhibition assays)

3.1.1 Ligand preparation

In silico approaches aims to investigate the binding ability of the phytochemicals from *A. indicum* to the α -glucosidase, pancreatic lipase and α -chymotrypsin enzyme acts as anti-diabetes, anti-obesity, and anti-ulcer. The 66 selected phytochemicals were drawn using ChemDraw Professional 15.0. The structures were optimized using the PyRx software and then converted file for all compounds to PDBQT format for docking investigations.

3.1.2 Protein preparation

The RCSB Protein Data Bank provided the receptors (PDB ID: 4J5T, 1LPB, and 5J4S). Using the protein setup in AutoDock to adjust structure, atom, and bond length, the protein structures were constructed before to the docking investigations. The protein structures were cleaned of water molecules and the original inhibitor, and any hydrogen atoms that were lacking were then added. The stable conformation was then provided by the optimization process, which was subsequently converted to PDBQT format for docking analysis.

3.1.3 Molecular docking

Molecular docking studies were performed using the default protocol in AutoDock Vina in PyRx software, The Scripps research Institute, USA. The active site of the enzymes was set into a grid box. The protein-ligand interactions were further analyzed using the Discovery Studio Visualizer (BIOVIA, San Diego, CA, USA).

3.1.4 Drug-likeness prediction

The structures of phytochemicals found in the *A. indicum* (**Table 1**) were obtained from PubChem database as SMILE files. SwissADME (<http://www.swissadme.ch/>) was used to evaluate drug-likeness according to the Lipinski's rule of five to predict their pharmacokinetic distinctive features such as the Absorption, Distribution, Metabolism, and Excretion (ADME).

3.1.5 Toxicity, carcinogenicity, and mutagenicity prediction

Using the canonical SMILE of the list of compounds in **Table 1**, their toxicity was further examined by Pro-Tox II software to predict their toxicity, including hepatotoxicity, carcinogenicity, immunotoxicity, mutagenicity, and cytotoxicity.

3.2 Plant Materials

The stems of *A. indicum* was collected from 13°59'03.2"N 100°14'04.4"E Bang Len, Nakhon Pathom in February 2020. A voucher specimen is deposited at the Department of Chemistry, Faculty of Science, Chulalongkorn University.

3.3 General Experimental Procedures

3.3.1 Thin-layer chromatography (TLC)

TLC analysis using Silicycle's aluminium sheet (Merck) coated with 0.2 mm silica gel 60 F₂₅₄, 20 x 20 cm was used to monitor the separation processes. The TLC reverse phase analysis was performed on Merck's aluminium sheets coated with silica gel 60 RP-18 F₂₅₄S. TLC was visualized under UV light at wavelength of 254 and 365 nm and by staining with *p*-anisaldehyde and ammonium molybdate ((NH₄)₆MO₇O₂₄) in 5% H₂SO₄/EtOH followed by heating on a hot plate for 1-2 mins at 105-120°C.

3.3.2 Column chromatography

Column chromatography (CC) was performed using Silica gel 60H (Merck code No. 7734 and No. 9385) as packing materials. Reverse-phase C18 (RP-18)

chromatography was performed using Silica gel C-18 (Wako code No. 237-01555) as packing materials. Size exclusion chromatography was performed by Sephadex LH-20 (Pharmacia Code No. 17-0090-01) to separate metabolites according to their molecular weight.

3.3.3 Nuclear magnetic resonance spectroscopy (NMR)

The NMR spectra were recorded on a JEOL (500 MHz for ^1H -NMR, 125 MHz for ^{13}C -NMR) using tetramethylsilane (TMS) as an internal standard. The chemical shifts (δ) were reported in parts per million (ppm) and the coupling constants (J) in Hertz (Hz). Mestrelab Research – MestReNova NMR software version 14.1.1-24571 was used to analyze the spectral data. Chloroform- d (CDCl_3), methanol- d_4 , and deuterium oxide (D_2O) were used in NMR experiments and chemical shifts were referenced to the signals of the residual solvent [for CDCl_3 at δ_{H} 7.26 ppm, δ_{C} 77.17 ppm; for CD_3OD at δ_{H} 3.31 ppm, δ_{C} 49.00 ppm; for D_2O at δ_{H} 4.79 ppm].

3.3.4 Mass spectrometry (MS)

High-resolution electrospray ionization mass spectrometry (HRESIMS) spectra were recorded on a Bruker Model micrOTOF-Q II spectrometer, Micromass UK Limited.

3.3.5 Fourier transforms infrared spectrophotometry (FT-IR)

FT-IR spectra were recorded on a Perkin-Elmer Model 1760X Fourier Transform Infrared Spectrophotometer. Solid samples were formally examined by incorporating the sample with potassium bromide (KBr) to form a pellet.

3.3.6 Ultraviolet-visible spectrophotometry (UV-Vis)

The UV data were recorded on a CARY 50 Probe UV-visible spectrophotometer.

3.3.7 High-performance liquid chromatography (HPLC)

Semi-preparative HPLC was carried out on a Thermo Finnigan SpectraSYSTEM HPLC with a Thermo Scientific Hypersil ODS (C18) column (250 mm x 10 mm I.D., 5 μ m) and UV detection at 220, 254, and 280 nm.

3.3.8 Microplate spectrophotometer

UV data of chromogenic methods were obtained from PowerWave XS2 (Biotek Instruments Inc, USA) microplate reader.

3.4 Chemicals

All commercial-grade solvents used in the present study, such as methanol (MeOH), acetone, ethyl acetate (EtOAc), dichloromethane (DCM), and *n*-hexane, were distilled prior to use. The reagent grade (AR) and HPLC grade solvents were purchased from Sigma-Aldrich, Burdick & Jackson, and Merck® (Germany) used for thin layer chromatography, crystallization and HPLC experiments.

3.5 *In vitro* α -Glucosidase inhibition assay

The α -glucosidase inhibition assay was determined as described by Srisurichan *et al.* (Figure 5) with slight modification [31]. Briefly, 10 μ L of the serially diluted test compound in DMSO (prepared concentration of 50 μ g/mL, 100 μ g/mL, and 200 μ g/mL) was transferred to each well of 96-well microplate. Then, 30 μ L of 0.1 M phosphate buffer (pH 6.8) and 10 μ L of α -glucosidase solution (1U/mL in 0.1 M phosphate buffer) were added and pre-incubated at 37°C for 15 min. The enzyme reaction was initiated by adding 50 μ L of *p*-nitrophenyl α -D-glucopyranoside (*p*-NPG) (1 mM in 0.1 phosphate buffer). After incubation at 37°C for 20 min, 100 μ L of Na₂CO₃ was added to stop the reaction. The α -glucosidase activity was determined by measuring the amount of *p*-nitrophenol released from *p*-NPG at 400 nm. The percentage inhibition is calculated using the following equation:

$$\% \text{ inhibition} = \left(1 - \frac{\text{Absorbance of the test well}}{\text{Absorbance of the untreated (control)}} \right) \times 100$$

The IC_{50} value is determined from a plot of percentage inhibition versus sample concentration.

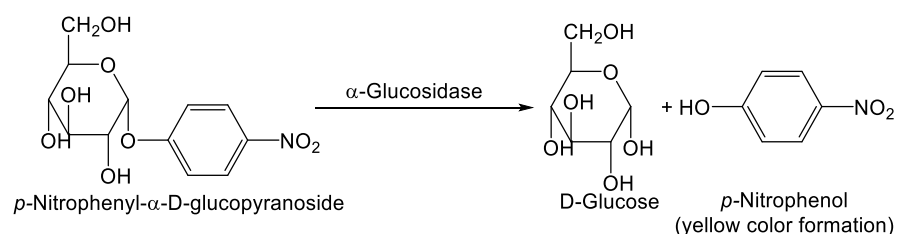
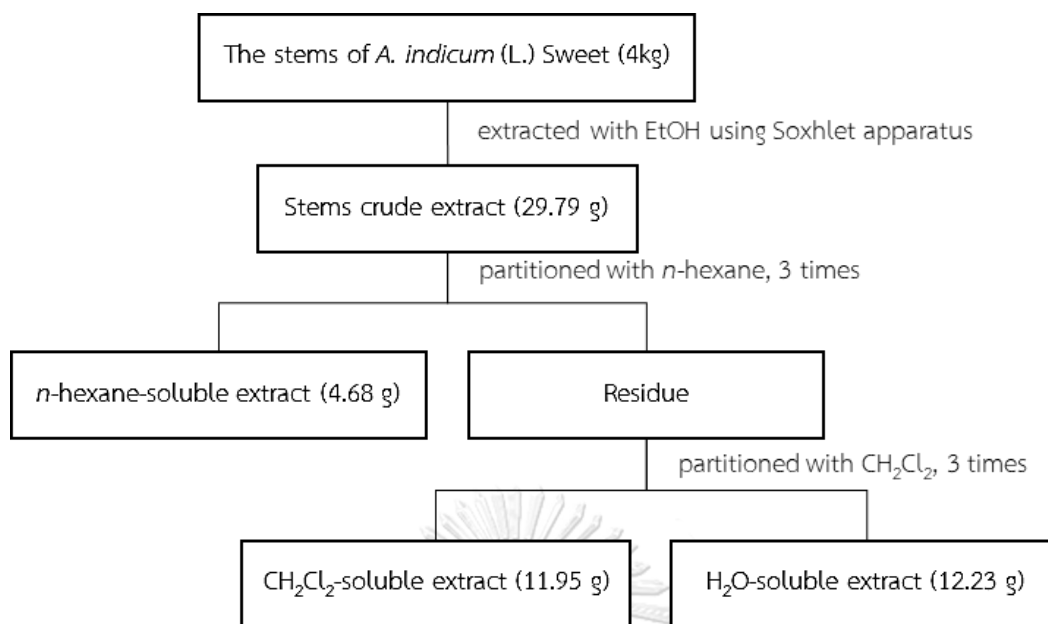


Figure 5 Mechanism of hydrolysis of *p*-nitrophenyl α -D-glucopyranoside (*p*-NPG) by α -glucosidase [158]

3.6 Extraction and isolation

3.6.1 Extraction of stems

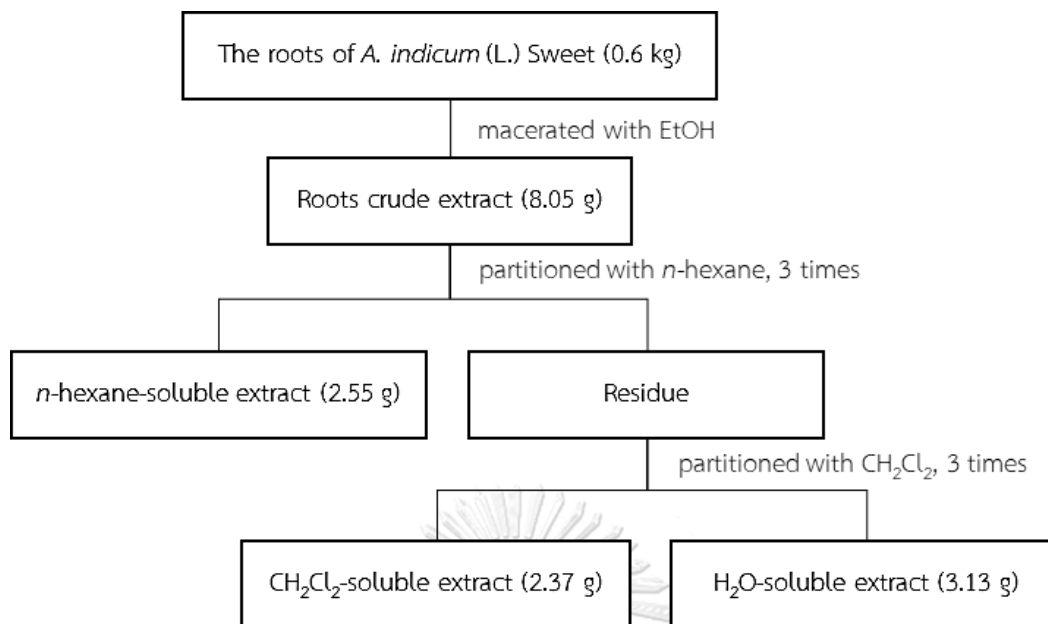
The fresh stems of *A. indicum* (6.5 kg) were cut into small pieces. The cut fresh stems were then dried in oven at 60°C and grounded. The ground plant (4.0 kg) was extracted using Soxhlet apparatus with ethanol (2.5 L) and concentrated under reduced pressure. The entire stems crude extract (29.79 g) was suspended in H₂O (250 mL) and then extracted successively with *n*-hexane (1 L x 3) and CH₂Cl₂ (1 L x 3) to give the *n*-hexane-soluble extract (4.68 g), CH₂Cl₂-soluble extract (11.95 g), methanol-soluble extract and H₂O-soluble extract (12.23 g), respectively. The extraction procedure is shown in **Scheme 1**.



Scheme 1 Extraction of *A. indicum* (L.) Sweet stems

3.6.2 Extraction of roots

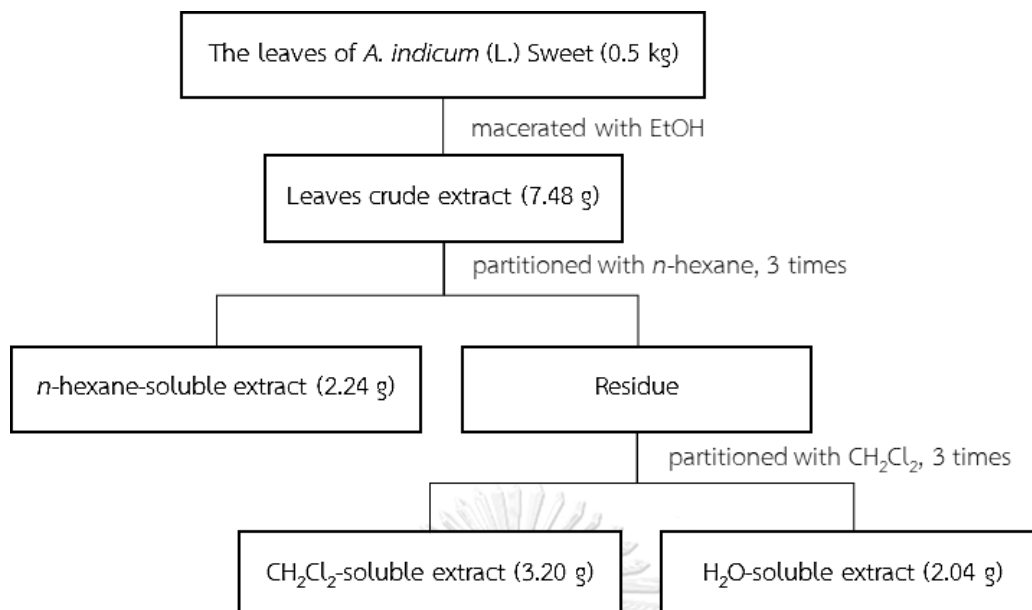
The roots of *A. indicum* were cleaned from any adhering soil and were cut into small pieces (1.5 kg). The cut roots were then dried in oven at 60°C and grounded. The ground plant (0.6 kg) was extracted by maceration with ethanol (2.5 L) and concentrated under reduced pressure. The stems crude extract (8.05 g) was suspended in H₂O (250 mL) and then extracted successively with *n*-hexane (1 L x 3) and CH₂Cl₂ (1 L x 3) to give the *n*-hexane-soluble extract (2.55 g), CH₂Cl₂-soluble extract (2.37 g), methanol-soluble extract and H₂O-soluble extract (3.13 g), respectively. The extraction procedure is shown in **Scheme 2**.



Scheme 2 Extraction of *A. indicum* (L.) Sweet roots

3.6.3 Extraction of leaves

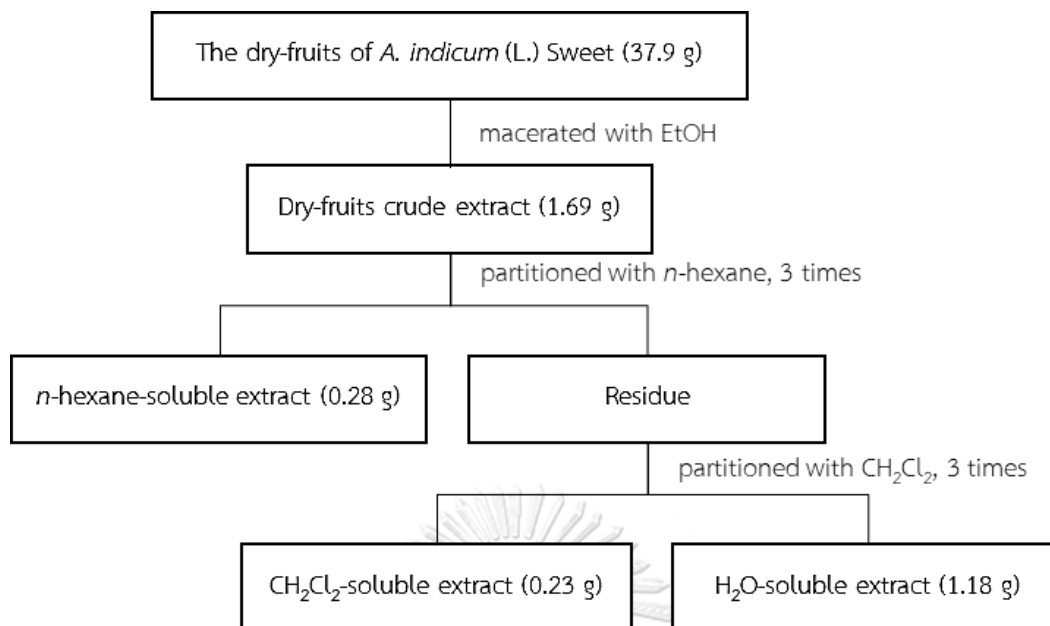
The leaves of *A. indicum* (1.1 kg) were dried in oven at 60°C and grounded. The ground plant (0.5 kg) was extracted by maceration with ethanol (2.5 L) and concentrated under reduced pressure. The leaves crude extract (7.48 g) was suspended in H₂O (250 mL) and then extracted successively with *n*-hexane (1 L x 3) and CH₂Cl₂ (1 L x 3) to give the *n*-hexane-soluble extract (2.24 g), CH₂Cl₂-soluble extract (3.20 g), methanol-soluble extract and H₂O-soluble extract (2.04 g), respectively. The extraction procedure is shown in **Scheme 3**.



Scheme 3 Extraction of *A. indicum* (L.) Sweet leaves

3.6.4 Extraction of dry-fruits

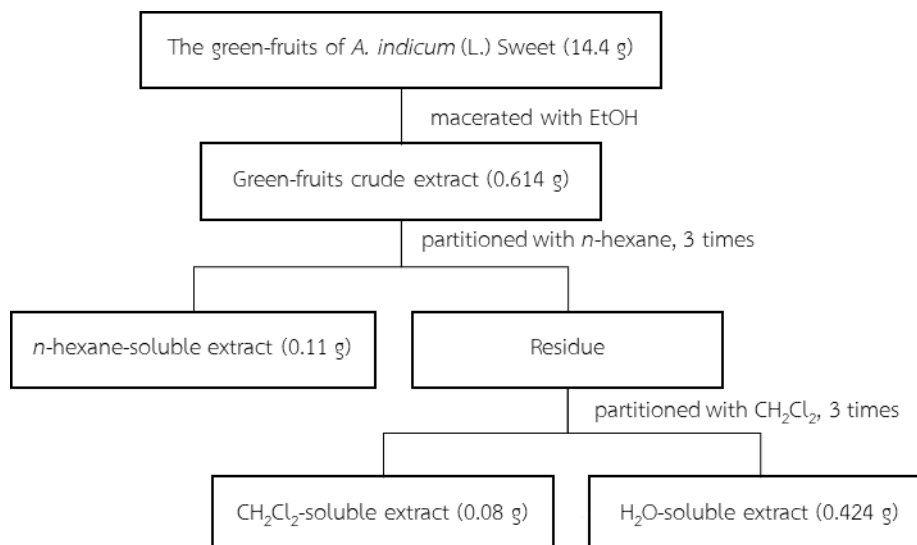
The dry-fruits of *A. indicum* (42.3 g) were dried in oven at 60°C and grounded. The ground plant (37.9 g) was extracted by maceration with ethanol and concentrated under reduced pressure. The dry-fruits crude extract (1.69 g) was suspended in H₂O and then extracted successively with *n*-hexane (3 times) and CH₂Cl₂ (3 times) to give the *n*-hexane-soluble extract (0.28 g), CH₂Cl₂-soluble extract (0.23 g), methanol-soluble extract and H₂O-soluble extract (1.18 g), respectively. The extraction procedure is shown in **Scheme 4**.



Scheme 4 Extraction of *A. indicum* (L.) Sweet leaves

3.6.5 Extraction of green-fruits

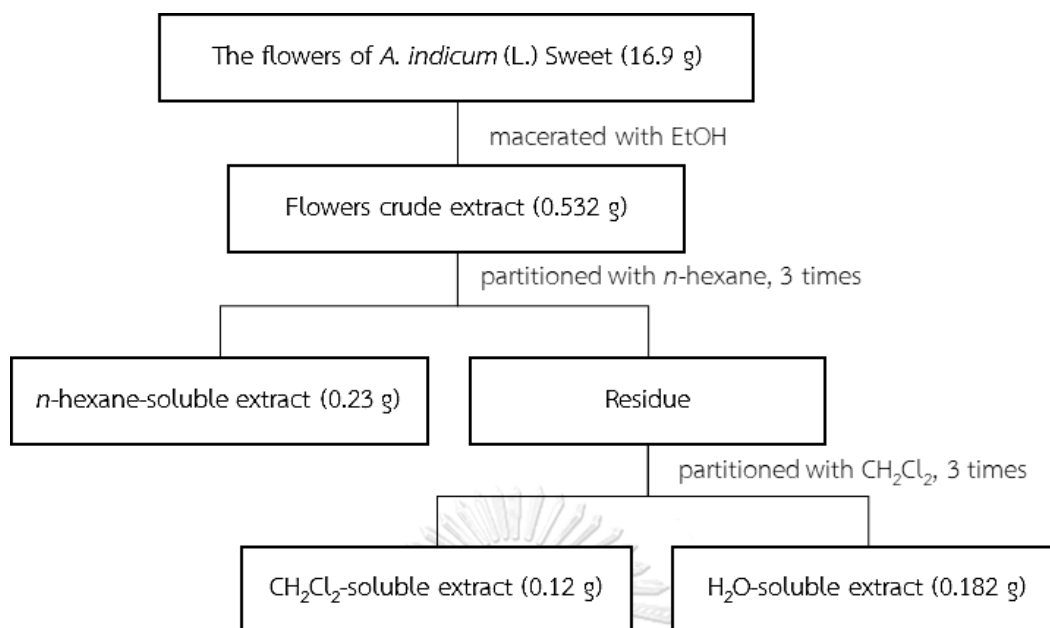
The green-fruits of *A. indicum* (30.4 g) were dried in oven at 60°C and grounded. The ground green-fruits (14.4 g) were extracted by maceration with ethanol and concentrated under reduced pressure. The green-fruits crude extract (0.614 g) was suspended in H₂O and then extracted successively with *n*-hexane (3 times) and CH₂Cl₂ (3 times) to give the *n*-hexane-soluble extract (0.11 g), CH₂Cl₂-soluble extract (0.08 g), methanol-soluble extract and H₂O-soluble extract (0.424 g), respectively. The extraction procedure is shown in **Scheme 5**.



Scheme 5 Extraction of *A. indicum* (L.) Sweet green-fruits

3.6.6 Extraction of flowers

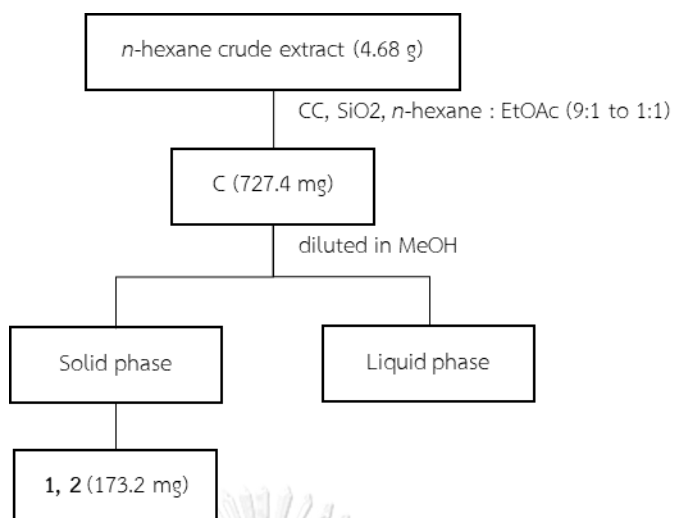
The roots of *A. indicum* were cleaned from any adhering soil and were cut into small pieces (38.0 g). The cut roots were then dried in oven at 60°C and grounded. The ground plant (16.9 g) was extracted by maceration with ethanol and concentrated under reduced pressure. The stems crude extract (0.532 g) was suspended in H₂O and then extracted successively with *n*-hexane (3 times) and CH₂Cl₂ (3 times) to give the *n*-hexane-soluble extract (0.23 g), CH₂Cl₂-soluble extract (0.12 g), methanol-soluble extract and H₂O-soluble extract (0.182 g), respectively. The extraction procedure is shown in **Scheme 6**.



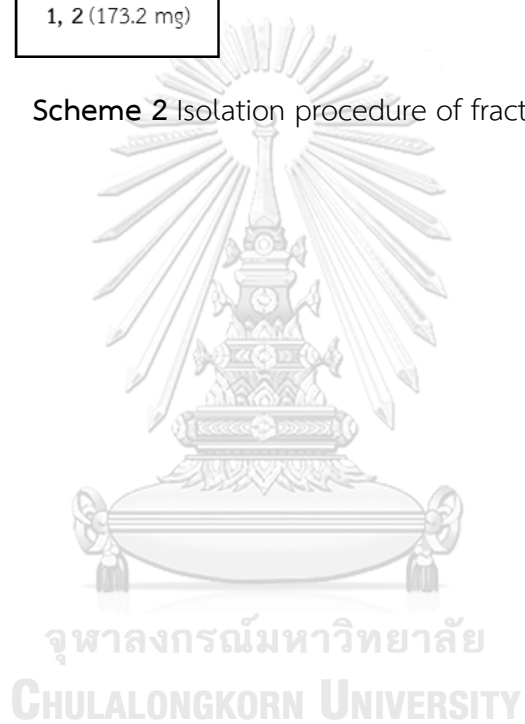
Scheme 6 Extraction of *A. indicum* (L.) Sweet green-fruits

3.6.7 Isolation of metabolite from *n*-hexane-soluble stems extract

The *n*-hexane-soluble extract was chromatographed to CC over silica gel 60 with gradient *n*-hexane : EtOAc (9:1 to 1:1) to give twelve fractions, A-L. Fraction C (727.4 mg) was diluted in methanol and formed a solid and liquid phases. The solid phase was washed with methanol to afford mixture of metabolite **1**, **2**, and **3** (93.3 mg). The isolation procedure is shown in **Scheme 2**.



Scheme 2 Isolation procedure of fraction C



CHAPTER IV

RESULTS AND DISCUSSION

4.1 *In vitro* α -glucosidase inhibition assay

The use of *p*-NPG, a colorless, artificial substrate for α -glucosidase, allowed researchers to study the chemicals' inhibitory effects. As illustrated in **Figure 17**, the hydrolysis product, *p*-nitrophenol or *p*-NP, is formed (yellow color) by adding quenching solution to approach pH 10. The 4-nitrophenolate form has a maximum of absorbance at 405 nm [159].



Figure 6 The deprotonation of 4-nitrophenol to 4-nitrophenoxide happened after the addition of base

The α -glucosidase inhibition by the crude extract was studied on the basis of enzymatic hydrolysis of *p*-NPG. *p*-Nitrophenol (*p*-NP), a yellow color, was measured at 405 nm [159]. The mature-brown fruit deployed the lowest inhibition with 2.0% at 0.025 $\mu\text{g/mL}$. While, flower extract exhibited highest inhibition with 21% at 0.25 $\mu\text{g/mL}$. Ten out of eighteen crude extracts depicted low percent inhibition (**Table 10**).

The dichloromethane (DCM) soluble roots and mature-brown fruits were active with 10.2% at 25 $\mu\text{g/mL}$ and 2.0% at 0.025 $\mu\text{g/mL}$, respectively, while the *n*-hexane and MeOH-soluble extracts of both plant parts were not active. The *n*-hexane and MeOH-soluble stem extracts were active with 11.0% at 25 $\mu\text{g/mL}$ and 8.0% at 0.25 $\mu\text{g/mL}$. The hexane, DCM, and MeOH-soluble leaves are active with 20.2% at 0.025 $\mu\text{g/mL}$; 20.0% at 0.025 $\mu\text{g/mL}$; and 14.6% at 2.5 $\mu\text{g/mL}$, respectively. The inhibition of the leaves might be caused by the abundance of chemicals in leaves and demonstrated inhibitory activity against α -glucosidase. On the contrary,

the crude extract of young-green fruits did not show any inhibitory activity. This probably due to less active compounds contained in the young-green fruits. While, fully grown fruits of mature-brown fruits showed higher activity. The *n*-hexane, DCM, and MeOH-soluble flowers extracts are active with 17.8% at 0.25 $\mu\text{g/mL}$; 20.6% at 0.25 $\mu\text{g/mL}$; and 12.3% at 2.5 $\mu\text{g/mL}$, respectively.

Table 2 The percent inhibition of the crude extract of *A. indicum* against α -glucosidase enzyme

Part of the plant	Percentage of inhibition, concentration in $\mu\text{g/mL}$		
	<i>n</i> -hexane	DCM	MeOH ³
Roots	NA ¹	10.2%, 25	NA
Stems	11.0%, 25	NA	8.0%, 0.25
Leaves	20.2%, 0.025 ²	20.0%, 0.025 ²	14.6%, 2.5 ²
Mature-brown fruits	NA	2.0%, 0.025	NA
Young-green fruits	NA	NA	NA
Flowers	17.8%, 0.25	20.6%, 0.25	12.3%, 2.5

¹NA is not active.

²Maximum concentration of leaves extracts at 0.025 $\mu\text{g/mL}$ was used as higher concentration had very intense color which interfered the absorbance measurement.

³Methanol extracts were obtained from the aqueous extract which dissolved in 5% water in methanol to get rid of the salts

Based on the literature, the ethanolic root extract of *A. indicum* exhibited a dose-dependent on the percent inhibition against α -glucosidase ranged from 8.1-24.4%, meanwhile the half maximum inhibitory concentration (IC_{50}) of the acarbose was 207.13 $\mu\text{g/mL}$ [160]. The methanolic leaves extract of *A. indicum* has IC_{50} value of 137.61 $\mu\text{g/mL}$, while the acarbose exhibited an IC_{50} of 272.72 $\mu\text{g/mL}$ against the α -glucosidase [161]. Phytochemical evaluation of the entire plant extract indicated the presence of alkaloids, flavonoids, and tannins in *A. indicum*, despite the fact that

the key components with antidiabetic action were not specifically identified in this study. Other studies revealed that *A. indicum* have contents of saponins and glycosides [11]. Glycosides, alkaloids, and flavonoids have been discovered in most of the plants demonstrated anti-diabetic effects [162]. Saponins and alkaloids have also been shown to impede glucose absorption, whereas flavonoids have been found to protect diverse cell types from oxidative stress-induced cell damage [163]. Glycosides have also been shown to enhance insulin secretion [25]. Glycosides are composed of sugars that structurally resemble carbohydrates and are thus likely substrate for the enzyme α -glucosidase [164]. Due to the active chemical components in the crude not having undergone further separation, they inhibited α -glucosidase at considerably lower levels than acarbose [165].

According to literature, quercetin (**9**) [30, 56, 58], β -amyrin (**42**) [56], lupeol (**45**) [56], and scopoletin (**49**) [27] which isolated from *A. indicum* showed activity against the α -glucosidase IC_{50} of 15.9 ± 1.2 ; 7.4 ± 1.34 ; 8.69 ± 2.10 ; and $52.76 \pm 1.96 \mu\text{M}$, respectively [166] and much higher than acarbose [167]. There are slightly different on the IC_{50} of **42** and **45**, indicating that removing the double bond at C-12 enhance the activity. Furthermore, at the ring E, 5-membered-ring with isopropenyl (**45**) exhibits higher activity than a 6-membered-ring with 2 methyl (**42**). Besides, extract has some intriguing action but not as powerful as a known positive control. Because a plant extract is a complex combination, it is unexpected that it has low bioactivity. Assuming that the unknown, relevant molecules exist but are present in low concentrations, fractionation can be used to increase the relative quantities of those key components in the hopes of observing better bioactivity [53]. The low activity or even inactivity of the crude extracts due to the loss of compound activity during the extraction process and storage period.

Only few reports on the stems were made, despite the fact that several studies on the phytochemical, pharmacological, and isolation work on *A. indicum* have been published. Metabolites in stem sections are significantly impacted by

changes in nutritional components resulting from various geographic factors. In order to find novel pharmacological prospects, this thesis focused on the stems of *A. indicum* (L.) Sweet.

4.2 *In silico* approach (α -glucosidase, pancreatic lipase and α -chymotrypsin inhibition assay)

4.2.1 *In silico* study of phytochemicals of *A. indicum* as α -glucosidase inhibitors

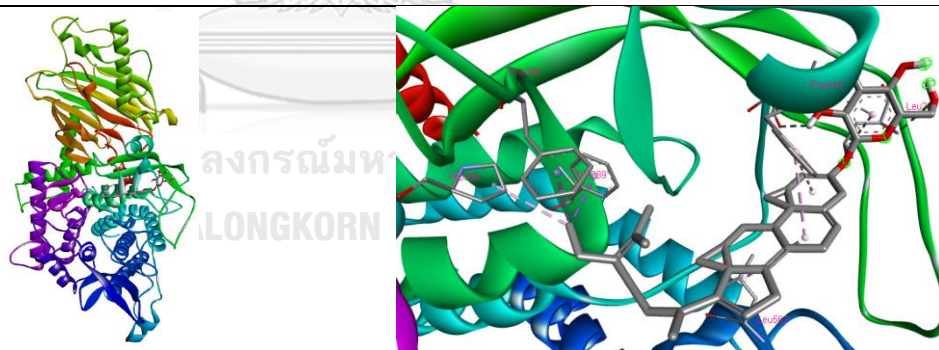
The crystal structure of α -glucosidase I (PDB ID: 4J5T) was obtained from RCSB Protein Data Bank [168]. The protein was prepared for docking studies by removing water molecules and the native ligand to provide the stable conformation. Chain A is the proposed active site pocket, and the ligands docked make polar contacts with the amino acid residues Trp391, Asp392, Arg428, Gly566, Asp568, Trp710, and Glu771 [168]. The calculated binding energy presented in the **Table 2** below.

Table 3 Calculated free binding energy (kcal/mol) of the phytochemicals (**1-66**) from *A. indicum* against processing α -glucosidase I (PDB code: 4J5T)

Phyto-chemical	Binding energy (kcal/mol)	Phyto-chemical	Binding energy (kcal/mol)	Phyto-chemical	Binding energy (kcal/mol)
1	-8.3	23	-8.3	45	-8.6
2	-9.9	24	-5.5	46	-6.6
3	-7.5	25	-4.9	47	-5.5
4	-7.9	26	-5.3	48	-6.0
5	-7.7	27	-5.9	49	-6.0

Phyto-chemical	Binding energy (kcal/mol)	Phyto-chemical	Binding energy (kcal/mol)	Phyto-chemical	Binding energy (kcal/mol)
6	-8.1	28	-5.8	50	-6.7
7	-7.9	29	-6.3	51	-9.2
8	-8.9	30	-6.9	52	-8.1
9	-7.9	31	-5.4	53	-8.2
10	-8.9	32	-7.5	54	-7.2
11	-10.2	33	-7.6	55	-7.0
12	-9.4	34	-5.9	56	-7.0
13	-8.8	35	-6.4	57	-6.7
14	-7.9	36	-6.2	58	-7.5
15	-9.1	37	-5.7	59	-7.6
16	-7.4	38	-5.3	60	-8.3
17	-9.1	39	-5.5	61	-6.5
18	-9.2	40	-6.7	62	-6.9
19	-9.9	41	-5.0	63	-8.1
20	-5.6	42	-7.8	64	-6.8
21	-5.5	43	-9.5	65	-5.9
22	-5.9	44	-8.7	66	-5.6
Acarbose	-8.5				

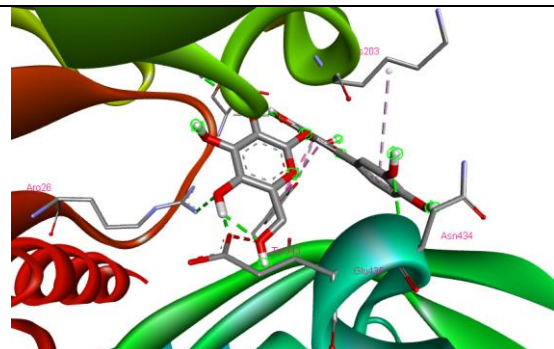
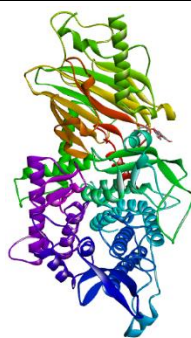
Fourteen phytochemicals (2, 8, 10, 11, 12, 13, 15, 17, 18, 19, 43, 44, 45, and 51) exhibited better binding score than the commercially available drugs for controlling hyperglycemia, acarbose (-8.5 kcal/mol). Phytochemical 2, 44, and 51 from whole plant, phytochemical 8 and 45 from the aerial part of the plant, Phytochemical 11, 12, 13, 18, 19 from flowers, phytochemical 43 from leaves, and phytochemical 10, 15, and 17 from flowers and leaves. Most of the phytochemicals exhibited better binding energy than acarbose attach to glycoside. The fact that a sugar moiety may bind to the enzyme's carbohydrate binding site and resemble the structure of disaccharides or oligosaccharides demonstrated that the inclusion of sugar moiety appeared to be essential for constructing α -glucosidase [169]. These medications structural similarity to carbs facilitates their attachment to the α -glucosidase enzyme's binding site [170]. The 3D presentation of the phytochemicals from *A. indicum* (1-66) in the active site of α -glucosidase (PDB code: 4J5T) were shown in Figure 7. It demonstrated that the phytochemicals occupying the same site as acarbose.



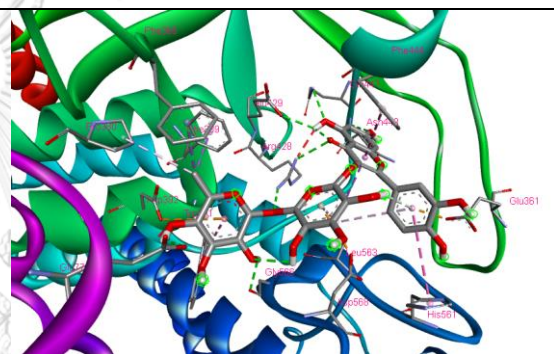
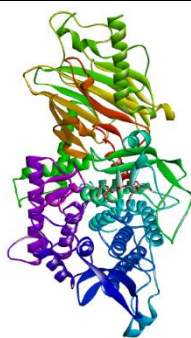
2



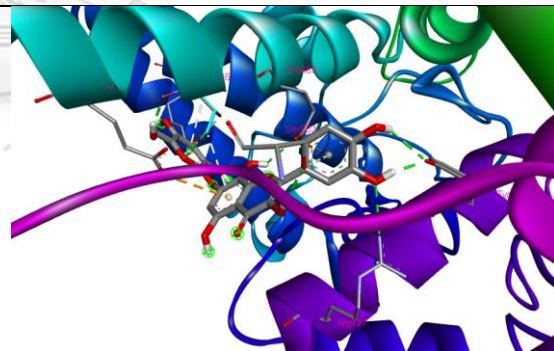
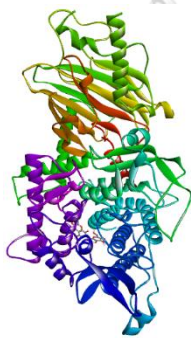
8



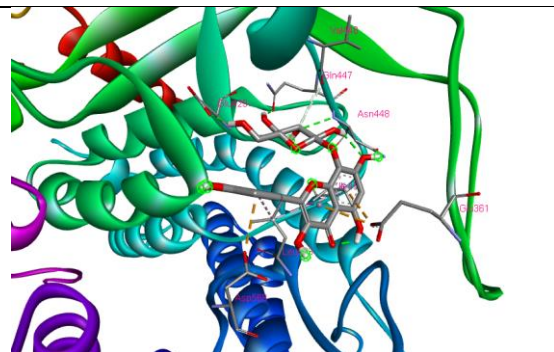
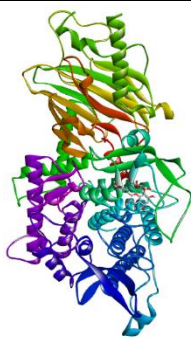
10



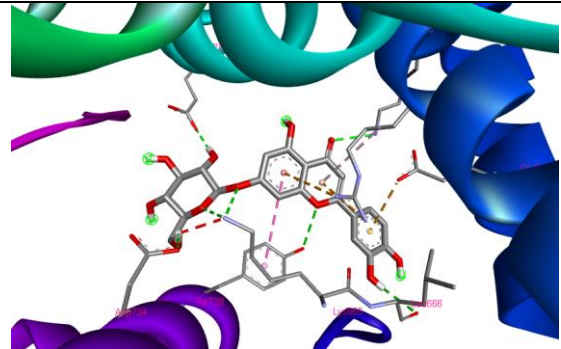
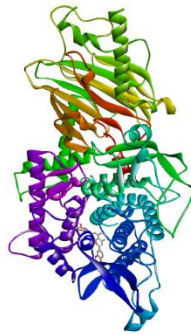
11



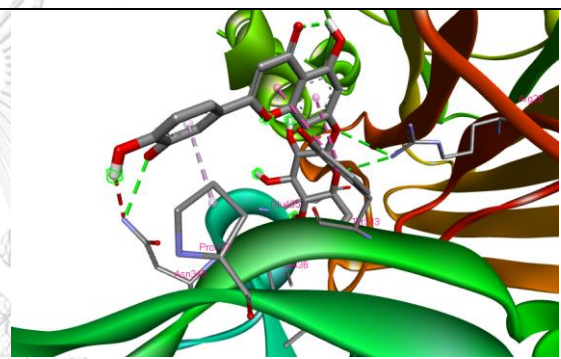
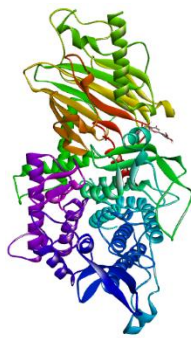
12



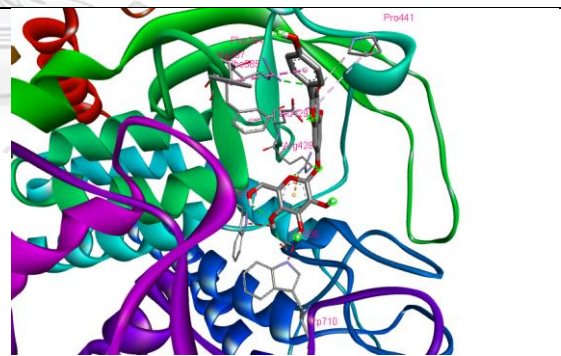
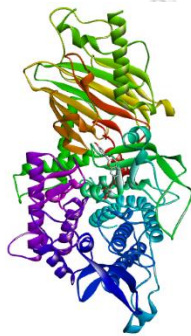
13



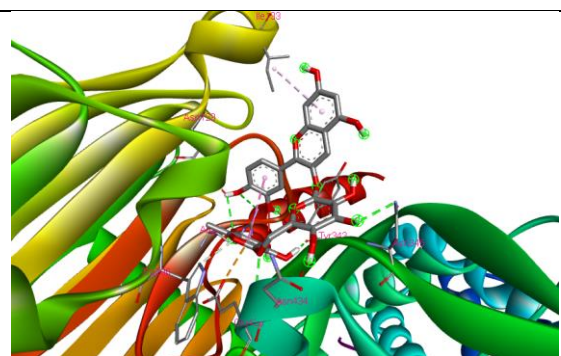
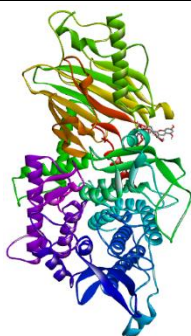
15



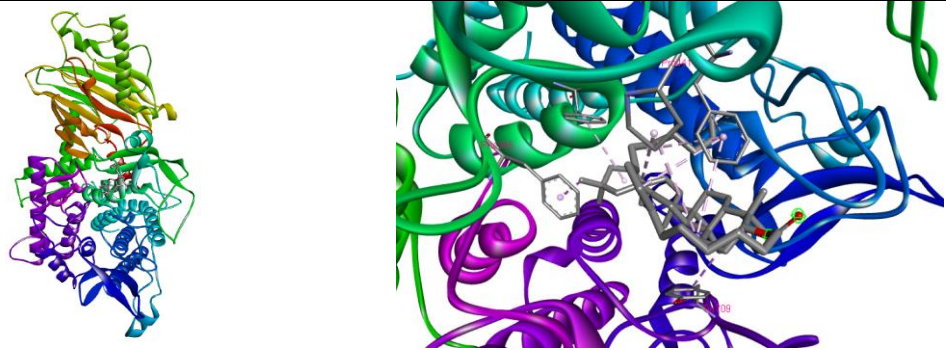
17



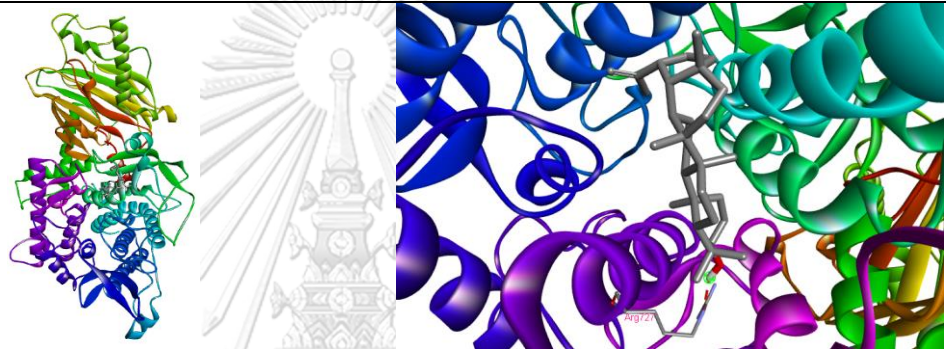
18



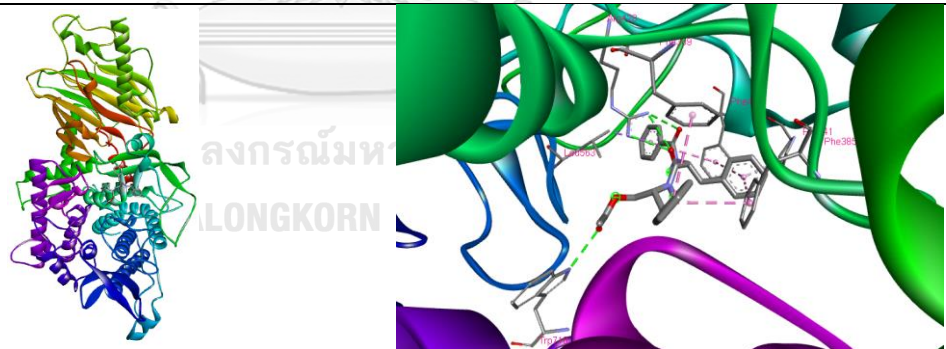
19



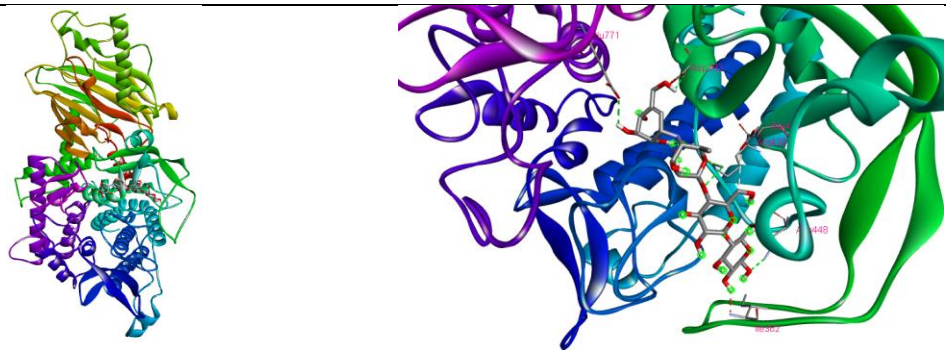
44



45



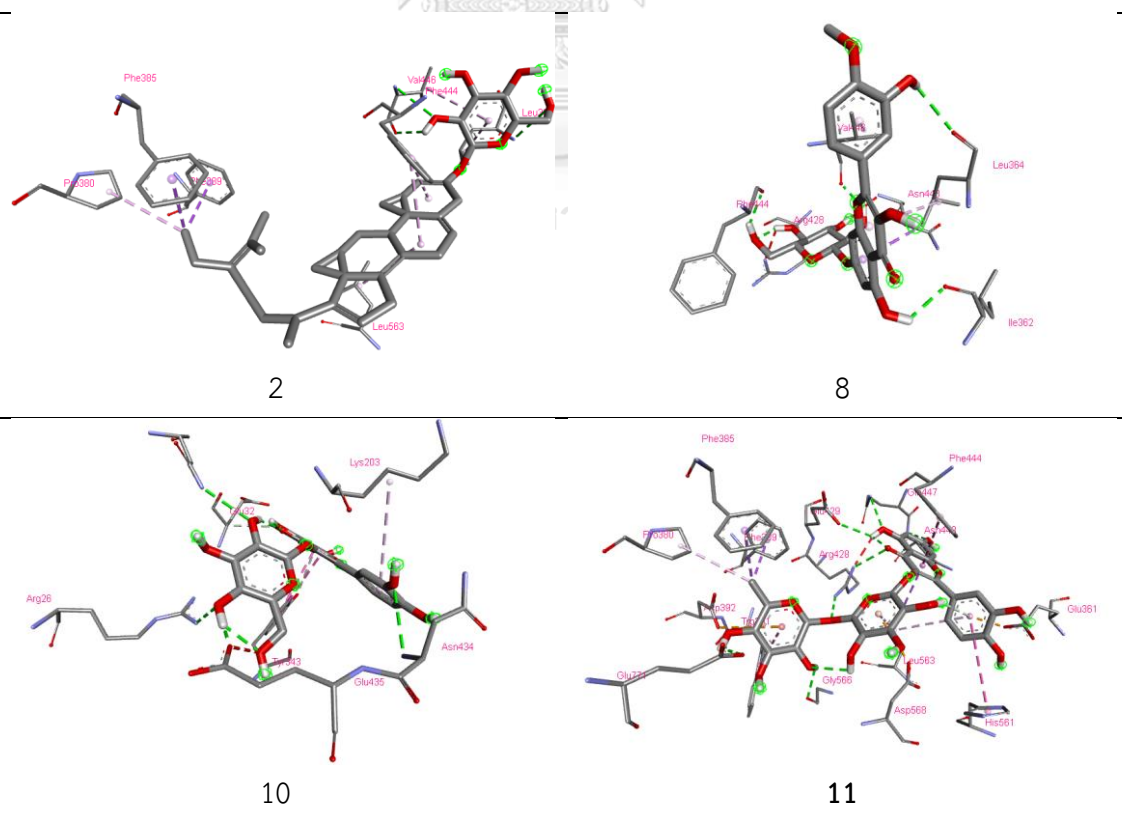
51

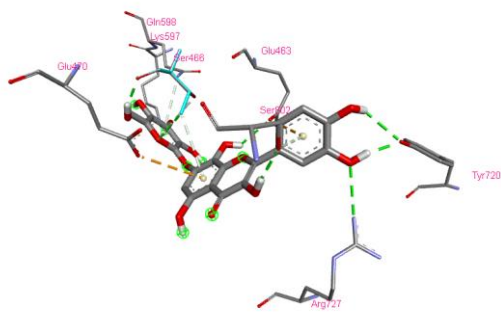


Acarbose

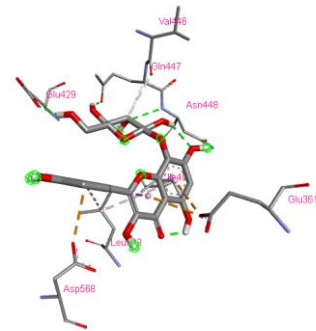
Figure 7 3D presentation of the phytochemicals from *A. indicum* in the active site of α -glucosidase (PDB code: 4J5T)

AGIs interact with a variety of enzyme residues, including Phe178, Phe303, His280, His351, Arg315, Arg442, and Tyr158 [171]. Acarbose is a pseudo-tetrasaccharide made up of a valienol moiety connected via nitrogen to isomaltotriose. Compared to natural oligosaccharides, this compound has an affinity for α -glucosidases that is 104 to 105 times higher. It competitively inhibits this enzyme [172]. Due to hydrogen bond configuration between Asp568 and the hydrogen atom of the amine group, acarbose has a substantially greater binding affinity to the enzyme than the typical sugar substrates [173]. **Figure 8** below showed the 3D molecular amino interaction of the phytochemicals of *A. indicum* in the binding site of α -glucosidase (PDB code: 4J5T).

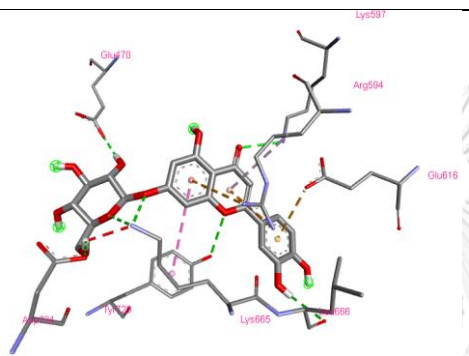




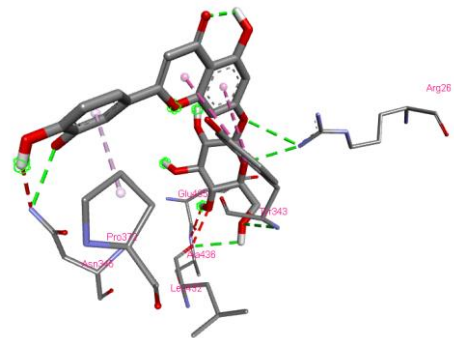
12



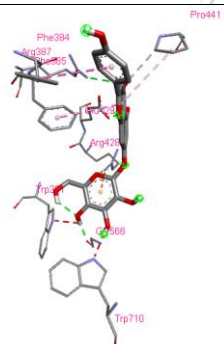
13



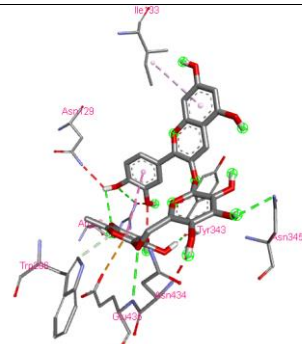
15



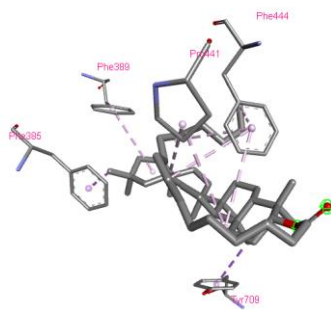
17



18



19



44



45

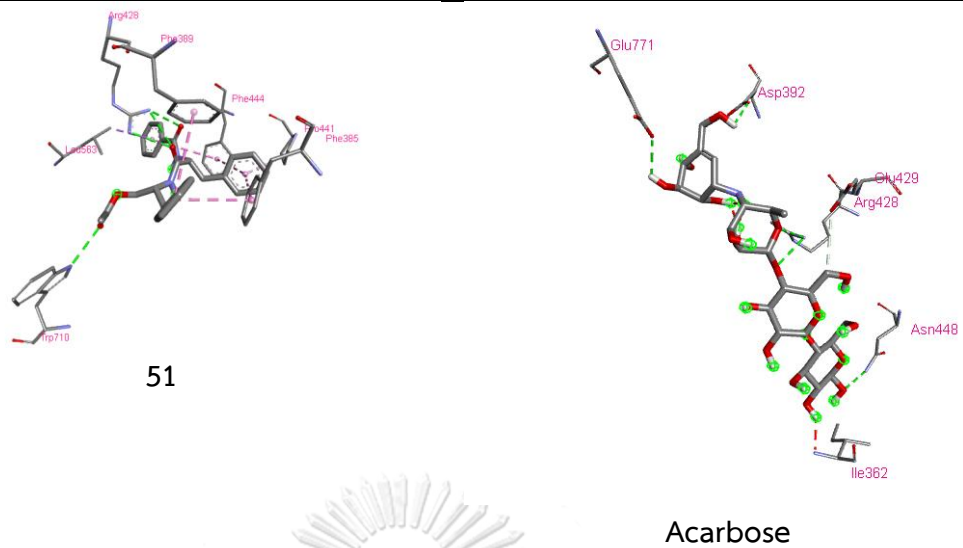
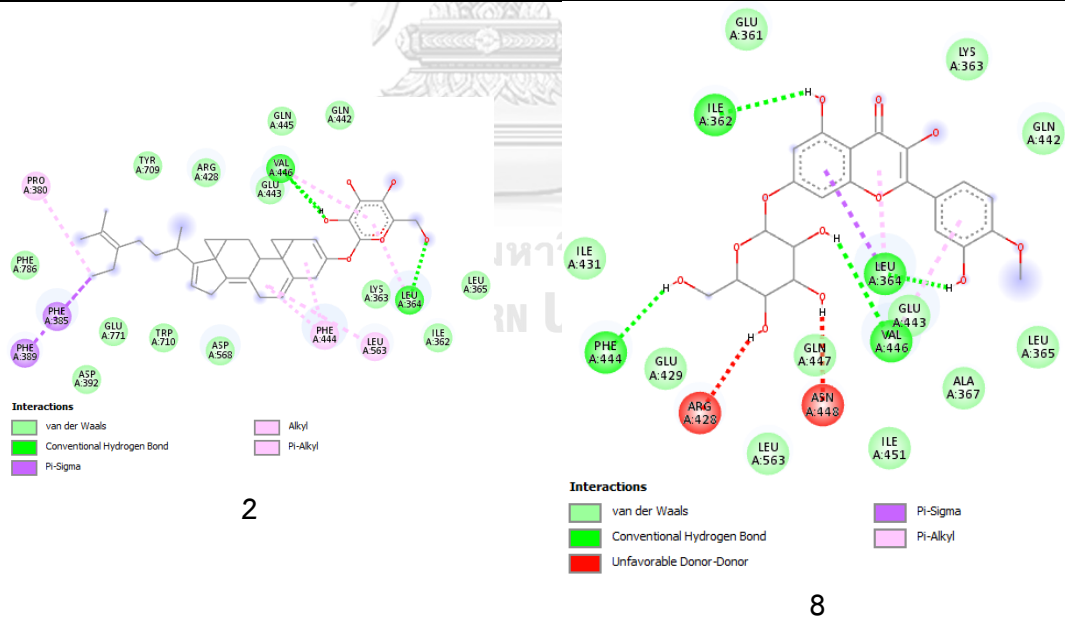
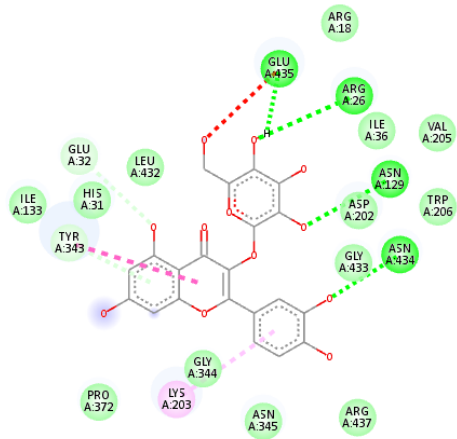


Figure 8 3D molecular amino interaction of the phytochemicals of *A. indicum* in the binding site of α -glucosidase (PDB code: 4J5T)

Figure 9 depicted the amino acids residual and its interaction types.

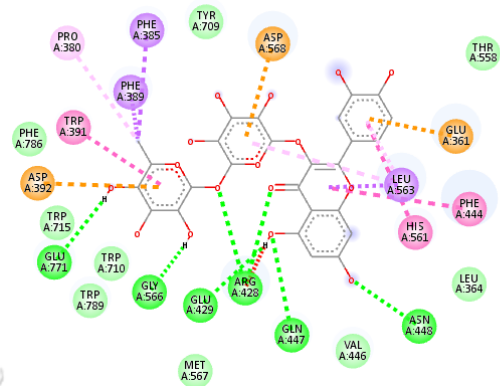




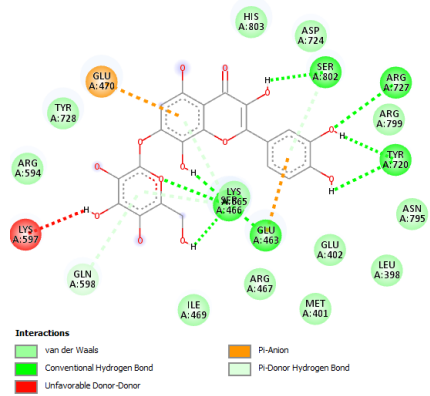
Interactions

- van der Waals
- Conventional Hydrogen Bond
- Carbon Hydrogen Bond
- Unfavorable Acceptor-Acceptor
- Pi-Donor Hydrogen Bond
- Pi-Pi T-shaped
- Pi-Alkyl

10



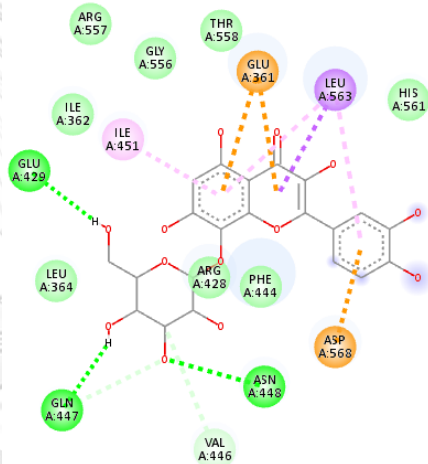
11



Interactions

- van der Waals
- Conventional Hydrogen Bond
- Carbon Hydrogen Bond
- Unfavorable Donor-Donor
- Pi-Anion
- Pi-Donor Hydrogen Bond

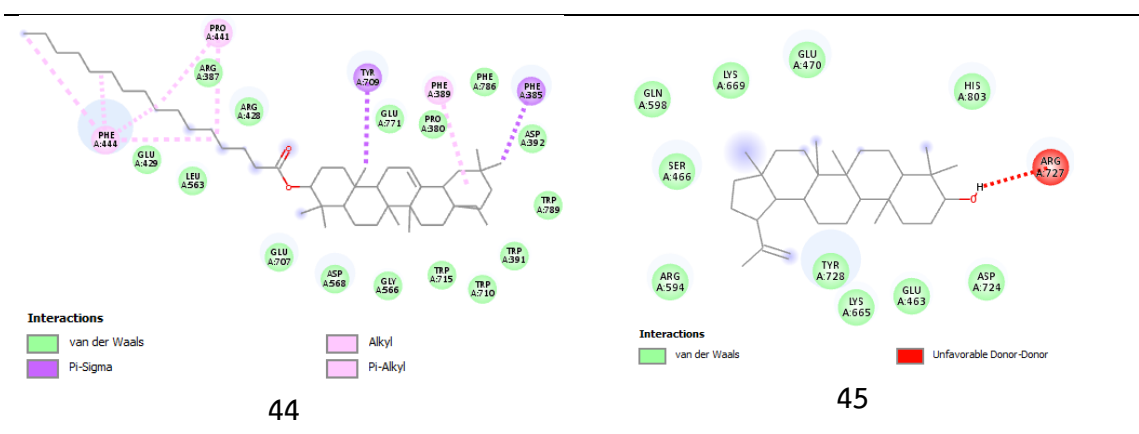
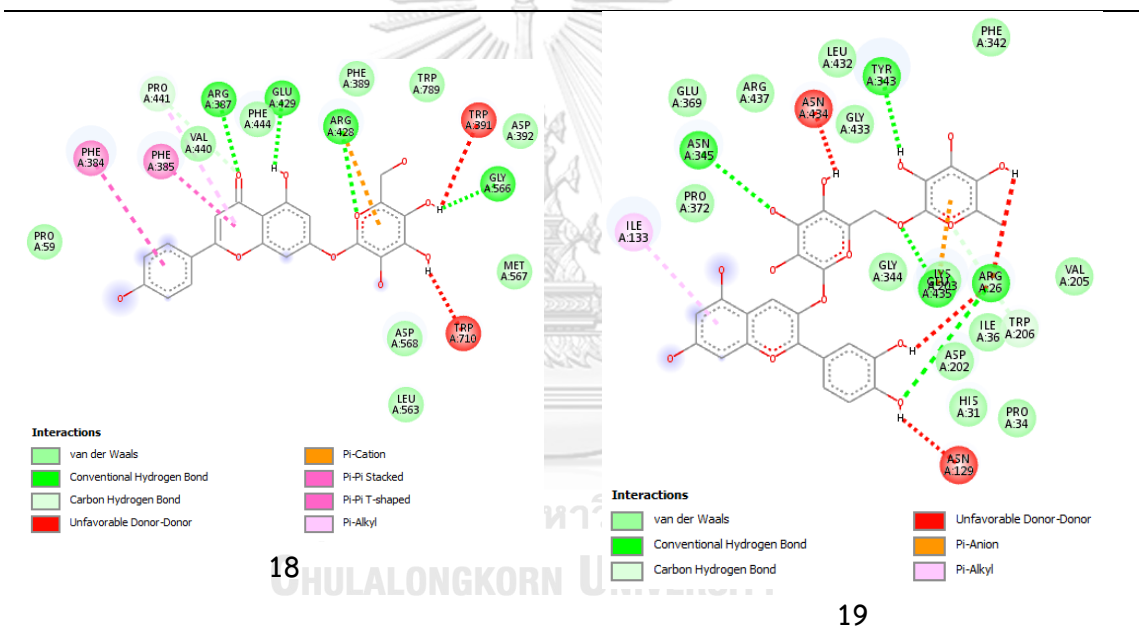
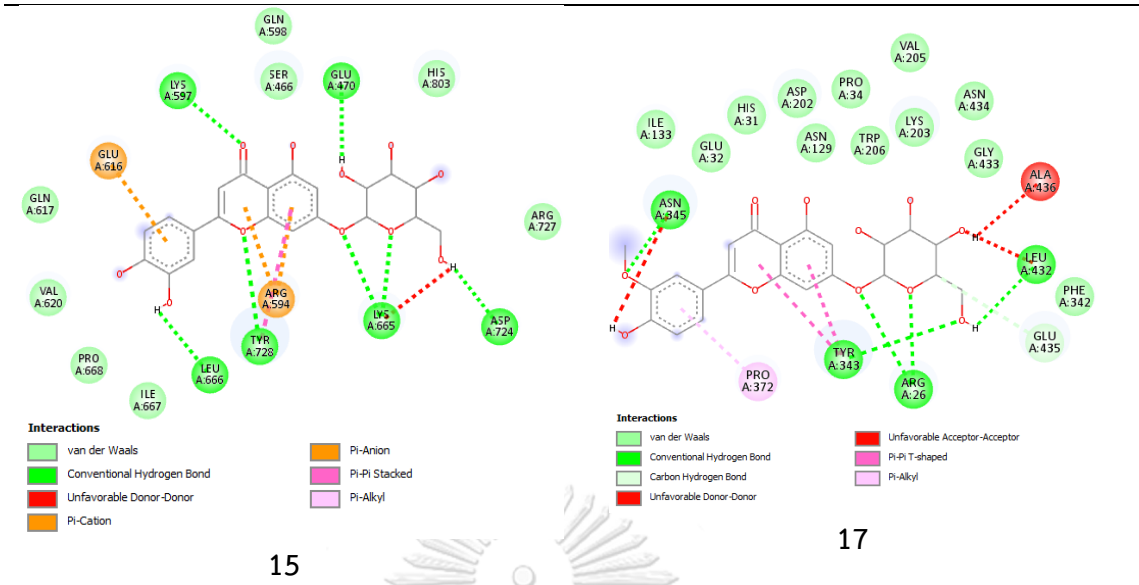
12 SHULALONGKORN UN



Interactions

- van der Waals
- Conventional Hydrogen Bond
- Carbon Hydrogen Bond
- Unfavorable Donor-Donor
- Pi-Anion
- Pi-Sigma
- Pi-Alkyl

13



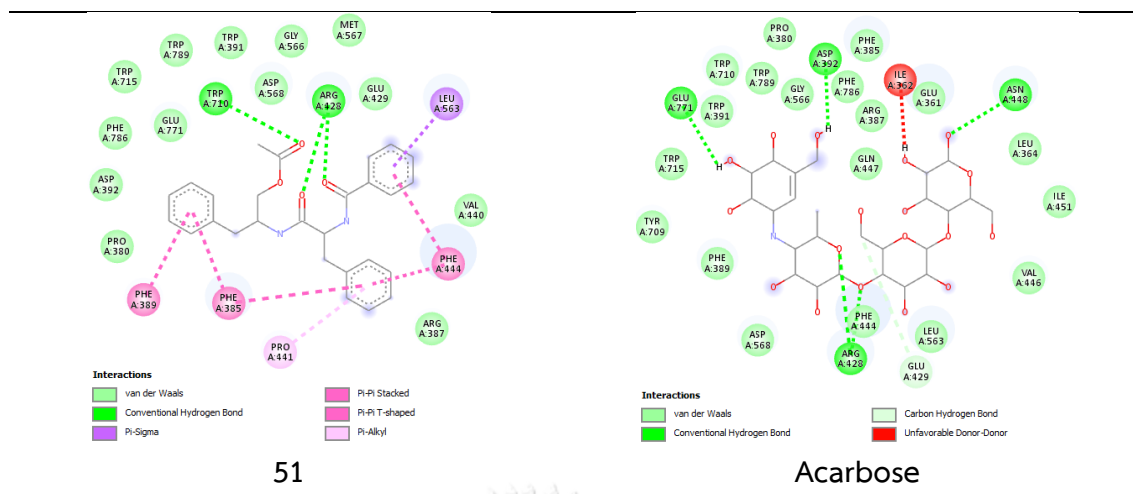


Figure 9 Amino acids residual interactions of the interacting pocket between α -glucosidase (PDB ID: 4J5T) and ligands

Table 3 below listed all the amino acids residue divided into 3 types of interaction (conventional hydrogen bond, hydrophobic/Pi-interaction, and Van der Waals force) with the active site of the α -glucosidase (PDB ID: 4J5T). The vital amino acid interaction between acarbose and the α -glucosidase (PDB ID: 4J5T) occurred between Asp392, Arg428, Asn448, and Glu771.

Table 4 The type of molecular interactions of the phytochemicals (1-66) within the active site of the α -glucosidase (PDB ID: 4J5T)

Comp.	Residual interactions		
	Conventional Hydrogen Bond	Hydrophobic/Pi-interaction	Van der Waals
1	-	Ile362, Phe444, Ile451, Leu563, Pro564	Glu361, Leu364, Glu443, Val446, Gln447, Asn448, Gly556, Thr558
2	Leu364, Val446	Leu364, Pro380, Phe385, Phe389, Phe444, Val446,	Ile362, Lys363, Leu365, Asp392, Arg428, Gln442, Glu443, Gln445, Asp568, Tyr709, Trp710, Glu771, Phe786

Comp.	Conventional Hydrogen Bond	Residual interactions	
		Hydrophobic/Pi- interaction	Van der Waals
		Leu563	
3	No interaction	-	-
4	-	Phe7, Asn500, Leu503	Phe0, Glu3, Tyr4, Lys6, Glu10, Asn496
5	-	Phe7	Phe0, Glu3, Tyr4, Ser11, Arg74, Lys98, Arg304, Met493, Asn496, Asn500, Leu503
6	-	Ile451, Leu563, Pro564	Glu361, Ile362, Lys363, Leu364, Leu365, Glu443, Phe444, Val446, Asn448, Gly556
7	Arg799, Ser802	Arg727, Tyr728, Ile734, Phe800, His803	Lys665, Asp724, Arg801
8	Ile362, Leu364, Phe444, Val446	Leu364, Arg428, Val446, Asn448	Glu361, Lys363, Leu365, Ala367, Glu429, Ile431, Gln442, Glu443, Gln447, Ile451, Leu563
9	Arg26, Glu32, Asp202	Asn129, Asp202, Lys203, Asn434	His31, Pro34, Ile36, Gly130, Ile133, Tyr343, Gly344, Asn345, Gly433, Glu435, Arg437
10	Arg26, Asn129, Asn434, Glu435	Glu32, Lys203, Tyr343, Glu435	Arg18, His31, Ile36, Ile133, Asp202, Val205, Trp206, Gly344, Asn345, Pro372, Leu432, Gly433, Arg437
11	Arg428, Glu429, Gln447, Asn448,	Glu361, Pro380, Phe385, Phe389,	Leu364, Val446, Thr558, Met567, Tyr709, Trp710, Trp715, Phe786,

Comp.	Conventional	Residual interactions	
	Hydrogen Bond	Hydrophobic/Pi- interaction	Van der Waals
	Gly566, Glu771	Trp391, Asp392, Arg428, Phe444, His561, Leu563, Asp568	Trp789
12	Glu463, Ser466, Tyr720, Arg727, Ser802	Ser466, Glu470, Lys597, Gln598, Ser802	Lys365, Leu398, Met401, Glu402, Arg467, Ile469, Arg594, Asp724, Tyr728, Asn795, Asp799, His803
13	Glu429, Gln447, Asn448	Glu361, Val446, Gln447, Ile451, Leu563, Asp568	Ile362, Leu364, Arg428, Phe444, Arg556, Arg557, Thr558, His561
14	Arg29, Glu32	Pro34, Asn129, Asp202, Lys203, Asn434	His31, Ile36, Gly130, Ile133, Gly344, Asn345, Gly433, Arg437
15	Glu470, Lys597, Lys665, Leu666, Asp724, Tyr728	Arg594, Glu616, Lys665, Tyr728	Ser466, Gln598, Gln617, Val620, Ile667, Pro668, Arg727, His803
16	-	Lys363, Leu364, Arg428, Val446, Ile451, Leu563	Glu361, Ile362, Glu443, Phe444, Asn448
17	Arg26, Tyr343, Asn345, Leu432, Ala436	Tyr343, Asn345, Pro372, Glu435, Ala436	His31, Glu32, Pro34, Asn129, Ile133, Asp202, Lys203, Val205, Trp206, Phe342, Gly433, Asn434
18	Arg387, Arg428,	Phe384, Phe385,	Pro59, Phe389, Asp392, Val440,

Comp.	Conventional	Residual interactions	
	Hydrogen Bond	Hydrophobic/Pi- interaction	Van der Waals
	Glu429, Gly566	Trp391, Pro441, Trp710	Phe444, Leu563, Met567, Asp568, Trp789
19	Arg26, Asn129, Tyr343, Asn345, Asn434, Glu435	Ile133, Trp206	His31, Pro34, Ile36, Asp202, Lys203, Val205, Phe342, Gly344, Glu369, Pro372, Leu432, Gly433, Arg437
20	Arg428, Gly566	Phe385, Phe389, Asp392, Glu771	Pro380, Trp391, Trp710, Trp715, Phe786, Trp789
21	Asp392, Trp710	Trp391	Arg428, Leu563, Gly566, Met567, Asp568, Asp569, Trp715, Glu771, Phe786, Trp789
22	Arg26, Asp202, Leu432, Asn434, Glu435	Asn129	His31, Pro34, Ile36, Lys203, Val205, Trp206, Tyr343, Gly344, Gly433, Ala436
23	Ser462, Ser477, Gln598, Glu616, Arg727	Asp724, Tyr728	Glu463, Glu470, Arg594, Lys597, Lys665, Lys669, Pro731, His803
24	Arg428	Trp391	Phe389, Asp392, Asn453, Leu563, Gly566, Asp568, Trp710, Trp715, Glu771, Phe786, Trp789
25	Gly566	Trp391, Asp392	Pro380, Phe385, Phe389, Arg428, Trp710, Trp715, Glu771, Phe786, Trp789

Comp.	Conventional	Residual interactions	
	Hydrogen Bond	Hydrophobic/Pi- interaction	Van der Waals
26	Arg26, Asp202, Asn434, Glu435	Pro34, Glu435	Ile36, Asn129, Lys203, Val205, Trp206, Gly433, Ala436
27	Arg26, Asn434, Glu435	Arg26, Ile36, Lys203, Val205, Tyr343, Glu435	Arg18, Pro34, Asn129, Asp202, Trp206, Gly433
28	Arg428	Phe385, Trp391, Trp710	Phe389, Asp392, Tyr709, Trp715, Glu771, Phe786, Trp789
29	Arg26	Arg18, Arg26, His31, Pro34, Val205, Trp206	Ile36, Asn129, Asp202, Lys203, Tyr343, Glu435
30	As20, Arg26, Tyr343, Pro386	Phe342, Glu435, Ala436	Arg18, Tyr341, Arg387, Leu432
31	Lys665, Arg727, Arg799, Ser802	Ser466, Arg727	Glu463, Asp724, Tyr728, His803
32	Asp392	Phe385, Asp568, Tyr709	Pro380, Phe389, Trp391, Arg428, Asn453, His561, Asp569, Leu563, Gly566, Glu707, Trp710, Trp715, Glu771, Phe786, Trp789
33	Arg26, His31, Glu32, Asn129, Asn345, Asn434	Ile36, Asp202, Lys203	Ser33, Pro34, Gly130, Ile133, Trp206, Tyr343, Gly344, Gly433, Glu435, Arg437
34	Gly566	Trp710, Glu771	Pro380, Phe385, Phe389, Trp391,

Comp.	Conventional		Residual interactions	
	Hydrogen Bond		Hydrophobic/Pi- interaction	Van der Waals
				Asp392, Met567, Asp568, Tyr709, Trp715, Phe786, Trp789
35	Asn448, Gly556	Ile362, Ile451		Thr360, Glu361, Leu364, Arg428, Val446, Gln447, Arg557, Thr558, Leu563
36	Arg26, Lys203, Asn434	Ile36, Asn129		Arg18, Pro34, Asp202, Val205, Trp206, Gly433, Glu435
37	Gly312, Lys324, Tyr748, Arg799	Gly312		Phe311, Glu313, Gly314, Pro315, Arg727, Ile734, Lys752, Ile796, Leu797
38	Arg26, Asn434	Lys203		Asp202, Trp206, Tyr343, Gly433, Glu435
39	Asn434, Gly435	Asn129		Arg26, His31, Glu32, Pro34, Asp202, Lys203, Trp206, Gly433
40	Glu361, Leu364	Leu364, Val446, Gly556		Ile362, Lys363, Leu365, Glu443, Phe444, Asn448, Ile451, Thr558, Leu563
41	Arg18, Arg26, Asn129, Asp202	Arg18		Pro34, Ile36, Lys203, Val205, Trp206, Glu435
42	-	Ile734		Gly312, Glu313, Arg727, Asp736, Tyr748, Lys752, Arg799, Phe800, Arg801, His803

Comp.	Conventional Hydrogen Bond	Residual interactions	
		Hydrophobic/Pi- interaction	Van der Waals
43	No interaction		
44	-	Phe385, Phe389, Pro441, Phe444, Tyr709	Pro380, Arg387, Trp391, Asp392, Arg428, Glu429, Leu563, Gly566, Asp568, Glu707, Trp710, Trp715, Glu771, Phe786, Trp789
45	-	Arg727	Glu463, Ser466, Glu470, Arg594, Gln598, Lys665, Lys669, Asp724, Tyr728, His803,
46	-	Leu347, Lys363, Ala367, Arg428, Val446, Ile451, Leu563	Glu361, Ile362, Leu364, Leu365, Glu443, Gln442, Phe444, Gln445, Gln447, Asn448,
47	Arg26, Trp206	Val205, Glu435	His31, Pro34, Ile36, Asn129, Asp202, Lys203, Tyr343, Gly433, Asn434
48	Tyr720	Met401, Glu402, Glu463, Ser466, Glu470, Ser802	Leu398, Arg467, Asp724, Arg727, Asn795, Arg799, His803
49	Asn9, Glu410	Tyr29, Ala413	Gln5, Arg28, Ser414, Glu417
50	Arg428, Trp710	Phe389, Trp391, Asp392	Pro380, Phe385, Leu563, Gly566, Met567, Asp568, Trp715, Glu771, Phe786, Trp789
51	Arg428, Trp710	Phe385, Phe389, Pro441, Phe444,	Pro380, Arg387, Trp391, Asp392, Glu429, Val440, Gly566, Met567,

Comp.	Conventional Hydrogen Bond	Residual interactions	
		Hydrophobic/Pi- interaction	Van der Waals
		Leu563	Asp568, Trp715, Glu771, Phe786, Trp789
52	Trp391	Asp568, Glu771	Pro380, Phe385, Phe389, Asp392, Arg428, Asn453, His561, Leu563, Gly566, Asp569, Glu707, Tyr709, Trp710, Trp715, Phe786, Trp789
53	Arg428, Val446	Leu364, Val446, Gln447, Ile451, Leu563	Glu361, Ile362, Lys363, Leu365, Gln442, Glu443, Phe444, Asn448, Gly556, Thr558
54	Asp568	Phe385, Asp392, Glu771	Pro380, Phe389, Trp391, Arg428, Leu563, Tyr709, Trp710, Trp715, Phe786, Trp789
55	Lys203, Asn434	Ile36, Val205, Glu435	Arg26, Asn129, Asp202, Trp206, Tyr343, Gly344, Gly433
56	Asp724, His803	Met401, Glu402, Glu463, Asp724, Ser802	Leu398, Arg467, Glu470, Tyr720, Arg727, Tyr728, Arg799
57	Phe444, Val446	Leu364, Val446	Glu361, Ile362, Lys363, Glu443, Gln447
58	Gly312	-	Phe311, Gly314, Pro315, Lys324, Ile734, Tyr748, Gly749, Lys752, Ile796, Ley797, Arg799, Phe800

Comp.	Conventional Hydrogen Bond	Residual interactions	
		Hydrophobic/Pi- interaction	Van der Waals
59	-	Phe389	Pro380, Phe385, Trp391, Asp392, Arg428, Tyr709, Trp710, Trp715, Glu771, Phe786, Trp789
60	Asn129, Asn434, Glu435	Lys203	His31, Glu32, Pro34, Ile133, Asp202, Trp206, Gly433
61	Arg428, Trp710	Pro380, Phe385, Phe389	Trp391, Asp392, Leu563, Asp568, Tyr709, Trp715, Glu771, Phe786, Trp789
62	-	Asp568	Pro380, Phe385, Phe389, Trp391, Asp392, Arg428, Gly566, Met567, Asp569, Trp710, Trp715, Glu771, Phe786, Trp789
63	Ser466, Arg727, Arg799	Lys665, Asp724, His803	Ser462, Glu463, Arg594, Gln598, Tyr720, Tyr728, Pro731, Ile734, Ser803
64	-	Arg26, Lys203, Asn345, Asn434	Ile36, Asn129, Asp202, Val205, Trp206, Gly344, Gly433, Glu435, Arg437
65	Tys343, Leu432	Arg18, Arg26, Phe342, Glu435, Ala436	Asn20, Tyr341, Gly433
66	Tyr709	Pro380, Phe385, Phe389, Pro441,	Phe384, Arg389, Trp391, Asp392, Arg428, Glu429, Val440, Leu563,

Comp.	Conventional Hydrogen Bond	Residual interactions	
		Hydrophobic/Pi- interaction	Van der Waals
		Phe444, Tyr709, Trp710, Trp715	Gly566, Asp568, Glu771, Phe786, Trp789
Acar- bose	Asp392, Arg428, Asn448, Glu771	Ile362, Glu429	Glu361, Leu364, Pro380, Phe382, Phe385, Arg387, Phe389, Trp391, Phe444, Val446, Gln447, Ile451, Leu563, Gly566, Asp568, Tyr709, Trp710, Trp715, Phe786, Trp789

Phytochemical **11** formed vital amino acid bonds with Arg428 (ketone, glycosidic bond, and hydroxyl group), Asn448 (hydroxyl group), Gly566 (hydroxyl group), and Glu771 (hydroxyl group). Phytochemical **13** formed a vital amino acid bond with Asn448 (glycosidic bond). Phytochemical **18** formed amino acid bonds with Arg428 (*O*-glucopyranose) and Gly566 (hydroxyl group). Lastly, phytochemical **51** formed vital amino acid with Arg428 (ketone) and Trp710 (hydroxyl group).

The binding energy values of the benzoic acid with one hydroxyl group (*p*-hydroxybenzoic acid (**20**)) on the benzene ring were less than the benzoic acid which has three hydroxyl groups (gallic acid (**30**)). This is likely because the addition of hydroxyl groups provides additional hydrogen binding opportunities to α -glucosidase that enhance their binding energy value. It appears that simple changes to the number of hydroxyl groups have different effects on the ability of the benzoic acids to bind to the α -glucosidase. Therefore, the effect of the hydroxyl groups on the binding ability of benzoic acid is likely to vary between the original structure and the hydroxylation position.

Although the number of methoxy groups on the benzene ring did not appear to have a significant effect on the inhibition of α -glucosidase, the methylation of hydroxyl groups resulted on decreased inhibitory activity of the benzoic acids. It may

reduce the polarity of the molecule, thereby enhances the ability to enter the hydrophobic cavity of the enzyme, it also reduces the number of hydrogen-bonding donors and acceptors that play a key role in the inhibition [174].

4.2.2 *In silico* study of phytochemicals of *A. indicum* as human pancreatic lipase (HPL) inhibitors

X-ray diffraction was used to ascertain the crystal structure of human pancreatic lipase (HPL) (PDB ID: 1LPB) [175]. Associated with colipase, HPL is a glycoprotein consisting of the N region (residues from 1 to 335) and the C region (residues from 336 to 449), [176-178]. The catalytic triad Ser152, Asp176, and His263 are located in the active site, which spans residues 247 to 258 in the N region. The disulfide bridge between residues Cys237 and Cys261 forms the surface loop that makes up the lid domain. The primary binding surface for colipase is found in the double ringed C region. Additionally, there are nine loops from amino acids 204-224 and two hair loop coils for amino acid 76 to 85 [177]. There are two states of HPL structure: closed state and open state. The lid domain opens the enzyme's catalytic site when it binds to the β 5-loop and β 9-loop coils through a van der Waals contact in the open state [175, 179]. Of the 66 phytochemicals from *A. indicum*, 42 phytochemicals have superior binding energy than orlistat, the drug is frequently prescribed to treat obesity, with -6.7 kcal/mol as listed in the **Table 4**.

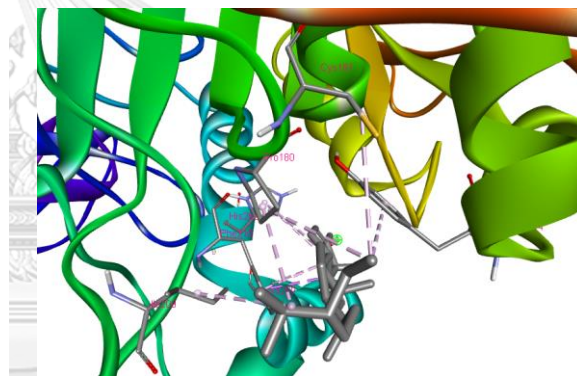
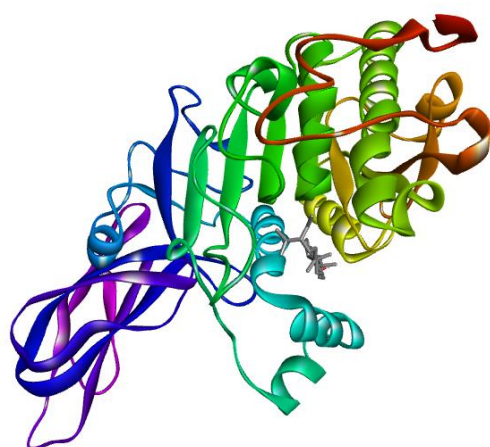
Table 5 Calculated free binding energy (kcal/mol) of the phytochemicals (1-66) from *A. indicum* against HPL (PDB ID: 1LPB)

Phyto-chemical	Binding energy (kcal/mol)	Phyto-chemical	Binding energy (kcal/mol)	Phyto-chemical	Binding energy (kcal/mol)
1	-9.1	23	-7.4	45	-7.8
2	-10.0	24	-5.8	46	-8.0

Phyto-chemical	Binding energy (kcal/mol)	Phyto-chemical	Binding energy (kcal/mol)	Phyto-chemical	Binding energy (kcal/mol)
3	-9.6	25	-5.4	47	-5.5
4	-10.0	26	-5.3	48	-6.4
5	-10.1	27	-5.5	49	-7.2
6	-8.3	28	-5.8	50	-7.1
7	-8.1	29	-5.8	51	-8.3
8	-9.6	30	-6.1	52	-8.7
9	-9.8	31	-5.7	53	-8.8
10	-8.0	32	-7.0	54	-8.2
11	-10.3	33	-8.1	55	-8.5
12	-9.3	34	-6.2	56	-8.5
13	-9.1	35	-6.6	57	-7.9
14	-9.5	36	-6.1	58	-7.2
15	-10.3	37	-6.2	59	-8.7
16	-8.2	38	-5.7	60	-8.8
17	-10.3	39	-6.3	61	-6.0
18	-9.1	40	-8.2	62	-6.3
19	-9.3	41	-5.0	63	-8.8
20	-5.7	42	-8.4	64	-7.3
21	-5.5	43	-9.1	65	-5.3

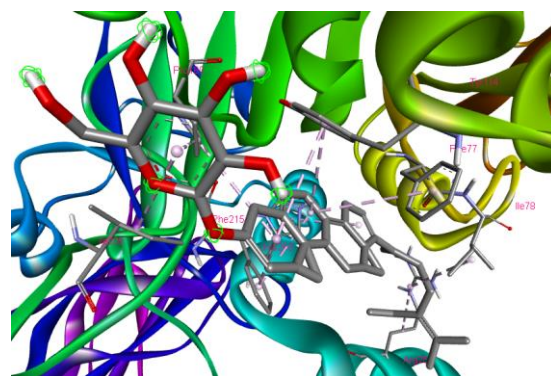
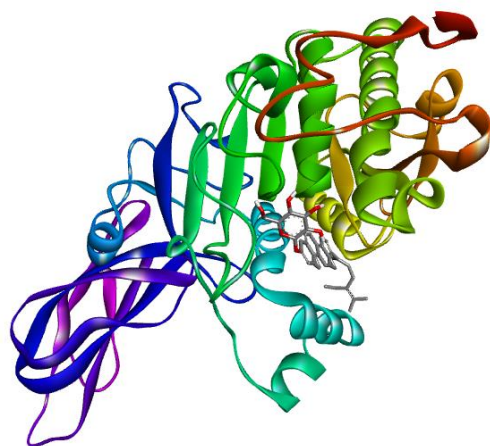
Phyto-chemical	Binding energy (kcal/mol)	Phyto-chemical	Binding energy (kcal/mol)	Phyto-chemical	Binding energy (kcal/mol)
22	-5.7	44	-7.8	66	-5.7
Orlistat	-6.7				

Figure 10 showed the 3D presentation of the phytochemicals from *A. indicum* (1-66) in the active site of HPL (PDB code: 1LPB). It demonstrated that the phytochemicals occupying the same site as orlistat.

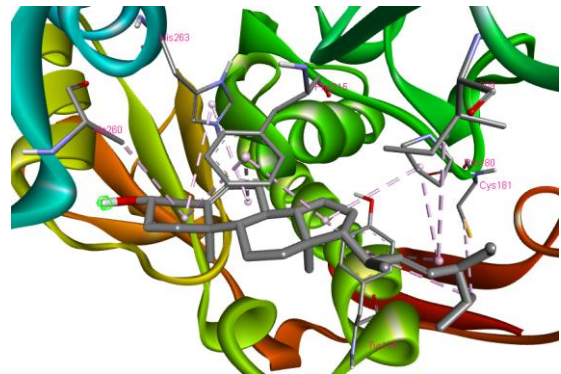
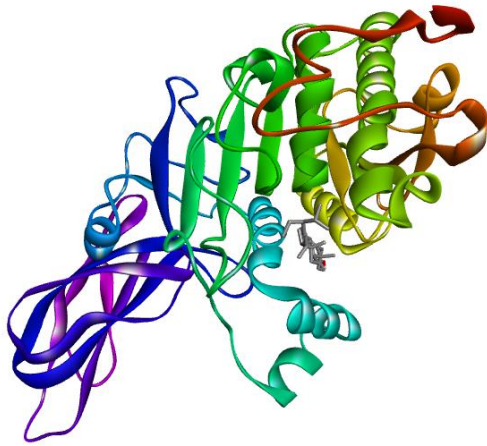


มหาวิทยาลัย
CHULALONGKORN UNIVERSITY

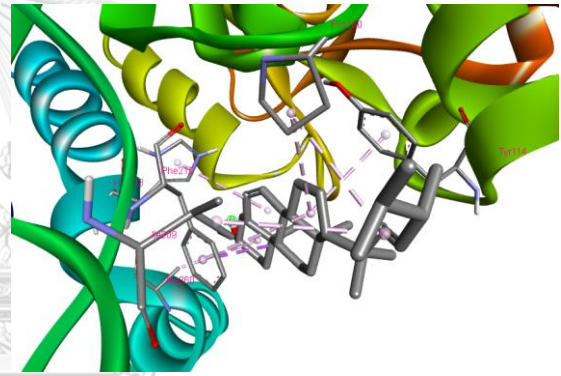
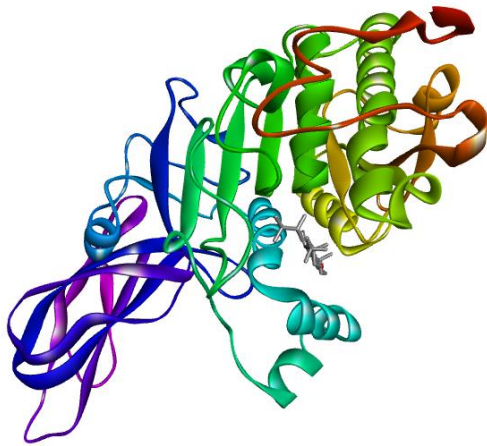
1



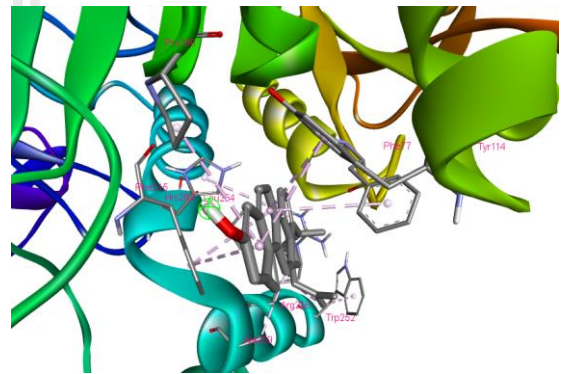
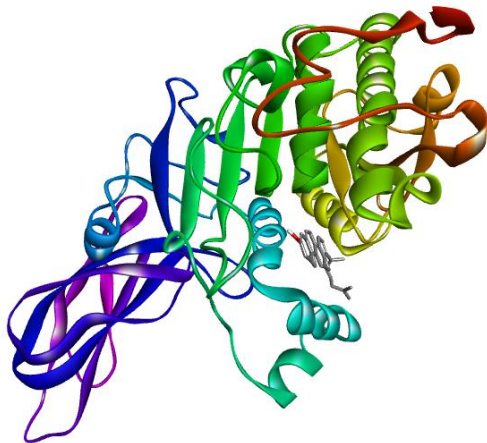
2



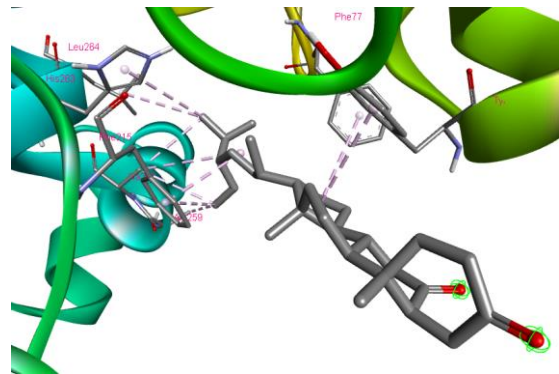
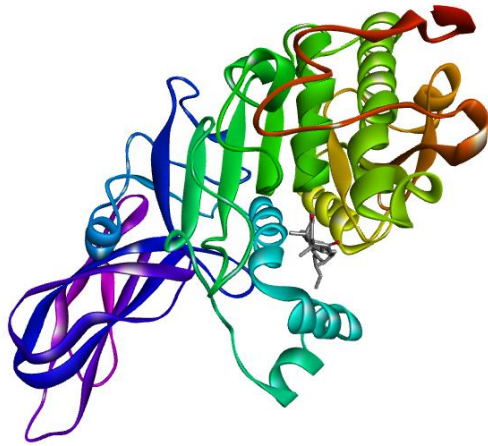
3



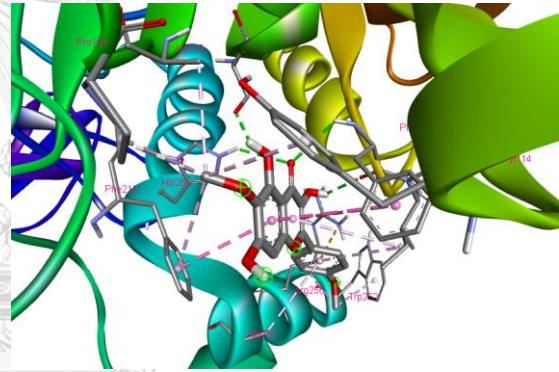
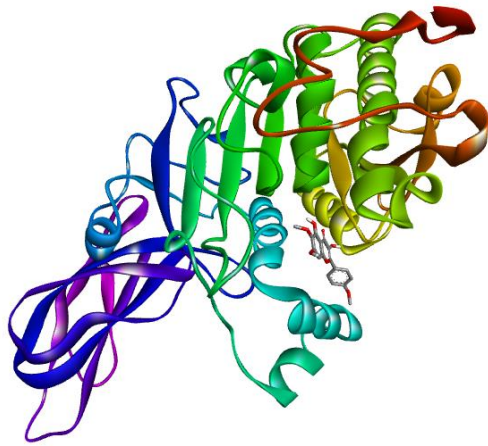
4



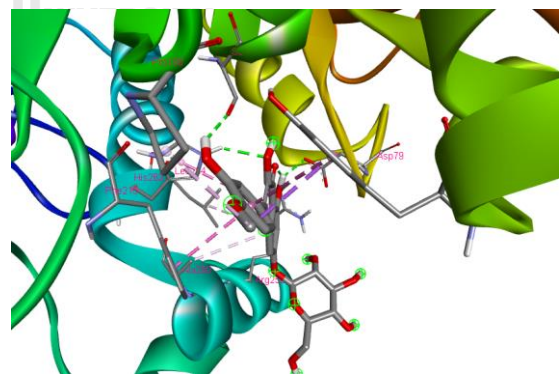
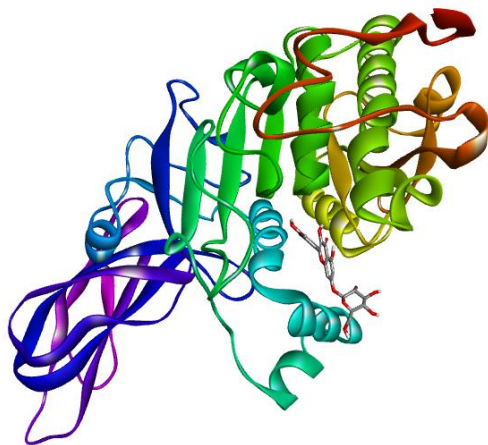
5



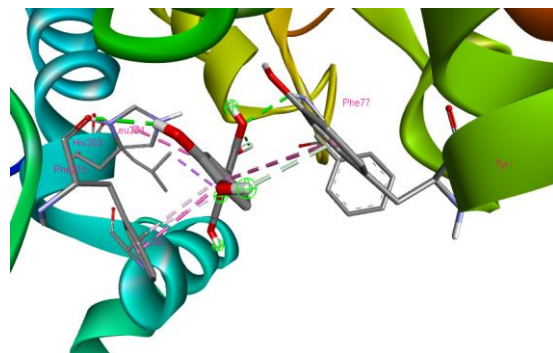
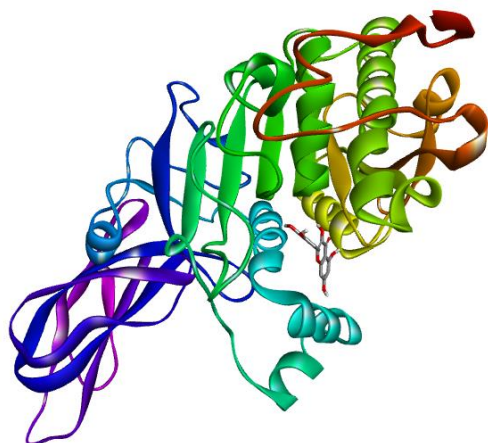
6



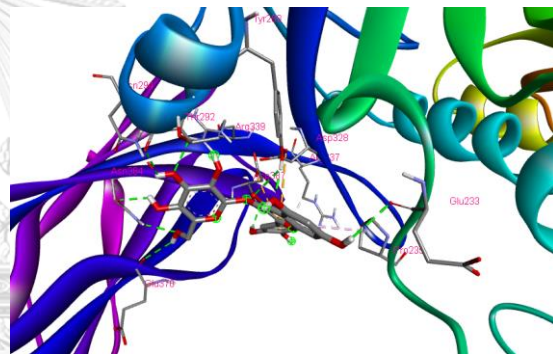
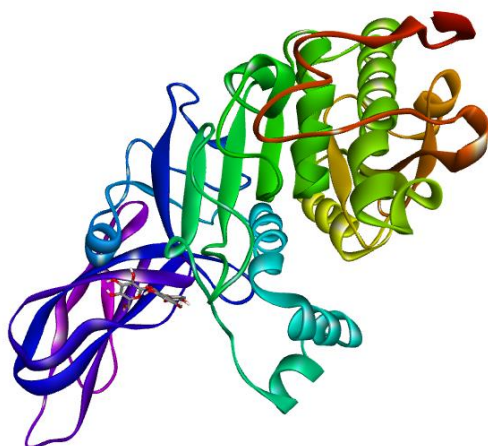
7



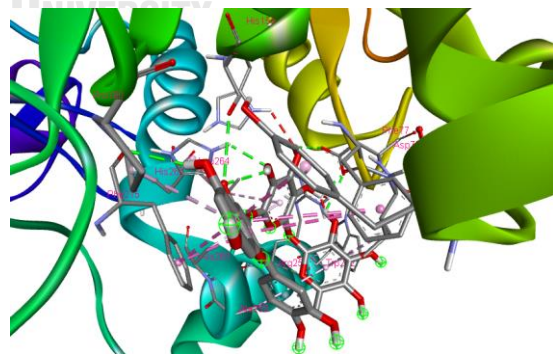
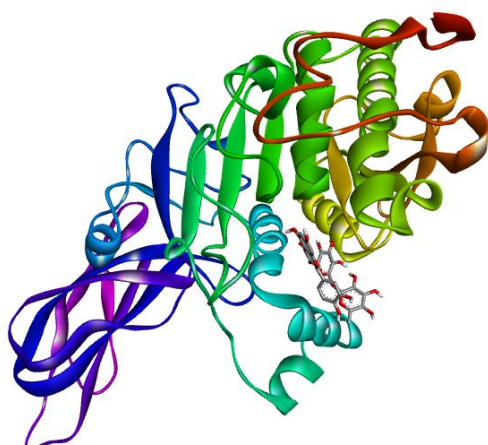
8



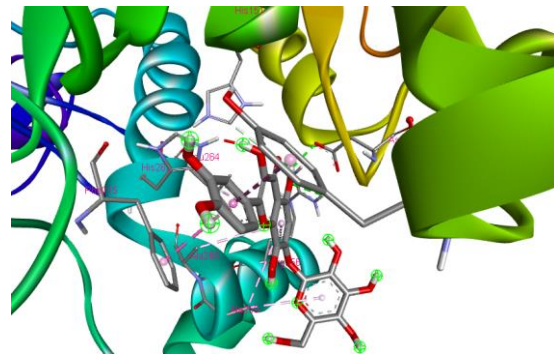
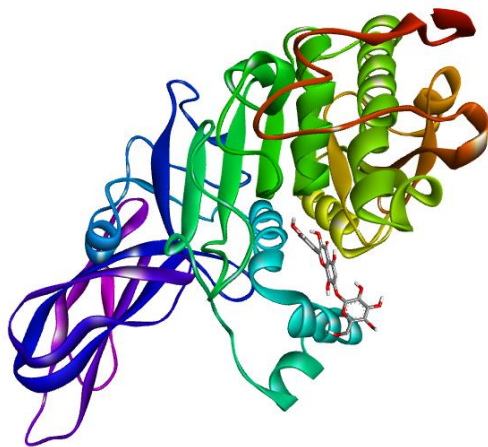
9



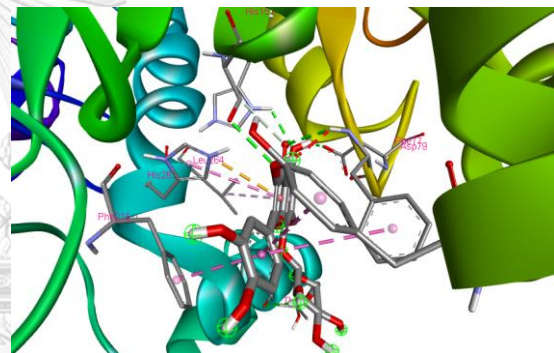
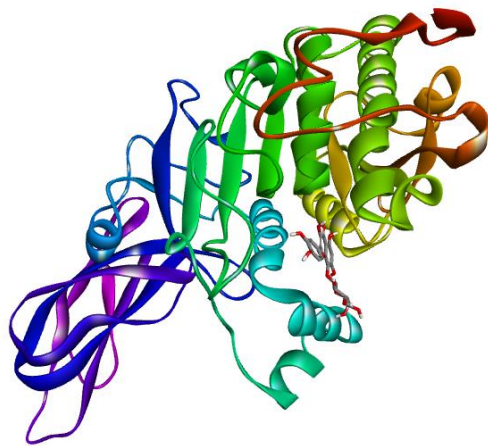
10



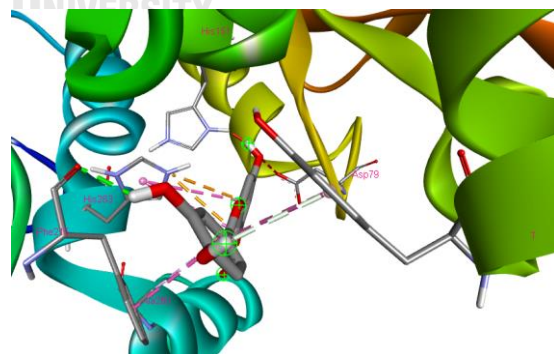
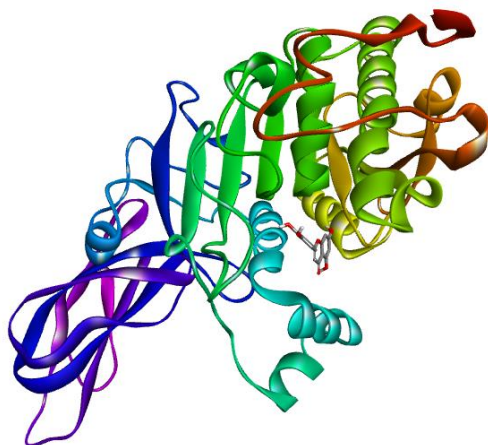
11



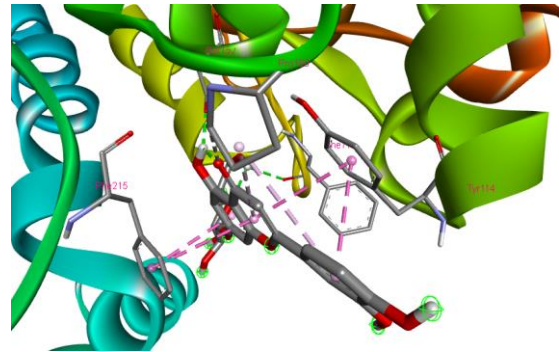
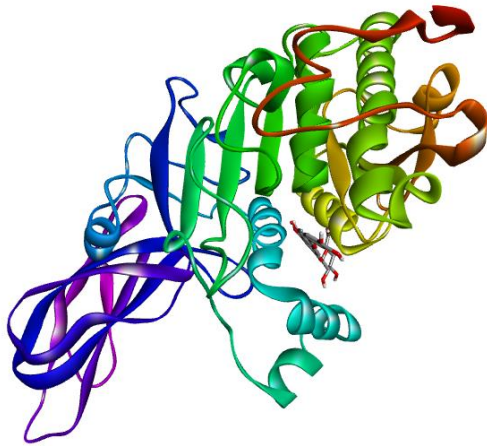
12



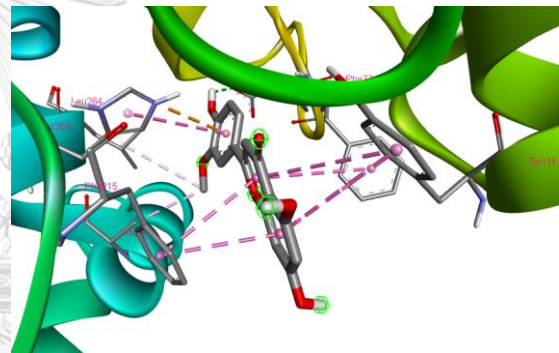
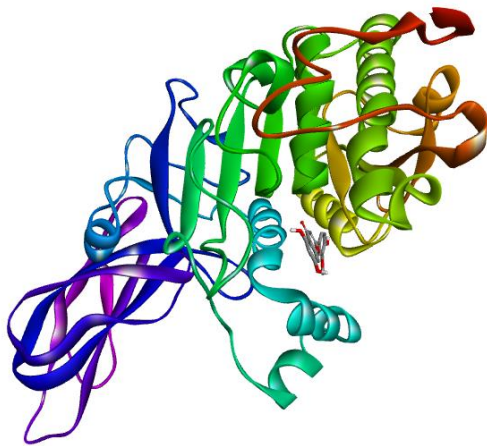
13



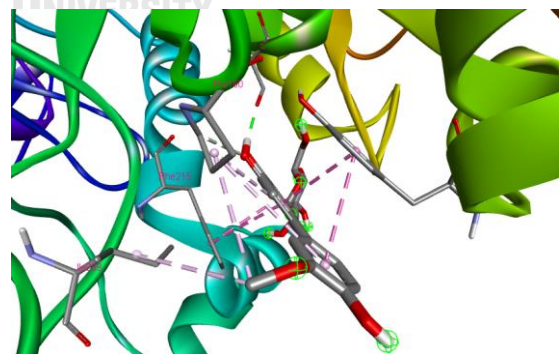
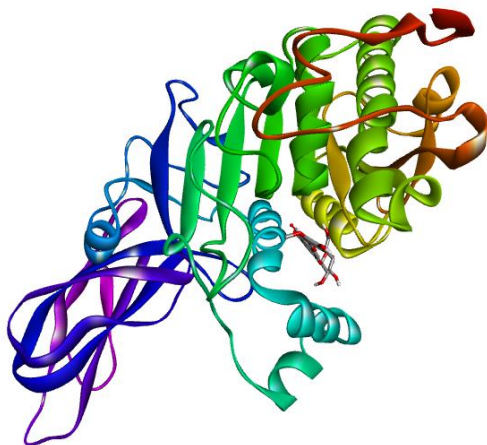
14



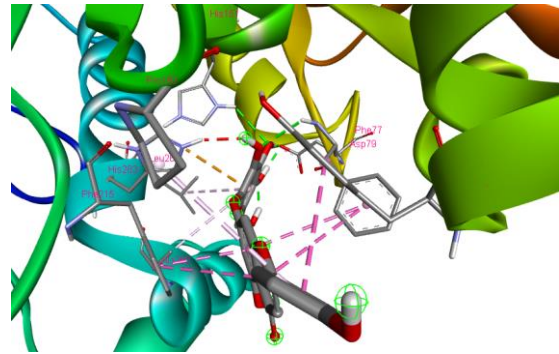
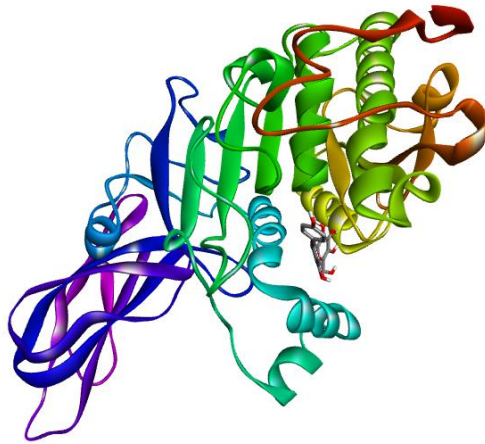
15



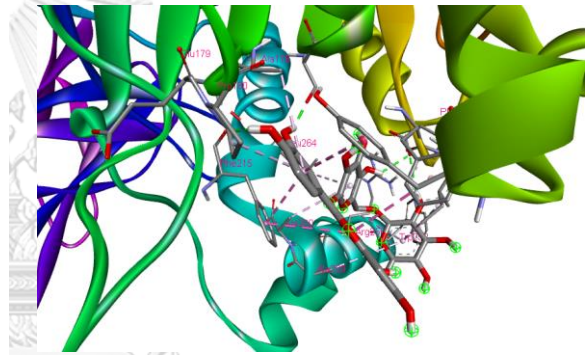
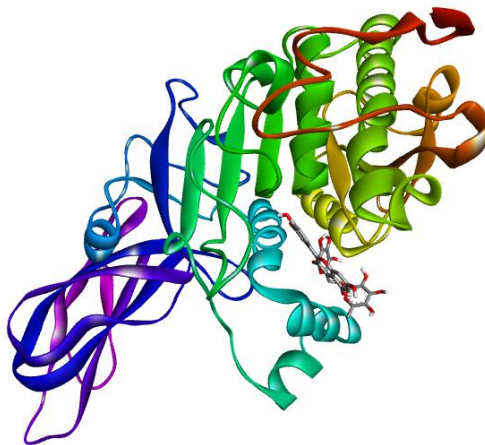
16



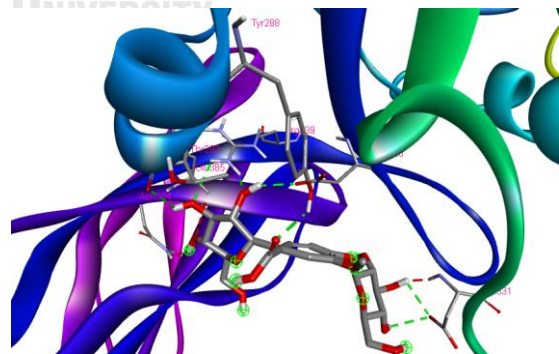
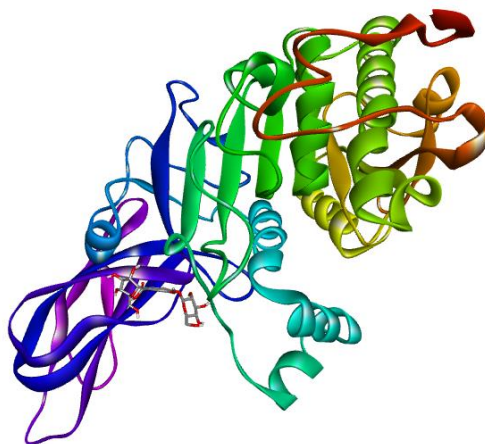
17



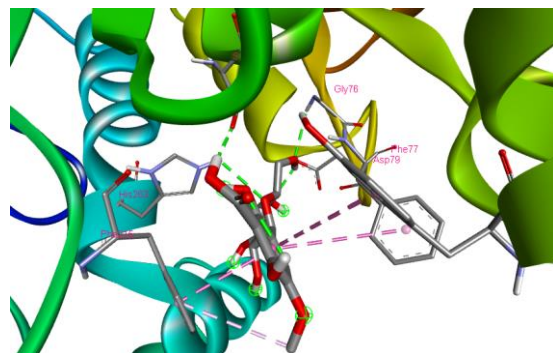
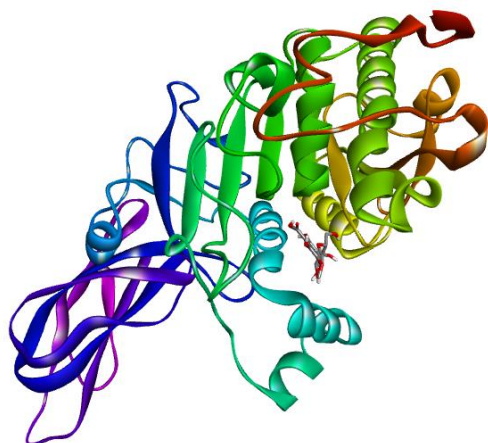
18



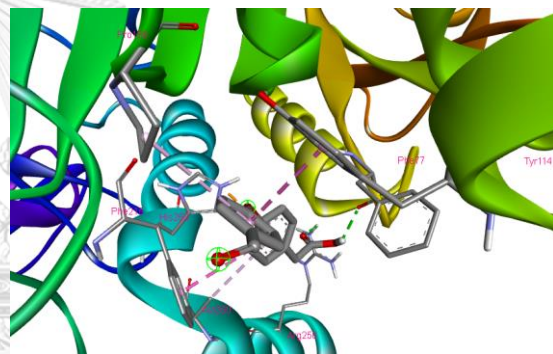
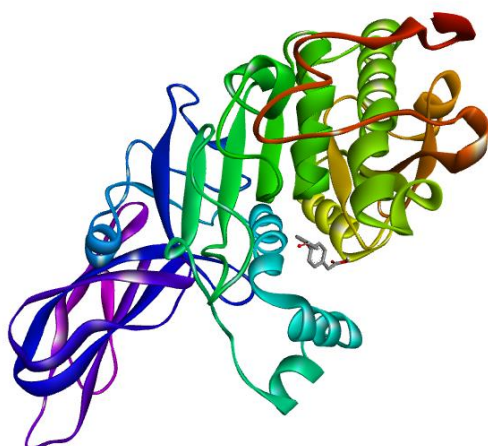
19



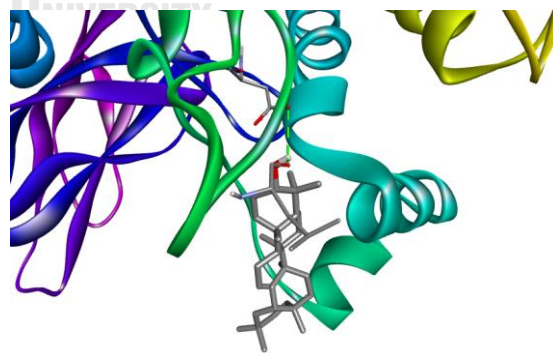
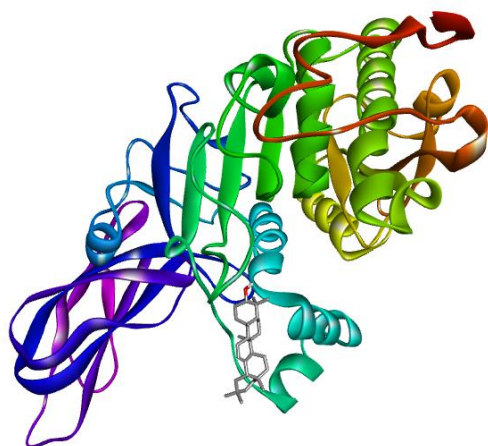
23



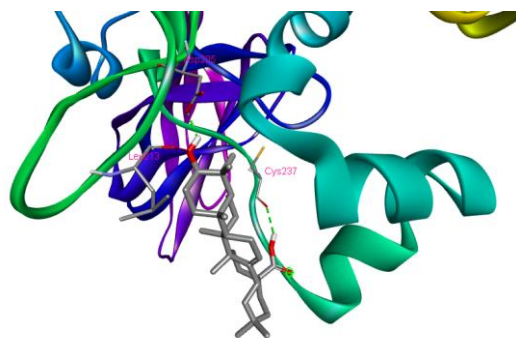
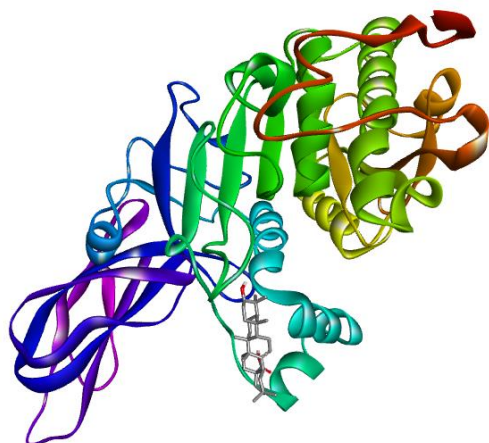
33



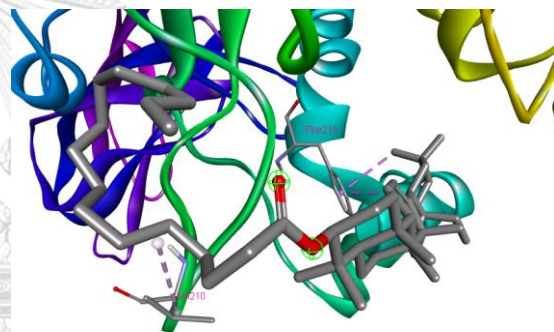
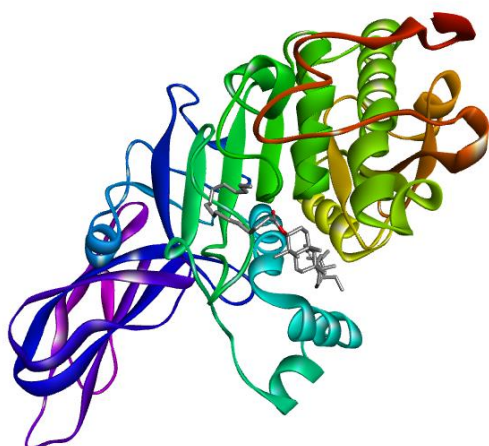
40



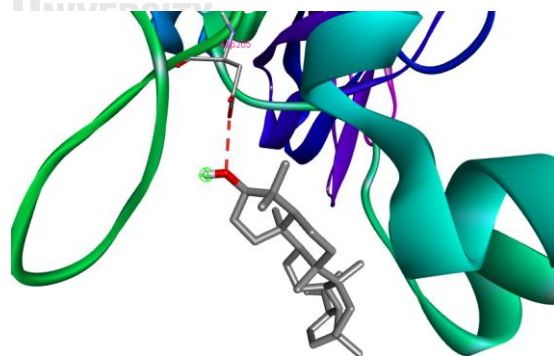
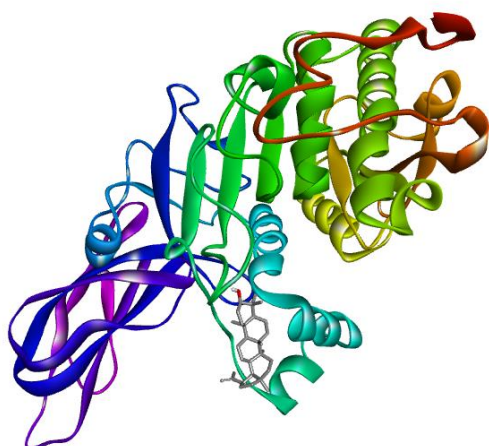
42



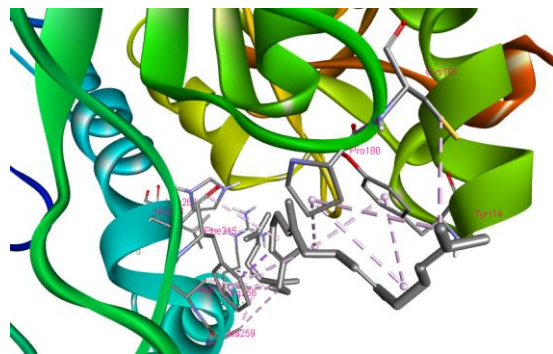
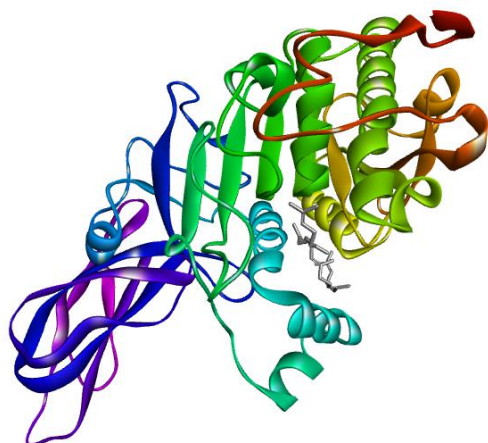
43



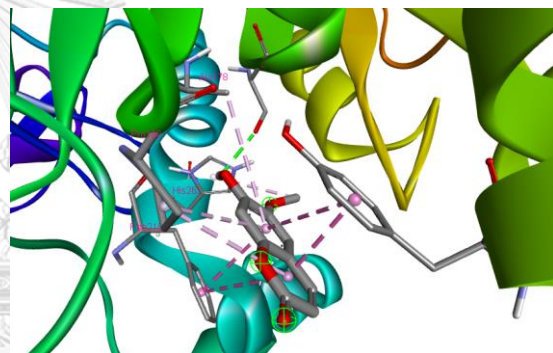
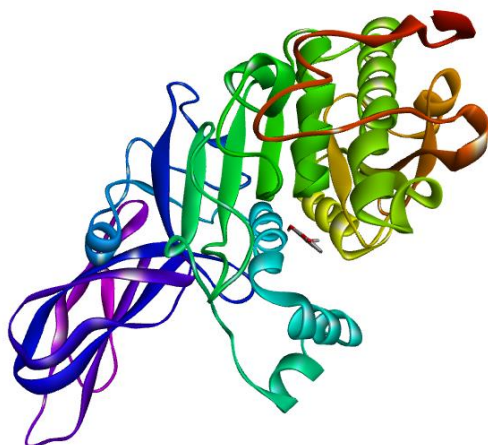
44



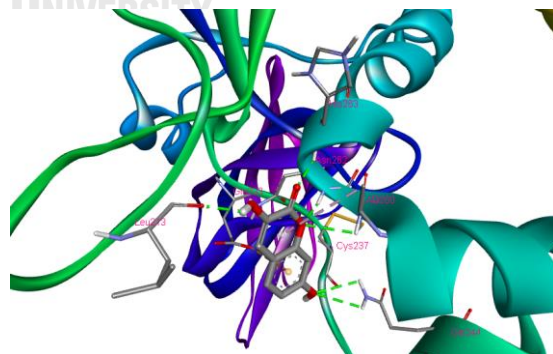
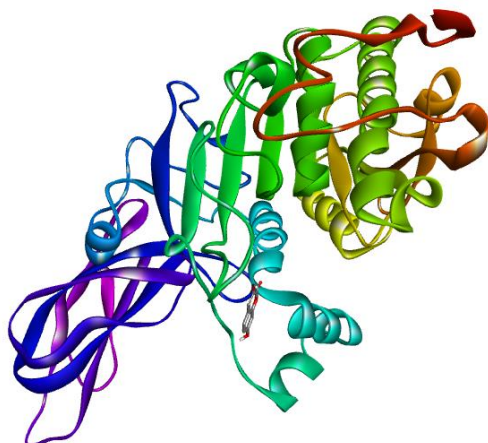
45



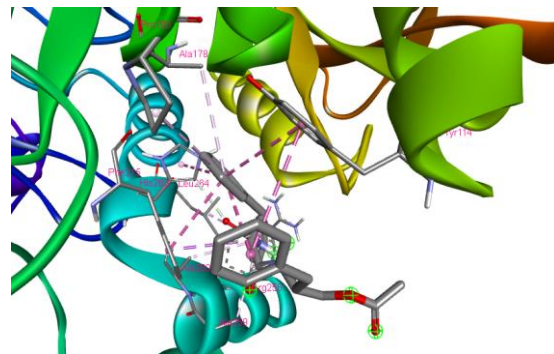
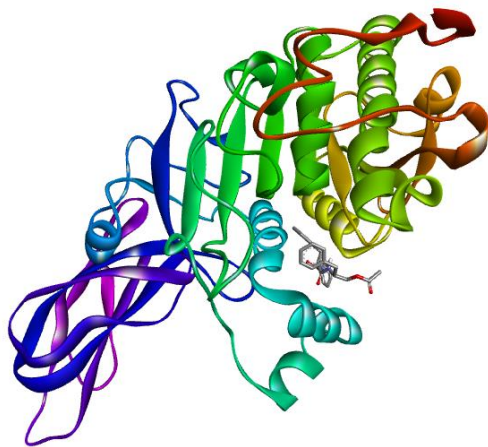
46



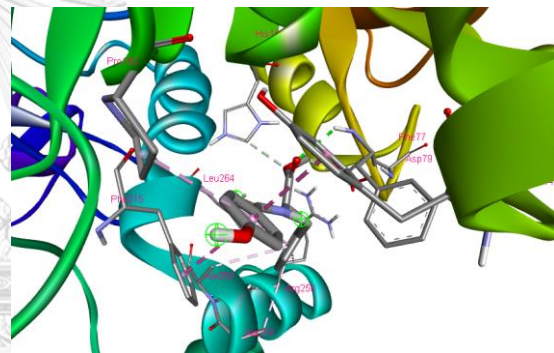
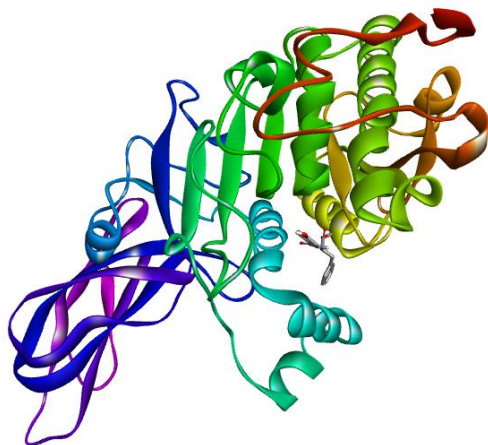
49



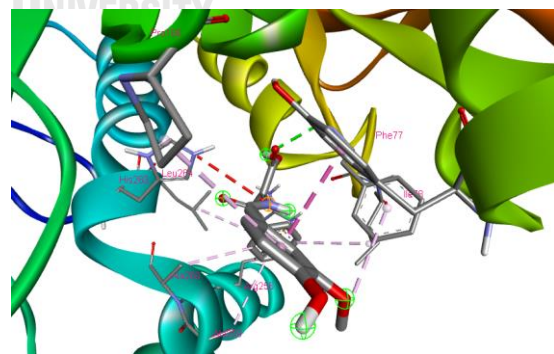
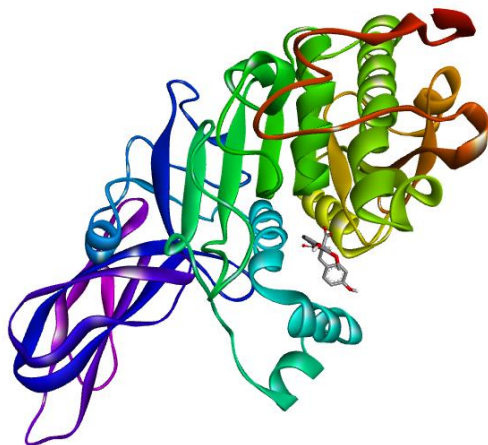
50



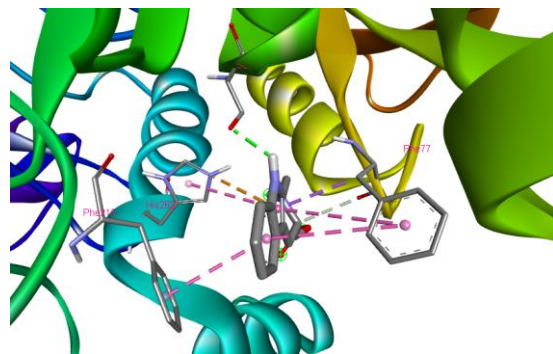
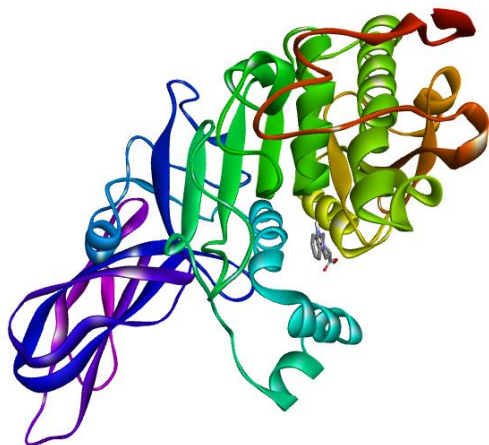
51



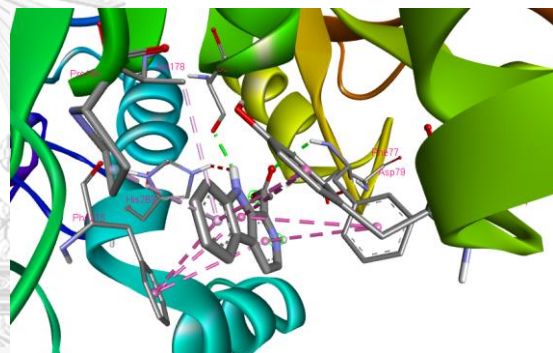
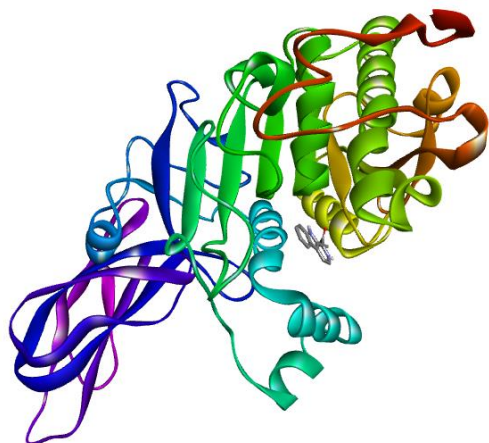
52



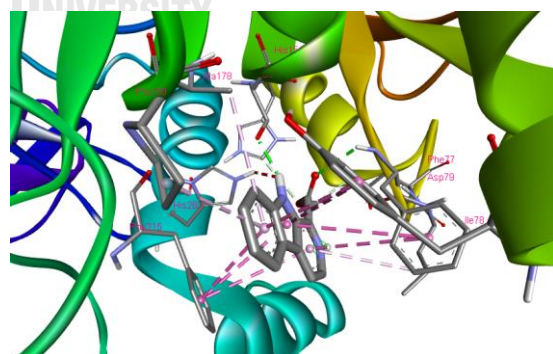
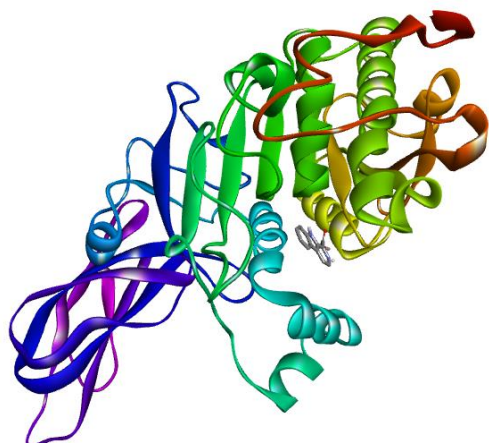
53



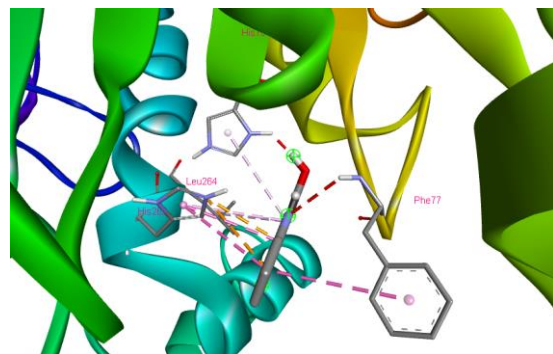
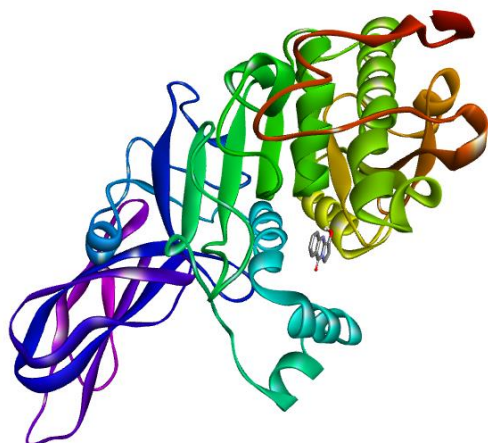
54



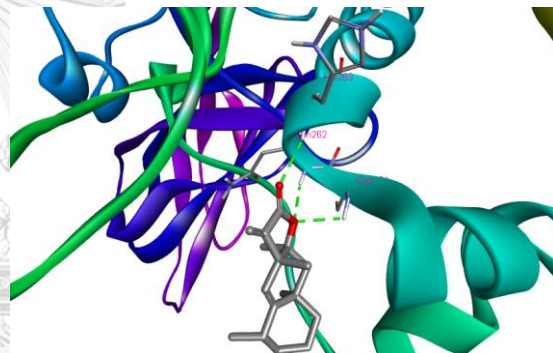
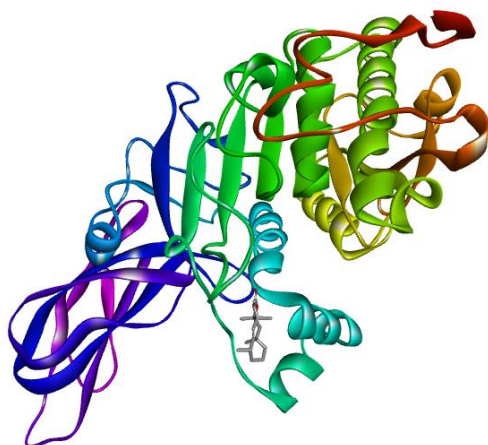
55



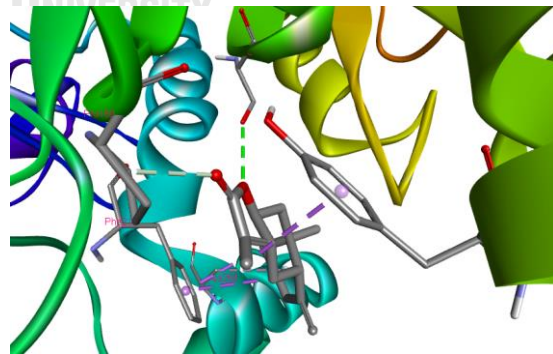
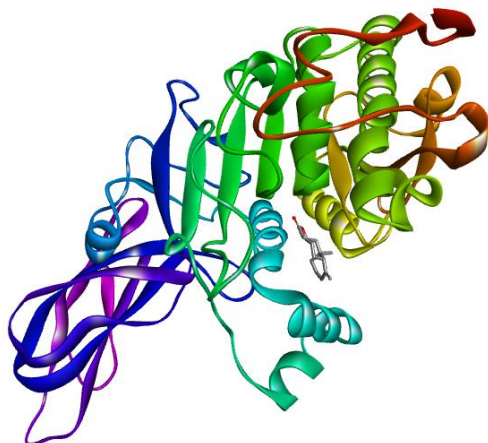
56



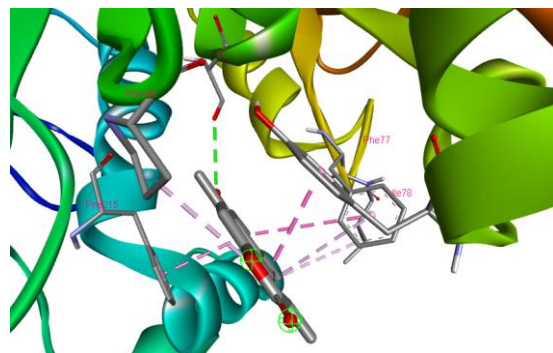
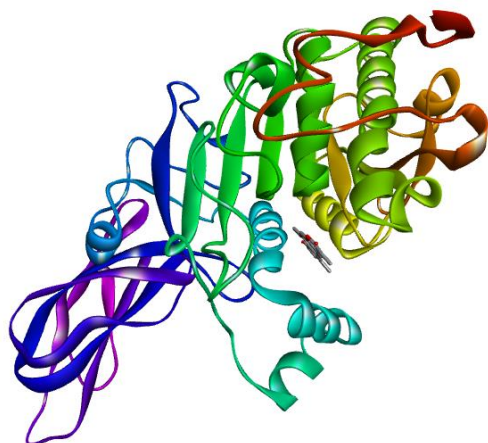
57



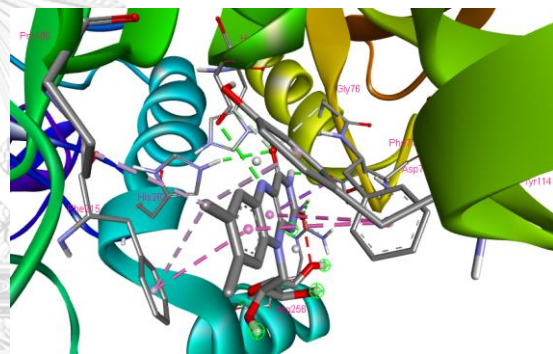
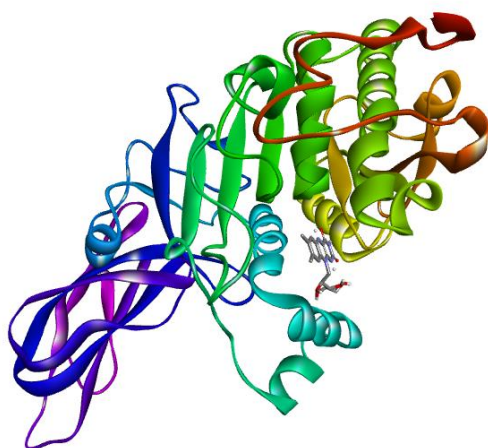
58



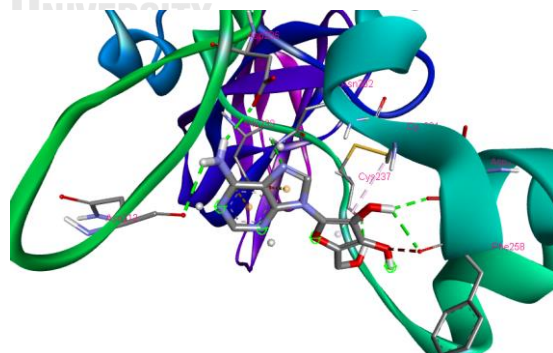
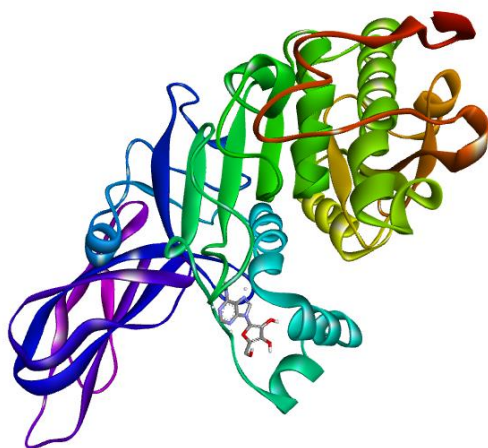
59



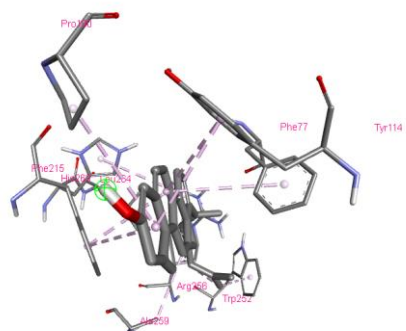
60



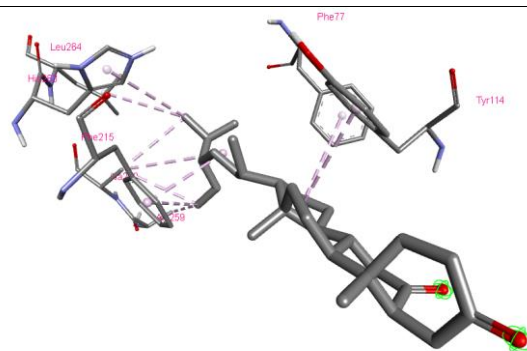
63



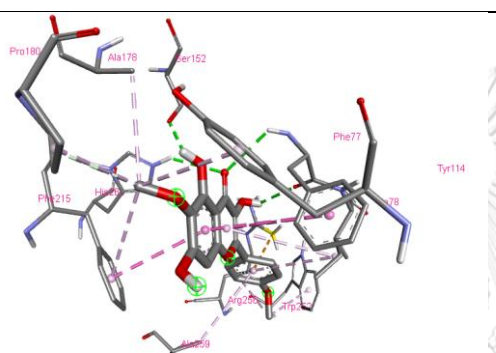
64



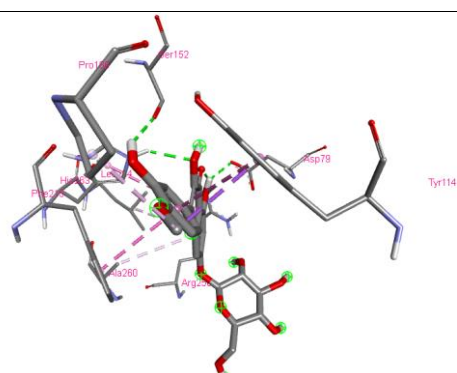
5



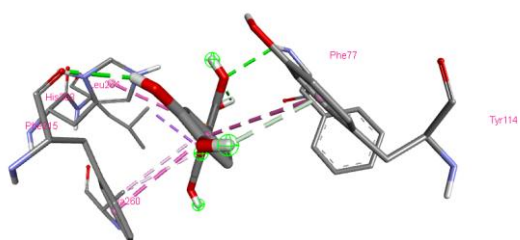
6



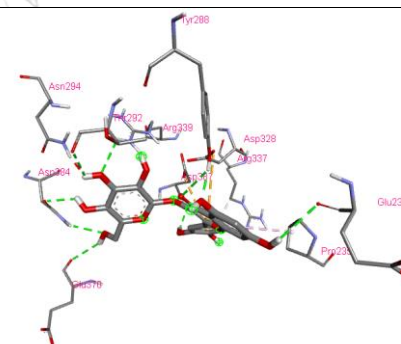
7



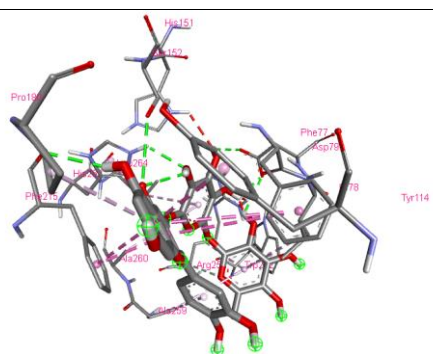
8



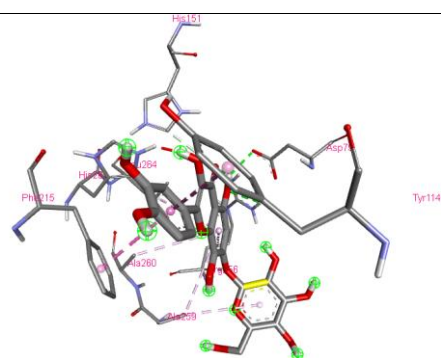
9



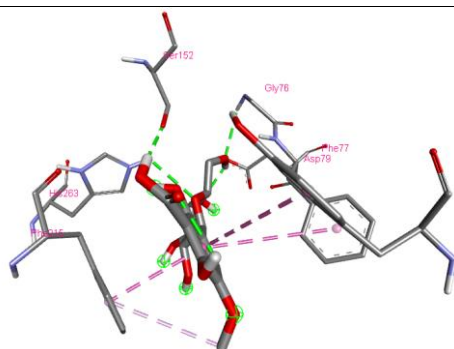
10



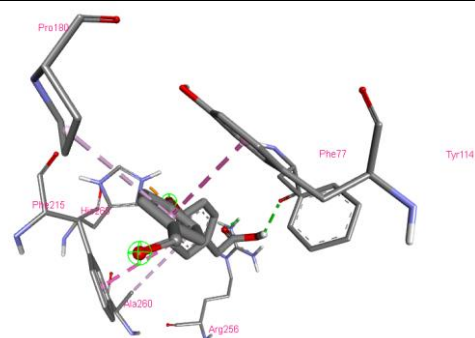
11



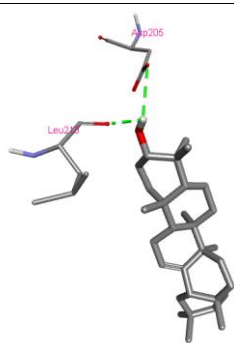
12



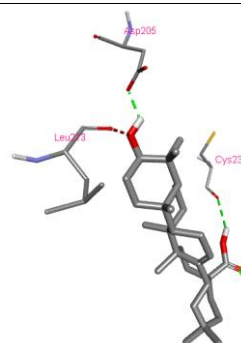
33



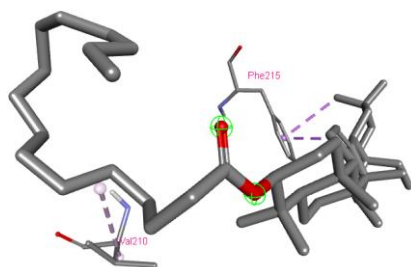
40



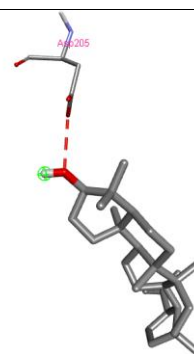
42



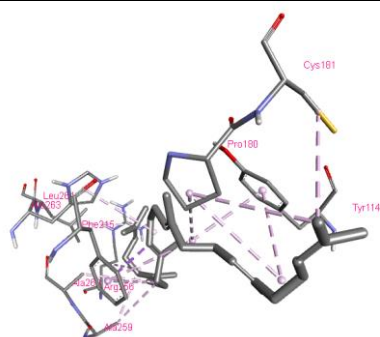
43



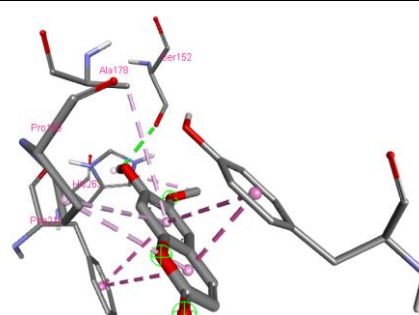
44



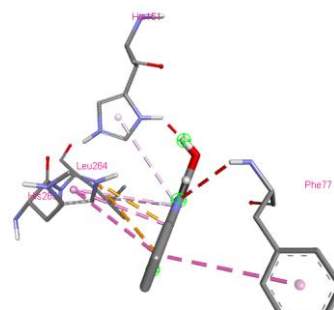
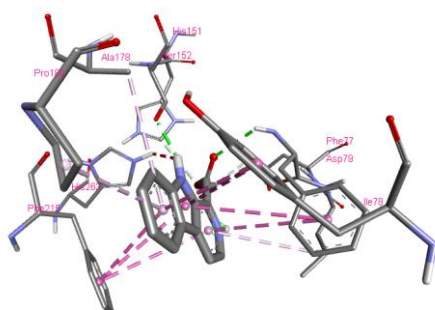
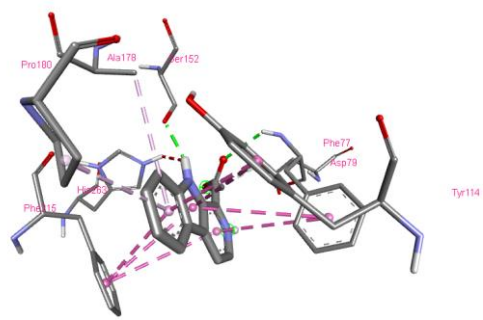
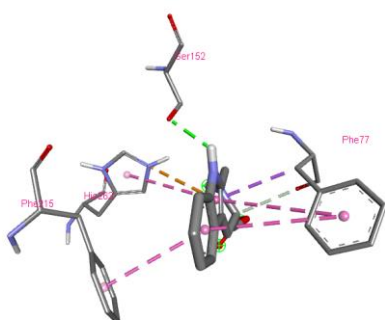
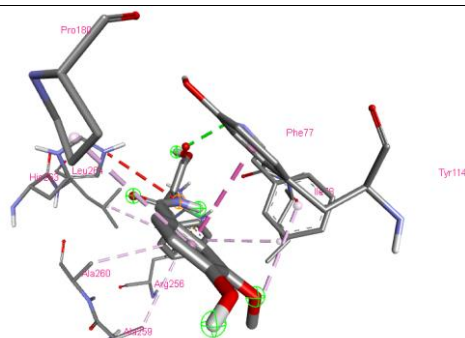
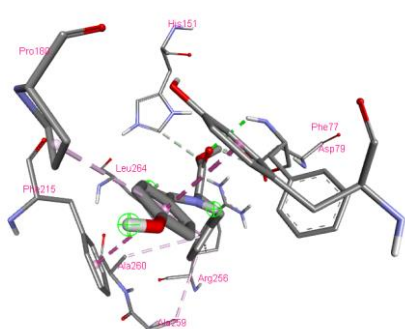
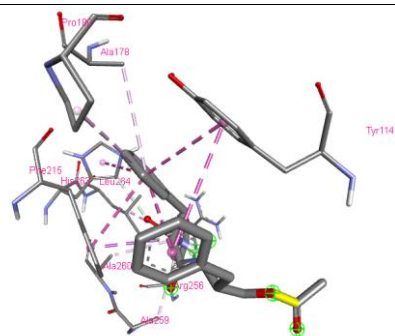
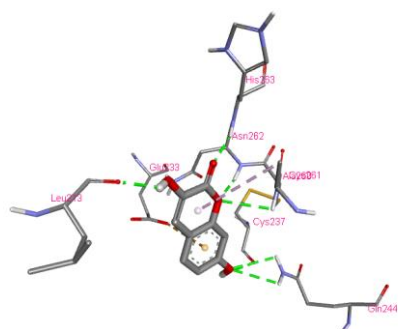
45



46



49



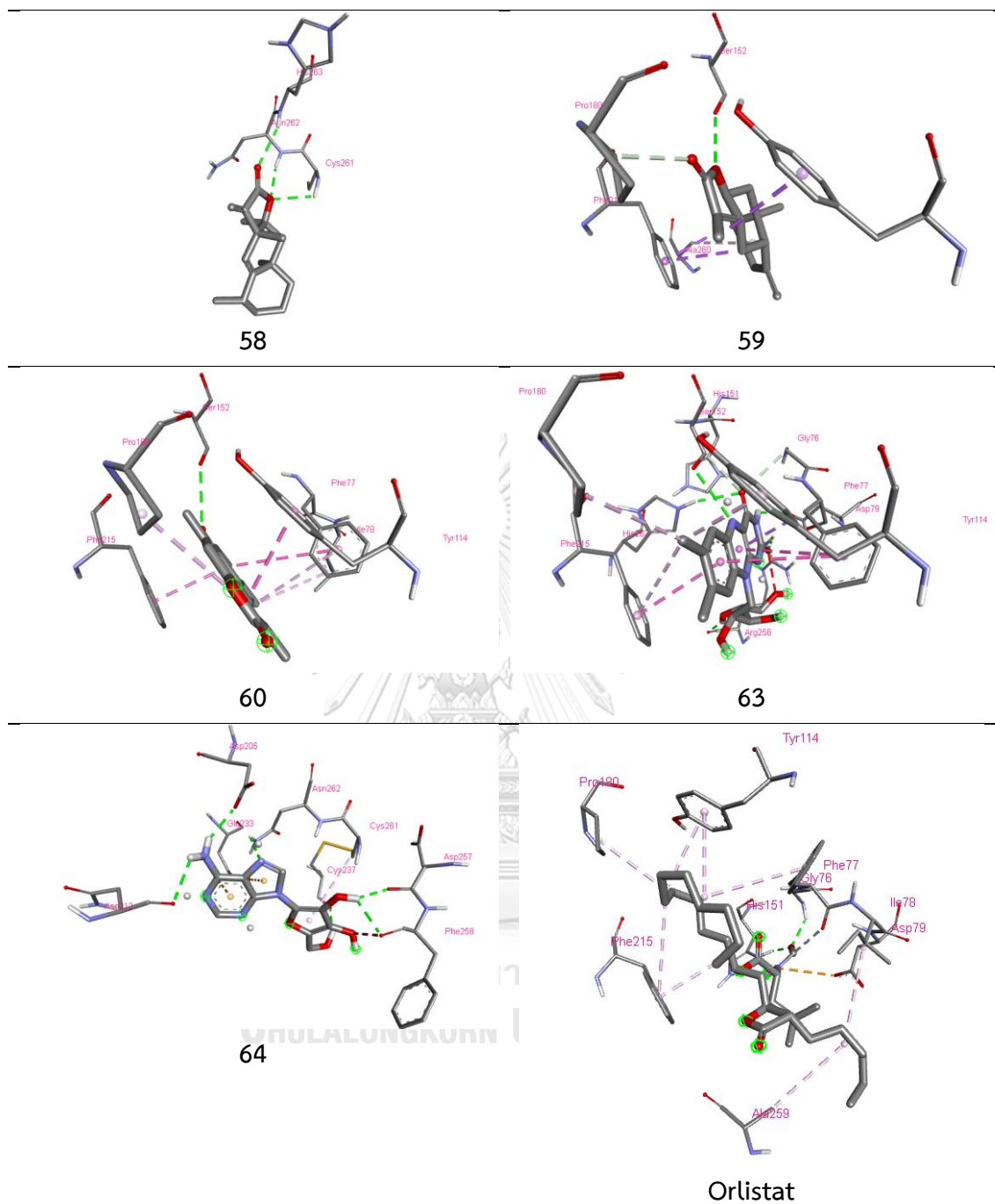
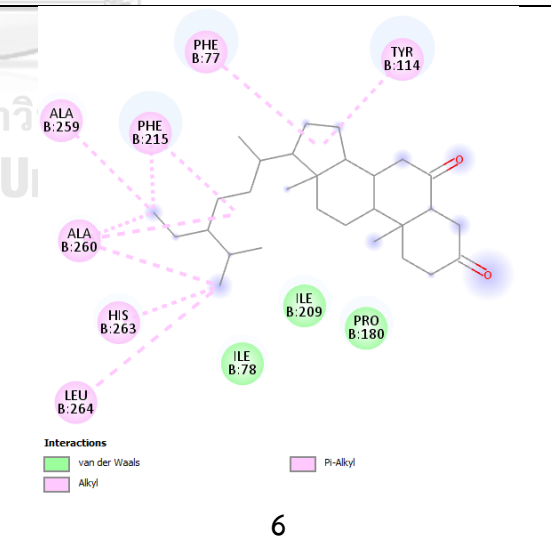
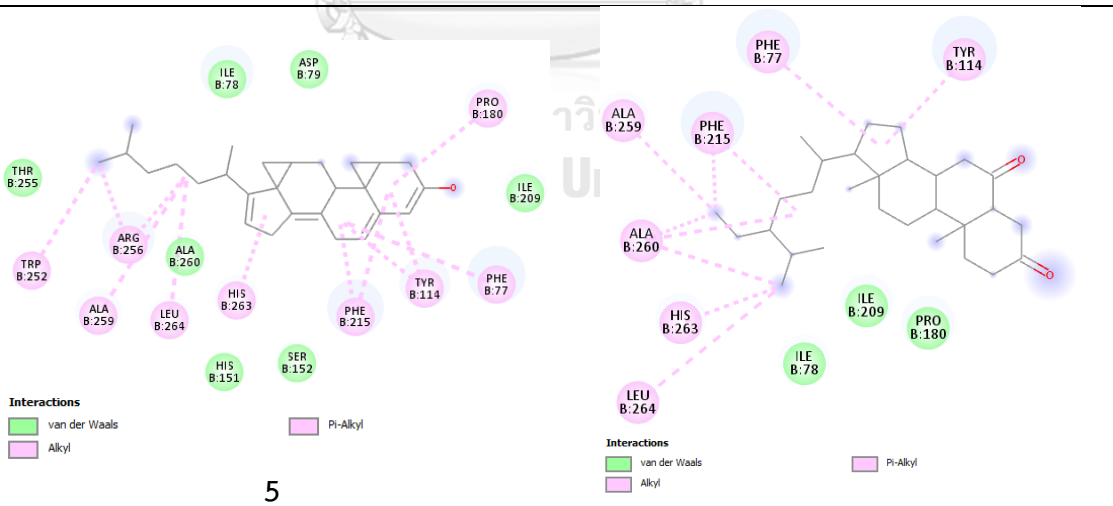
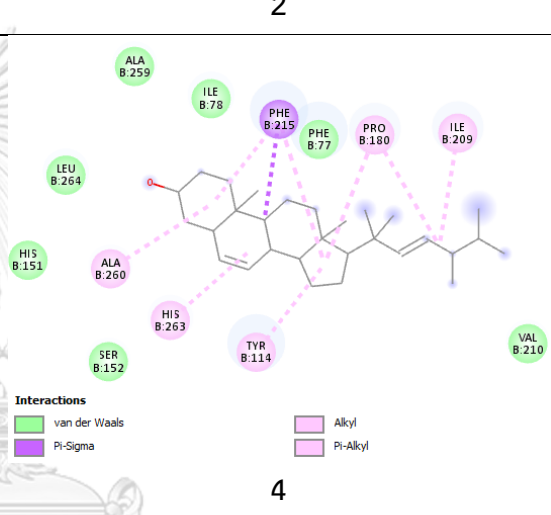
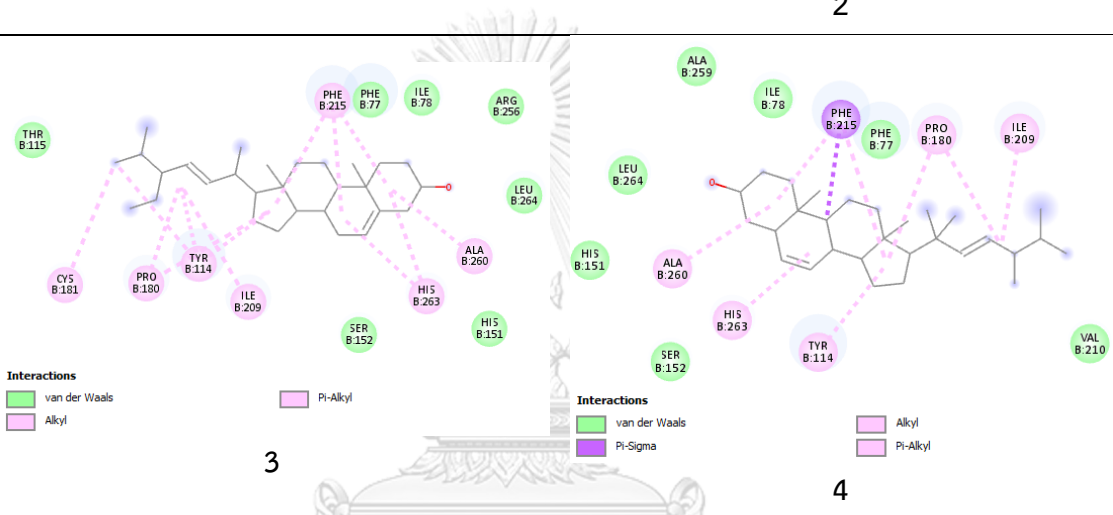
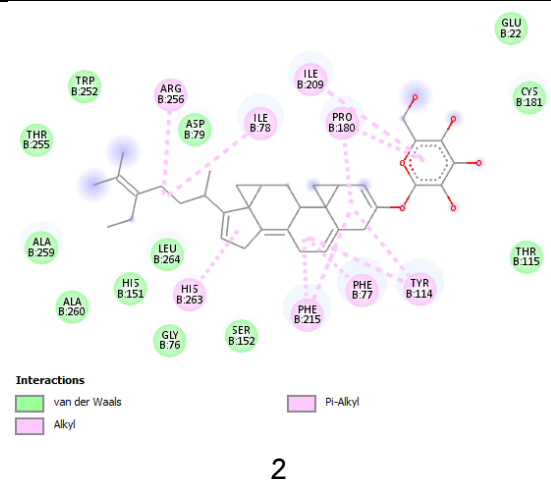
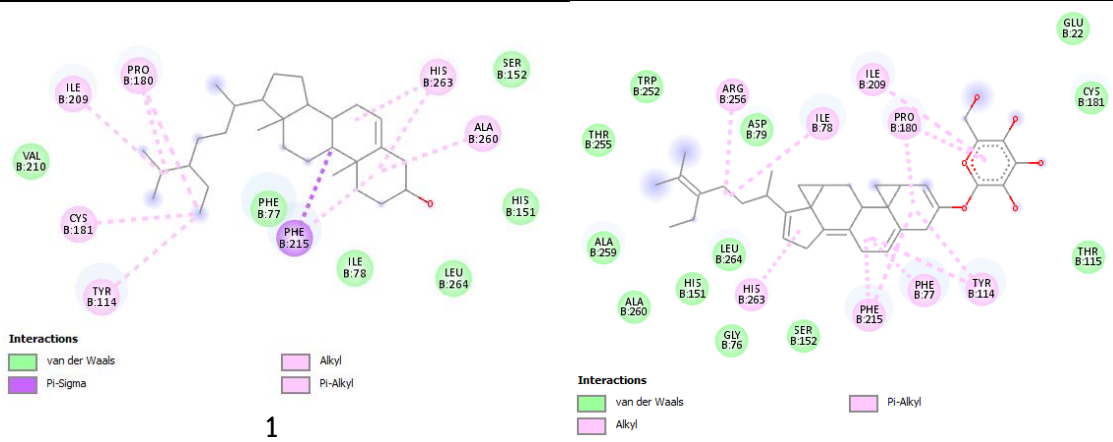
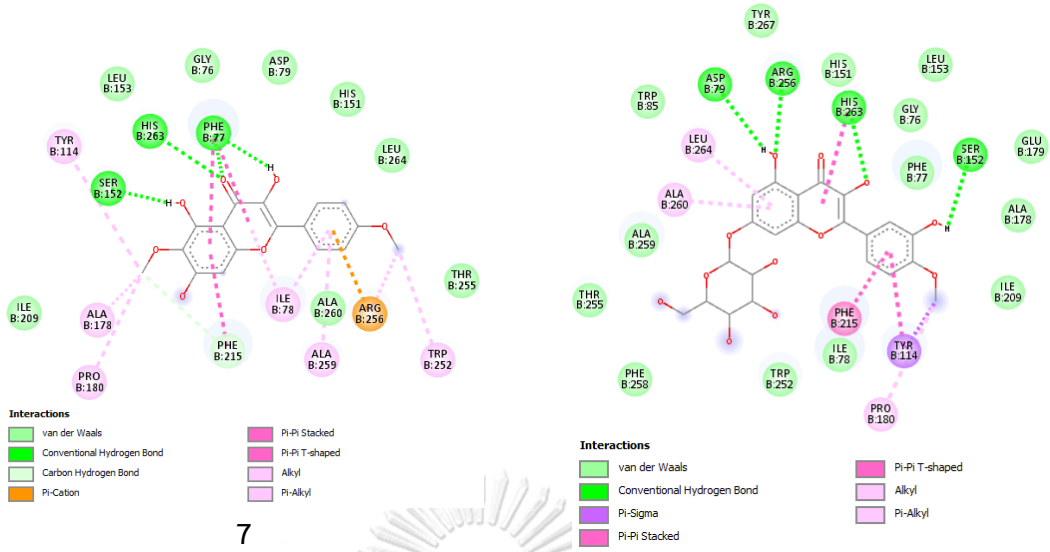


Figure 11 3D molecular amino interaction of the phytochemicals of *A. indicum* in the binding site of HPL (PDB code: 1LPB)

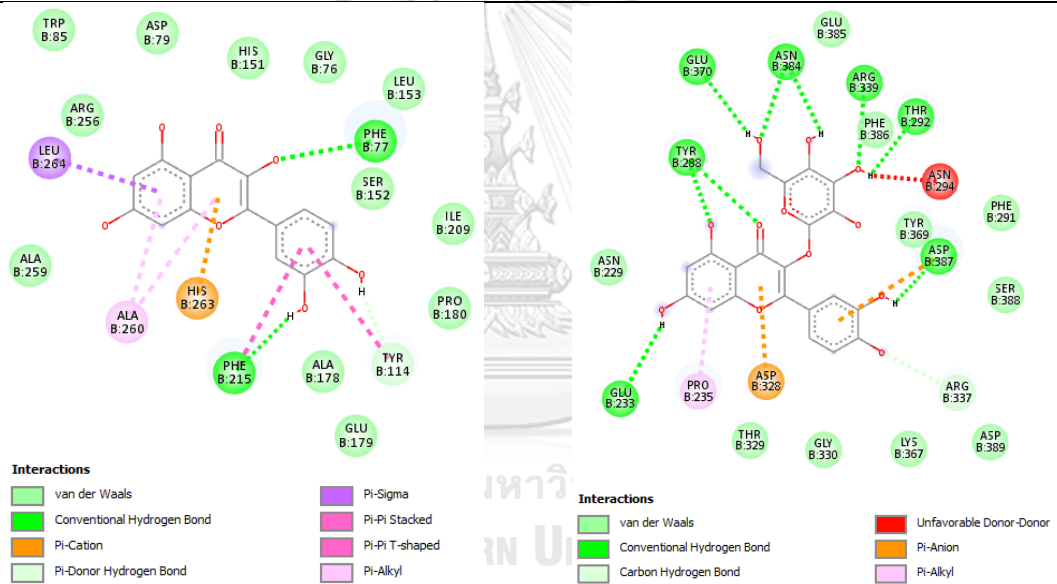
Figure 12 depicted the amino acids residual and its interaction types.





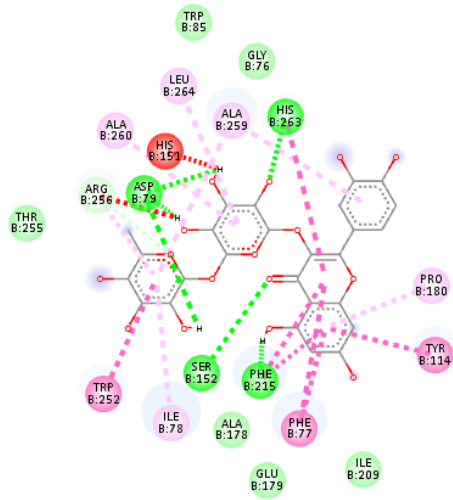
7

8



9

10

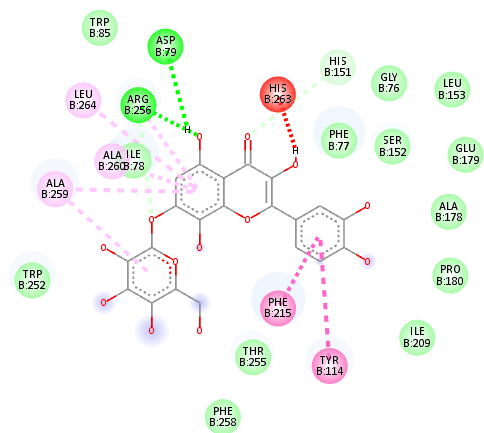


Interactions

- van der Waals
- Conventional Hydrogen Bond
- Carbon Hydrogen Bond
- Unfavorable Donor-Donor

- Pi-Pi Stacked
- Pi-Pi T-shaped
- Pi-Alkyl

11

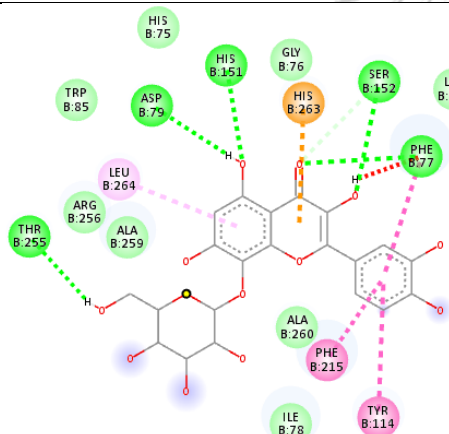


Interactions

- van der Waals
- Conventional Hydrogen Bond
- Carbon Hydrogen Bond

- Unfavorable Donor-Donor
- Pi-Pi Stacked
- Pi-Alkyl

12

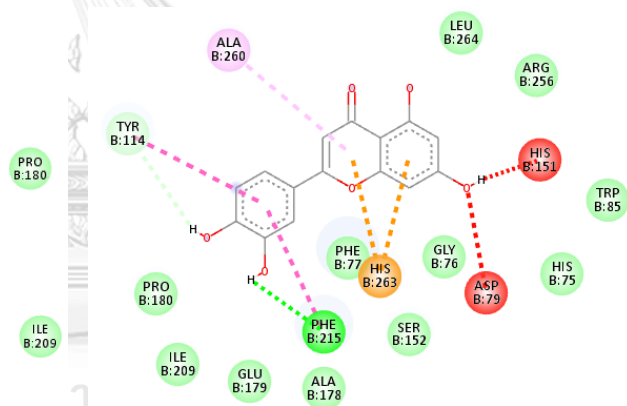


Interactions

- van der Waals
- Conventional Hydrogen Bond
- Carbon Hydrogen Bond
- Unfavorable Donor-Donor

- Pi-Cation
- Pi-Pi Stacked
- Pi-Pi T-shaped
- Pi-Alkyl

13

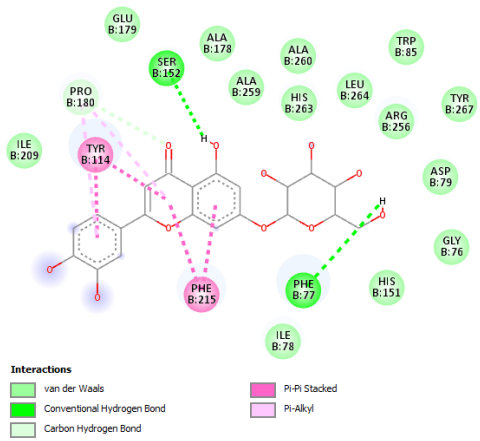


Interactions

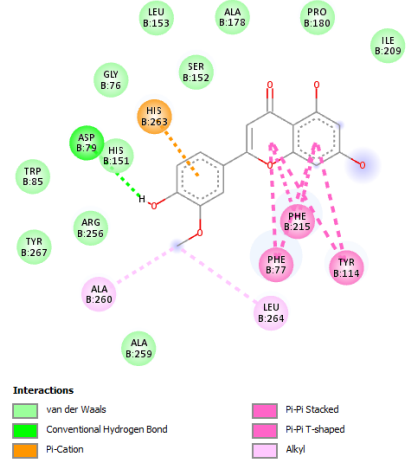
- van der Waals
- Conventional Hydrogen Bond
- Unfavorable Donor-Donor
- Unfavorable Acceptor-Acceptor
- Pi-Cation

- Pi-Donor Hydrogen Bond
- Pi-Pi Stacked
- Pi-Pi T-shaped
- Pi-Alkyl

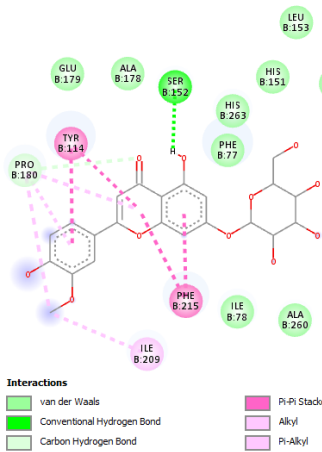
14



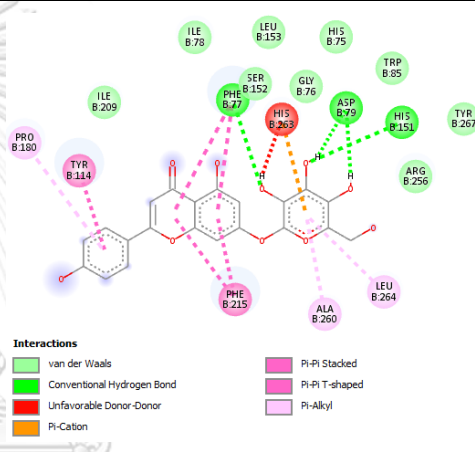
15



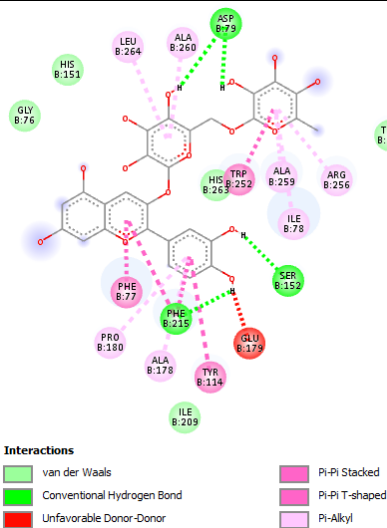
16



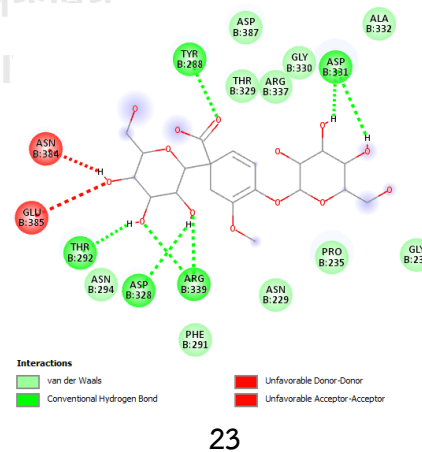
17



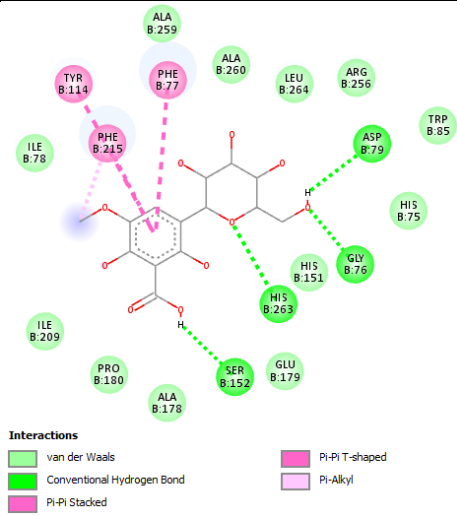
18



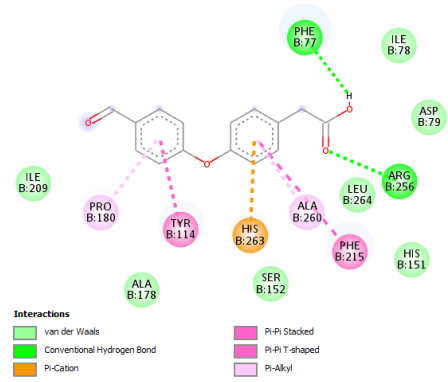
19



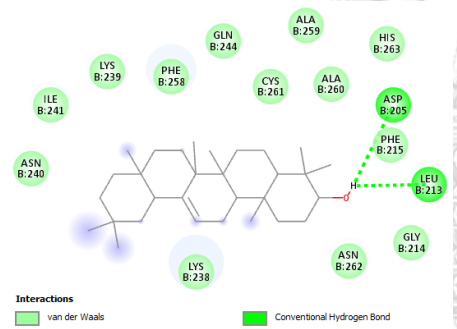
23



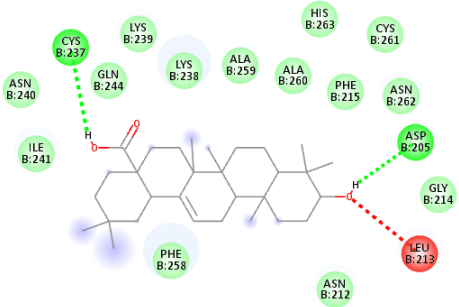
33



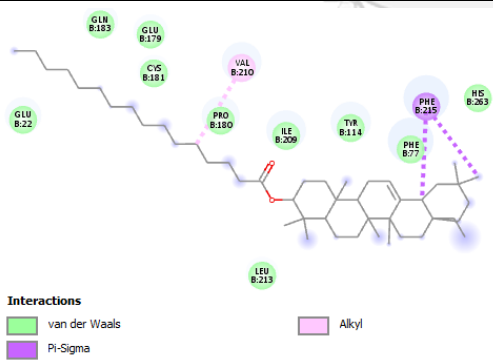
40



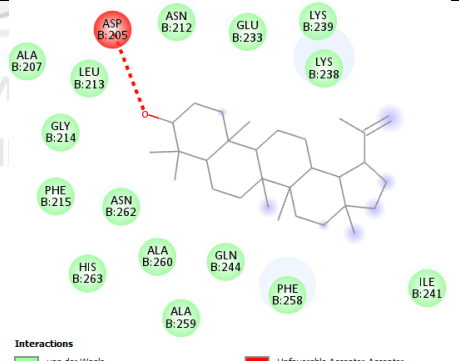
42



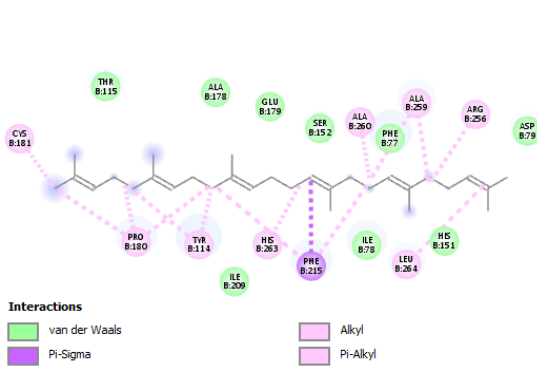
43



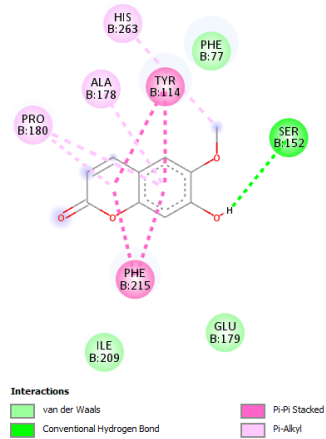
44



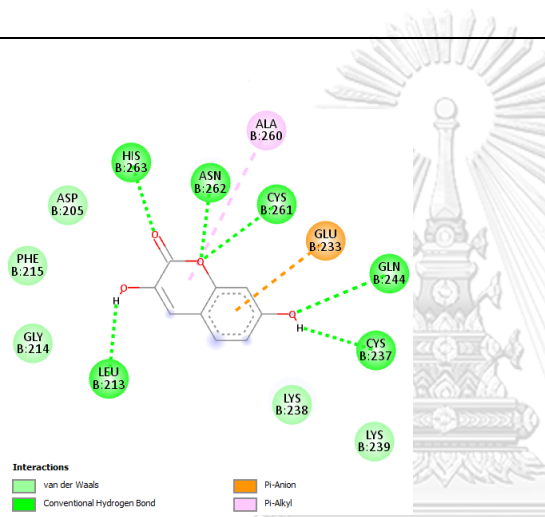
45



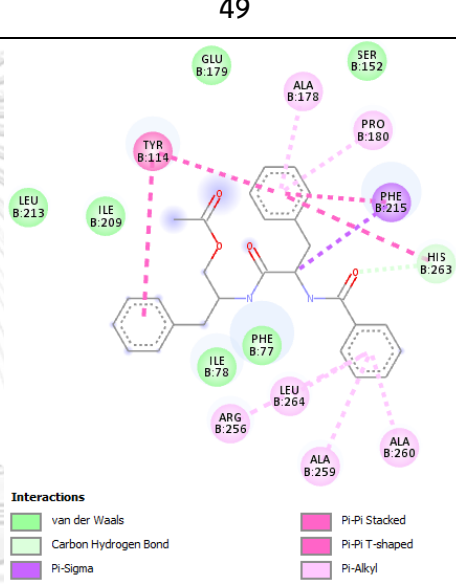
46



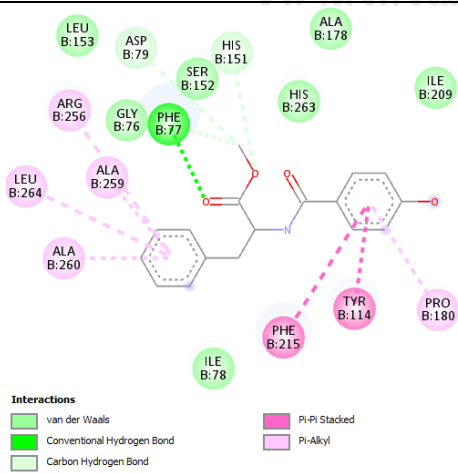
49



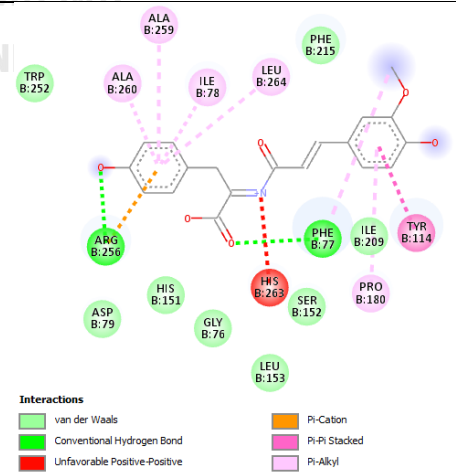
50



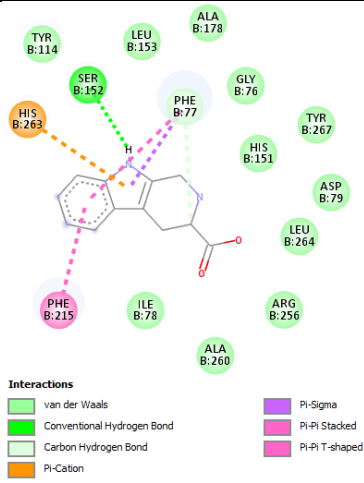
51



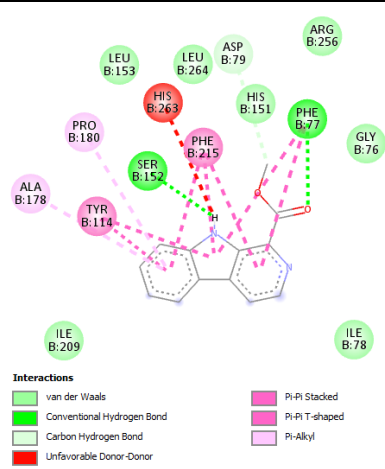
52



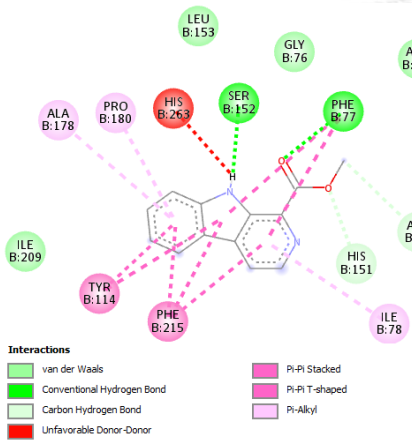
53



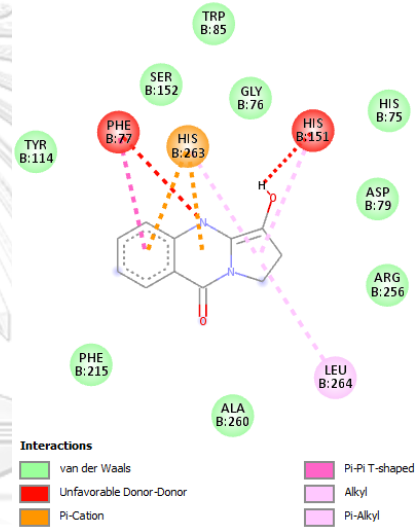
54



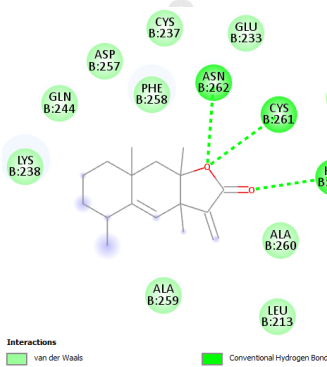
55



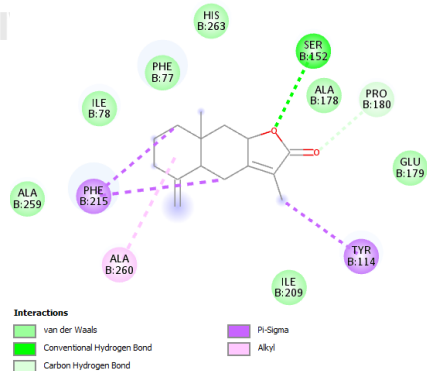
56



57



58



59

จุฬาลงกรณ์มหาวิทยาลัย

KORN UNI

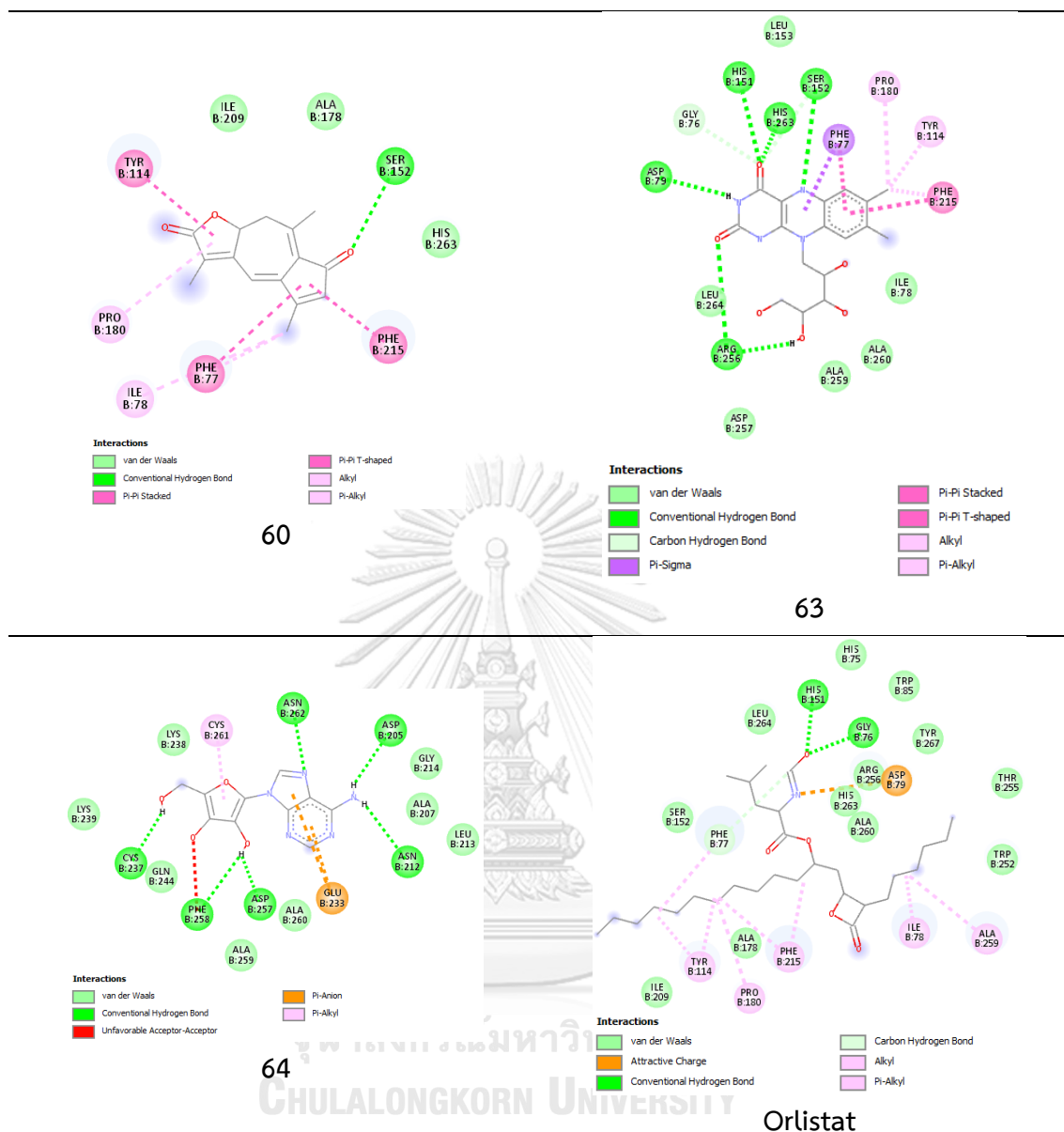


Figure 12 Amino acids residual interactions of the interacting pocket between HPL (PDB ID: 1LPB) and ligands

Table 6 The type of molecular interactions of the phytochemicals (1-66) within the active site of the HPL (PDB ID: 1LPB)

Comp.	Conventional Hydrogen Bond	Residual interactions
		Hydrophobic/Pi-interaction
		Van der Waals

Comp.	Conventional		Residual interactions	
	Hydrogen Bond	Hydrophobic/Pi-interaction	Van der Waals	
1	-	Tyr114, Pro180, Cys181, Ile209, Phe215, Ala260, His263	Phe77, Ile78, His151, Ser152, Val210, Leu264	
2	-	Phe77, Ile78, Tyr114, Pro180, Ile209, Phe215, Arg256, His263	Glu22, Gly76, Asp79, Thr115, His151, Ser152, Cys181, Trp252, Thr255, Ala259, Ala260, Leu264	
3	-	Tyr114, Pro180, Cys181, Ile209, Phe215, Ala260, His263	Phe77, Ile78, Ths115, His151, Ser152, Arg256, Leu264	
4	-	Tyr114, Pro180, Ile209, Phe215, Ala260, His263	Phe77, Ile78, His151, Ser152, Val210, Ala259, Leu264	
5	-	Phe77, Tyr114, Pro180, Phe215, Trp252, Arg256, Ala259, His263, Leu264	Ile78, Asp79, His151, Ser152, Ile209, Thr255, Ala260	
6	-	Ile78, Pro180, Ile209	Phe77, Tyr114, Phe215, Ala259, Ala260, His263, Leu264	
7	Phe77, Ser152,	Phe77, Ile78, Tyr114, Ala178,	Gly76, Asp79, His151, Leu153, Ile209, Thr255, Ala260, Leu264	

Comp.	Conventional	Residual interactions	
	Hydrogen Bond	Hydrophobic/Pi-interaction	Van der Waals
	His263	Pro180, Phe215, Trp252, Arg256, Ala259	
8	Asp79, Ser152, Arg256, His263	Tyr114, Pro180, Phe215, Ala260, His263, Leu264	Gly76, Phe77, Ile78, Trp85, His151, Leu153, Ala178, Glu179, Ile209, Trp252, Thr255, Phe258, Ala259, Tyr267
9	Phe77, Phe215	Tyr114, Phe215, Ala260, His263, Leu264	Gly76, Asp79, Trp85, His151, Ser152, Leu153, Ala178, Glu179, Pro180, Ile209, Arg256, Ala259
10	Glu233, Tyr288, Thr292, Arg339, Glu370, Asn384, Asp387	Pro235, Asn294, Asp328, Arg337, Asp387	Asn229, Phe291, Thr329, Gly330, Lys367, Tyr369, Glu385, Phe386, Ser388, Asp389,
11	Asp79, Ser152, Phe215, His263	Phe77, Ile78, Tys114, His151, Pro180, Phe215, Trp252, Arg256, Ala259, Ala260, His263, Leu264	Gly76, Trp85, Ala178, Glu179, Ile209, Thr255

Comp.	Conventional	Residual interactions	
	Hydrogen Bond	Hydrophobic/Pi-interaction	Van der Waals
12	Asp79, Arg256	Tyr114, His151, Phe215, Arg256, Ala259, Ala260, His263, Leu264	Gly76, Phe77, Ile78, Trp85, Ser152, Leu153, Ala178, Glu179, Pro180, Ile209, Trp252, Thr255, Phe258
13	Phe77, Asp79, His151, Ser152, Thr255	Phe77, Tyr114, Ser152, Phe215, His263, Leu264	His75, Gly76, Ile78, Trp85, Leu153, Pro180, Ile209, Arg256, Ala259, Ala260
14	Phe215	Asp79, Tyr114, His151, Phe215, Ala260, His263	His75, Gly76, Phe77, Trp85, Ser152, Ala178, Glu179, Pro180, Ile209, Arg256, Leu264
15	Phe77, Ser152	Tyr114, Phe215, Pro180	Gly76, Ile78, Asp79, Trp85, His151, Ala178, Glu179, Ile209, Arg256, Ala259, Ala260, His263, Leu264, Tyr267
16	Asp79	Phe77, Tyr114, Phe215, Ala260, His263, Leu264	Gly76, Trp85, His151, Ser152, Leu153, Ala178, Pro180, Ile209, Arg256, Ala259, Tyr167
17	Ser152	Tyr114, Pro180, Ile209, Phe215	Gly76, Phe77, Ile78, Asp79, His151, Leu153, Ala178, Glu179, Arg256, Ala259, Ala260, His263, Leu264, Tyr267
18	Phe77, Asp79, His151	Phe77, Tys114, Pro180, Phe215, Ala260, His263, Leu264	His75, Gly76, Ile78, Trp85, Ser152, Leu153, Ile209, Arg256, Tyr267

Comp.	Conventional	Residual interactions	
	Hydrogen Bond	Hydrophobic/Pi-interaction	Van der Waals
19	Asp79, Ser152, Phe215	Phe77, Ile78, Tyr114, Ala178, Glu179, Pro180, Phe215, Trp252, Arg256, Ala259, Ala260, Leu264	Gly76, His151, Ile209, Thr255, His263
20	Ser152, His263	Tyr114, Ala178, Pro180, Phe215	Gly76, Phe77, Gly179, Ile209
21	Ser152	Tyr114, Ala178, Pro180, Phe215, His263	Phe77, Leu153, Ile209
22	Ser152	Tyr114, Ala178, Pro180, Phe215, His263	Phe77, Glu179
23	Tyr288, Thr292, Asp328, Asp331, Arg339	Asn384, Glu385	Asn229, Pro235, Gly236, Phe291, Asn294, Thr329, Gly330, Ala332, Arg337, Asp387
24	-	Tyr114, Ala178, Pro180, Phe215	Phe77, Ser152, Ile209, His263
25	Ser152	Tyr114, Ala178, Pro180, Phe215	Phe77, Ile209, His263

Comp.	Conventional		Residual interactions	
	Hydrogen Bond	Hydrophobic/Pi-interaction	Van der Waals	
26	His263	Ala260, Leu264	Gly76, Phe77, Asp79, His151, Ser152, Arg256, Ala259	
27	-	His151, Arg256, Ala260, His263, Leu264	Gly76, Phe77, Asp79, Ser152, Phe215, Ala259, Tyr267	
28	-	Phe215, His263	Gly76, Phe77, Tyr114, Ser152, Leu153, Ala178, Pro180, Ile209	
29	Phe77, Ser152, Phe215	His151, His263	Gly76, Ile78, Tyr114, Ala178, Glu179, Pro180, Ala260	
30	-	His151, His263	His75, Gly76, Phe77, Asp79, Trp85, Ser152, Phe215, Arg256, Ala260, Leu264, Tyr267	
31	Asp257, Phe258, Asn262	Glu233, Lys238, Cys261	Cys237, Gln244, Ala259, Ala260, His263	
32	Leu213, Asp257, Phe258	Asn262	Asp205, Asn212, Gly214, Glu233, Lys239, Asn240, Ile241, Gln244, Ala260, Cys261, His263	
33	Gly76, Asp79, Ser152, His263	Phe77, Tyr114, Phe215	His75, Ile78, Trp85, His151, Ala178, Glu179, Pro180, Ile209, Arg256, Ala259, Ala260, Leu264	
34	Phe77	Tyr114, Ala178,	Gly76, Asp79, His151, Ser152, Ile209, His263, Leu264	

Comp.	Conventional		Residual interactions	
	Hydrogen Bond	Hydrophobic/Pi-interaction	Van der Waals	
		Pro180, Phe215		
35	Asp79, His151, Ser152	Gly76, His263	His75, Phe77, Trp85, Ala178, Phe215, Arg256, Leu264	
36	Ser152	Tyr114, Ala178, Phe215, His263	Phe77, Glu179, Pro180, Ile209	
37	Ser152	Tyr114, Ala178, Pro180, Phe215, His263	Phe77, Ile209	
38	Phe77, Ser152	Tyr114, Pro180, Ile209, Phe215	Gly76, Ile78, Ala178, His263	
39	Phe77	Tyr114, Pro180, Phe215	Gly76, His151, Ser152, Ala178, Ile209, Ala260, His263, Leu264	
40	Phe77, Arg256	Tyr114, Pro180, Phe215, Ala260, His263	Ile78, Asp79, His151, Ser152, Ala178, Ile209, Leu264	
41	Ser12, Arg122, Glu160, Arg163	-	-	
42	Asp205, Leu213	-	Gly214, Phe215, Lys238, Lys239, Asn240, Ile241, Gln244, Phe258, Ala259, Ala260, Cys261, Asn262, His263	

Comp.	Conventional		Residual interactions	
	Hydrogen Bond	Hydrophobic/Pi-interaction	Van der Waals	
43	Asp205, Cys237	Leu213	Asn212, Gly214, Phe215, Lys238, Lys239, Asn240, Ile241, Gln244, Phe258, Ala259, Ala260, Cys261, Asn262, His263	
44	-	Val210, Phe215	Glu22, Phe77, Ile78, Tyr114, Glu179, Pro180, Cys181, Gln183, Ile209, Leu213, His263	
45	-	Asp205	Ala207, Asn212, Leu213, Gly214, Phe215, Glu233, Lys238, Lys239, Ile241, Gln244, Phe258, Ala259, Ala260, Asn262, His263,	
46	-	Tyr114, Pro180, Cys181, Phe215, Arg256, Ala259, Ala260, His263, Leu264	Phe77, Ile78, Asp79, Thr115, His151, Ser152, Ala178, Glu179, Ile209	
47	Gly76, His151	His263	Phe77, Asp79, Ser152, Phe215, Arg256, Ala260, Leu264	
48	-	Phe77, Ile78, Tyr114, His151, Pro180, Phe215, His263	Gly76, Ser152, Ala178, Ile209	
49	Ser152	Tyr114, Ala178, Pro180, Phe215, His263	Phe77, Glu179, Ile209	
50	Leu213, Cys237, Gln244,	Glu233, Ala260	Asp205, Gly214, Phe215, Lys238, Lys239	

Comp.	Conventional	Residual interactions	
	Hydrogen Bond	Hydrophobic/Pi-interaction	Van der Waals
	Cys261, Asn262, His263		
51	-	Tyr114, Ala178, Pro180, Phe215, Arg256, Ala259, Ala260, His263, Leu264	Phe77, Ile78, Ser152, Glu179, Ile209, Leu213
52	Phe77	Asp79, Tyr114, His151, Pro180, Phe215, Arg256, Ala259, Ala260, Leu264	Gly76, Ile78, Ser152, Leu153, Ala178, Ile209, His263
53	Phe77, Arg256	Phe77, Ile78, Tyr114, Pro180, Arg256, Ala259, Ala260, His263, Leu264	Gly76, Asp79, His151, Ser152, Leu153, Ile209, Phe215, Trp252
54	Ser152	Phe77, Phe215, His263	Gly76, Ile78, Asp79, Tyr114, His151, Leu153, Ala178, Arg256, Ala260, Leu264, Tyr267
55	Phe77, Ser152	Phe77, Asp79, Tyr114, Ala178, Pro180, Phe215,	Gly76, Ile78, His151, Leu153, Ile209, Arg256, Leu264

Comp.	Conventional		Residual interactions	
	Hydrogen Bond	Hydrophobic/Pi-interaction	Van der Waals	
		His263		
56	Phe77, Ser152	Phe77, Ile78, Asp79, Tyr114, His151, Ala178, Pro180, Phe215, His263	Gly76, Leu153, Ile209, Arg256, Leu264	
57	-	Phe77, His151, His263, Leu264	His75, Gly76, Asp79, Trp85, Tyr114, Ser152, Phe215, Arg256, Ala260	
58	Cys261, Asn262, His263	-	Asp205, Leu213, Glu233, Cys237, Lys238, Gln244, Asp257, Phe258, Ala259, Ala260,	
59	Ser152	Tyr114, Pro180, Phe215, Ala260	Phe77, Ile78, Ala178, Glu179, Ile209, Ala259, His263	
60	Ser152	Phe77, Ile78, Tyr114, Pro180, Phe215	Ala178, Ile209, His263	
61	-	Phe215, Ala259	Phe77, Ile78, Tyr114, Ser152, Ala178, Pro180, Ala260, His263	
62	Ser152	Phe215, Ala260, His263	Phe77, Tyr114, Ala178, Pro180, Ile209	
63	Asp79, His151, Ser152,	Gly76, Phe77, Tyr114, Pro180, Phe215	Ile78, Leu153, Asp257, Ala259, Ala260, Leu264	

Comp.	Conventional	Residual interactions	
	Hydrogen Bond	Hydrophobic/Pi-interaction	Van der Waals
	Arg256, His263		
64	Asp205, Asn212, Cys237, Asp257, Phe258, Asn262	Glu233, Cys261	Ala207, Leu213, Gly214, Lys238, Lys239, Gn244, Ala259, Ala260
65	Phe77, Asp79	Ala260, His263, Leu264	His75, Gly76, Trp85, His151, Ser152, Arg256, Tyr267
66	Arg256	Ile78, Tyr114, Ala178, Pro180, Ile209, Phe215, Ala259, Ala260, His263	Phe77, Asp79, His151, Ser152, Leu153, Leu213, Leu264
Orlistat	Gly76, His151	Phe77, Ile78, Asp79, Tyr114, Pro180, Phe215, Ala259	His75, Trp85, Ser152, Ala178, Ile209, Trp252, Thr255, Arg256, Ala260, His263, Leu264, Tyr267

Table 5 listed all the amino acids residue divided into 3 types of interaction (conventional hydrogen bond, hydrophobic/Pi-interaction, and Van der Waals force) with the active site of the HPL.

The lactone ring in orlistat acts as the catalyst and has been discovered to interact covalently with Ser152, a crucial amino acid in the catalytic triad. Five phytochemicals (**48**, **49**, **50**, **59**, and **60**) out of the 66 presented with lactone. **48**,

Due to the fact that phytochemicals **7-13** are flavonols and flavonol glycosides, which has been reported to have pancreatic lipase inhibitory activity, they showed a good binding energy [180, 181]. The bioavailability of flavonoids increased by glycosylation, which significantly improves their water solubility. Glycosides typically exhibit less biological activity, including antioxidants, although certain particular bioactivities are boosted [182].

4.2.3 *In silico* study of phytochemicals of *A. indicum* as α -chymotrypsin inhibitors

Molecular docking studies were performed against protein structure of α -chymotrypsin (PDB ID: 5J4S) [183]. An amino acid replacement in P1 of carboxyl-protected BBI was made possible because of the earlier protein chemistry study on the protein, showing that Leu43 could be substituted by Met, Phe, or Trp and still maintain the α -chymotrypsin inhibition [184]. Two phytochemicals have shown the binding scores less than chymostatin with -9.1 kcal/mol (**Table 6**).

Table 7 Calculated free binding energy (kcal/mol) of the phytochemicals (**1-66**) from *A. indicum* against α -chymotrypsin (PDB ID: 5J4S)

Phyto-chemicals	Binding energy (kcal/mol)	Phyto-chemicals	Binding energy (kcal/mol)	Phyto-chemicals	Binding energy (kcal/mol)
1	-6.8	23	-7.8	45	-7.7
2	-8.3	24	-5.3	46	-3.9
3	-7.2	25	-5.1	47	-5.9
4	-6.8	26	-5.4	48	-5.7

Phyto-chemicals	Binding energy (kcal/mol)	Phyto-chemicals	Binding energy (kcal/mol)	Phyto-chemicals	Binding energy (kcal/mol)
5	-6.8	27	-5.7	49	-5.4
6	-6.8	28	-5.3	50	-5.9
7	-7.1	29	-5.0	51	-6.8
8	-8.5	30	-6.6	52	-7.0
9	-7.7	31	-6.1	53	-7.5
10	-7.7	32	-7.2	54	-6.9
11	-9.2	33	-6.5	55	-6.4
12	-9.3	34	-6.3	56	-6.4
13	-8.5	35	-5.1	57	-6.7
14	-7.0	36	-5.3	58	-6.3
15	-8.7	37	-5.3	59	-6.8
16	-6.9	38	-5.8	60	-6.9
17	-8.4	39	-6.1	61	-5.3
18	-8.6	40	-6.1	62	-5.1
19	-8.3	41	-4.8	63	-7.3
20	-5.3	42	-8.2	64	-7.4
21	-5.8	43	-7.2	65	-5.8
22	-6.1	44	-6.9	66	-4.3
Chymo-	-9.1				

Phyto-chemicals	Binding energy (kcal/mol)	Phyto-chemicals	Binding energy (kcal/mol)	Phyto-chemicals	Binding energy (kcal/mol)
-----------------	---------------------------	-----------------	---------------------------	-----------------	---------------------------

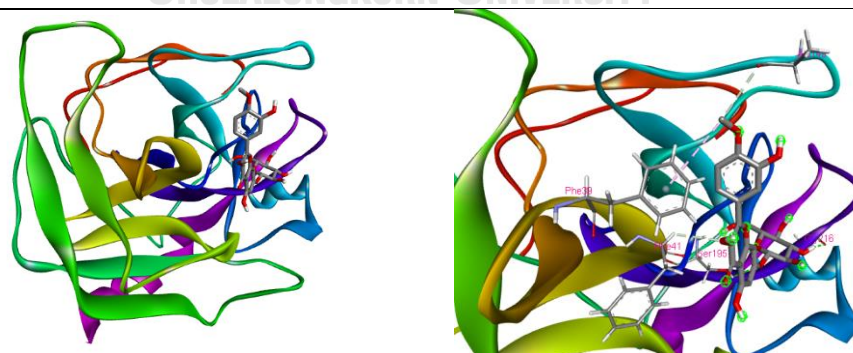
statin

Two flavonoids from flowers, quercetin-3-*O*- α -rhamnopyranosyl (1 \rightarrow 6)- β -glucopyranoside (**11**) and gossypetin-8-*O*-glucoside (**12**), out of 66 phytochemicals from *A. indicum* exhibited better binding energy than good α -chymotrypsin with -9.1 kcal/mol.

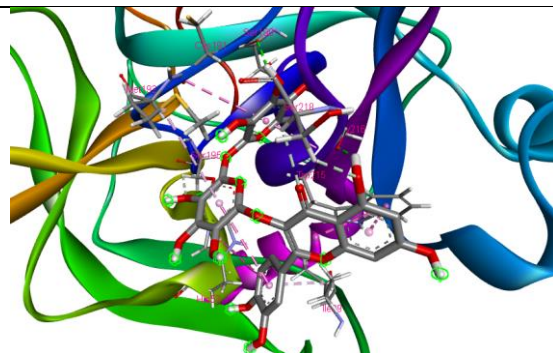
Figure 13 showed the 3D presentation of the phytochemicals from *A. indicum* (1-66) in the active site of α -chymotrypsin (PDB code: 5J45). It demonstrated that the phytochemicals occupying the same site as chymostatin.



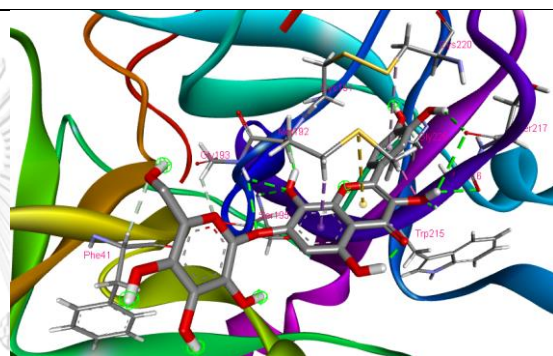
2



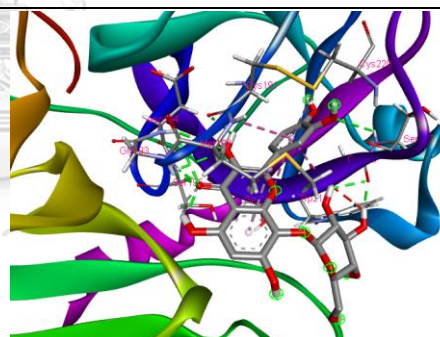
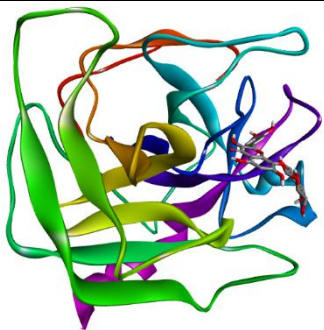
8



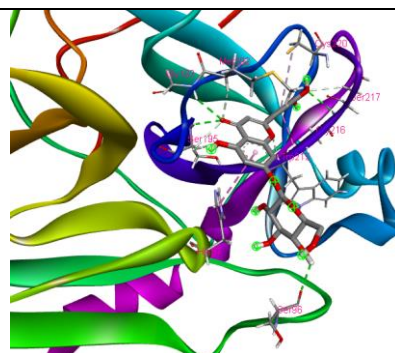
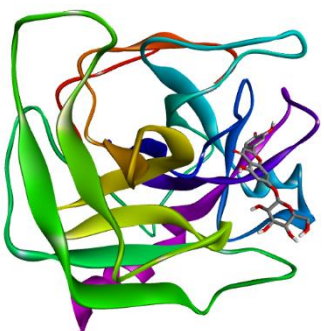
11



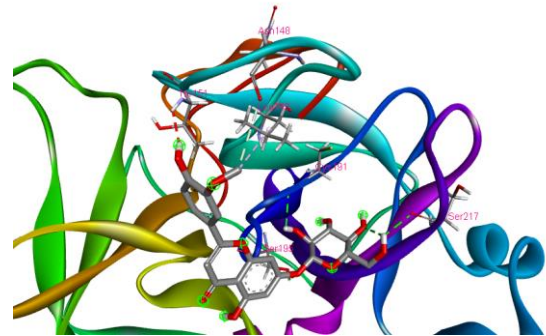
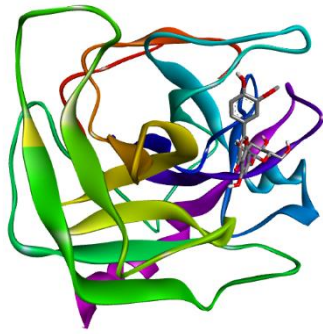
12



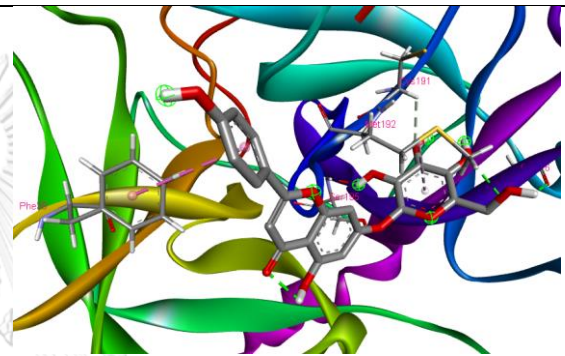
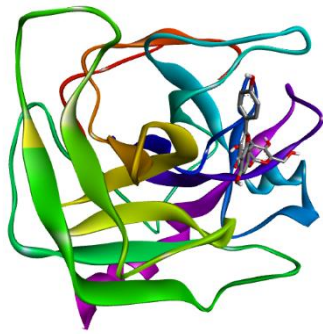
13



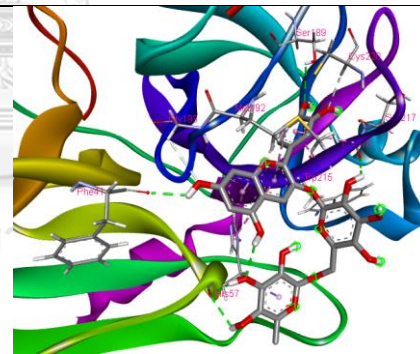
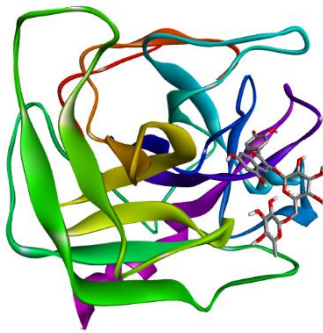
15



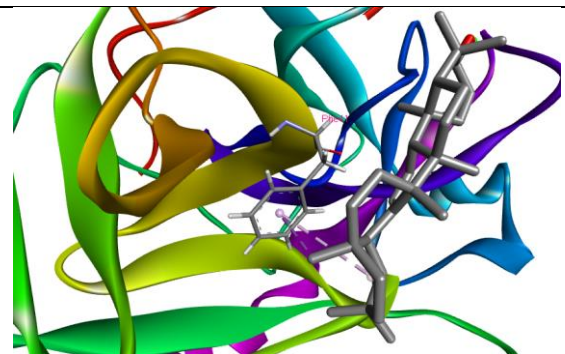
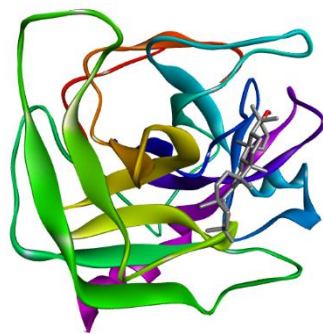
17



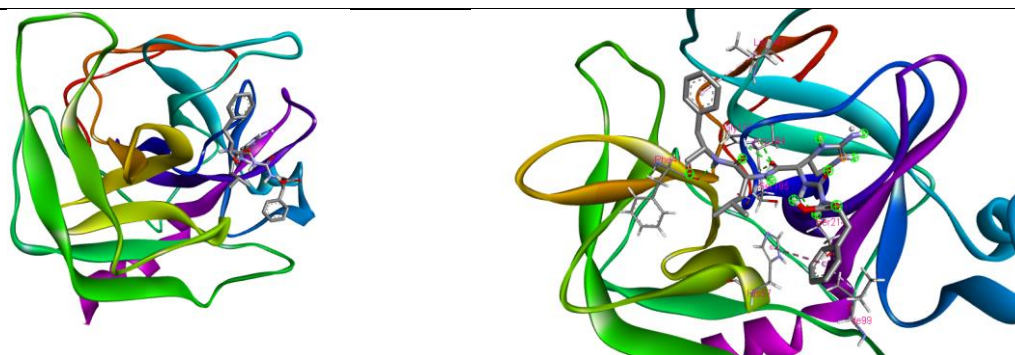
18



19

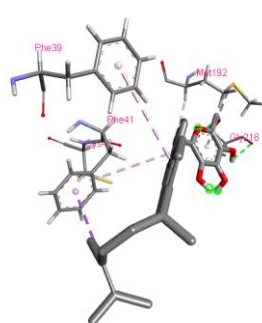


42

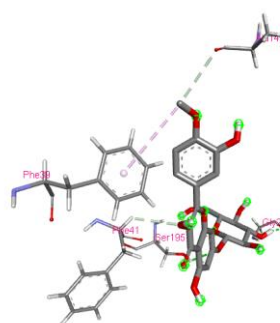


Chymostatin

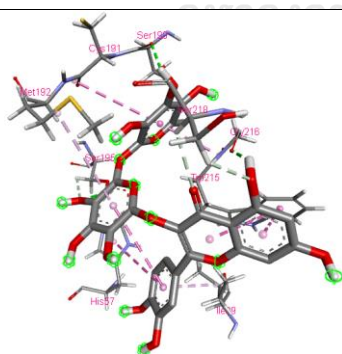
Figure 13 3D presentation of the phytochemicals from *A. indicum* in the active site of α -chymotrypsin (PDB code: 5J4S)



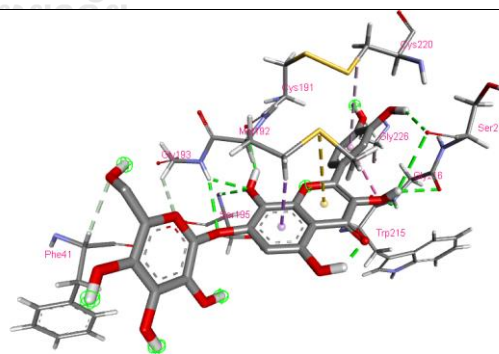
2



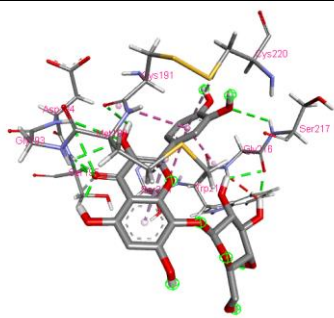
8



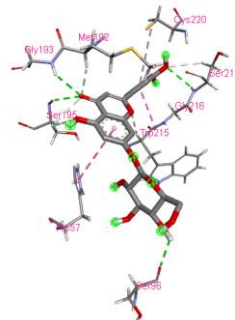
11



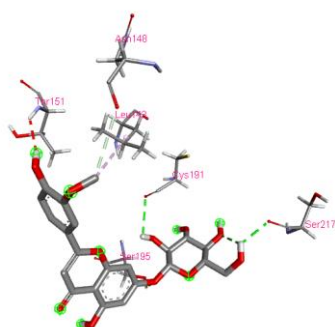
12



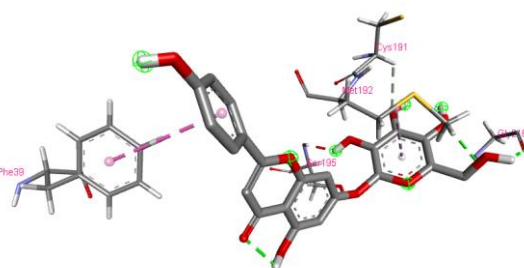
13



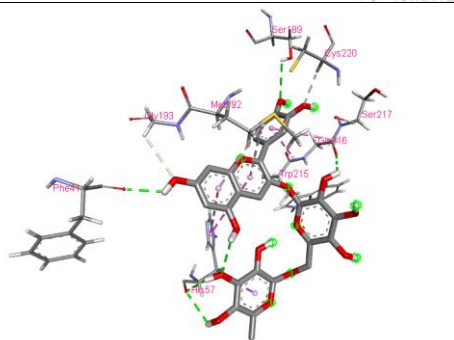
15



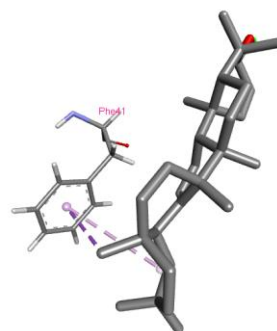
17



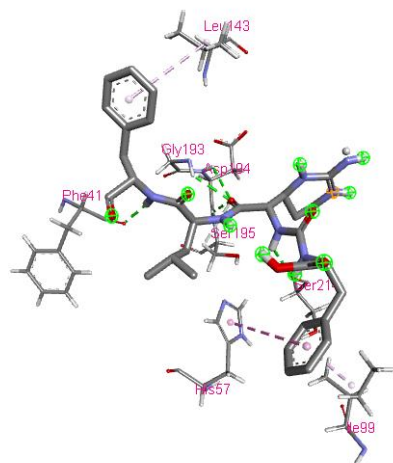
18



19



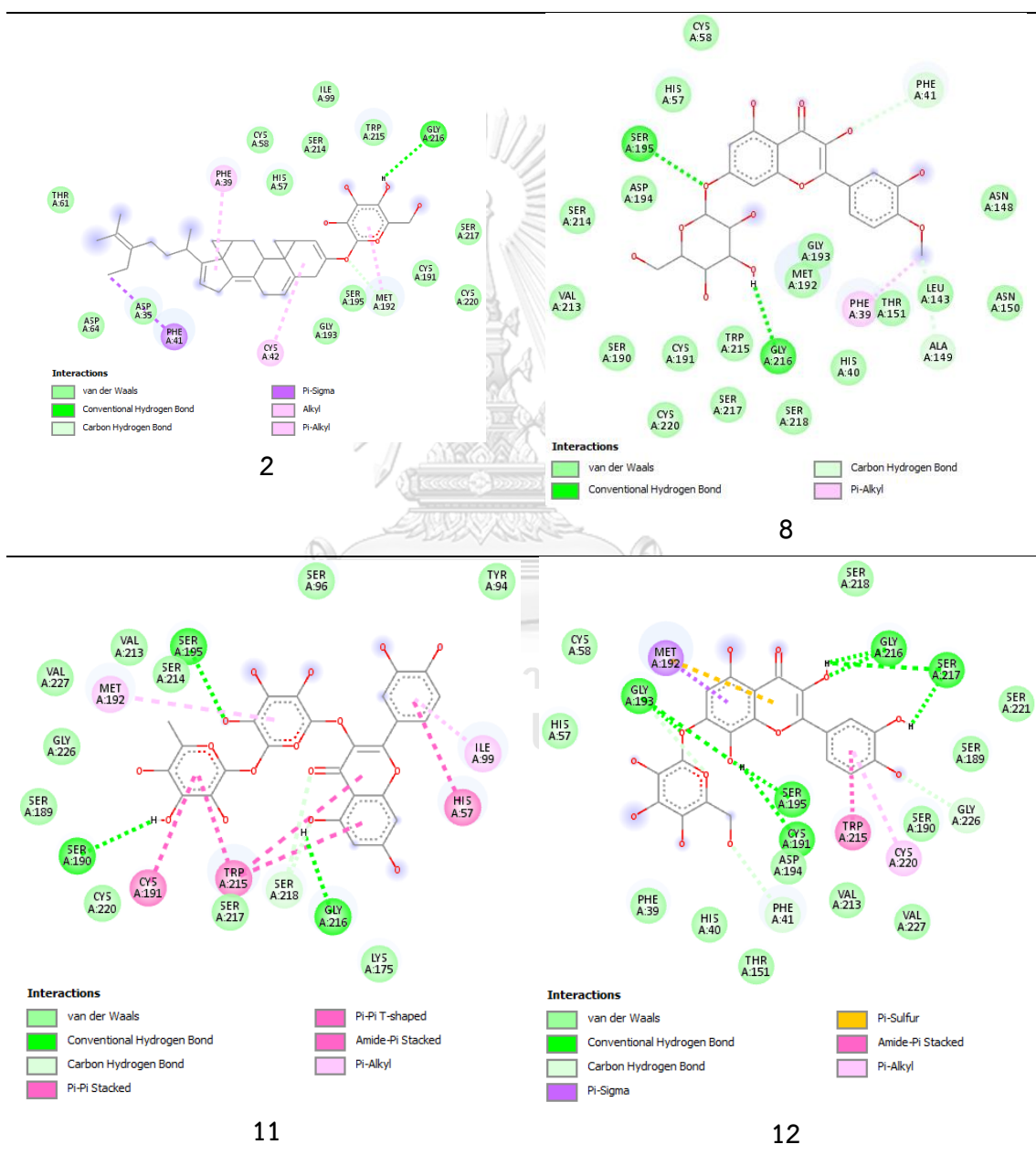
42

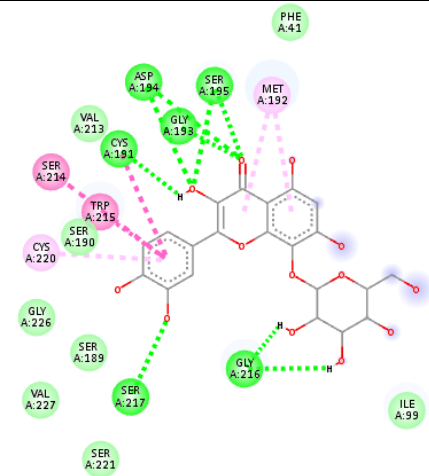


Chymostatin

Figure 14 3D molecular amino interaction of the phytochemicals of *A. indicum* in the binding site of α -chymotrypsin (PDB code: 5J4S)

Figure 15 depicted the amino acids residual and its interaction types.





Interactions

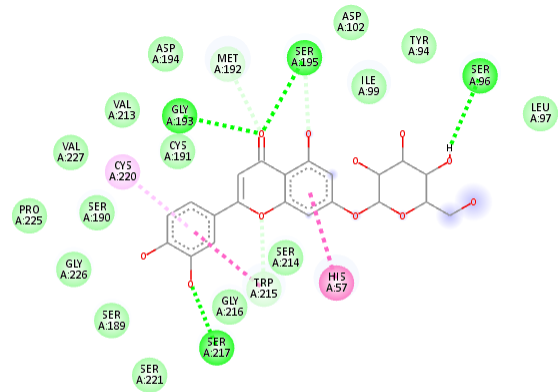
- van der Waals
- Conventional Hydrogen Bond
- Carbon Hydrogen Bond

■ Unfavorable Donor-Donor

■ Amide-Pi Stacked

■ Pi-Alkyl

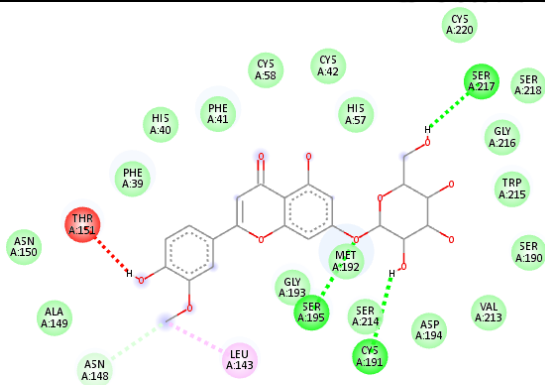
13



Interactions

- van der Waals
- Conventional Hydrogen Bond
- Carbon Hydrogen Bond
- Pi-Pi T-shaped
- Amide-Pi Stacked
- Pi-Alkyl

15



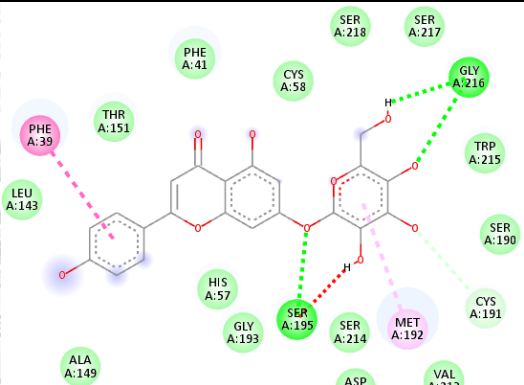
Interactions

- van der Waals
- Conventional Hydrogen Bond
- Carbon Hydrogen Bond

■ Unfavorable Donor-Donor

■ Alkyl

17



Interactions

- van der Waals
- Conventional Hydrogen Bond
- Carbon Hydrogen Bond

■ Unfavorable Donor-Donor

■ Pi-Pi T-shaped

■ Pi-Alkyl

18

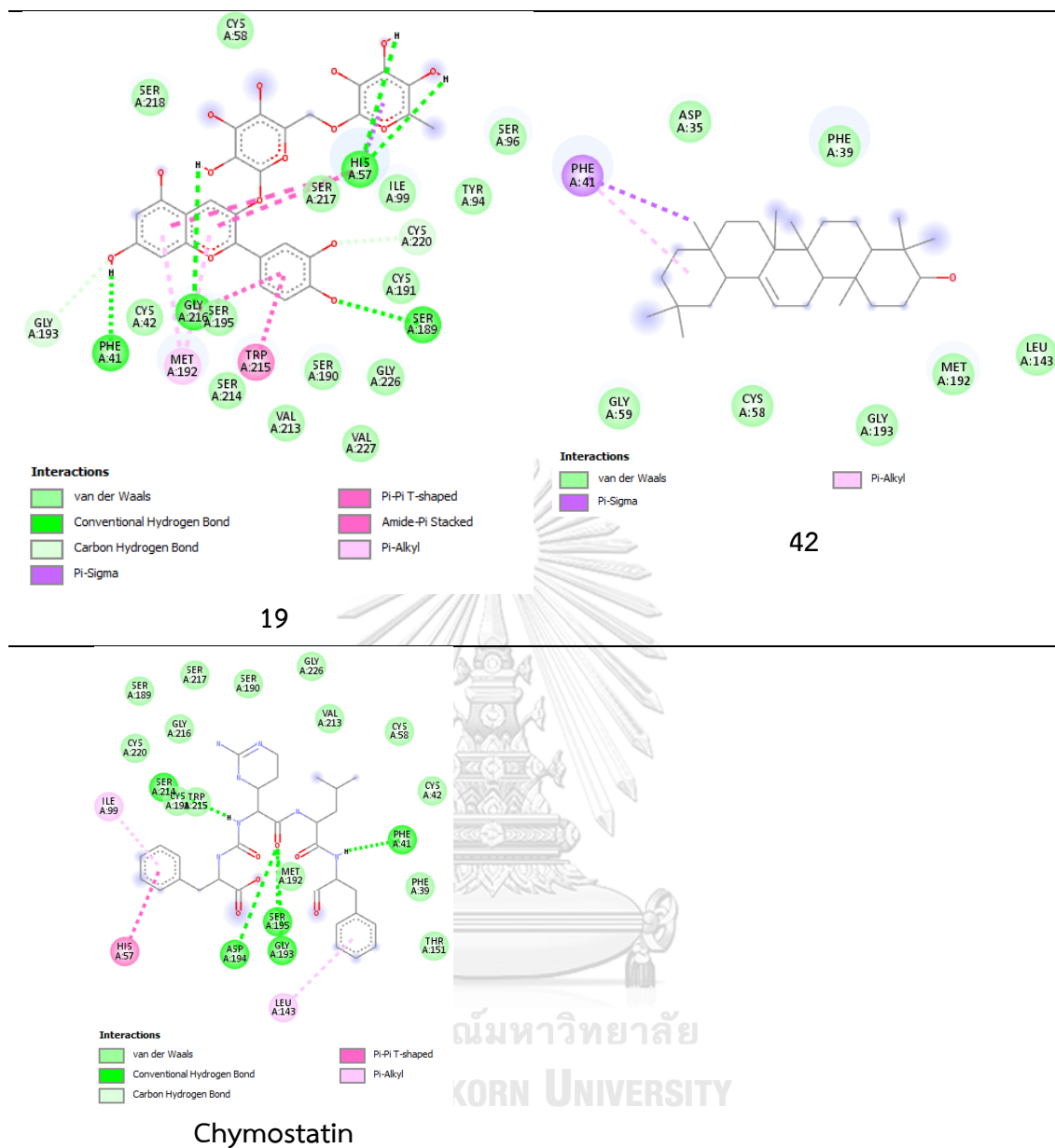


Figure 15 Amino acids residual interactions of the interacting pocket between α -chymotrypsin (PDB ID: 5J4S) and ligands

Table 7 below listed all the amino acids residue divided into 3 types of interaction (conventional hydrogen bond, hydrophobic/Pi-interaction, and Van der Waals force) with the active site of the α -chymotrypsin (PDB ID: 5J4S).

Table 8 The type of molecular interactions of the phytochemicals (1-66) within the active site of the α -chymotrypsin (PDB ID: 5J4S)

Comp.	Conventional Hydrogen Bond	Residual interactions	
		Hydrophobic/Pi- interaction	Van der Waals
1	Gly59, Asp64	Phe41	Asp35, Phe39, Cys58, Val60, Thr61, Leu143, Ala149, Thr151, Met192, Gly193
2	Gly216	Phe39, Phe41, Cys42, Met192	Asp35, His57, Cys58, Thr61, Asp64, Ile99, Cys191, Gly193, Ser195, Ser214, Trp215, Ser217, Cys220
3	-	Ser63, Asp64	Asp35, Phe39, His40, Phe41, Cys58, Gly59, Val60, Thr61, Thr151, Met192, Gly193
4	-	Phe39, Phe41, Ser63, Asp64	Asp35, Cys58, Gly59, Thr61
5	Asp64	Phe39, Phe41	Asp35, His40, Cys58, Gly59, Val60, Thr61, Leu143, Thr151, Met192, Gly193
6	-	His57, Trp172, Trp215	Tyr94, Ser96, Ile99, Lys175, Gly216, Ser218
7	Gly193, Asp194, Ser195, Gly216	Ser190, Ser192, Ser217, Cys220	Phe41, Cys42, His57, Cys191, Val213, Trp215, Ser218
8	Ser195, Gly216	Phe39, Phe41, Ala149	His40, His57, Cys58, Leu143, Asn148, Asn150, Thr151, Ser190, Cys191, Met192, Gly193, Asp194, Val213, Ser214, Trp215, Ser217, Ser218,

Comp.	Conventional	Residual interactions	
	Hydrogen Bond	Hydrophobic/Pi- interaction	Van der Waals
			Cys220
9	Ser190, Cys191, Ser217	Trp215, Gly216, Cys220	His57, Ser189, Met192, Gly193, Asp194, Ser195, Val213, Ser214, Gly226
10	Cys58, Cys191, Gly193, Ser195	Cys42, His57, Met192	Phe41, Gly59, Ile99, Ser190, Asp194, Val213, Ser214, Trp215, Gly216, Ser217
11	Ser190, Ser195, Gly216	His57, Ile99, Cys191, Met192, Trp215, Ser218	Tyr94, Ser96, Lys175, Ser189, Val213, Ser214, Ser217, Cys220, Gly226, Val227
12	Cys191, Gly193, Ser195, Gly216, Ser217	Phe41, Met192, Trp215, Cys220, Gly226	Phe39, His40, His57, Cys58, Thr151, Ser189, Ser190, Asp194, Val213, Ser218, Ser221, Val227
13	Cys191, Gly193, Asp194, Ser195, Gly216, Ser217	Cys191, Met192, Ser214, Trp215, Cys220	Phe41, Ile99, Ser189, Ser190, Val213, Ser221, Gly226, Val227
14	Ser96, Ser195, Ser217	His57, Ile99, Met192	Tyr94, Leu97, Cys191, Gly193, Asp194, Ser214, Trp215, Gly216, Ser218, Cys220
15	Ser96, Gly193, Ser195, Ser217	His57, Met192, Ser195, Trp215, Cys220	Tyr94, Leu97, Ile99, Asp102, Ser189, Ser190, Cys191, Asp194, Val213, Ser214, Gly216, Ser221, Pro225, Gly226, Val227
16	Ser96, Ser195, Ser217	His57, Ile99,	Cys191, Gly193, Asp194, Ser214,

Comp.	Conventional Hydrogen Bond	Residual interactions	
		Hydrophobic/Pi- interaction	Van der Waals
		Met192	Trp215, Gly216, Cys220
17	Cys191, Ser195, Ser217	Leu143, Asn148, Thr151	Phe39, His40, Phe41, Cys42, His57, Cys58, Ala149, Asn150, Ser190, Met192, Gly193, Asp194, Val213, Ser214, Trp215, Gly216, Ser218, Cys220
18	Ser195, Gly216	Phe39, Cys191, Met192	Phe41, His57, Cys58, Leu143, Ala149, Thr151, Ser190, Gly193, Asp194, Val213, Ser214, Trp215, Ser217, Ser218
19	Phe41, His57, Ser189, Gly216	His57, Met192, Gly193, Trp215, Gly216, Cys220	Cys42, Cys58, Tyr94, Ser96, Ile99, Cys190, Cys191, Ser195, Val213, Ser214, Ser217, Ser218, Gly226, Val227
20	Ser190, Ser217	Trp215	Ser189, Cys191, Met192, Val213, Ser214, Gly216, Cys220, Gly226
21	Ser190, Ser217	Trp215, Cys220	Ser189, Cys191, Met192, Ser195, Val213, Ser214, Gly216, Gly226
22	Ser189, Ser190, Ser214, Ser217	Met192, Trp215, Gly216	His57, Cys191, Ser195, Val213, Ser218, Cys220, Gly226
23	His57, Ser96, Cys191, Gly216	Gly193, Asp194, Ser195, Trp215,	Cys58, Tyr94, Ile99, Ser189, Ser190, Met192, Val213, Ser214, Ser217,

Comp.	Conventional Hydrogen Bond	Residual interactions	
		Hydrophobic/Pi- interaction	Van der Waals
		Ser218	Gly226
24	Gly193, Asp194, Ser195	Ser190, Cys191, Met192	Val213, Trp215, Gly216, Ser217, Gly226
25	Ser195	Cys191, Met192, Ser214, Cys220	Ser189, Ser190, Asp194, Val213, Trp215, Gly216, Ser217
26	Ser217	Ser190, Cys191, Met192, Val213, Ser214, Cys220, Tyr228	Ser189, Gly193, Asp194, Ser195, Trp215, Gly216, Gly226, Val227
27	Cys220, Val227	Cys191, Ser214, Cys220, Pro225, Gly226	Ser189, Ser190, Met192, Ser195, Val213, Trp215, Gly216, Ser217, Tyr228
28	Ser214	-	His57, Ser189, Ser190, Cys191, Met192, Gly193, Asp194, Ser195, Val213, Trp215, Gly216, Ser217, Gly226
29	Ser195	His57, Ser190, Cys191, Met192, Val213, Trp215	Asp194, Ser214, Gly216, Ser217, Ser218
30	Ser190, Cys191, Gly193	Met192, Ser214, Cys220	Ser189, Asp194, Ser195, Val213, Trp215, Gly216, Ser217, Gly226,

Comp.	Conventional		Residual interactions	
	Hydrogen Bond		Hydrophobic/Pi- interaction	Van der Waals
				Val227
31	Ser189, Ser190, Ser217	Met192, Cys220		Cys191, Gly193, Ser195, Val213, Ser214, Trp215, Gly216, Gly226, Val227
32	Phe41, Gly193, Ser195, Ser217	Ser190, Cys191, Met192, Ser214, Gly216		His57, Cys58, Asp194, Val213, Trp215, Cys220, Gly226
33	His57, Cys191	Phe41, Ser190, Met192, Asp194, Ser195, Trp215		Phe39, Cys42, Cys58, Gly193, Val213, Ser214, Gly216, Ser217
34	Ser189, Ser195, Ser217	Gly193, Ser214, Trp215, Cys220		Ser190, Cys191, Met192, Asp194, Val213, Gly216, Ser221, Gly226, Val227
35	Cys58, Asp64	Phe41		Asp35, Phe39, Gly59, Val60
36	Phe41, Gly193, Gly216	Met192		Cys42, His57, Cys191, Ser195, Ser214, Trp215, Ser217
37	Gly193, Gly216, Ser217	Met192		Phe41, Cys42, His57, Cys58, Cys191, Ser195, Trp215, Ser218
38	Gly193, Ser195	Ser190, Met192		His57, Ser189, Cys191, Asp194, Val213, Ser214, Trp215, Gly216, Ser217, Gly226, Val227

Comp.	Conventional Hydrogen Bond	Residual interactions	
		Hydrophobic/Pi- interaction	Van der Waals
39	Gly193, Asp194, Ser195	Cys191, Ser214, Cys220	Ser189, Ser190, Met192, Val213, Trp215, Gly216, Ser217, Ser221, Gly226
40	Ser190	Cys191, Ser214, Trp215	His57, Ile99, Ser189, Met192, Ser195, Val213, Gly216, Ser217, Cys220, Gly226, Val227
41	Asp194	Ser190, Met192, Ser214	Cyr191, Gly193, Ser195, Val213, Trp215, Gly216, Val227
42	-	Phe41	Asp35, Phe39, Cys58, Gly59, Leu143, Met192, Gly193
43	Gly69, Glu78	-	Ile6, Pro24, Gly25, Glu70, Phe71, Lys79, Ser115, Gln116, Thr117
44	-	His57, Ile99, Met192	Phe41, Cys58, Gly59, Asp64, Asp95, Phe99, Cys191, Gly193, Ser195, Ser214, Trp215, Gly216, Ser217, Ser218
45	No interaction		
46	-	Lys36, Phe41	Asp35, Thr37, Cys58, Gly59, Thr61, Ser63, Asp64
47	-	Met192, Ser214, Cys220, Val227	Ser189, Ser190, Cys191, Ser195, Val213, Trp215, Gly216, Ser217, Gly226, Tyr228

Comp.	Conventional	Residual interactions	
	Hydrogen Bond	Hydrophobic/Pi- interaction	Van der Waals
48	Gly193, Ser195	His57, Met192	Phe41, Ser190, Cys191, Asp194, Trp215, Gly216
49	Gly216	His57, Met192, Trp215	Ser189, Ser190, Cys191, Ser195, Val213, Ser214, Ser217, Cys220
50	Gly193	Ser192, Met192, Gly216	Cys191, Asp194, Ser195, Val213, Trp215, Ser217, Ser218
51	Gly193, Ser195, Ser214	His57, Ile99, Met192	Tyr94, Ser96, Ser190, Cys191, Asp194, Val213, Trp215, Gly216, Ser217
52	-	His57, Trp215	Phe41, Cys42, Ile99, Ser189, Ser190, Cys191, Met192, Gly193, Ser195, Val213, Ser214, Gly216, Ser217, Cys220, Pro225, Gly226
53	Ser189, Cys191, Ser214, Ser217	Ile99, Trp215, Cys220	Lys175, Ser190, Met192, Gly193, Asp194, Ser195, Ser213, Gly216, Ser221, Gly226
54	Ser189, Ser217	Met192, Trp215, Cys220	His57, Ser190, Cys191, Ser195, Val213, Ser214, Gly216, Gly226, Val227
55	His57, Asp194, Ser195	His57, Met192	Phe41, Ile99, Cys191, Gly193, Ser214, Trp215, Gly216
56	His57, Asp194,	Met192	Phe41, Ile99, Cys191, Gly193,

Comp.	Conventional		Residual interactions	
	Hydrogen Bond		Hydrophobic/Pi- interaction	Van der Waals
	Ser195			Ser214, Trp215, Gly216
57	Gly193, Asp194, Ser195, Gly216, Ser217	Met192		Ser190, Cys191, Val213, Trp215, Ser218
58	Thr151	-		Thr37, Gly38, Phe39, His40, Gln73, Pro152, Asp153
59	Thr222, Ser223	Arg145		Val17, Tyr146, Thr147, Thr219, Cys220, Ser221
60	Tyr146, Thr147, Ser223	-		Val17, Arg145, Thr219, Ser221, Thr222
61	Gly69, Lys79, Thr117	Pro24, Phe71		Ile6, Gly25, Glu78, Ile80
62	Gly216	Trp215		His57, Tyr94, Ser96, Ile99, Ser214
63	Phe41, Asp194, Ser195	Met192, Gly216		Cys42, His57, Cys58, Ser190, Cys191, Gly193, Val213, Ser214, Trp215, Ser218
64	Trp215, Gly216, Val227	Met192, Trp215		Ser189, Ser190, Cys191, Ser195, Val213, Ser214, Ser217, Cys220, Pro225, Gly226, Tyr228
65	-	Cys191, Met192, Ser214, Trp215, Cys220		Ser189, Ser190, Val213, Gly216, Ser217, Gly226, Val227

Comp.	Conventional Hydrogen Bond	Residual interactions	
		Hydrophobic/Pi- interaction	Van der Waals
66	Gly193, Asp194, Ser195	Phe41, Leu143	Asp35, Phe39, His40, Cys58, Gly59, Thr151, Cys191, Met192
Chymo- statin	Phe41, Gly193, Asp194, Ser195, Ser214	His57, Ile99, Leu143	Phe39, Cys42, Cys58, Thr151, Ser189, Ser190, Cys191, Met192, Val213, Trp215, Gly216, Ser217, Cys220, Gly226,

Several bonds in the insulin molecule are broken by the trypsin and α -chymotrypsin enzymes. Nevertheless, in order to make the most intact, physiologically active insulin available for absorption, insulin must nevertheless be preserved from the pancreatic digesting enzymes. The potential to increase the absorption of bioactive insulin from the intestine has been demonstrated when different enzyme inhibitors, either non-specific or specific for trypsin or chymotrypsin, are administered together with insulin [185-191]. In non-diabetic human patients, oral administration of chymotrypsin inhibitor with insulin dosages of 1.4–4.2 U/kg resulted in a significant reduction in blood glucose [190].

Furthermore, in type II diabetic individuals who have just been diagnosed, the trypsin/chymotrypsin inhibitor can slow the pace of stomach emptying and lower postprandial plasma glucose, plasma gastric inhibitory polypeptide (GIP), and serum insulin levels. Treatment for type II diabetes may be unique or adjunctive in that it delays stomach emptying in diabetic patients [192]. The delayed stomach emptying might contribute to the development of gastric ulcers. On the other hand, the development of duodenal ulcer may be influenced by fast stomach emptying coupled with gastric acid hypersecretion [193].

4.2.4 The physicochemical properties of the phytochemicals from *A. indicum* based in Lipinski's rule of five

The 66 phytochemicals from *A. indicum* were investigated for the drug-like properties using the ADME (Adsorption, Distribution, Metabolism, and Excretion). In the examination of the structures of orally administered drugs, and potential pharmaceuticals, Lipinski's rule of five highlights the significance of lipophilicity, molecular weight (MW), number of hydrogen bond donors, and number of hydrogen bond acceptors [194, 195]. The test compounds must meet certain requirements, such as the molecular weight (MW) ≤ 500 g/mol, the number of hydrogen bond acceptors ≤ 10 , the number of hydrogen donors ≤ 5 , and the $\log P_{o/w} \leq 5$, and a maximum of 1 violation.

Table 9 The physicochemical properties of the phytochemicals from *A. indicum* based on Lipinski's rule of five

Comp.	Molecular weight (g/mol) (≤ 500)	Σ H-bond acceptors (≤ 10)	Σ H-bond donors (≤ 5)	Log $P_{o/w}$ (≤ 5)	Violation (≤ 1)
1	414.71	1	1	7.24	1
2	576.85	6	4	5.5	1
3	412.69	1	1	6.98	1
4	412.69	1	1	6.86	1
5	386.65	1	1	6.74	1
6	428.69	2	0	6.64	1
7	330.29	7	3	2.02	0
8	478.4	12	7	0.13	2
9	302.24	7	5	1.23	0
10	464.38	12	8	-0.48	2
11	596.49	16	10	-1.66	3
12	480.38	13	9	-0.7	2
13	480.38	13	9	-0.71	2

Comp.	Molecular weight (g/mol) (≤ 500)	Σ H-bond acceptors (≤ 10)	Σ H-bond donors (≤ 5)	Log $P_{o/w}$ (≤ 5)	Violation (≤ 1)
14	286.24	6	4	1.73	0
15	448.38	11	7	0.15	2
16	300.26	6	3	2.18	0
17	448.38	11	7	0.15	2
18	432.38	10	6	0.52	1
19	597.54	15	11	-1.6	3
20	122.12	2	1	1.44	0
21	138.12	3	2	1.05	0
22	168.15	4	2	1.08	0
23	492.43	14	8	-2.51	2
24	136.15	2	1	1.41	0
25	122.12	2	1	1.17	0
26	152.15	3	1	1.2	0
27	182.17	4	1	0.93	0
28	152.15	3	1	1.46	0
29	212.2	5	1	1.36	0
30	170.12	5	4	0.21	0
31	168.15	4	2	0.88	0
32	300.26	8	5	-0.76	0
33	346.29	10	7	-1.45	1
34	164.16	3	2	1.26	0
35	180.16	4	3	0.93	0
36	194.18	4	2	1.36	0
37	208.21	4	1	1.76	0
38	180.2	4	0	1.86	0
39	178.18	3	1	1.81	0
40	256.25	4	1	2.46	0

Comp.	Molecular weight (g/mol) (≤ 500)	Σ H-bond acceptors (≤ 10)	Σ H-bond donors (≤ 5)	Log $P_{o/w}$ (≤ 5)	Violation (≤ 1)
41	116.07	4	2	-0.35	0
42	426.72	1	1	7.27	1
43	426.72	1	1	7.2	1
44	665.13	2	0	12.5	2
45	426.72	1	1	7.27	1
46	410.72	0	0	9.38	1
47	168.15	4	0	0.22	0
48	206.19	4	0	1.84	0
49	192.17	4	1	1.52	0
50	178.14	4	2	1.18	0
51	444.52	4	2	3.89	0
52	299.32	4	2	2.27	0
53	126.11	2	2	0.15	0
54	357.36	6	4	1.92	0
55	216.24	3	3	0.22	0
56	226.23	3	1	2.25	0
57	175.18	2	1	1.97	0
58	260.37	2	0	3.91	0
59	232.32	2	0	3.19	0
60	242.27	3	0	2.18	0
61	208.30	2	1	2.42	0
62	210.31	2	2	2.28	0
63	376.36	8	5	-0.19	0
64	267.24	7	4	-1.49	0
65	135.13	3	2	-0.12	0
66	466.82	2	0	10.54	1
Acarbose	645.60	19	14	-6.22	3

Comp.	Molecular weight (g/mol) (≤ 500)	Σ H-bond acceptors (≤ 10)	Σ H-bond donors (≤ 5)	Log $P_{o/w}$ (≤ 5)	Violation (≤ 1)
Orlistat	495.73	5	1	7.16	1
Chymostatin	607.7	7	6	1.13	3

Four out of the 66 phytochemicals, **2**, **11**, **19**, and **44**, as well as acarbose and chymostatin have molecular weight more than 500 g/mol. Nine from the 66 have hydrogen bond acceptors more than 10 which are phytochemical **8**, **10**, **11**, **12**, **13**, **15**, **17**, **19**, and **23**. Of the 66, phytochemical **8**, **10**, **11**, **12**, **13**, **15**, **17**, **18**, **19**, **23**, and orlistat have hydrogen bond donor more than 5. HBA and HBD total hydrogen bond counts are significant indicators of high oral bioavailability. The $P_{o/w}$ of phytochemical **1**, **3**, **4**, **5**, **6**, **42**, **44**, **45**, **46**, and **66** are more than 5. In conclusion, 10 phytochemicals, **8**, **10**, **11**, **12**, **13**, **15**, **17**, **19**, **23**, and **44** as well as acarbose and chymostatin violate the the Lipinski's rule of five more than 1. Although 10 phytochemicals did not fit the Lipinski's rule of five as it violated more than one rules. Hence, these natural compounds are nevertheless acceptable as drug-likeness compounds despite their low solubility and permeability. In order to create physiologically active molecules with high molecular weight and plenty of rotatable bonds, nature has figured out how to preserve low hydrophobicity and intermolecular hydrogen bond donating potential [196].

4.2.5 Toxicity of the phytochemicals of *A. indicum*

The toxicity of the phytochemicals was calculated by ProTox-II webserver. The toxicity prediction was demonstrated in **Table 9**. The ProTox-II differentiated the classification system of toxicity into oral toxicity, organ toxicity (hepatotoxicity), toxicological endpoints (such as mutagenicity, carcinogenicity, cytotoxicity, and immunotoxicity), toxicological pathways (AOPs) and toxicity targets. The rule that identifies the compound's acute toxicity (rodent) was based on the analysis of the two-dimensional (2D) similarity with known LD_{50} values and identification of

fragments over-represented in toxic compounds. The hepatotoxicity was based on Random Forest with SMOTE TC (Synthetic Minority Over-Sampling-using Tanimoto Coefficient) sampling. The carcinogenicity, mutagenicity and cytotoxicity were based on machine learning with over sampling, while immunotoxicity was based on the Multinomial Naïve Bayes [197].

Table 10 Toxicity of the phytochemicals of *A. indicum*

Comp.	LD ₅₀ value (mg/kg)	Toxicity class	Hepato-toxicity	Carcino-genicity	Immune-toxicity	Mutage-nicity	Cyto-toxicity
1	890	4	I; 0.87	I; 0.60	A; 0.99	I; 0.98	I; 0.94
2	8000	6	I; 0.94	I; 0.71	A; 0.99	I; 0.83	I; 0.96
3	890	4	I; 0.87	I; 0.60	A; 0.99	I; 0.98	I; 0.94
4	2260	5	I; 0.83	I; 0.73	A; 0.55	I; 0.92	I; 0.91
5	890	4	I; 0.85	I; 0.59	A; 0.99	I; 0.96	I; 0.95
6	775	4	I; 0.78	I; 0.62	A; 0.99	I; 0.93	A; 0.58
7	3919	5	I; 0.71	I; 0.69	A; 0.85	I; 0.91	I; 0.90
8	5000	5	I; 0.83	I; 0.90	A; 0.96	I; 0.65	I; 0.58
9	159	3	I; 0.69	A; 0.68	I; 0.87	A; 0.51	I; 0.99
10	5000	5	I; 0.82	I; 0.85	A; 0.66	I; 0.76	I; 0.69
11	5000	5	I; 0.73	A; 0.50	A; 0.99	I; 0.71	I; 0.93
12	5000	5	I; 0.82	I; 0.85	A; 0.75	I; 0.76	I; 0.69
13	5000	5	I; 0.82	I; 0.85	A; 0.74	I; 0.76	I; 0.69
14	5000	5	I; 0.69	A; 0.68	I; 0.97	A; 0.51	I; 0.99
15	5000	5	I; 0.82	I; 0.85	I; 0.74	I; 0.76	I; 0.69
16	4000	5	I; 0.72	I; 0.68	I; 0.77	I; 0.94	I; 0.95
17	5000	5	I; 0.83	I; 0.90	A; 0.72	I; 0.65	I; 0.58
18	5000	5	I; 0.82	I; 0.86	I; 0.93	A; 0.59	I; 0.69
19	5000	5	I; 0.75	I; 0.85	A; 0.91	I; 0.74	I; 0.66
20	290	3	A; 0.54	I; 0.74	I; 0.99	I; 0.99	I; 0.86
21	2200	5	I; 0.52	I; 0.51	I; 0.99	I; 0.99	I; 0.86
22	2000	4	I; 0.55	I; 0.64	I; 0.97	I; 0.96	I; 0.93

Comp.	LD ₅₀ value (mg/kg)	Toxicity class	Hepato- toxicity	Carcino- genicity	Immune- toxicity	Mutage- nicity	Cyto- toxicity
23	2260	5	I; 0.87	I; 0.85	I; 0.68	I; 0.80	I; 0.73
24	1500	4	I; 0.54	I; 0.50	I; 0.99	I; 0.98	I; 0.84
25	2250	5	I; 0.55	A; 0.50	I; 0.99	I; 0.99	I; 0.83
26	1000	4	I; 0.52	I; 0.60	I; 0.55	I; 0.98	I; 0.94
27	2000	4	I; 0.57	I; 0.64	I; 0.71	I; 0.96	I; 0.97
28	2000	4	A; 0.57	I; 0.63	I; 0.99	I; 0.96	I; 0.86
29	2000	4	A; 0.50	I; 0.69	I; 0.94	I; 0.92	I; 0.94
30	2000	4	I; 0.61	A; 0.56	I; 0.99	I; 0.94	I; 0.91
31	490	4	I; 0.62	I; 0.70	I; 0.97	I; 0.81	I; 0.75
32	4000	5	I; 0.89	I; 0.78	I; 0.99	I; 0.75	I; 0.88
33	2170	5	I; 0.82	I; 0.82	I; 0.84	I; 0.73	I; 0.81
34	2850	5	I; 0.51	A; 0.50	I; 0.91	I; 0.93	I; 0.81
35	2980	5	I; 0.57	A; 0.78	I; 0.50	I; 0.98	I; 0.86
36	1772	4	I; 0.51	I; 0.61	A; 0.91	I; 0.96	I; 0.88
37	978	4	A; 0.56	I; 0.67	A; 0.97	I; 0.89	I; 0.94
38	1550	4	A; 0.51	I; 0.68	I; 0.98	I; 0.80	I; 0.82
39	2850	5	A; 0.60	I; 0.63	I; 0.57	I; 0.81	I; 0.84
40	750	4	A; 0.53	I; 0.81	I; 0.99	I; 0.91	I; 0.90
41	1350	4	I; 0.88	I; 0.78	I; 0.99	I; 0.99	I; 0.76
42	2000	4	I; 0.91	I; 0.63	A; 0.57	I; 0.95	I; 0.97
43	70000	6	I; 0.75	I; 0.75	A; 0.93	I; 0.92	I; 0.95
44	339	4	I; 0.71	I; 0.52	A; 0.99	I; 0.98	I; 0.84
45	2000	4	I; 0.91	I; 0.63	A; 0.57	I; 0.95	I; 0.97
46	5000	5	I; 0.79	I; 0.76	A; 0.99	I; 0.98	I; 0.81
47	2842	5	I; 0.65	I; 0.67	A; 0.93	I; 0.90	I; 0.79
48	280	3	I; 0.69	A; 0.53	I; 0.74	I; 0.61	I; 0.89
49	3800	5	I; 0.69	A; 0.53	A; 0.54	I; 0.56	I; 0.91
50	2991	4	I; 0.75	I; 0.50	I; 0.97	I; 0.74	I; 0.93

Comp.	LD ₅₀ value (mg/kg)	Toxicity class	Hepato-toxicity	Carcino-genicity	Immune-toxicity	Mutage-nicity	Cyto-toxicity
51	550	4	I; 0.70	I; 0.66	I; 0.99	I; 0.70	I; 0.62
52	550	4	I; 0.68	I; 0.64	I; 0.99	I; 0.68	I; 0.74
53	1923	4	I; 0.70	A; 0.83	I; 0.99	I; 0.93	I; 0.85
54	600	4	I; 0.67	I; 0.65	I; 0.74	I; 0.69	I; 0.65
55	300	3	I; 0.76	I; 0.76	I; 0.98	I; 0.88	I; 0.76
56	1600	4	A; 0.52	I; 0.60	I; 0.86	I; 0.80	I; 0.84
57	1425	4	A; 0.56	I; 0.56	I; 0.99	I; 0.78	I; 0.90
58	5000	5	I; 0.61	A; 0.54	A; 0.87	I; 0.97	I; 0.77
59	3424	5	I; 0.58	I; 0.53	A; 0.78	I; 0.92	A; 0.67
60	200	3	I; 0.64	A; 0.56	I; 0.83	I; 0.76	I; 0.82
61	9000	6	A; 0.53	I; 0.69	I; 0.75	I; 0.79	I; 0.92
62	288	3	I; 0.76	I; 0.67	I; 0.98	I; 0.77	I; 0.91
63	10000	6	I; 0.93	I; 0.75	I; 0.94	I; 0.72	I; 0.75
64	8	2	I; 0.84	I; 0.71	I; 0.99	I; 0.87	A; 0.74
65	570	4	A; 0.57	A; 0.66	I; 0.93	A; 0.57	I; 0.85
66	5000	5	I; 0.58	I; 0.55	I; 0.99	I; 0.98	A; 0.73
Acarbose	24000	6	A; 0.65	I; 0.84	A; 0.99	I; 0.76	I; 0.70
Orlistat	1300	4	A; 0.70	I; 0.55	I; 0.68	I; 0.81	I; 0.70
Chymo-statin	2400	5	I; 0.71	I; 0.58	I; 0.99	I; 0.69	I; 0.76

LD₅₀: median lethal dose; I: Inactive; A: Active

The GHS guidelines classify the substances into six groups, with the highest group having the lowest likelihood of being dangerous or harmful. Class 1 ($LD_{50} \leq 5$) and 2 ($5 < LD_{50} \leq 50$) signifies that the compounds are lethal and almost certainly will result in death. Adenine (**64**) has been identified belong to class 2. Class 3 ($50 < LD_{50} \leq 300$), indicates potential toxicity hazards from oral exposure. Six phytochemicals, 3,5,5'-Trihydroxy-4' methoxy flavone-7O-b-D-glucopyranoside (**9**),

benzoic acid (20), scoparone (48), 1-methoxycarbonyl- β -carboline (55), 3-hydroxy- β -damascone (60), and riboflavin (62), were found in class 3. Class 4 ($300 < \text{LD50} \leq 2000$) classifies substances that are most likely to be dangerous when consumed. Twenty-eight phytochemicals including fall in class 4. Compounds that are less likely to be hazardous after oral consumption are included under class 5 ($2000 < \text{LD50} \leq 5000$). Among the 66 phytochemicals, 27 phytochemicals as well as chymostatin were classified in class 5. Finally, class 6 ($\text{LD50} > 5000$) reflects the non-toxic compounds [197, 198]. Four phytochemicals, β -sitosterol-3-*O*- β -D-glucopyranoside (2), oleanic acid (43), 3-hydroxy- β -ionol (61), and riboflavin (62), were found to be class 6 members, including acarbose.

The functional groups of the molecule might potentially be used to estimate its potential for mutagenicity and carcinogenicity. Acyl halide, haloalkene, epoxide, aliphatic halogen, alkyl nitrate, aldehyde, hydrazine, isocyanate, polyaromatic hydrocarbon, azide, alkyl/aromatic nitro, coumarin, diazo aromatic, benzyl sulfinyl ether, alkyl halide, and thiocarbonyl are the functional groups that are either carcinogenic or mutagenic [199]. Overall, nineteen phytochemicals (15, 16, 21, 22, 23, 24, 26, 27, 31, 32, 33, 41, 50, 51, 52, 54, 55, 62, and 63) out of 66 were calculated as non-toxic phytochemicals of *A. indicum*.

Based on the *in silico* study, ADME calculation, and toxicity prediction, nine phytochemicals (2, 8, 11, 12, 13, 15, 17, 18, and 19) were potential to be developed as novel inhibitors for α -glucosidase, HPL, and α -chymotrypsin.

4.3 Structure elucidation of isolated metabolites

4.3.1 Structure elucidation of metabolite 1

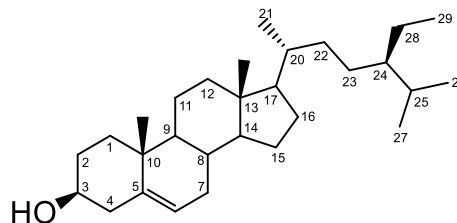


Figure 16 Structure of metabolite 1

Metabolite **1** was observed as a white amorphous solid. From the HR-ESI-MS result, the molecular ion peaks at m/z 413.3249 $[M+H]^+$ suggested β -sitosterol with molecular formula $C_{29}H_{50}O$. The structure of metabolite **1** was established as shown in **Figure 17** and it was β -sitosterol by comparing its 1H and ^{13}C NMR data to the previous report (**Table 11** and **12**) [200-202]. The ^{13}C NMR has given signal at 140.5 and 122.4 ppm for $C_5=C_6$ double bond respectively, 71.9 ppm for C_3 β -hydroxyl group, 19.5 and 11.9 for angular methyl carbon atoms for C_{19} and C_{18} respectively. The value for C_{18} is lower due to γ -gauche interaction that increases the screening of the C_{18} hence lower chemical shift. However, the loss of H in C_6 results in decrease in screening of the C_{19} leading to increase in ^{13}C chemical shift to higher frequency. The proton NMR has revealed the existence of signals for olefinic proton at 5.358 (br, s), angular methyl proton at 0.68 (s), 0.699 (s), and 1.01 (s) corresponding to C_{18} and C_{19} proton respectively. The weak molecular ions were given at m/z 413.3249 $[M+H]^+$. The molecular weights and the fragmentation pattern indicate that the compounds present in the mixture are β -sitosterol and stigmasterol, respectively. The loss of $C_{10}H_{21}$ and the dehydration of β -sitosterol yielded m/z 255. The above 1H and ^{13}C NMR, 1H - 1H COSY, HMQC, HR-ESI-MS data, and comparison of the ^{13}C NMR signal with those describes in the literatures showed that the white amorphous solid to be the mixture of β -sitosterol and stigmasterol. The only difference between the two compounds is the presence of $C_{22}=C_{23}$ double bond in stigmasterol and $C_{22}-C_{23}$ double bond in β -sitosterol. Hence the lack of practical difference in their R_f despite

the use of several solvent systems. Furthermore, literatures have shown that β -sitosterol is difficult to be obtained in pure state [203].

Table 11 ^1H NMR data of β -sitosterol (chloroform-*d*, 500 MHz) (500 MHz, CDCl_3)

Position	δ_{H} (ppm), mult, <i>J</i> in Hz	Position	δ_{H} (ppm), mult, <i>J</i> in Hz
1	1.00, 1.70	16	1.85, 1.25
2	2.15, 1.75	17	1.11
3	3.52, m	18	0.680, s
4	2.76, 2.50	19	1.01 s
5	-	20	1.39
6	5.358, br s	21	0.92, (d, 6.4)
7	5.40	22	1.19
8	1.36	23	1.25
9	0.90	24	1.01
10	-	25	1.69
11	1.45, 1.55	26	0.814, (d, 6.5)
12	1.90, 1.00	27	0.833, (d, 6.5)
13	-	28	1.30
14	0.85	29	0.845 (t, 7.5)
15	1.00, 1.55		

Table 12 ^{13}C -NMR data of metabolites **1** (500 MHz, CDCl_3)

Position	δ_c (ppm)			
	Ref 1a [200]	Ref 1b [202]	Ref 1c [201]	1 ^a
1	37.3	37.4	37.3	37.3
2	31.9	31.9	31.6	31.7
3	71.9	71.8	71.8	71.9
4	42.3	42.3	42.2	42.3
5	140.8	140.3	140.8	140.5
6	121.8	121.7	121.7	122.4
7	31.7	31.7	31.9	31.9
8	32.0	32.0	31.9	31.9
9	50.2	50.1	51.2	50.2
10	36.6	36.5	36.5	36.6
11	21.2	21.1	21.1	21.1
12	39.8	39.6	39.8	39.8
13	42.4	42.3	42.3	42.4
14	56.8	56.7	56.8	56.8
15	24.4	24.3	24.3	24.4
16	28.3	28.6	28.3	28.3
17	56.1	55.9	56.0	56.1
18	11.9	11.6	11.9	11.9
19	19.5	19.4	19.4	19.5
20	36.2	36.2	36.2	36.2
21	18.9	18.8	18.8	18.8
22	34.0	34.0	33.9	33.9
23	26.2	26.1	26.1	26.1
24	46.0	45.8	45.9	45.5

Position	δ_c (ppm)			
	Ref 1a [200]	Ref 1b [202]	Ref 1c [201]	1 ^a
25	29.2	29.2	29.2	28.3
26	19.9	19.8	19.8	19.9
27	19.1	19.0	19.3	19.1
28	23.1	23.1	23.1	23.0
29	12.1	12.0	12.2	12.2

4.3.2 Structure elucidation of metabolites 2

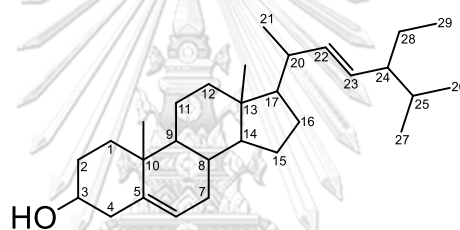


Figure 17 Structure of metabolite 2

Metabolite **2** was obtained as a white amorphous solid with molecular formula $C_{29}H_{48}O$ established by 1H and ^{13}C NMR data (**Table 13** and **14**). The existence The structure of metabolite **2** was established as shown in **Figure 19** and it was stigmasterol by comparing its NMR data to the previous report [200-202].

Table 13 1H NMR data of metabolite **2** (500 MHz, $CDCl_3$)

Position	δ_{H} (ppm), mult, J in Hz	Position	δ_{H} (ppm), mult, J in Hz
1	1.00, 1.70	16	1.85, 1.25
2	2.15, 1.75	17	1.11
3	3.52, m	18	0.699, s
4	2.76, 2.50	19	1.01, s
5	-	20	1.39
6	5.357, br s	21	1.02 (d, 7.5)
7	5.40	22	1.19
8	1.36	23	1.25
9	0.90	24	1.01
10	-	25	1.69
11	1.45, 1.55	26	0.795 (d, 6.5)
12	1.90, 1.00	27	0.846 (d, 6.5)
13	-	28	1.30
14	0.85	29	0.804 (t, 7.5)
15	1.00, 1.55		

Table 14 ^{13}C NMR data of metabolites **2** (500 MHz, CDCl_3)

Position	δ_c (ppm)			
	Ref 2a [204]	Ref 2b [202]	Ref 2c [201]	1 ^a
1	37.3	37.1	37.3	37.3
2	31.7	31.6	31.6	31.7
3	71.9	71.8	71.8	71.9
4	42.3	41.5	42.3	42.3
5	140.8	140.3	140.8	140.5
6	121.8	121.7	121.7	122.4
7	32.1	31.7	31.9	31.9
8	32.0	32.0	31.9	31.9
9	50.2	50.1	51.2	50.2
10	36.6	36.7	36.5	36.6
11	21.2	20.8	21.1	21.1
12	39.8	39.6	39.7	39.8
13	42.4	42.3	42.3	42.4
14	56.8	56.7	56.9	56.8
15	24.4	24.3	24.4	24.4
16	28.3	28.6	28.4	28.3
17	56.1	55.9	56.1	56.1
18	11.9	11.6	11.0	11.9
19	19.1	19.2	21.2	19.5
20	40.6	40.1	40.5	36.2
21	20.0	20.5	21.2	18.8
22	138.4	138.0	138.3	33.9
23	129.2	129.2	129.3	26.1
24	51.3	51.1	51.2	45.5

Position	δ_c (ppm)			
	Ref 2a [204]	Ref 2b [202]	Ref 2c [201]	1 ^a
25	34.0	32.0	31.9	28.3
26	21.3	21.2	21.2	19.9
27	18.9	19.0	19.0	19.1
28	25.5	25.4	25.4	23.0
29	12.1	12.0	12.1	12.2

4.3.3 Structure elucidation of metabolites **3**

Further research on *in vitro* pancreatic lipase inhibition assay by ricinoleic acid was needed as pancreatic lipase activity was inhibited in a concentration-dependent manner in the presence linoleic acid and oleic acid. In comparison to linoleic acid, which showed an IC₅₀ of 23.1 g/mL (0.08 M/mL), oleic acid demonstrated greater levels of inhibition over the whole concentration range with an IC₅₀ of 11.7 g/mL (0.04 M/mL) [205]. It proved that fatty acid lowers the absorption of TAGs into circulation after an oral fat load. It is reasonable to assume that these fatty acids attenuate postprandial triglyceridemia by targeting pancreatic lipase, the single most significant determinant of lipid absorption, as this finding coincided with the discovery that these fatty acids were effective pancreatic lipase inhibitors *in vitro*. Future study is still needed to determine the profile of safe and effective levels as well as the dose-response relationship for both the individual free fatty acids and the combination of these free fatty acids [205].

CHAPTER V

CONCLUSIONS

In conclusion, purification of the *n*-hexane and dichloromethane crude extracts of *A. indicum* stems yielded three known compounds identified as β -sitosterol (1), stigmasterol (2), and ricinoleic acid (3). All crude extract were evaluated for their α -glucosidase inhibitory activity. The *n*-hexane and MeOH-soluble stem extracts were active with 11.0% at 25 $\mu\text{g/mL}$ and 8.0% at 0.25 $\mu\text{g/mL}$. The hexane, DCM, and MeOH-soluble leaves extracts are active with 20.2% at 0.025 $\mu\text{g/mL}$; 20.0% at 0.025 $\mu\text{g/mL}$; and 14.6% at 2.5 $\mu\text{g/mL}$, respectively. Furthermore, sixty-six phytochemicals of *A. indicum* were studied for their interaction against α -glucosidase, pancreatic lipase, α -chymotrypsin through molecular docking. Based on the *in silico* study, ADME investigation, and toxicity prediction, nine phytochemicals (2, 8, 11, 12, 13, 15, 17, 18, and 19) out of 66 phytochemicals were potential to be developed as novel inhibitor for α -glucosidase, human pancreatic lipase, and α -chymotrypsin. The result demonstrated that phytochemicals from *A. indicum* potential to be an anti-diabetes, anti-obesity, and anti-ulcer drugs.

REFERENCES



จุฬาลงกรณ์มหาวิทยาลัย
CHULALONGKORN UNIVERSITY

- [1] Natural products isolation. in *Methods in Molecular Biology*, Sarker, S.D. and Nahar, L., Editors. 2012, Humana Press. XII, 552.
- [2] Dias, D.A., Urban, S., and Roessner, U. A historical overview of natural products in drug discovery. *Metabolites* 2(2) (2012): 303-336.
- [3] Dewick, P.M. Medicinal Natural Products: A Biosynthetic Approach, 3rd Edition. 2011, Wiley & Sons Ltd.
- [4] Kim, J. and Park, E.J. Cytotoxic anticancer candidates from natural resources. *Current Medicinal Chemistry Anti-cancer Agents* 2(4) (2002): 485-537.
- [5] Butler, M.S. The role of natural product chemistry in drug discovery. *Journal of Natural Products* 67(12) (2004): 2141-2153.
- [6] Western Oregon University. *Chemistry CH105: Consumer Chemistry (Chapter 6 - A Brief History of Natural Products and Organic Chemistry)* [Online]. 2021.
- [7] Altmann, K.-H. and Gertsch, J. Anticancer drugs from nature—Natural products as a unique source of new microtubule-stabilizing agents. *Natural Product Reports* 24 (2007): 327-357.
- [8] Roshan, S., Ali, S., Khan, A., Tazneem, B., and Purohit, M.G. Wound healing activity of *Abutilon indicum*. *Pharmacognosy Magazine* 4(15) (2008): 85-88.
- [9] Brown, D.G., Lister, T., and May-Dracka, T.L. New natural products as new leads for antibacterial drug discovery. *Bioorganic & Medicinal Chemistry Letters* 24(2) (2014): 413-418.
- [10] El Sayed, K.A. Natural products as antiviral agents. *Studies in Natural Products Chemistry* 24 (2000): 473-572.
- [11] Seetharam, Y.N., Chalageri, G., and Setty, S.R. Hypoglycemic activity of *Abutilon indicum* leaf extracts in rats. *Fitoterapia* 73(2) (2002): 156-159.
- [12] Newman, D.J. and Cragg, G.M. Natural products as sources of new drugs over the 30 years from 1981 to 2010. *Journal of Natural Products* 75(3) (2012): 311-335.
- [13] Füllbeck, M., Michalsky, E., Dunkel, M., and Preissner, R. Natural products: sources and databases. *Natural Product Reports* 23(3) (2006): 347-356.

- [14] Gomaa, A., Samy, M., Yehia, S., and Kamel, M. Phytochemistry and pharmacological activities of genus *Abutilon*: a review (1972-2015). Journal of Advanced Biomedical and Pharmaceutical Sciences 1 (2018): 56-74.
- [15] PLANT GENERA *Abutilon* Mill. - MALVACEAE [Online]. 2018. Available from: https://www.dnp.go.th/Botany/detail_eng.html?menu=PlantGenera_Eng_Abutilon_Eng [15 January 2021]
- [16] Rajeshwari, S. and Sevarkodiyone, S.P. Medicinal properties of *Abutilon indicum*. International Journal of Research in Phytochemical and Pharmacological Sciences 1(1) (2018): 1-4.
- [17] Mahanthesh, M.C. and Jalalpure, S. Pharmacognostical evaluation and anticonvulsant activity of stem of *Abutilon indicum* Linn. Sweet. International Journal of Pharmacy and Pharmaceutical Sciences 8(8) (2016): 58-70.
- [18] Konsue, A. and Talubmook, C. Effect of Thai folklore recipe from *Abutilon indicum* and *Mimosa pudica* in streptozotocin-induced diabetic rats. Pharmacognosy Journal 10(3) (2018): 480-485.
- [19] Singh, D. and Singh, V.S. Phytochemical analysis and antimicrobial activity of chloroform extract of *Abutilon indicum*. American Journal of Applied Chemistry 4(6) (2016): 242-246.
- [20] Chandrashekar, V.M., Nagappa, A.N., Channeshh, T.S., Habbu, P.V., and Rao, K.P. Anti-diarrhoeal activity of *Abutilon indicum* Linn. leaf extract. Journal of Natural Remedies 4(2) (2004): 12-16.
- [21] Ushakumari, J., Ramana, V.V., and Reddy, K.J. Ethnomedicinal plants used for wounds and snake-bites by tribal of Kinnerasani region. Journal of Pharmacognosy 3(2) (2012): 79–81.
- [22] Abat, J.K., Kumar, S., and Mohanty, A. Ethnomedicinal, phytochemical and ethnopharmacological aspects of four medicinal plants of Malvaceae used in Indian traditional medicines: A review. Medicines (Basel) 4(4) (2017).
- [23] Khanduri, N.C. Fertility control of female rat through *Abutilon indicum* seeds. International Journal of Technology Enhancements and Emerging Engineering Research 2(3) (2014): 89-91.

- [24] Kaushik, P., Kaushik, D., Khokra, S., and Sharma, A. Antidiabetic activity of the plant *Abutilon indicum* in streptozotocin- induced experimental diabetes in rats. (2010).
- [25] Krisanapun, C., Peungvicha, P., Temsiririrkkul, R., and Wongkrajang, Y. Aqueous extract of *Abutilon indicum* Sweet inhibits glucose absorption and stimulates insulin secretion in rodents. Nutrition Research 29(8) (2009): 579-587.
- [26] Krisanapun, C., Seong-Ho, L., Peungvicha, P., Temsiririrkkul, R., and Seung Joon, B. Antidiabetic activities of *Abutilon indicum* (L.) Sweet are mediated by enhancement of adipocyte differentiation and activation of the GLUT1 promoter. Evidence-Based Complementary and Alternative Medicine 2011 (2011).
- [27] Kuo, P.C., et al. Chemical constituents from *Abutilon indicum*. Journal of Asian Natural Product Research 10(7-8) (2008): 699-703.
- [28] Macabeo, A. and Lee, C.A. Sterols and triterpenes from the non-polar antitubercular fraction of *Abutilon indicum*. Pharmacognosy Journal 6 (2014): 49-52.
- [29] Tiwari, S., Mishra, S., Dharm, R., Misra, and Upadhyay, R. Identification of new bioactive compounds from fruit of *Abutilon indicum* through GCMS analysis. (2019).
- [30] Yasmin, S., Kashmiri, M.A., Ahmad, I., Adnan, A., and Ahmad, M. Biological activity of extracts in relationship to structure of pure isolates of *Abutilon indicum*. Pharmaceutical Biology 46(10-11) (2008): 673-676.
- [31] Srisurichan, S. and Pornpakakul, S. Triterpenoids from the seedpods of *Holarrhena curtisii* King and Gamble. Phytochemistry Letters 12 (2015): 282–286.
- [32] Survase, S.A., Sarwade, B.P., and Chavan, D.P. Antibacterial activity of various extracts of *Abutilon pannosum* (Forst.f.) Schlecht. leave. African Journal of Plant Science 7 (2013): 128-130.
- [33] Beha, E., Jung, A., Wiesner, J., Rimpler, H., Lanzer, M., and Heinrich, M. Antimalarial activity of extracts of *Abutilon grandiflorum* G. Don - A traditional Tanzanian medicinal plant. Phytotherapy Research 18(3) (2004): 236-240.

- [34] Banso, A. and Adeyemo, S. Phytochemical screening and antimicrobial assessment of *Abutilon mauritianum*, *Bacopa monnifera* and *Datura stramonium*. Biokemistri 18(1) (2010).
- [35] Imran, M., et al. *In-vitro* and *in-silico* antioxidant, α -glucosidase inhibitory potentials of abutilins C and D, new flavonoide glycosides from *Abutilon pakistanicum*. Arabian Journal of Chemistry 14(4) (2021): 103021.
- [36] Fern, K., Fern, A., and Morris, R. Useful Tropical Plants *Abutilon indicum* [Online]. 2019. Available from: <https://tropical.theferns.info/viewtropical.php?id=Abutilon+indicum> [17 July]
- [37] Dhanalakshmi, S., Lakshmanan, K.K., and Subramanian, M.S. Pharmacognostical and phytochemical studies of *Abutilon* L. Journal of Research and Education in Indian Medicine 1(1) (1990): 21-25.
- [38] Jain, A., Katewa, S.S., Chaudhary, B.L., and Galav, P. Folk herbal medicines used in birth control and sexual diseases by tribals of southern Rajasthan, India. Journal of Ethnopharmacology 90(1) (2004): 171-177.
- [39] Jain, A., Katewa, S.S., Galav, P.K., and Sharma, P. Medicinal plant diversity of Sitamata wildlife sanctuary, Rajasthan, India. Journal of Ethnopharmacology 102(2) (2005): 143-157.
- [40] Kumar, V.P., Chauhan, N.S., Padh, H., and Rajani, M. Search for antibacterial and antifungal agents from selected Indian medicinal plants. Journal of Ethnopharmacology 107(2) (2006): 182-188.
- [41] Ganesan, S., Ramar Pandi, N., and Banumathy, N. Ethnomedicinal survey of Alagarkoil Hills (reserved forest), Tamil Nadu, India. eJournal of Indian Medicine 1(2007-2008) (2007): 1-18.
- [42] Mohapatra, S.P. and Sahoo, H.P. An ethno-medico-botanical study of Bolangir, Orissa, India: native plant remedies against gynaecological diseases. Ethnobotanical Leaflets 12(2008) (2008): 846-850.
- [43] Ignacimuthu, S., Ayyanar, M., and Sankarasivaraman, K. Ethnobotanical study of medicinal plants used by Paliyar tribals in Theni district of Tamil Nadu, India. Fitoterapia 79(7-8) (2008): 562-568.

- [44] Samy, R.P., Thwin, M.M., Gopalakrishnakone, P., and Ignacimuthu, S. Ethnobotanical survey of folk plants for the treatment of snakebites in Southern part of Tamilnadu, India. Journal of Ethnopharmacology 115(2) (2008): 302-312.
- [45] Ali, Z.A. Folk veterinary medicine in Moradabad District (Uttar Pradesh), India. Fitoterapia 70(4) (1999): 340-347.
- [46] Singh, A.K., Raghubanshi, A.S., and Singh, J.S. Medical ethnobotany of the tribals of Sonaghati of Sonbhadra district, Uttar Pradesh, India. Journal of Ethnopharmacology 81(1) (2002): 31-41.
- [47] Forest Herbarium. Thai plant names *Abutilon* [Online]. Available from: <https://www.dnp.go.th/Botany/mplant/words.html?groupcode=genus&keyword=Abutilon> [17 July]
- [48] Thailand Nature Project. Thailand nature project *Abutilon indicum* (L.) Sweet [Online]. 2020. [17 July]
- [49] Gujarat Forestry Research Foundation. E-Flora of Gandhinagar, Gujarat, India *Abutilon indicum* [Online]. Available from: <https://www.efloraofgandhinagar.in/shrub/abutilon-indicum> [17 July]
- [50] Nadkarni, K.M. Indian materia medica : with Ayurvedic, Unani-Tibbi, Siddha, allopathic, homeopathic, naturopathic & home remedies. 1996, Popular Prakashan (Pvt) Ltd.
- [51] Rahuman, A.A., Gopalakrishnan, G., Venkatesan, P., and Geetha, K. Isolation and identification of mosquito larvicidal compound from *Abutilon indicum* (Linn.) Sweet. Parasitology Research 102(5) (2008): 981-988.
- [52] Kumar, V. Chemical examination of *Abutilon indicum*, *Tamarix gallica* and *Xanthium strumarium*. Ph.D., Chemistry Department, R. H Government (P.G.) College Kumaun University, 2008.
- [53] Liu, N., Jia, L., and Sun, Q. Chemical constituents of *Abutilon indicum* (L.) Sweet. Journal of Chongyang Pharmaceutical University 26 (2009): 196-197.
- [54] Yasmin, S. Studies on bioactive natural products of selected species of family Malvaceae. Ph. D., Chemistry Department, Government College, Lahore University, Pakistan, 2008.

- [55] Amit, K. and Gyanender, S. Determination of the bioactive components of *Abutilon indicum* L. International Journal of Pharma and Bio Sciences 4(4) (2013): 898-901.
- [56] Rajput, A.P. and Patel, M.K. Isolation and characterization of phytoconstituents from the chloroform extract of *Abutilon indicum* leaves (Family: Malvaceae). Asian Journal of Research in Chemistry 5(11) (2012): 1375-1380.
- [57] Prabhuji, S., Singh, D.K., Srivastava, A.K., and Rahul, S. Antifungal activity of a new steroid isolated from *Abutilon indicum* (L.). Medicinal Plants 2(3) (2010): 215-218.
- [58] Vairavasundaram, R. and Senthil, K. Antimycotic activity of the componenets of *Abutilon indicum* (Malvaceae). Drug Invention Today 1(2) (2009): 137-139.
- [59] Matławska, I. and Sikorska, M. Flavonoid compounds in the flowers of *Abutilon indicum* (L.) Sweet (Malvaceae). Acta Poloniae Pharmaceutica 59(3) (2002): 227-229.
- [60] Singh, D. and Gupta, R.S. Modulatory influence of *Abutilon indicum* leaves on hepatic antioxidant status and lipid peroxidation against alcohol-induced liver damage in rats. Pharmacologyonline 1 (2008): 253-262.
- [61] Subramanian, S. and Nair, A. Flavonoids of four Malvaceous plants. Phytochemistry 11 (1972): 1518-1519.
- [62] Gaind, K.N. and Chopra, K.S. Phytochemical investigation of *Abutilon indicum*. Planta Medica 30(2) (1976): 174-188.
- [63] Pandey, D.P., Rather, M.A., Nautiyal, D.P., and Bachheti, R.K. Phytochemical analysis of *Abutilon indicum*. International Journal of ChemTech Research 3(2) (2011): 642-645.
- [64] Ambarsing, P.R. and Milind, K.P. Chemical investigation and biological activity of phytoconstituents from methanol extract of *Abutilon indicum* leaves. Journal of Chemical and Pharmaceutical Research 4(8) (2012): 3959-3965.
- [65] Sharma, P.V. and Ahmad, Z.A. Two sesquiterpene lactones from *Abutilon indicum*. Phytochemistry 28(12) (1989): 3525.
- [66] Lakshmayya, Nelluri, N.R., Kumar, P., Agarwal, N.K., Shivaraj, G.T., and Ramachandra, S.S. Phytochemical and pharmacological evaluation of leaves

- of *Abutilon indicum*. Indian Journal of Traditional Knowledge 2(1) (2003): 79-83.
- [67] Srikanth, P., Karthik, P.S., Siricha, M., and Sashikanth, C. Evaluation of antioxidant and anticancer properties of methanolic extracts of *Abutilon indicum* and *Blumea mollis*. Journal of Pharmacy Research 5(4) (2012): 2373-2376.
- [68] Musthafa, S.A., Kasinathan, T., Bhattacharyya, R., Muthu, K., Kumar, S., and Munuswamy-Ramanujam, G. Gallic acid synergistically enhances the apoptotic ability of *Abutilon indicum* Linn. stem fraction in human U87 glioblastoma cells. Materials Today: Proceedings 40 (2021): S216-S223.
- [69] Kaladhar, D.S.V.G.K., Swathi, S.K., Varahalarao, V., and Nagendra, S.Y. Evaluation of anti-inflammatory and anti-proliferative activity of *Abutilon indicum* L. plant ethanolic leaf extract on lung cancer cell line A549 for system network studies. Journal of Cancer Science and Therapy 6(6) (2014): 195-201.
- [70] Mukherjee, P.K., Kumar, V., Mal, M., and Houghton, P.J. Acetylcholinesterase inhibitors from plants. Phytomedicine 14(4) (2007): 289-300.
- [71] Pandey, D.K., Tripathi, N.N., Tripathi, R.D., and Dixit, S.N. Antifungal activity of some seed extracts with special reference to that of *Pimpinella diversifolia* D. International Journal of Crude Drug Research 21(4) (1983): 177-182.
- [72] Dashputre, N.L. and Naikwade, N. Immunomodulatory activity of *Abutilon Indicum* Linn. on albino mice. International Journal of Pharma Sciences and Research (IJPSR) 1(3) (2010): 178-184.
- [73] Johri, R.K., Pahwa, G.S., Sharma, S.C., and Zutshi, U. Determination of estrogenic/antiestrogenic potential of antifertility substances using rat uterine peroxidase assay. Contraception 44(5) (1991): 549-557.
- [74] Deshpande, V., Jadhav, V.M., and Kadam, V.J. *In-vitro* anti-arthritic activity of *Abutilon indicum* (Linn.) Sweet. Journal of Pharmacy Research 2(4) (2009): 644-645.

- [75] Dash, G.K., Samanta, A., Kanungo, S.K., Suresh, P., and Ganapaty, S. Hepatoprotective activity of leaves of *Abutilon indicum*. Indian Journal of Natural Products 16(2) (2000): 25-27.
- [76] Porchezian, E. and Ansari, S.H. Hepatoprotective activity of *Abutilon indicum* on experimental liver damage in rats. Phytomedicine 12(1-2) (2005): 62-64.
- [77] American Diabetes Association. Diagnosis and classification of diabetes mellitus. Diabetes Care 32 (2009): S62-S67.
- [78] Genetics Home Reference. Type 2 diabetes [Online]. 2020. Available from: <https://medlineplus.gov/genetics/condition/type-2-diabetes/> [20 July]
- [79] World Health Organization. Diabetes [Online]. 2021. Available from: https://www.who.int/health-topics/diabetes#tab=tab_1 [23 July]
- [80] Al-Hourani, H.M. and Atoum, M.F. Body composition, nutrient intake and physical activity patterns in young women during Ramadan. Singapore Medical Journal 48(10) (2007): 906-910.
- [81] Bello, N.A., et al. Retinopathy and clinical outcomes in patients with type 2 diabetes mellitus, chronic kidney disease, and anemia. BMJ Open Diabetes Research & Care 2(1) (2014).
- [82] Jiao, Y., Hua, D., Huang, D., Zhang, Q., and Yan, C. Characterization of a new heteropolysaccharide from green guava and its application as an α -glucosidase inhibitor for the treatment of type II diabetes. Food and Function 9 (2018): 3997-4007.
- [83] Kumar, S., Narwal, S., Kumar, V., and Prakash, O. α -glucosidase inhibitors from plants: a natural approach to treat diabetes. Pharmacognosy Review 5(9) (2011): 19-25.
- [84] Ghani, U. Re-exploring promising α -glucosidase inhibitors for potential development into oral anti-diabetic drugs: finding needle in the haystack. European Journal of Medicinal Chemistry 103 (2015): 133-162.
- [85] Patil, P., Mandal, S., Tomar, S.K., and Anand, S. Food protein-derived bioactive peptides in management of type 2 diabetes. European Journal of Nutrition 54(6) (2015): 863-880.

- [86] Krentz, A.J. and Bailey, C.J. Oral antidiabetic agents: current role in type 2 diabetes mellitus. Drugs 65(3) (2005): 385-411.
- [87] Altmann, S.W., et al. Niemann-Pick C1 Like 1 protein is critical for intestinal cholesterol absorption. Science 303(5661) (2004): 1201-1204.
- [88] Davis, H.R., Jr., et al. Niemann-Pick C1 Like 1 (NPC1L1) is the intestinal phytosterol and cholesterol transporter and a key modulator of whole-body cholesterol homeostasis. Journal of Biological Chemistry 279(32) (2004): 33586-92.
- [89] Pan, X. and Hussain, M.M. Gut triglyceride production. Biochimica et Biophysica Acta 1821(5) (2012): 727-735.
- [90] Klop, B., Wouter Jukema, J., Rabelink, T.J., and Castro Cabezas, M. A physician's guide for the management of hypertriglyceridemia: the etiology of hypertriglyceridemia determines treatment strategy. Panminerva Medica 54(2) (2012): 91-103.
- [91] Goldberg, I.J., Eckel, R.H., and Abumrad, N.A. Regulation of fatty acid uptake into tissues: lipoprotein lipase- and CD36-mediated pathways. Journal of Lipid Research 50 Suppl(Suppl) (2009): S86-S90.
- [92] McQuaid, S.E., et al. Downregulation of adipose tissue fatty acid trafficking in obesity: a driver for ectopic fat deposition? Diabetes 60(1) (2011): 47-55.
- [93] Karpe, F., Dickmann, J.R., and Frayn, K.N. Fatty acids, obesity, and insulin resistance: time for a reevaluation. Diabetes 60(10) (2011): 2441-2449.
- [94] Ooi, E.M., Barrett, P.H., Chan, D.C., and Watts, G.F. Apolipoprotein C-III: understanding an emerging cardiovascular risk factor. Clinical Science (Lond) 114(10) (2008): 611-24.
- [95] Brunzell, J.D., Hazzard, W.R., Porte, D., Jr., and Bierman, E.L. Evidence for a common, saturable, triglyceride removal mechanism for chylomicrons and very low density lipoproteins in man. Journal of Clinical Investigation 52(7) (1973): 1578-1585.
- [96] Baldo, A., et al. The adipisin-acylation stimulating protein system and regulation of intracellular triglyceride synthesis. Journal of Clinical Investigation 92(3) (1993): 1543-7.

- [97] Germinario, R., Sniderman, A.D., Manuel, S., Lefebvre, S.P., Baldo, A., and Cianflone, K. Coordinate regulation of triacylglycerol synthesis and glucose transport by acylation-stimulating protein. Metabolism 42(5) (1993): 574-80.
- [98] Abumrad, N.A. and Davidson, N.O. Role of the gut in lipid homeostasis. Physiol Rev 92(3) (2012): 1061-1085.
- [99] Evans, K., Burdge, G.C., Wootton, S.A., Clark, M.L., and Frayn, K.N. Regulation of dietary fatty acid entrapment in subcutaneous adipose tissue and skeletal muscle. Diabetes 51(9) (2002): 2684-2690.
- [100] Beisiegel, U., Weber, W., and Bengtsson-Olivecrona, G. Lipoprotein lipase enhances the binding of chylomicrons to low density lipoprotein receptor-related protein. Proceedings of the National Academy of Sciences of the United States of America 88(19) (1991): 8342-8346.
- [101] Hussain, M.M., et al. Clearance of chylomicron remnants by the low density lipoprotein receptor-related protein/alpha 2-macroglobulin receptor. Journal of Biological Chemistry 266(21) (1991): 13936-13940.
- [102] Kowal, R.C., Herz, J., Goldstein, J.L., Esser, V., and Brown, M.S. Low density lipoprotein receptor-related protein mediates uptake of cholesteryl esters derived from apoprotein E-enriched lipoproteins. Proceedings of the National Academy of Sciences of the United States of America 86(15) (1989): 5810-5814.
- [103] Mahley, R.W., Huang, Y., and Rall, S.C., Jr. Pathogenesis of type III hyperlipoproteinemia (dysbetalipoproteinemia). Questions, quandaries, and paradoxes. Journal of Lipid Research 40(11) (1999): 1933-1949.
- [104] Mahley, R.W. and Ji, Z.S. Remnant lipoprotein metabolism: key pathways involving cell-surface heparan sulfate proteoglycans and apolipoprotein E. Journal of Lipid Research 40(1) (1999): 1-16.
- [105] Sultan, F., Lagrange, D., Jansen, H., and Griglio, S. Inhibition of hepatic lipase activity impairs chylomicron remnant-removal in rats. Biochimica et Biophysica Acta (BBA) 1042(1) (1990): 150-152.
- [106] Goldstein, J.L. and Brown, M.S. The LDL receptor. Arteriosclerosis, Thrombosis, and Vascular Biology 29(4) (2009): 431-438.

- [107] Lambert, G., Sjouke, B., Choque, B., Kastelein, J.J.P., and Hovingh, G.K. The PCSK9 decade: Thematic review series: New lipid and lipoprotein targets for the treatment of cardiometabolic diseases. Journal of Lipid Research 53(12) (2012): 2515-2524.
- [108] Raal, F., et al. Low-density lipoprotein cholesterol-lowering effects of AMG 145, a monoclonal antibody to proprotein convertase subtilisin/kexin type 9 serine protease in patients with heterozygous familial hypercholesterolemia: the Reduction of LDL-C with PCSK9 Inhibition in Heterozygous Familial Hypercholesterolemia Disorder (RUTHERFORD) randomized trial. Circulation 126(20) (2012): 2408-2417.
- [109] Diabetes.co.uk: the global diabetes community. Diabetes and obesity [Online]. 2019. Available from: <https://www.diabetes.co.uk/diabetes-and-obesity.html> [29 July]
- [110] Al-Goblan, A.S., Al-Alfi, M.A., and Khan, M.Z. Mechanism linking diabetes mellitus and obesity. Diabetes, Metabolic Syndrome & Obesity 7 (2014): 587-591.
- [111] Proctor, S.D., Vine, D.F., and Mamo, J.C. Arterial retention of apolipoprotein B(48)- and B(100)-containing lipoproteins in atherosclerosis. Current Opinion in Lipidology 13(5) (2002): 461-470.
- [112] Proctor, S.D. and Mamo, J.C.L. Intimal retention of cholesterol derived from apolipoprotein B100- and apolipoprotein B48-containing lipoproteins in carotid arteries of Watanabe heritable hyperlipidemic rabbits. Arteriosclerosis, Thrombosis, and Vascular Biology 23(9) (2003): 1595-1600.
- [113] Klop, B., Proctor, S.D., Mamo, J.C., Botham, K.M., and Castro Cabezas, M. Understanding postprandial inflammation and its relationship to lifestyle behaviour and metabolic diseases. International Journal of Vascular Medicine 2012 (2012): 947417.
- [114] Tabas, I., Williams, K.J., and Borén, J. Subendothelial lipoprotein retention as the initiating process in atherosclerosis. Circulation 116(16) (2007): 1832-1844.

- [115] Klop, B. and Castro Cabezas, M. Chylomicrons: A key biomarker and risk factor for cardiovascular disease and for the understanding of obesity. Current Cardiovascular Risk Reports 6(1) (2012): 27-34.
- [116] Subramanian, S. and Chait, A. Hypertriglyceridemia secondary to obesity and diabetes. Biochimica et Biophysica Acta (BBA) 1821(5) (2012): 819-25.
- [117] Proctor, S.D., Vine, D.F., and Mamo, J.C. Arterial permeability and efflux of apolipoprotein B-containing lipoproteins assessed by in situ perfusion and three-dimensional quantitative confocal microscopy. Arteriosclerosis, Thrombosis, and Vascular Biology 24(11) (2004): 2162-2167.
- [118] Pacifico, L., et al. Low 25(OH)D₃ levels are associated with total adiposity, metabolic syndrome, and hypertension in Caucasian children and adolescents. European Journal Endocrinology 165(4) (2011): 603-611.
- [119] Watts, G.F., Chan, D.C., Barrett, P.H., Martins, I.J., and Redgrave, T.G. Preliminary experience with a new stable isotope breath test for chylomicron remnant metabolism: a study in central obesity. Clinical Sciences (London) 101(6) (2001): 683-690.
- [120] Taskinen, M.R., et al. Dual metabolic defects are required to produce hypertriglyceridemia in obese subjects. Arteriosclerosis, Thrombosis, and Vascular Biology 31(9) (2011): 2144-2150.
- [121] Caron, S., et al. Transcriptional activation of apolipoprotein CIII expression by glucose may contribute to diabetic dyslipidemia. Arteriosclerosis, Thrombosis, and Vascular Biology 31(3) (2011): 513-519.
- [122] Seongkyu, K., Je-Hein, K., Su Hyun, S., and Eun-Seok, P. Anti-obesity effect with reduced adverse effect of the co-administration of mini-tablets containing orlistat and mini-tablets containing xanthan gum: *In-vitro* and *in-vivo* evaluation. International Journal of Pharmaceutics 591 (2020).
- [123] Kordik, C.P.a.R., A. B. Pharmacological treatment of obesity: therapeutic strategies. Journal of Medicinal Chemistry 42 (1999): 181-201.
- [124] Cavaliere, H., Floriano, I., and Medeiros-Neto, G. Gastrointestinal side effects of orlistat may be prevented by concomitant prescription of natural fibers

- (psyllium mucilloid). International Journal of Obesity and Related Metabolic Disorders 25(7) (2001): 1095-1099.
- [125] Demidova-Rice, T.N., Hamblin, M.R., and Herman, I.M. Acute and impaired wound healing: pathophysiology and current methods for drug delivery, part 1: normal and chronic wounds: biology, causes, and approaches to care. Advanced in Skin & Wound Care 25(7) (2012): 304-314.
- [126] McCarty, S.M. and Percival, S.L. Proteases and delayed wound healing. Advance in Wound Care (New Rochelle) 2(8) (2013): 438-447.
- [127] Latha, B., Ramakrishnan, K.M., Jayaraman, V., and Babu, M. Action of trypsin:chymotrypsin (Chymoral forte DS) preparation on acute-phase proteins following burn injury in humans. Burns 23 Suppl 1 (1997): S3-7.
- [128] Chandanwale, A., Langade, D., Sonawane, D., and Gavai, P. A randomized, clinical trial to evaluate efficacy and tolerability of Trypsin:Chymotrypsin as compared to Serratiopeptidase and Trypsin:Bromelain:Rutoside in wound management. Advances in Therapy 34(1) (2017): 180-198.
- [129] Toriseva, M. and Kähäri, V.M. Proteinases in cutaneous wound healing. Cellular and Molecular Life Sciences 66(2) (2009): 203-224.
- [130] Shah, J.M., Omar, E., Pai, D.R., and Sood, S. Cellular events and biomarkers of wound healing. Indian Journal of Plastic Surgery 45(2) (2012): 220-228.
- [131] Singh, N. and Bhattacharyya, D. Proteases in wound healing and immunity. in Chakraborti, S., Chakraborti, T., and Dhalla, N.S. (eds.), Proteases in Human Diseases, pp. 147-170. Singapore: Springer Singapore, 2017.
- [132] Gonzalez, A.C., Costa, T.F., Andrade, Z.A., and Medrado, A.R. Wound healing - A literature review. Annais Brasileiros de Dermatologia 91(5) (2016): 614-620.
- [133] Frykberg, R.G. and Banks, J. Challenges in the treatment of chronic wounds. Advances in Wound Care (New Rochelle) 4(9) (2015): 560-582.
- [134] Lenselink, E.A. Role of fibronectin in normal wound healing. International Wound Journal 12(3) (2015): 313-316.
- [135] Latha, B., Ramakrishnan, M., Jayaraman, V., and Babu, M. Serum enzymatic changes modulated using trypsin: chymotrypsin preparation during burn wounds in humans. Burns 23(7-8) (1997): 560-564.

- [136] Latha, B., Ramakrishnan, M., Jayaraman, V., and Babu, M. The efficacy of Trypsin: Chymotrypsin preparation in the reduction of oxidative damage during burn injury. Burns 24(6) (1998): 532-538.
- [137] Villines, Z. How does diabetes affect wound healing? in *Medical News Today*. 2019.
- [138] American Diabetes Association. The uncomplicated guide to diabetes complications. 3rd ed.: American Diabetes Association, Alexandria (VA), 2009.
- [139] Reiber, G.E. The epidemiology of diabetic foot problems. Diabetic Medicine 13 (1996): S6-S11.
- [140] Bakker, K.a.S., N. C. (on behalf of the International Working Group on the Diabetic Foot Editorial Board). The development of global consensus guidelines on the management and prevention of the diabetic foot 2011. Diabetes/ Metabolism Research and Reviews 28(Supplement 1) (2012): 116-118.
- [141] Guiso, M., Marra, C., and Farina, A. A new efficient resveratrol synthesis. Tetrahedron Letters 43(4) (2002): 597-598.
- [142] Zhang, P., Lu, J., Jing, Y., Tang, S., Zhu, D., and Bi, Y. Global epidemiology of diabetic foot ulceration: a systematic review and meta-analysis. Annals of Medicine 49(2) (2017): 106-116.
- [143] Abbas, Z.G. and Archibald, L.K. Epidemiology of the diabetic foot in Africa. Medicinal Science Monitor 11(8) (2005): RA262-RA270.
- [144] Ngwogu, K.O., Ekpo, B. O., Akpuaka, F. C., Ngwogu, A.C., and Okhiai, O. The prevalence of obesity as indicated by body mass index among apparently healthy adult living in Ava, Abia State, Nigeria. International Journal of Basic, Applied and Innovative Research 1(1) (2012): 19-24.
- [145] Tuttolomondo, A., Maida, C., and Pinto, A. Diabetic foot syndrome: immune-inflammatory features as possible cardiovascular markers in diabetes. World Journal of Orthopedics 6(1) (2015): 62-67.
- [146] Bakker, K., Apelqvist, J., Lipsky, B.A., and Van Netten, J.J. The 2015 IWGDF guidance documents on prevention and management of foot problems in

- diabetes: development of an evidence-based global consensus. Diabetes/Metabolism Research and Reviews 32 Suppl 1 (2016): 2-6.
- [147] Tellechea, A., Leal, E., Veves, A., and Carvalho, E. Inflammatory and angiogenic abnormalities in diabetic wound healing: role of neuropeptides and therapeutic perspectives. The Open Circulation & Vascular Journal 3 (2010): 43-55.
- [148] Shah, D. and Mital, K. The role of trypsin: chymotrypsin in tissue repair. Advances in Therapy 35(1) (2018): 31-42.
- [149] Xue, M. and Jackson, C.J. Extracellular Matrix Reorganization During Wound Healing and Its Impact on Abnormal Scarring. Advance in Wound Care (New Rochelle) 4(3) (2015): 119-136.
- [150] Libby, P. and Goldberg, A.L. Effects of chymostatin and other proteinase inhibitors on protein breakdown and proteolytic activities in muscle. Biochemical Journal 188(1) (1980): 213-220.
- [151] Merza, J., Mallet, S., Litaudon, M., Dumontet, V., Séraphin, D., and Richomme, P. New cytotoxic guttiferone analogues from *Garcinia virgata* from New Caledonia. Planta Medica 72(01) (2006): 87-89.
- [152] Phukhatmuen, P., Raksat, A., Laphookhieo, S., Charoensup, R., Duangyod, T., and Maneerat, W. Bioassay-guided isolation and identification of antidiabetic compounds from *Garcinia cowa* leaf extract. Heliyon 6(4) (2020): e03625.
- [153] Lambert, C., et al. Comparative analyses of stilbenoids in canes of major *Vitis vinifera* L. cultivars. Journal of Agricultural and Food Chemistry 61(47) (2013): 11392-11399.
- [154] Mattivi, F., et al. Profiling of resveratrol oligomers, important stress metabolites, accumulating in the leaves of hybrid *Vitis vinifera* (Merzlingx Teroldego) genotypes infected with *Plasmopara viticola*. Journal of Agricultural and Food Chemistry 59(10) (2011): 5364-5375.
- [155] Baderschneider, B. and Winterhalter, P. Isolation and characterization of novel stilbene derivatives from Riesling wine. Journal of Agricultural and Food Chemistry 48(7) (2000): 2681-2686.

- [156] Seo, E.-K., et al. Resveratrol tetramers from *Vatica diospyroides*. The Journal of Organic Chemistry 64(19) (1999): 6976-6983.
- [157] Sasikumar, P., et al. Isolation and characterization of resveratrol oligomers from the stem bark of *Hopea ponga* (Dennst.) Mabb. and their antidiabetic effect by modulation of digestive enzymes, protein glycation and glucose uptake in L6 myocytes. Journal of Ethnopharmacology 236 (2019): 196-204.
- [158] Ain, Q., Ashiq, U., Jamal, R., Saleem, M., and Mahroof-Tahir, M. Alpha-glucosidase and carbonic anhydrase inhibition studies of Pd(II)-hydrazide complexes. Arabian Journal of Chemistry 10 (2017): 488-499.
- [159] Dudoit, A., et al. α -glucosidase inhibitory activity of Tannat grape phenolic extracts in relation to their ripening stages. Biomolecules 10(8) (2020).
- [160] Arce, F., Jr., Concepcion, J.E., Mayol, K.M.C., and See, G.L. *In-vitro* α -amylase and α -glucosidase inhibition activity of tabing *Abutilon indicum* (Linn 1836) root extracts. International Journal of Toxicological and Pharmacological Research 8 (2016): 391-396.
- [161] Sakulkeo, O., Wattanapiromsakul, C., Pitakbut, T., and Dej-Adisai, S. Alpha-glucosidase inhibition and molecular docking of isolated compounds from traditional Thai medicinal plant, *Neuropeltis racemosa* Wall. Molecules 27(3) (2022).
- [162] Odetola, A., Akinloye, O., Egunjobi, C., Adekunle, W., and Ayoola, A. Possible antidiabetic and antihyperlipidaemic of fermented *Parkia biglobosa* (JACQ) extract in alloxan-induced diabetes rats. Clinical and Experimental Pharmacology and Physiology 33(9) (2006): 808-812.
- [163] Eidi, A., Eidi, M., and Sokhteh, M. Effect of fenugreek (*Trigonella foenum-graecum* L) seeds on serum parameters in normal and streptozotocin-induced diabetic rats. Nutrition Research 27(11) (2007): 728-733.
- [164] Sugiwati, S., Setiasih, S., and Afifah, E. Antihyperglycemic activity of the mahkota dewa leaf extracts as an alpha-glucosidase inhibitor. Seri Kesehatan (Health Series); Vol 13, No 2 (2009): December 13 (2010).

- [165] Andrade-Cetto, A., Becerra-Jiménez, J., and Cárdenas-Vázquez, R. Alfa-glucosidase-inhibiting activity of some Mexican plants used in the treatment of type 2 diabetes. Journal of Ethnopharmacology 116(1) (2008): 27-32.
- [166] Quispe, Y.N.G., Hwang, S.H., Wang, Z., Zuo, G., and Lim, S.S. Screening *in-vitro* targets related to diabetes in herbal extracts from Peru: Identification of active compounds in *Hypericum laricifolium* Juss. by offline high-performance liquid chromatography. International Journal of Molecular Sciences 18(12) (2017).
- [167] Thiantongin, P. Study of α -glucosidase and α -amylase inhibitory activities of Thai folk anti-diabetes remedies and phytochemical study of *Vitex glabrata* stem bark and its chemical constituents. Master, Thai Traditional Medicine Prince of Songkla University, 2014.
- [168] Barker, M.K. and Rose, D.R. Specificity of processing α -glucosidase I is guided by the substrate conformation: crystallographic and *in-silico* studies. Journal of Biological Chemistry 288(19) (2013): 13563-13574.
- [169] Sohrabi, M., Binaeizadeh, M.R., Iraj, A., Larijani, B., Saeedi, M., and Mahdavi, M. A review on α -glucosidase inhibitory activity of first row transition metal complexes: a futuristic strategy for treatment of type 2 diabetes. RSC Advances 12(19) (2022): 12011-12052.
- [170] Dirir, A.M., Daou, M., Yousef, A.F., and Yousef, L.F. A review of alpha-glucosidase inhibitors from plants as potential candidates for the treatment of type-2 diabetes. Phytochemistry Reviews (2021): 1-31.
- [171] Ernawati, T. *In-silico* evaluation of molecular interactions between known α -glucosidase inhibitors and homologous α -glucosidase enzymes from *Saccharomyces cerevisiae*, *Rattus norvegicus*, and GANC-human. Thai Journal of Pharmaceutical Sciences (TJPS) 42(1) (2018).
- [172] Rosak, C. and Mertes, G. Critical evaluation of the role of acarbose in the treatment of diabetes: patient considerations. Diabetes, Metabolic Syndrome and Obesity: Targets and Therapy 5 (2012): 357-367.

- [173] Abuelizz, H.A., Anouar, E.H., Ahmad, R., Azman, N., Marzouk, M., and Al-Salahi, R. Triazoloquinazolines as a new class of potent α -glucosidase inhibitors: in vitro evaluation and docking study. *PLoS One* 14(8) (2019): e0220379.
- [174] Guan, L., Long, H., Ren, F., Li, Y., and Zhang, H. A structure-activity relationship study of the inhibition of α -amylase by benzoic acid and its derivatives. *Nutrients* 14(9) (2022).
- [175] Egloff, M.P., Marguet, F., Buono, G., Verger, R., Cambillau, C., and van Tilbeurgh, H. The 2.46 Å resolution structure of the pancreatic lipase-colipase complex inhibited by a C11 alkyl phosphonate. *Biochemistry* 34(9) (1995): 2751-2762.
- [176] Nguyen, P.T.V., Huynh, H.A., Truong, D.V., Tran, T.D., and Vo, C.T. Exploring aurone derivatives as potential human pancreatic lipase inhibitors through molecular docking and molecular dynamics simulations. *Molecules* 25(20) (2020).
- [177] Winkler, F.K., D'Arcy, A., and Hunziker, W. Structure of human pancreatic lipase. *Nature* 343(6260) (1990): 771-774.
- [178] Lowe, M.E. Structure and function of pancreatic lipase and colipase. *Annual Review of Nutrition* 17 (1997): 141-158.
- [179] van Tilbeurgh, H., Egloff, M.P., Martinez, C., Rugani, N., Verger, R., and Cambillau, C. Interfacial activation of the lipase-procolipase complex by mixed micelles revealed by X-ray crystallography. *Nature* 362(6423) (1993): 814-20.
- [180] Park, J.-Y., Kim, C.S., Park, K.-M., and Chang, P.-S. Inhibitory characteristics of flavonol-3-O-glycosides from *Polygonum aviculare* L. (common knotgrass) against porcine pancreatic lipase. *Scientific Reports* 9(1) (2019): 18080.
- [181] Lunagariya, N.A., Patel, N.K., Jagtap, S.C., and Bhutani, K.K. Inhibitors of pancreatic lipase: state of the art and clinical perspectives. *Excli j* 13 (2014): 897-921.
- [182] Slámová, K., Kapešová, J., and Valentová, K. "Sweet Flavonoids": Glycosidase-Catalyzed Modifications. *Int J Mol Sci* 19(7) (2018).

- [183] Tornøe, C.W., Johansson, E., and Wahlund, P.-O. Divergent protein synthesis of Bowman–Birk protease inhibitors, their hydrodynamic behavior and co-crystallization with α -chymotrypsin. Synlett 28(15) (2017): 1901-1906.
- [184] Odani, S. and Ono, T. Chemical substitutions of the reactive site leucine residue in soybean Bowman-Birk proteinase inhibitor with other amino acids. The Journal of Biochemistry 88(5) (1980): 1555-1558.
- [185] Schilling, R.J. and Mitra, A.K. Degradation of insulin by trypsin and alpha-chymotrypsin. Pharmaceutical Research 8(6) (1991): 721-727.
- [186] Laskowski Jr, M., Haessler, H., Miech, R., Peanasky, R., and Laskowski, M. Effect of trypsin inhibitor on passage of insulin across the intestinal barrier. Science 127(3306) (1958): 1115-1116.
- [187] Danforth, E. and Moore, R.O. Intestinal absorption of insulin in the rat. Endocrinology 65(1) (1959): 118-123.
- [188] Kidron, M., Bar-On, H., Berry, E.M., and Ziv, E. The absorption of insulin from various regions of the rat intestine. Life Sciences 31(25) (1982): 2837-2841.
- [189] Fujii, S., Yokoyama, T., Ikegaya, K., Sato, F., and Yokoo, N. Promoting effect of the new chymotrypsin inhibitor FK-448 on the intestinal absorption of insulin in rats and dogs. Journal of Pharmacy and Pharmacology 37(8) (1985): 545-549.
- [190] Shinomiya, M., Shirai, K., Saito, Y., Yoshida, S., and Matsuoka, N. Effect of new chymotrypsin inhibitor (FK-448) on intestinal absorption of insulin. The Lancet 325(8437) (1985): 1092-1093.
- [191] Ziv, E., Lior, O., and Kidron, M. Absorption of protein via the intestinal wall: A quantitative model. Biochemical Pharmacology 36(7) (1987): 1035-1039.
- [192] Schwartz, J.G., Guan, D., Green, G.M., and Phillips, W.T. Treatment with an oral proteinase inhibitor slows gastric emptying and acutely reduces glucose and insulin levels after a liquid meal in type II diabetic patients. Diabetes Care 17(4) (1994): 255-262.

- [193] Harasawa, S., et al. Gastric emptying in normal subjects and patients with peptic ulcer: a study using the acetaminophen method. Journal of Gastroenterology 14(1) (1979): 1-10.
- [194] Hou, T., Wang, J., Zhang, W., and Xu, X. ADME evaluation in drug discovery. 6. Can oral bioavailability in humans be effectively predicted by simple molecular property-based rules? Journal of Chemical Information Model 47(2) (2007): 460-463.
- [195] Veber, D.F., Johnson, S.R., Cheng, H.Y., Smith, B.R., Ward, K.W., and Kopple, K.D. Molecular properties that influence the oral bioavailability of drug candidates. Journal of Medicinal Chemistry 45(12) (2002): 2615-2623.
- [196] Ganesan, A. The impact of natural products upon modern drug discovery. Current Opinion in Chemical Biology 12(3) (2008): 306-317.
- [197] Banerjee, P., Eckert, A.O., Schrey, A.K., and Preissner, R. ProTox-II: a webserver for the prediction of toxicity of chemicals. Nucleic Acids Research 46(W1) (2018): W257-w263.
- [198] Pokharkar, O., Lakshmanan, H., Zyryanov, G., and Tsurkan, M. *In-silico* evaluation of antifungal compounds from marine sponges against COVID-19-associated mucormycosis. Marine Drugs 20(3) (2022): 215.
- [199] Rangsinth, P., Sillapachaiyaporn, C., Nilkhet, S., Tencomnao, T., Ung, A.T., and Chuchawankul, S. Mushroom-derived bioactive compounds potentially serve as the inhibitors of SARS-CoV-2 main protease: An *in-silico* approach. Journal of Traditional and Complementary Medicine 11(2) (2021): 158-172.
- [200] Alam, M.S., Chopra, N., Ali, M., and Niwa, M. Oleanen and stigmasterol derivatives from *Ambroma augusta*. Phytochemistry 41(4) (1996): 1197-1200.
- [201] Garba, M.A. and Iliya, I. Isolation of stigmasterol, β -sitosterol and 2-hydroxyhexadecanoic acid methyl ester from the rhizomes of *Stylochaeton lancifolius* Pyer and Kotchy (Araceae). in, 2009.
- [202] Kamal, N., Clements, C., Gray, A., and Edrada-Ebel, R. Anti-infective activities of secondary metabolites from *Vitex pinnata*. Journal of Applied Pharmaceutical Science 6 (2016): 102-106.

- [203] Pollock, J.R.A.S.R.S. Dictionary of organic compounds 4th edition. Vol. 5: Eyre and Spottiswoode Ltd., 1965.
- [204] Mahato, S.B. and Kundu, A.P. ^{13}C NMR spectra of pentacyclic triterpenoids—a compilation and some salient features. Phytochemistry 37(6) (1994): 1517-1575.
- [205] Li, X., et al. Free Linoleic Acid and Oleic Acid Reduce Fat Digestion and Absorption In Vivo as Potent Pancreatic Lipase Inhibitors Derived from Sesame Meal. Molecules 27(15) (2022): 4910.





จุฬาลงกรณ์มหาวิทยาลัย
CHULALONGKORN UNIVERSITY

APPENDIX

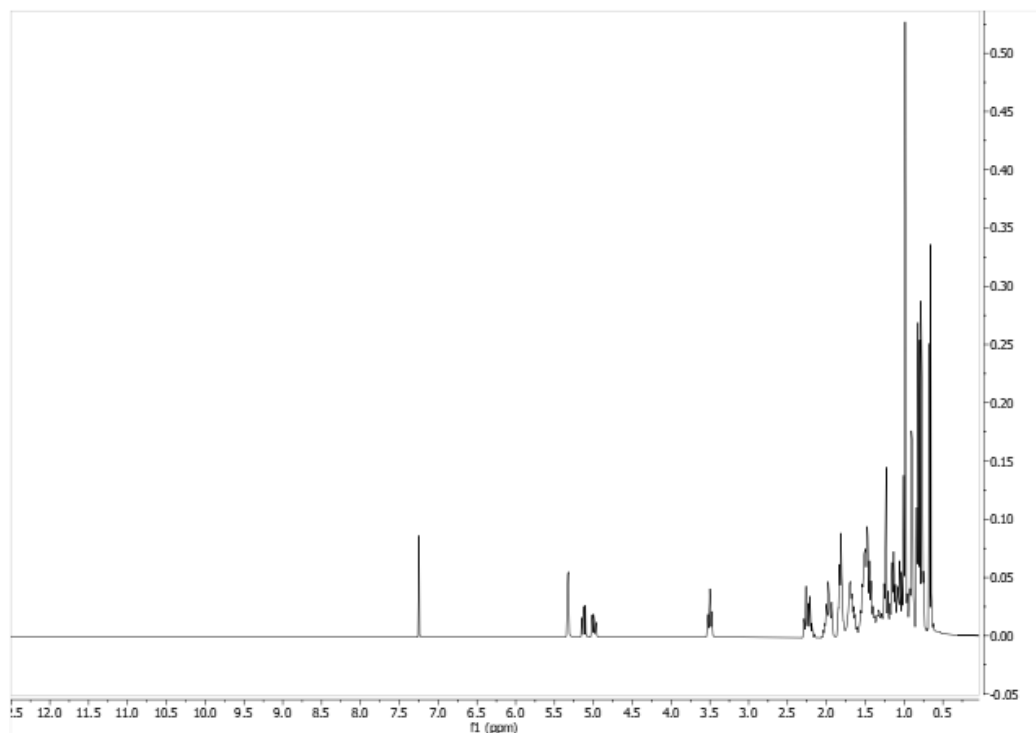


Figure A.1 ^1H NMR spectrum (500 MHz, CDCl_3) of mixture (metabolite 1 and 2)

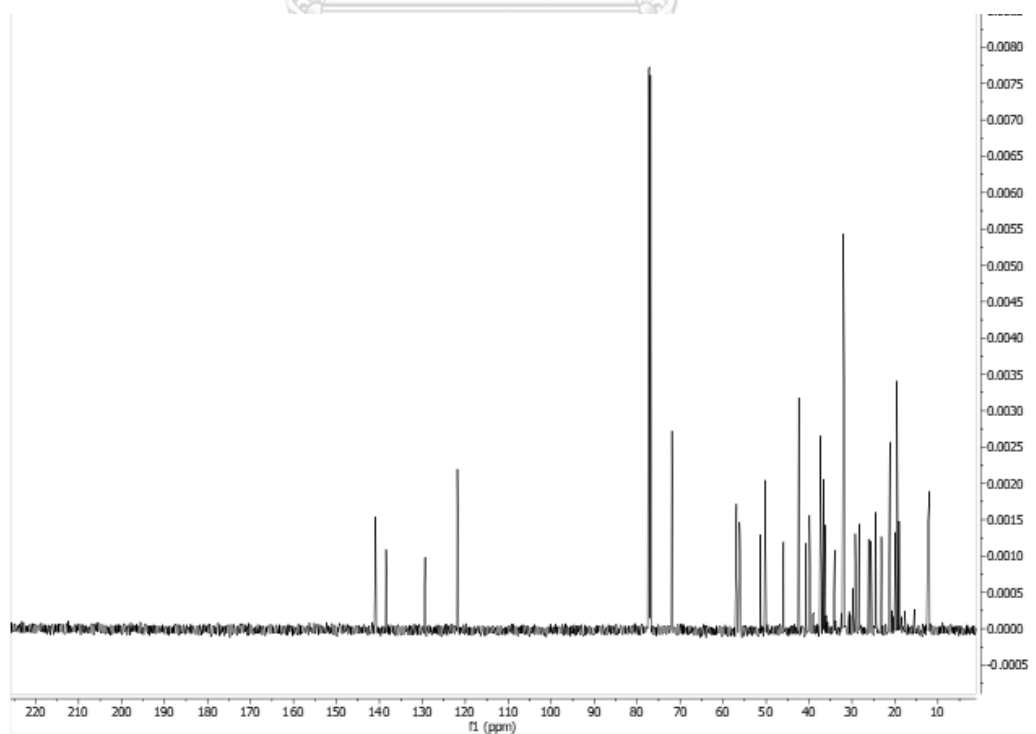


Figure A.2 ^{13}C NMR spectrum (500 MHz, CDCl_3) of mixture (metabolite 1 and 2)

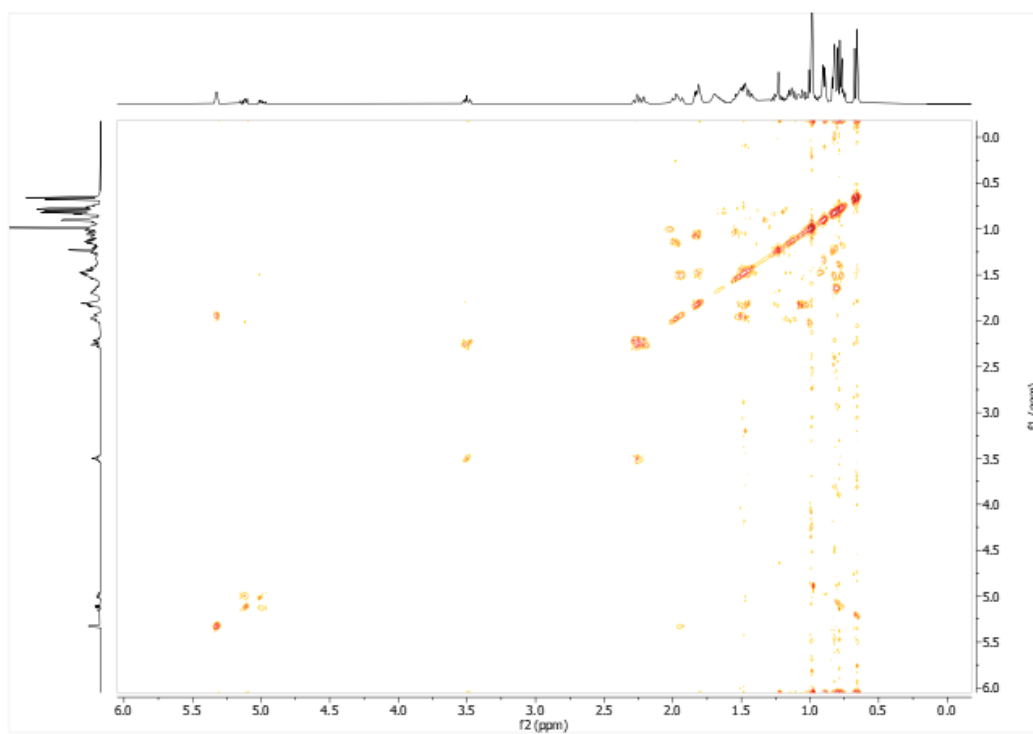


Figure A.3 ^1H - ^1H COSY spectrum (500 MHz, CDCl_3) of mixture (metabolite 1 and 2)

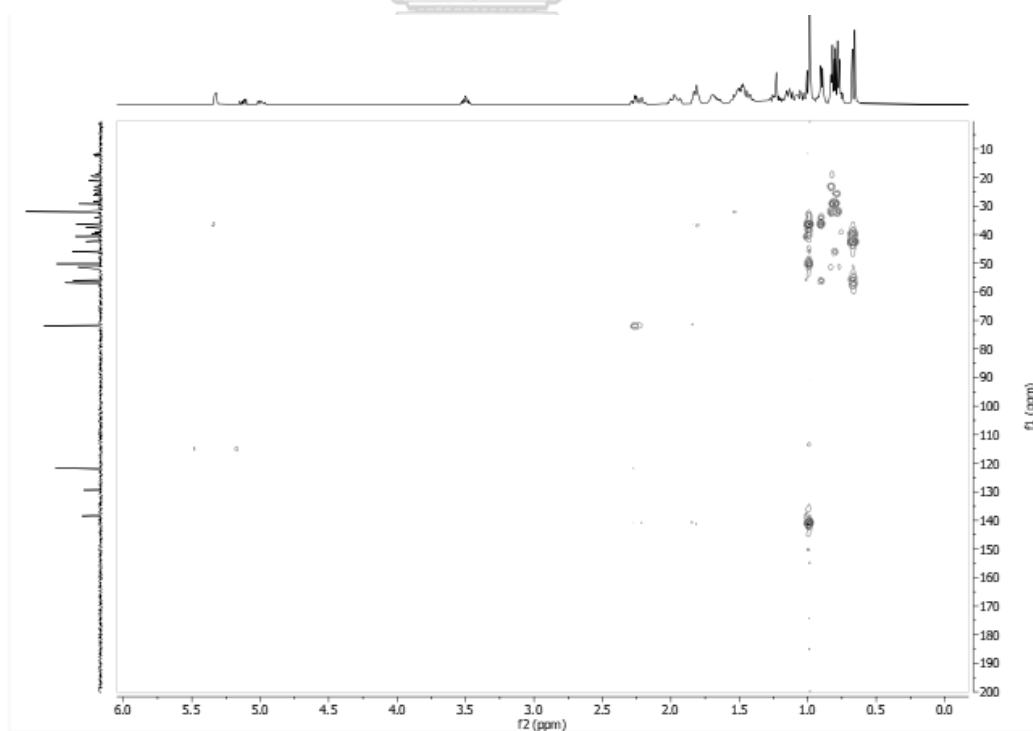


Figure A.4 HMBC spectrum (500 MHz, CDCl_3) of mixture (metabolite 1 and 2)

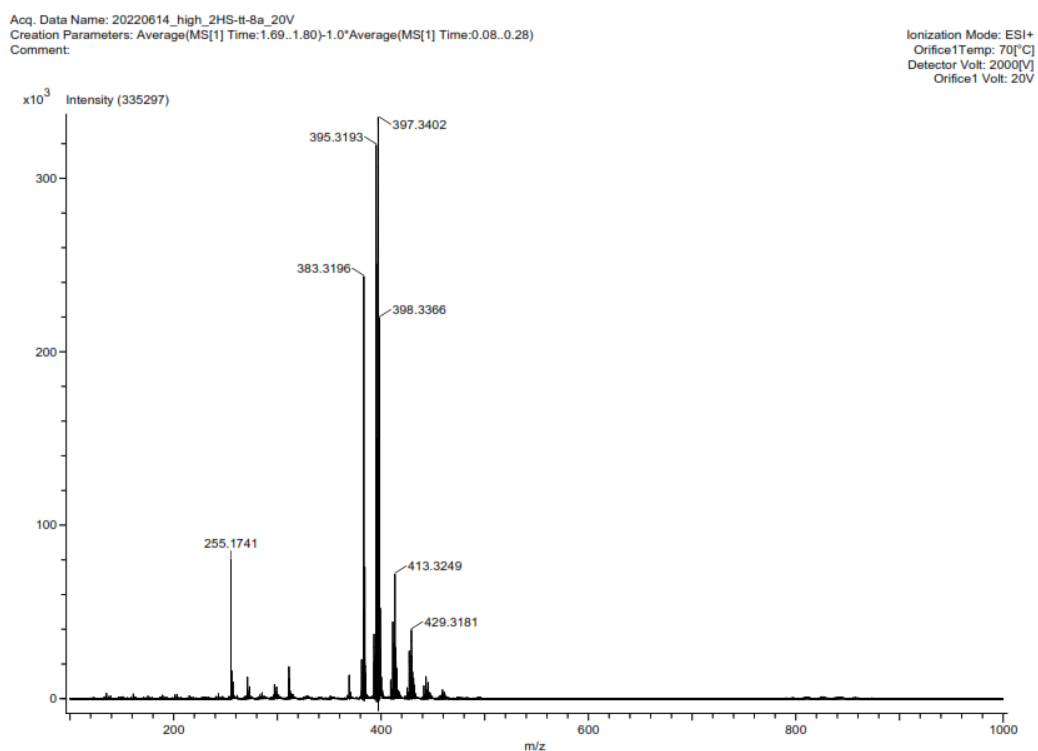


Figure A.5 HR-ESI-MS spectrum of mixture (metabolite 1 and 2)

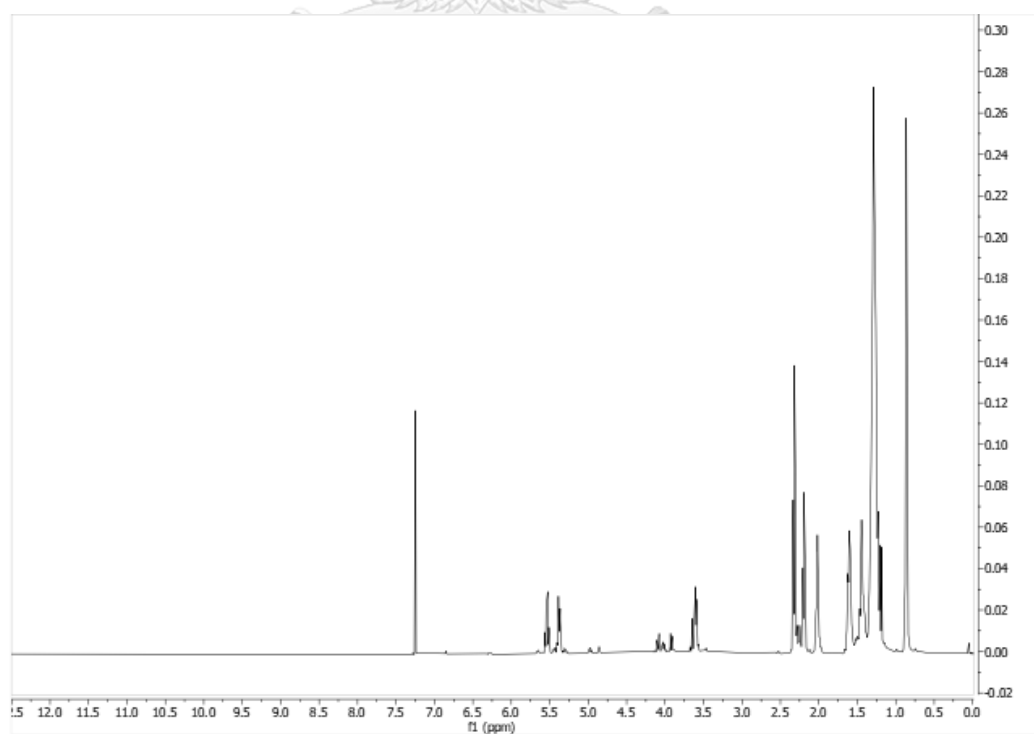


Figure A.6 ^1H NMR spectrum (500 MHz, CDCl_3) spectrum of metabolite 3

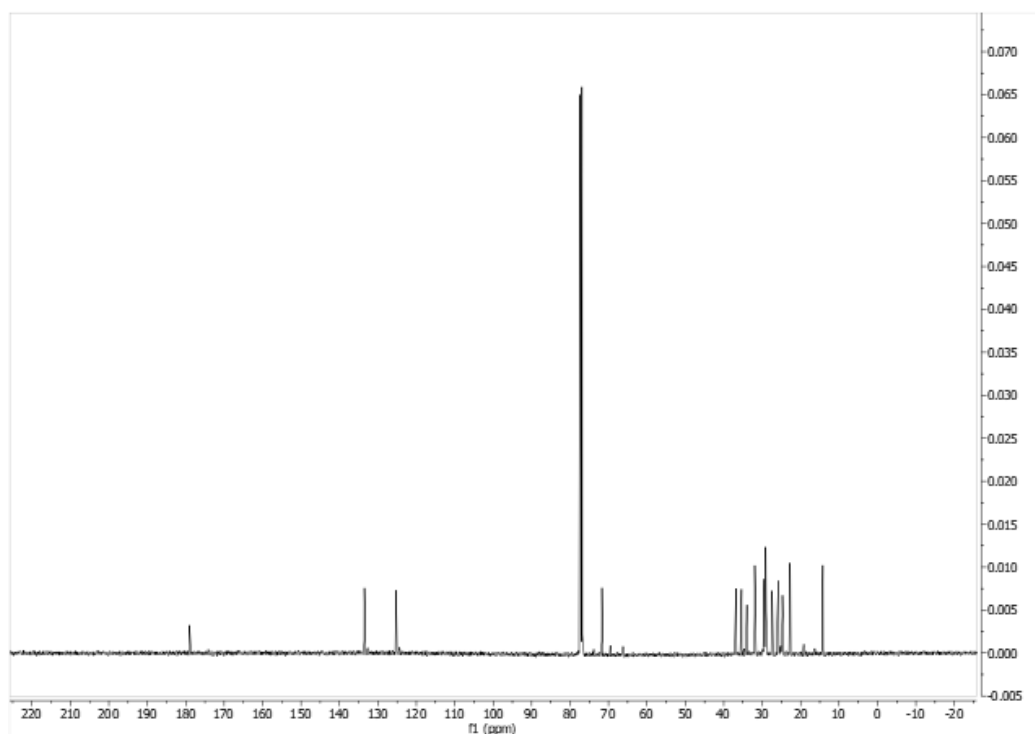


Figure A.7 ^{13}C NMR spectrum (500 MHz, CDCl_3) of metabolite 3

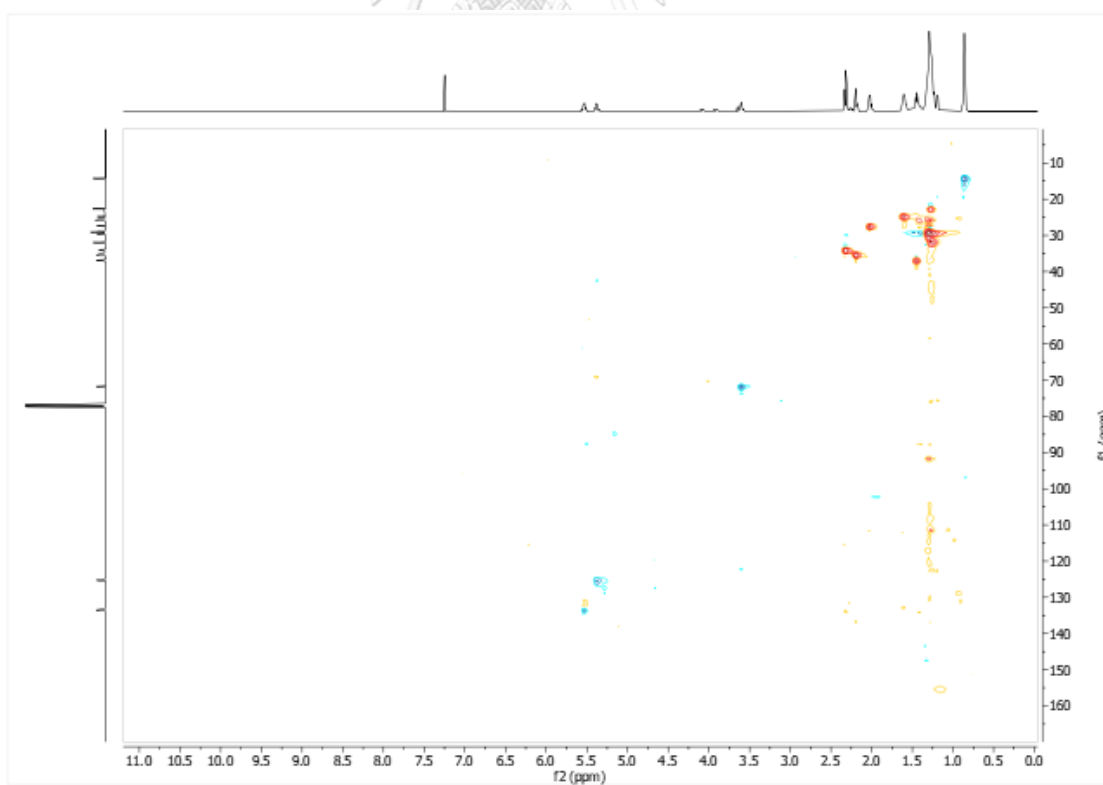


Figure A.8 HSQC spectrum (500 MHz, CDCl_3) of metabolite 3

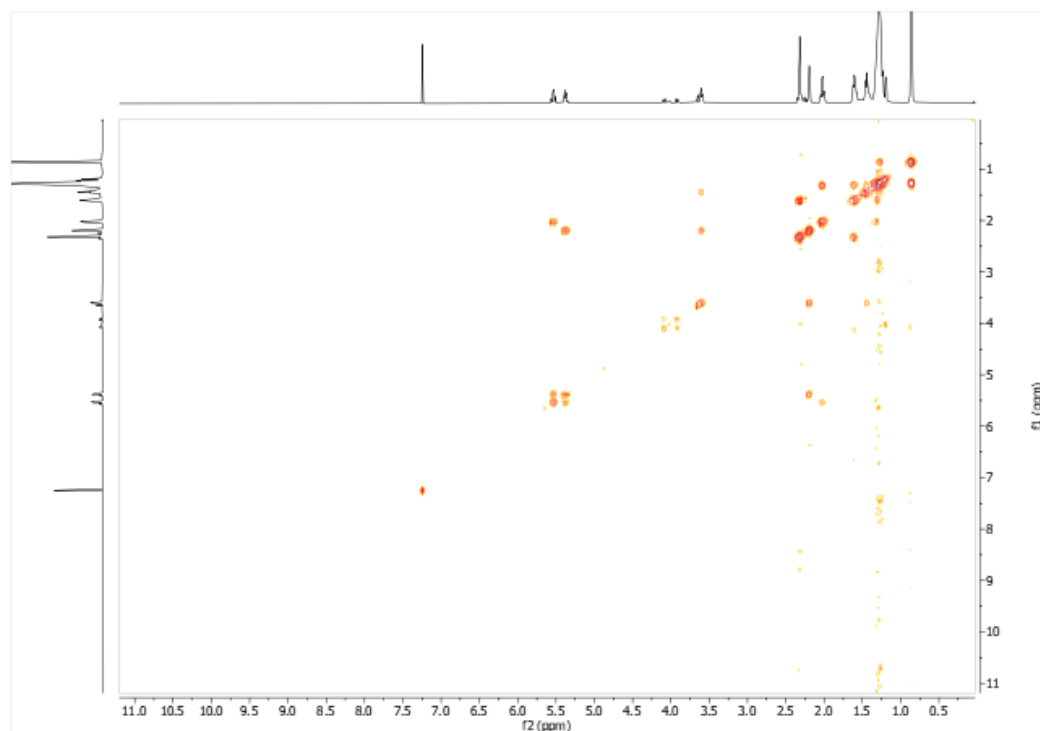


Figure A.9 ^1H - ^1H COSY spectrum (500 MHz, CDCl_3) of metabolite 3

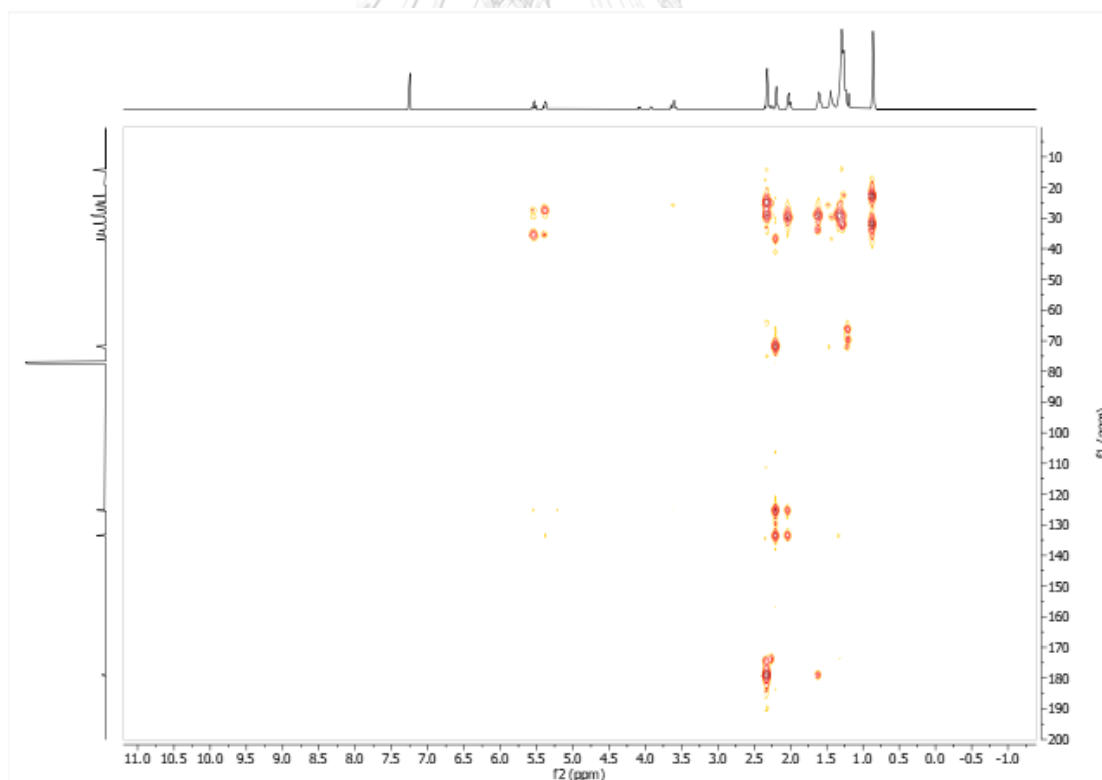


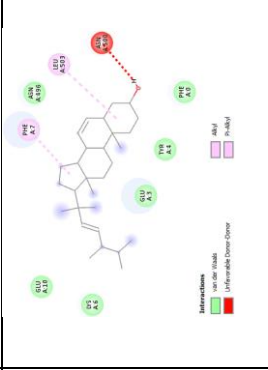

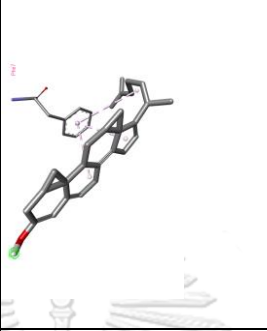
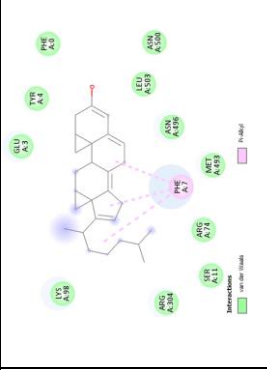
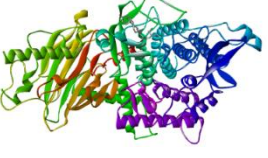
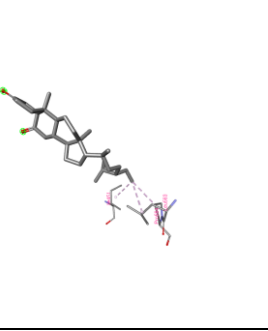
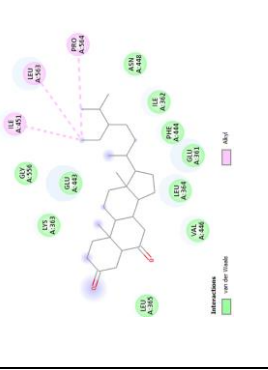
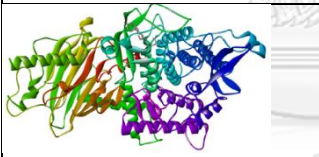

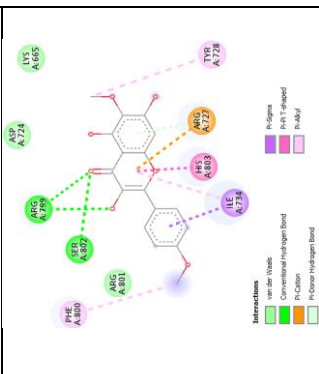
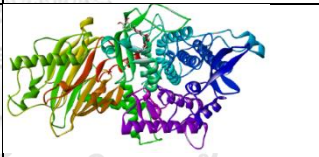

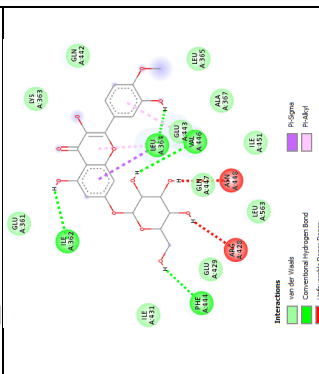
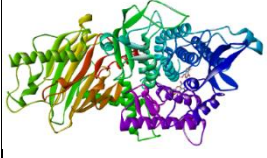
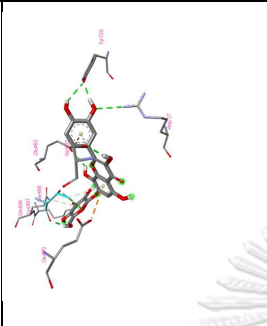
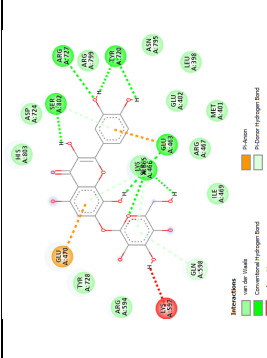
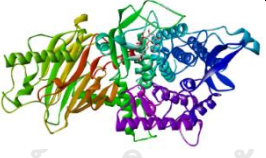
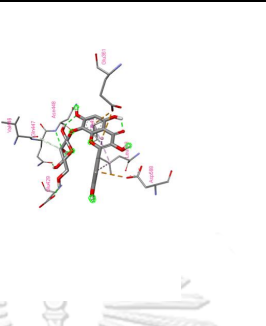
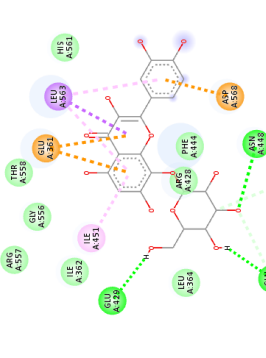
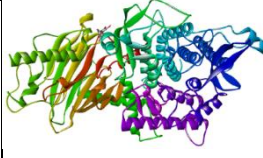
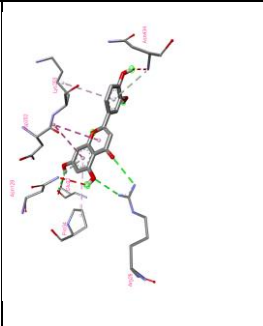
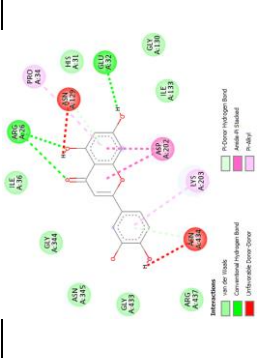



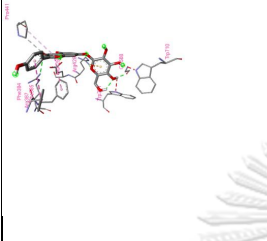
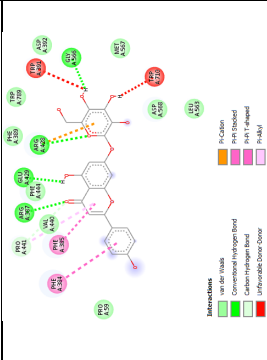
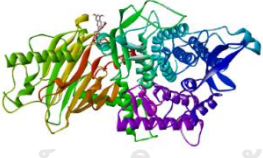
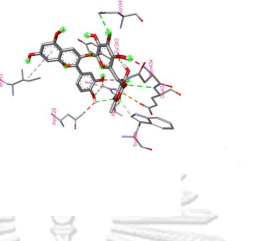
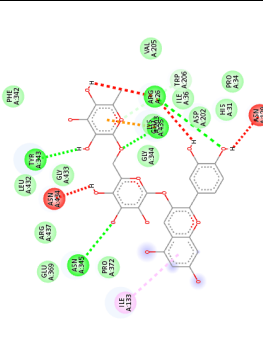

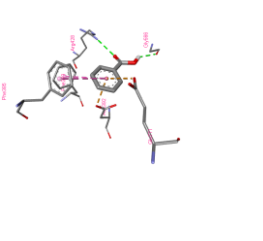
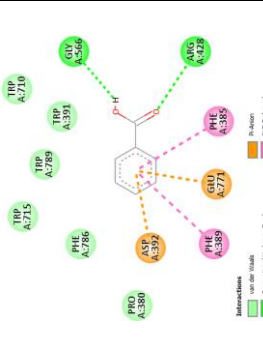
Figure A.10 HMBC spectrum (500 MHz, CDCl_3) of metabolite 3

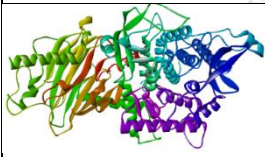
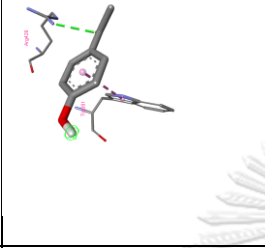
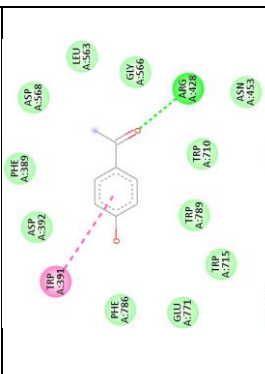

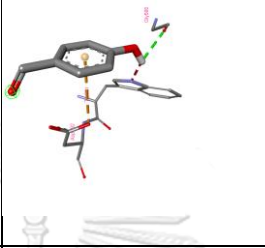
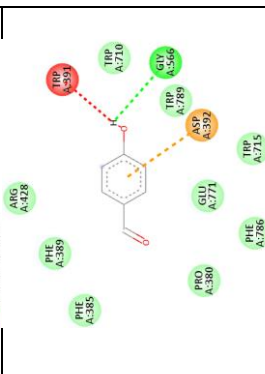

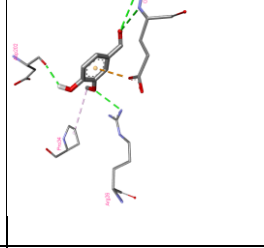
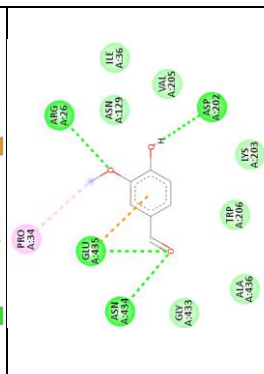
No	Phytochemical name	Binding energy (kcal/mol)	Phytochemicals in the active site of α -glucosidase	3D molecular amino acid interaction	2D molecular amino acid interaction
4	20, 23-Dimethylcholesta-6, 22-dien-3 β -ol	-7.9			
5	Cholesterol	-7.7			
6	(24R)-5 α -stigmastane-3,6-dione	-8.1			


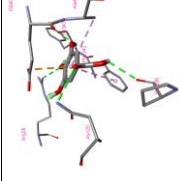
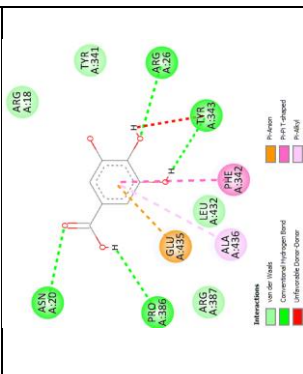
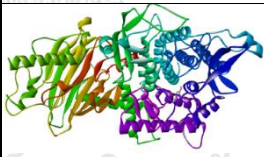
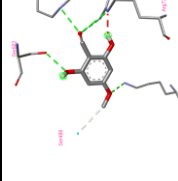
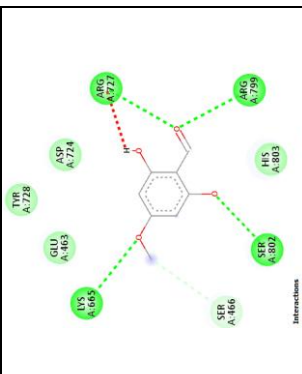
No	Phytochemical name	Binding energy (kcal/mol)	Phytochemicals in the active site of α -glucosidase	3D molecular amino acid interaction	2D molecular amino acid interaction
7	4',6-Dimethoxy kaempferol	-7.9			
8	3,5,5'-Trihydroxy-4'-methoxy flavone-7O- β -D-glucopyranoside	-8.9			


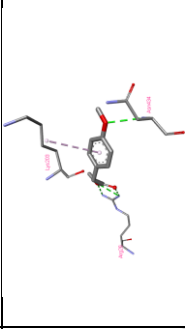
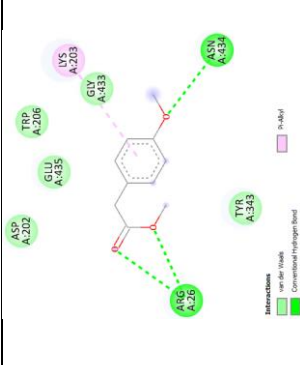

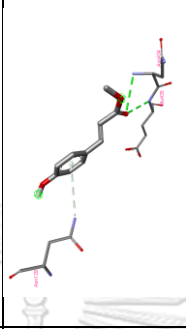
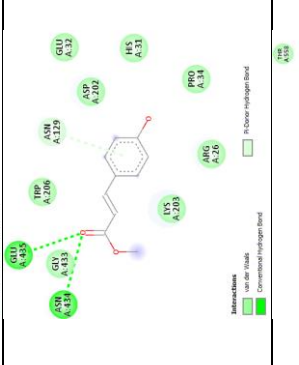
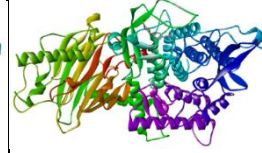
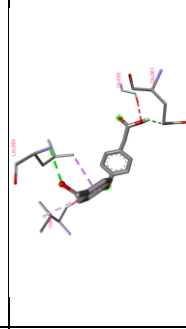
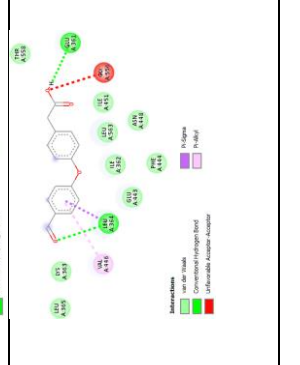
No	Phytochemical name	Binding energy (kcal/mol)	Phytochemicals in the active site of α -glucosidase	3D molecular amino acid interaction	2D molecular amino acid interaction
9	Quercetin	-7.9			
10	Quercetin-3-O- β -D-glucopyranoside	-8.9			
11	Quercetin-3-O- α -rhamnopyranosyl (1 \rightarrow 6)- β -glucopyranoside	-10.2			

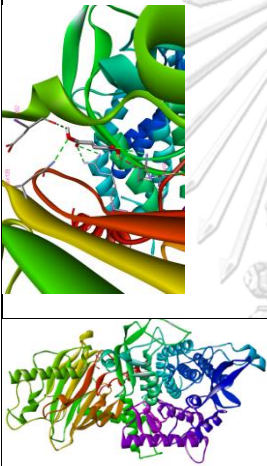
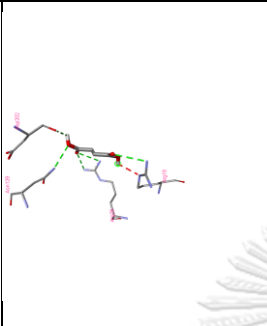
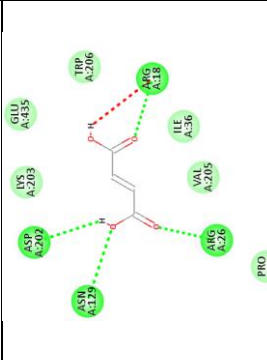
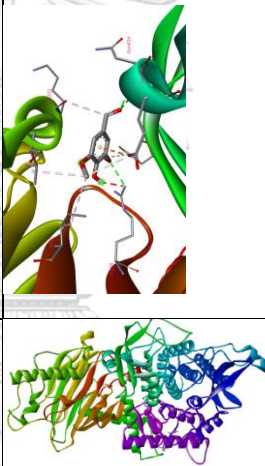
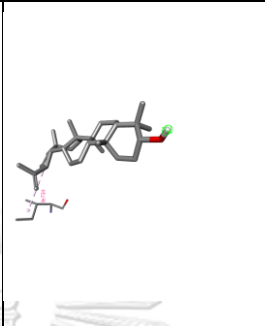
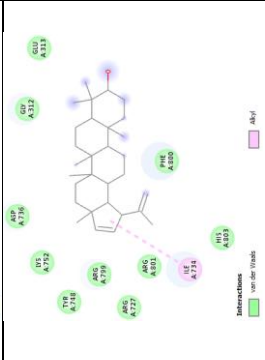

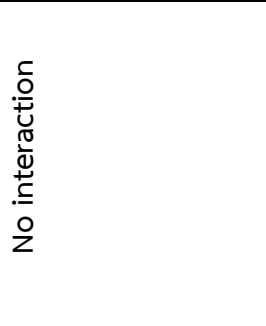

No	Phytochemical name	Binding energy (kcal/mol)	Phytochemicals in the active site of α -glucosidase	3D molecular amino acid interaction	2D molecular amino acid interaction
12	Gossypetin-7-O- β -glucoside	-9.4			
13	Gossypetin-8-O- β -glucoside	-8.8			
14	Luteolin	-7.9			

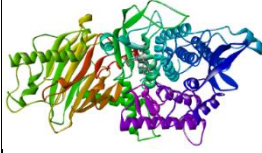
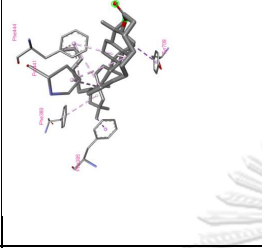
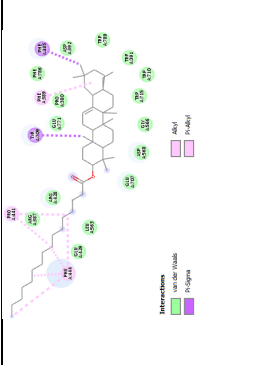
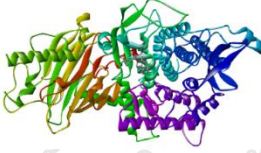
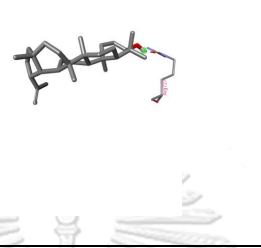
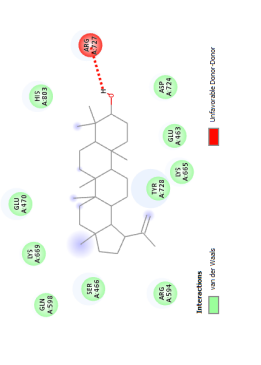

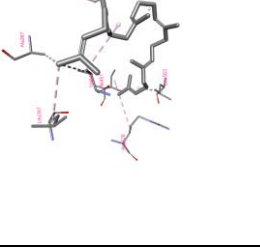
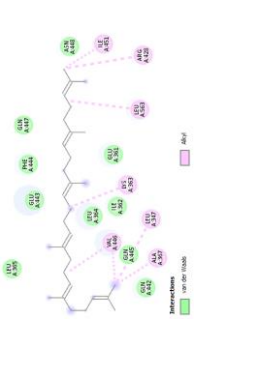
No	Phytochemical name	Binding energy (kcal/mol)	Phytochemicals in the active site of α -glucosidase	3D molecular amino acid interaction	2D molecular amino acid interaction
18	Apigenin-7-O- β -glupyranoside	-9.2			
19	Cyanidin-3-O-rutinoside	-9.9			
20	Benzoic acid	-5.6			

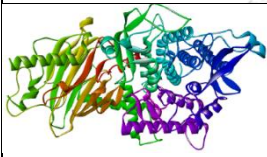
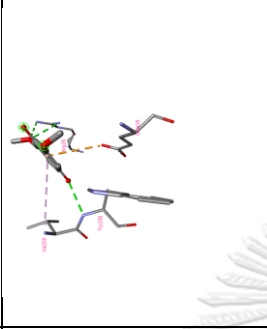
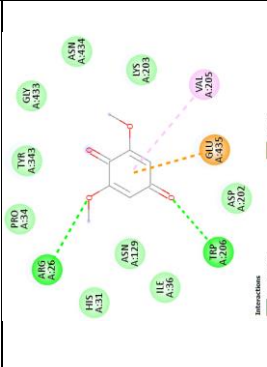
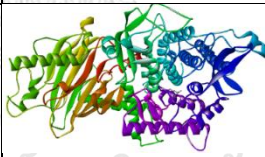

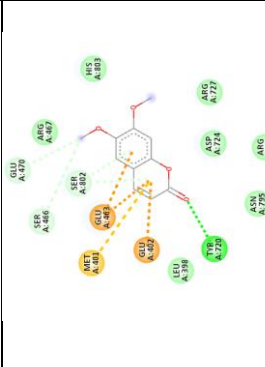
No	Phytochemical name	Binding energy (kcal/mol)	Phytochemicals in the active site of α -glucosidase	3D molecular amino acid interaction	2D molecular amino acid interaction
24	4-Hydroxyacetophenone	-5.5			
25	4-Hydroxybenzaldehyde	-4.9			
26	Vanillin	-5.3			

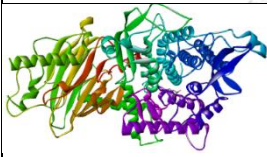
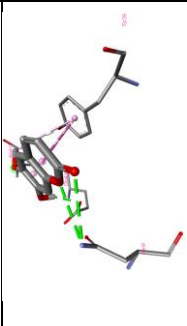
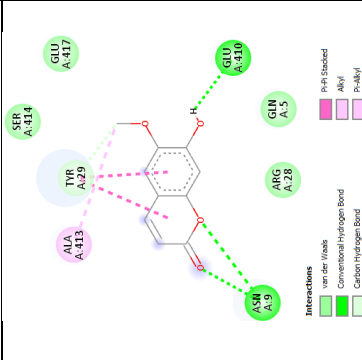
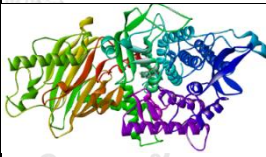
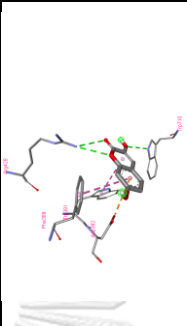
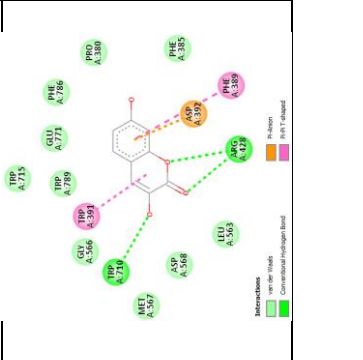
No	Phytochemical name	Binding energy (kcal/mol)	Phytochemicals in the active site of α -glucosidase	3D molecular amino acid interaction	2D molecular amino acid interaction
30	Gallic acid	-6.9			
31	2,6-Dihydroxy-4-methoxyacetophenone	-5.4			


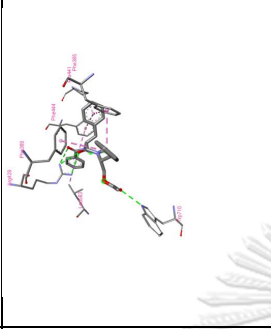
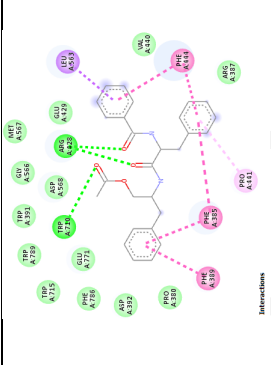
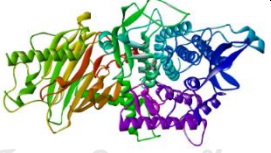
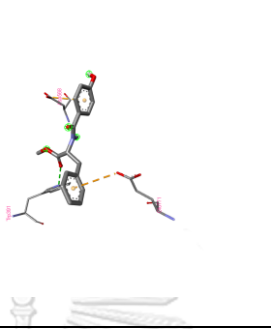
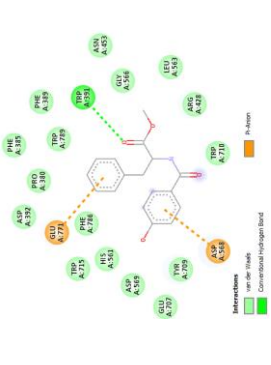

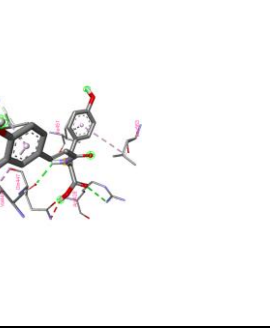
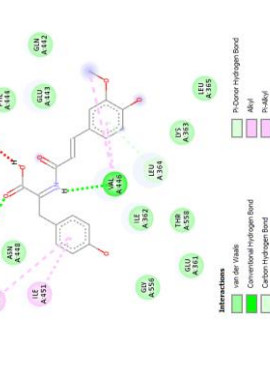
No	Phytochemical name	Binding energy (kcal/mol)	Phytochemicals in the active site of α -glucosidase	3D molecular amino acid interaction	2D molecular amino acid interaction
38	Methyl 4-hydroxyphenylacetate	-5.3			
39	Methylcoumarate	-5.5			
40	Abutilin A	-6.7			

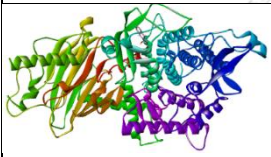
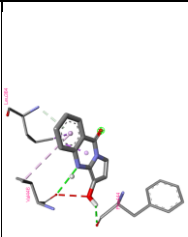
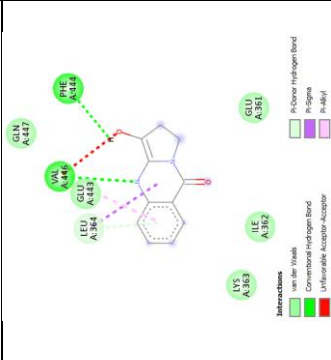

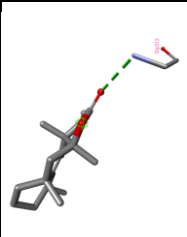
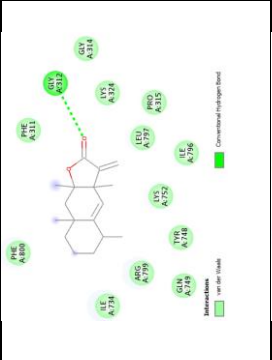
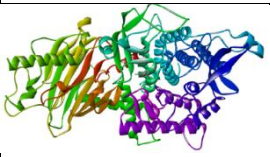
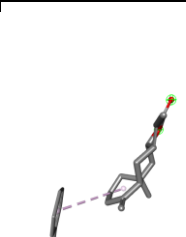
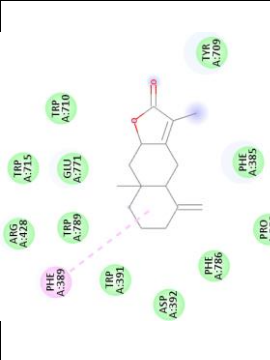
No	Phytochemical name	Binding energy (kcal/mol)	Phytochemicals in the active site of α -glucosidase	3D molecular amino acid interaction	2D molecular amino acid interaction
41	Fumaric acid	-5.0			
42	β -Amyrin	-7.8			
43	β -Amyrin-3-palmitate	-9.5			

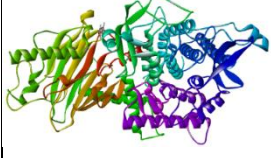
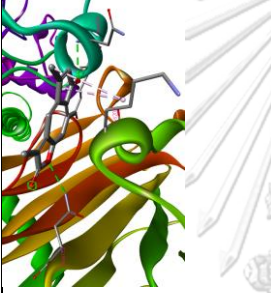

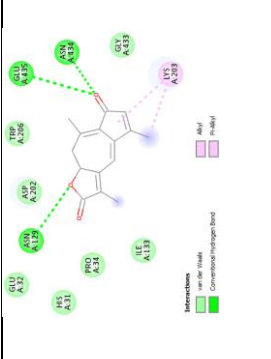

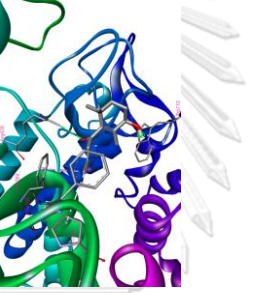
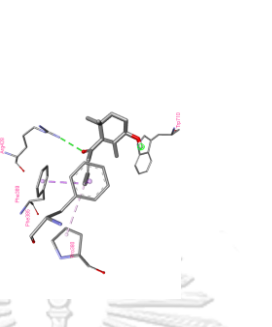
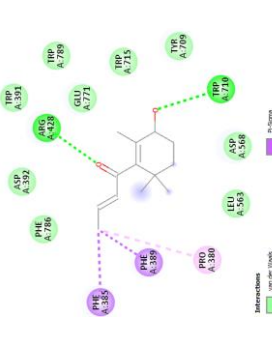
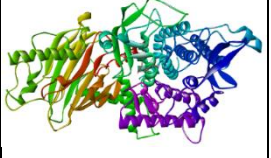
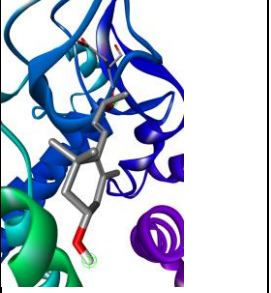
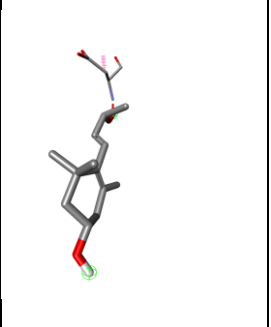
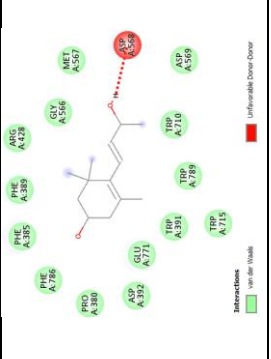
No	Phytochemical name	Binding energy (kcal/mol)	Phytochemicals in the active site of α -glucosidase	3D molecular amino acid interaction	2D molecular amino acid interaction
44	Oleanic acid	-8.7			
45	Lupeol	-8.6			
46	Squalene	-6.6			


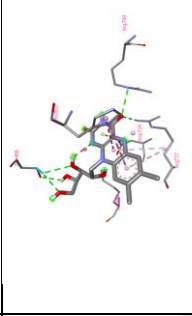
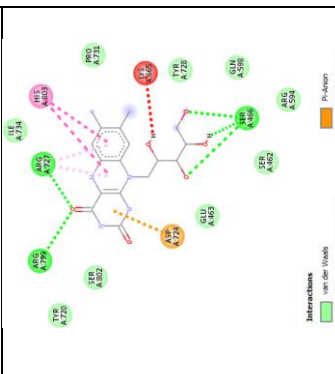
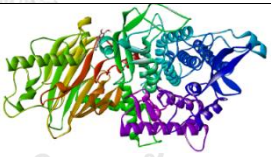
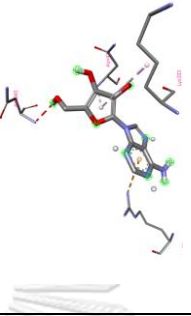
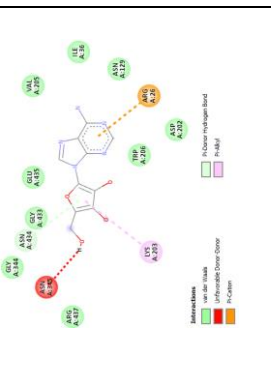
No	Phytochemical name	Binding energy (kcal/mol)	Phytochemicals in the active site of α -glucosidase	3D molecular amino acid interaction	2D molecular amino acid interaction
47	2,6-Dimethoxy-4-benzoquinone	-5.5			
48	Scoparone	-6.0			



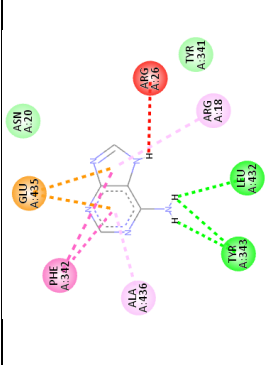

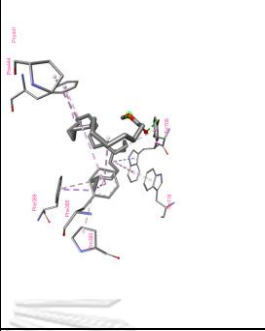
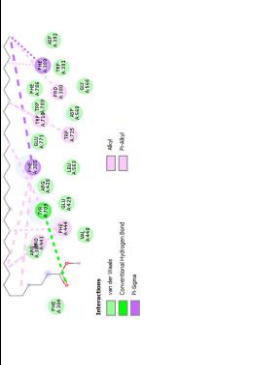
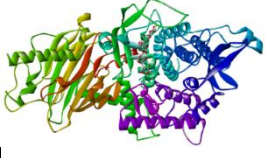
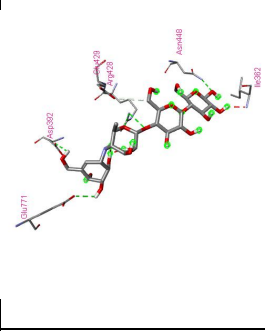
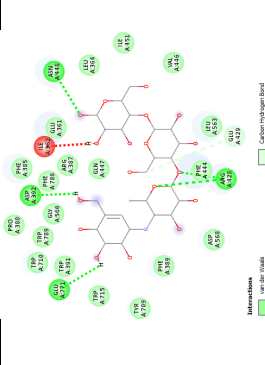
No	Phytochemical name	Binding energy (kcal/mol)	Phytochemicals in the active site of α -glucosidase	3D molecular amino acid interaction	2D molecular amino acid interaction
49	Scopoletin	-6.0			
50	3,7-Dihydroxychromen-2-one	-6.7			

No	Phytochemical name	Binding energy (kcal/mol)	Phytochemicals in the active site of α -glucosidase	3D molecular amino acid interaction	2D molecular amino acid interaction
51	Aurantiamide acetate	-9.2			
52	(R)-N-(1'-Methoxycarbonyl-2 phenylethyl)-4-hydroxybenzamide	-8.1			
53	N-Feruloyl tyrosine	-8.2			

No	Phytochemical name	Binding energy (kcal/mol)	Phytochemicals in the active site of α -glucosidase	3D molecular amino acid interaction	2D molecular amino acid interaction
57	Vasicine	-6.7			
58	Alantolactone	-7.5			
59	Isoalantolactone	-7.6			

No	Phytochemical name	Binding energy (kcal/mol)	Phytochemicals in the active site of α -glucosidase		3D molecular amino acid interaction	2D molecular amino acid interaction
60	3-Hydroxy- β -damascone	-8.3				
61	3-Hydroxy- β -ionol	-6.5				
62	Riboflavin	-6.9				

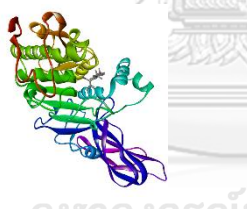
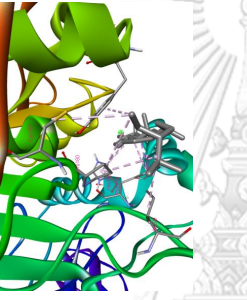
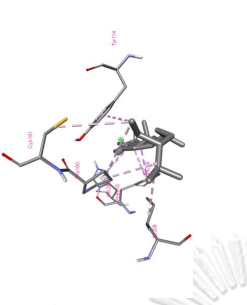
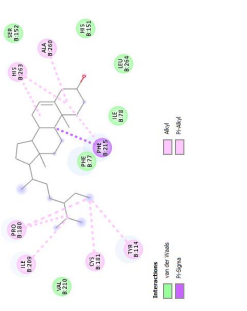
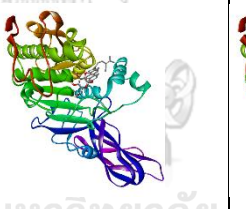
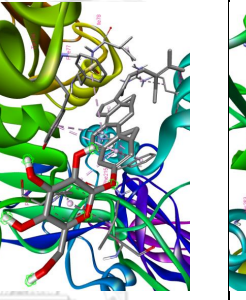
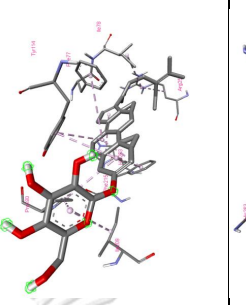
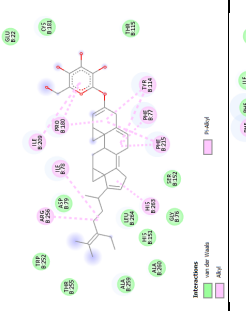
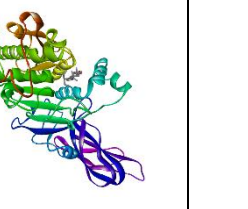
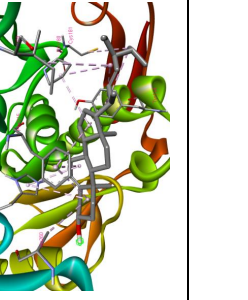
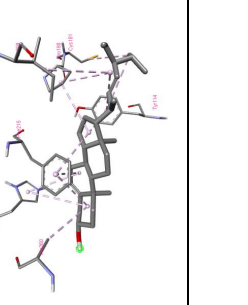
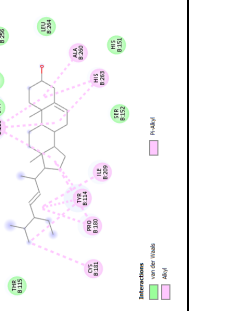
No	Phytochemical name	Binding energy (kcal/mol)	Phytochemicals in the active site of α -glucosidase	3D molecular amino acid interaction	2D molecular amino acid interaction
63	Adenosine	-8.1			
64	Adenine	-6.8			

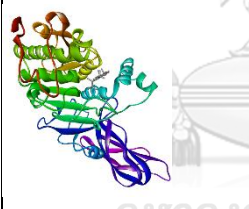
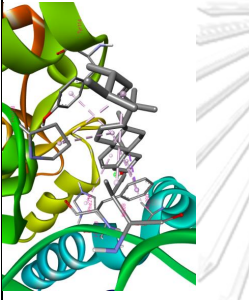
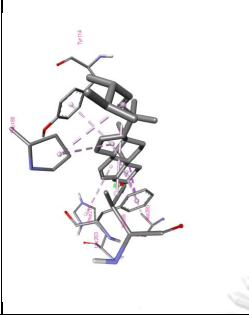
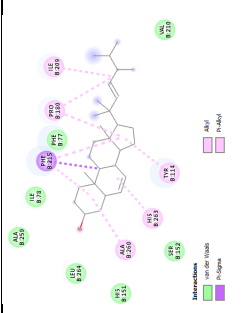
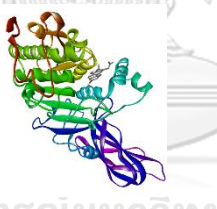
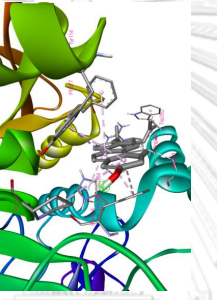
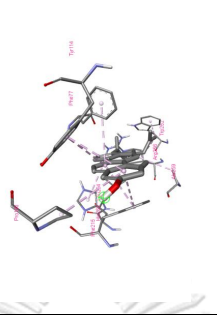
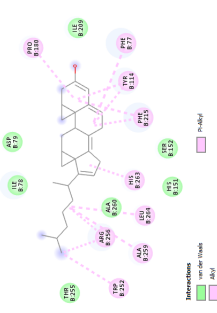
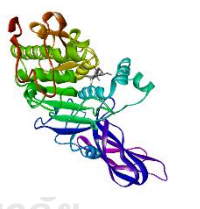
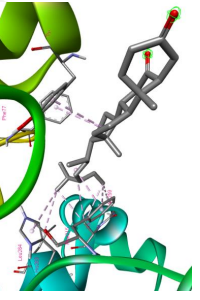
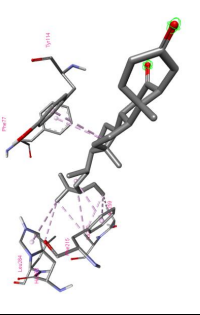
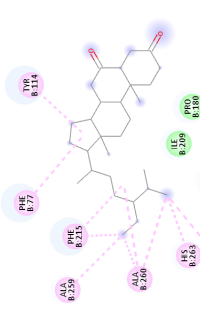
No	Phytochemical name	Binding energy (kcal/mol)	Phytochemicals in the active site of α -glucosidase	3D molecular amino acid interaction	2D molecular amino acid interaction
65	Thymine	-5.9			
66	Methyl triacontanoate	-5.6			
	Acarbose	-8.5			

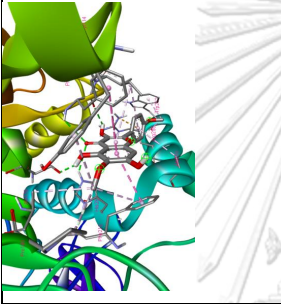
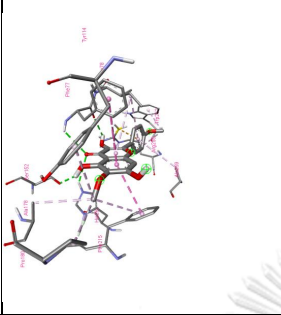
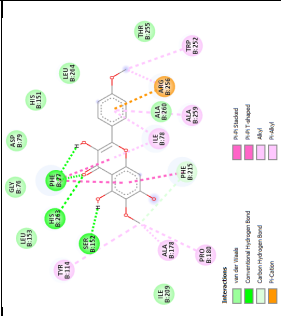
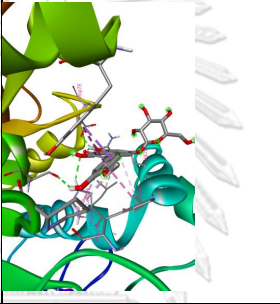
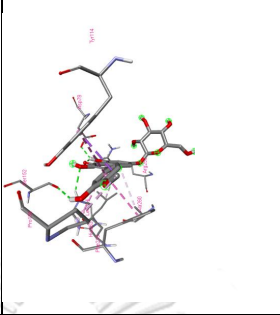
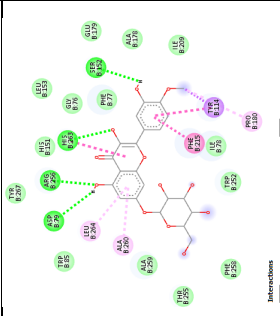


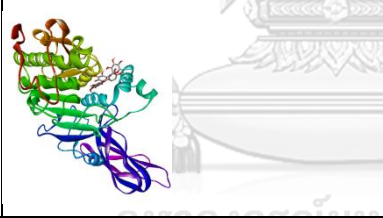
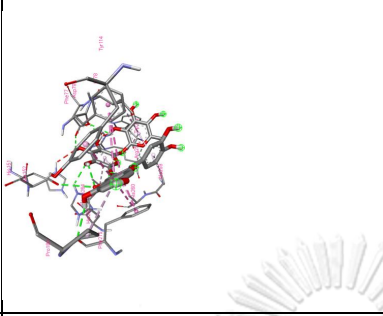
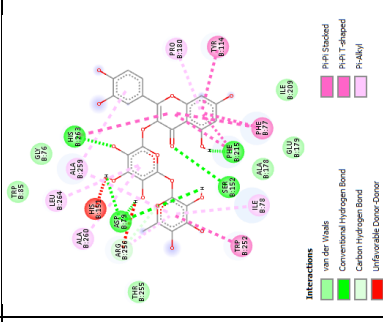
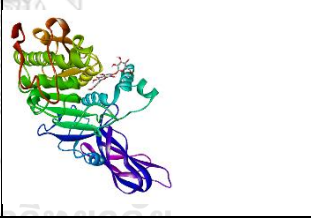
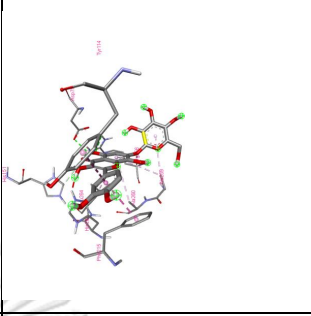
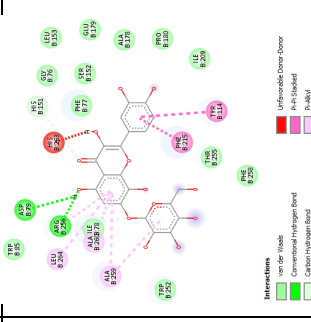
จุฬาลงกรณ์มหาวิทยาลัย
CHULALONGKORN UNIVERSITY

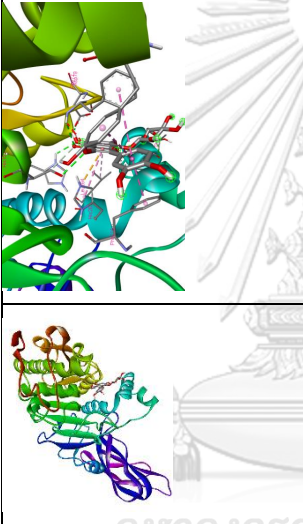
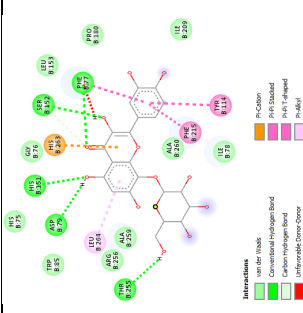
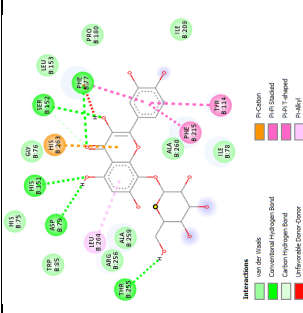
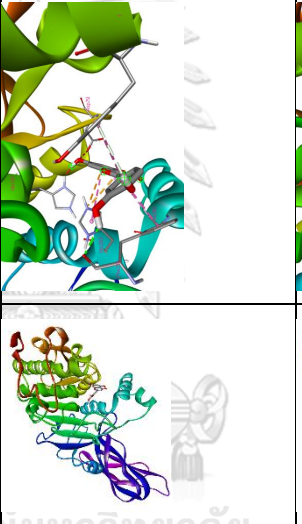
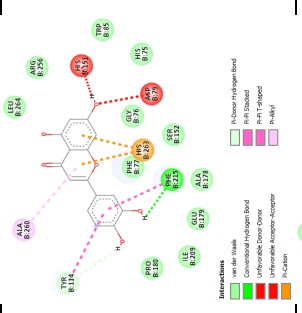
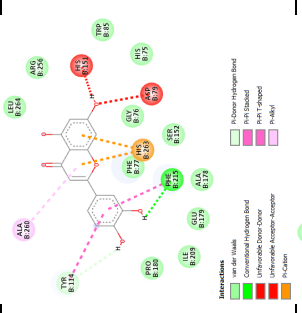
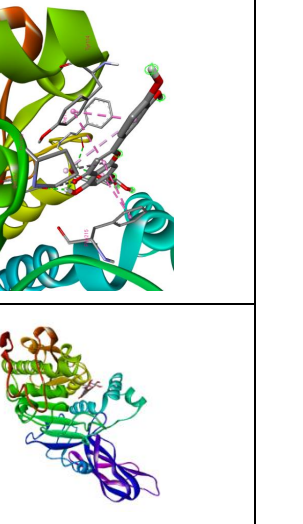
Table A.2 *In silico* approach of the phytochemicals in the active site of human pancreatic lipase (HPL) (PDB ID: 1LPB)


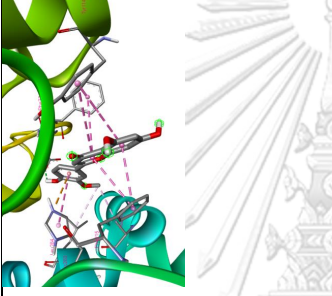
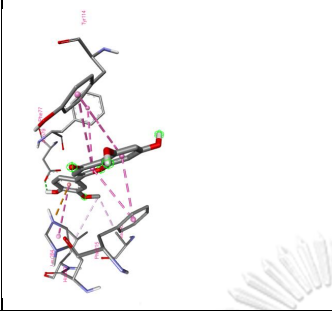
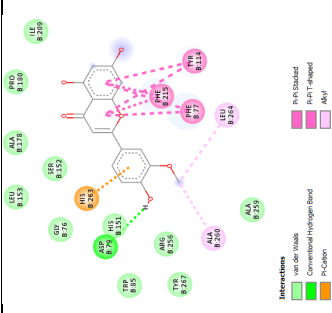

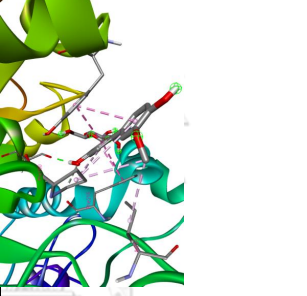
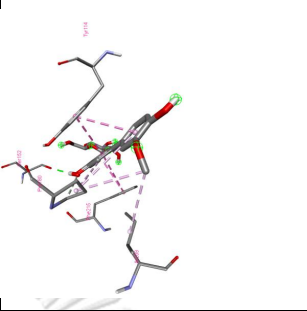
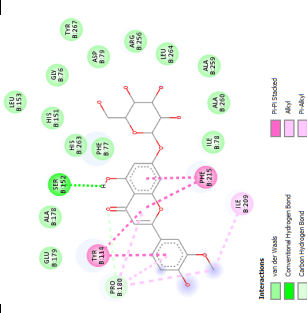
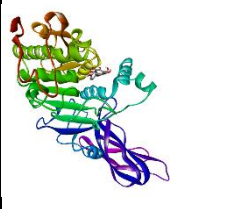
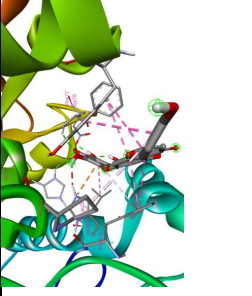
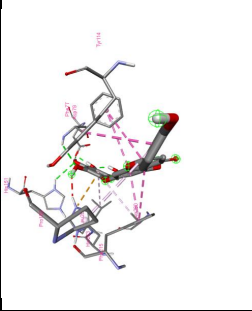
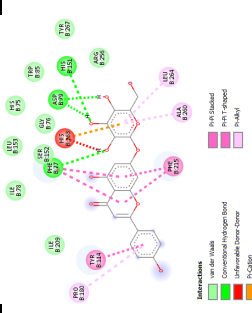
No	Phytochemical name	Binding energy (kcal/mol)	Phytochemicals in the active site of α -glucosidase		3D molecular amino acid interaction	2D molecular amino acid interaction
1	β -sitosterol	-9.1				
2	β -sitosterol-3-O- β -D-glucopyranoside	-10.0				
3	Stigmasterol	-9.6				

No	Phytochemical name	Binding energy (kcal/mol)	Phytochemicals in the active site of α -glucosidase		3D molecular amino acid interaction	2D molecular amino acid interaction
4	20, 23-Dimethylcholesta-6, 22-dien-3 β -ol	-10.0				
5	Cholesterol	-10.1				
6	(24R)-5 α -stigmastane-3,6-dione	-8.3				

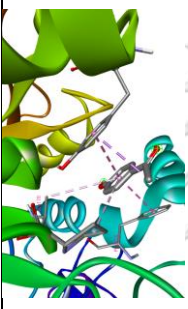
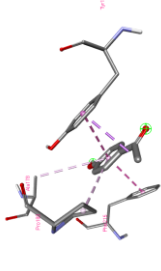
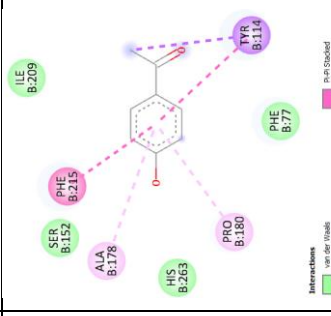
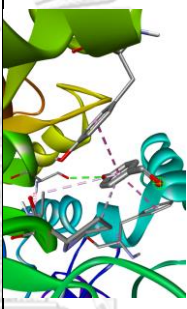
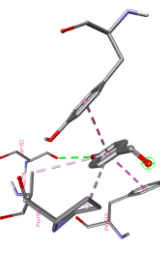
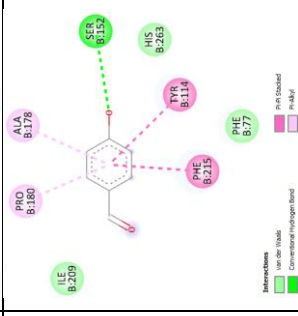

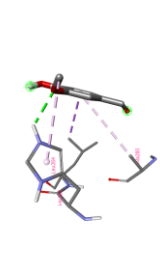
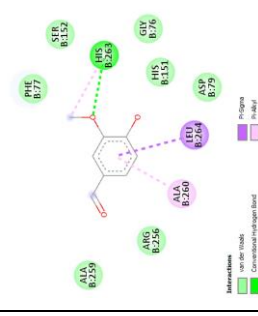
No	Phytochemical name	Binding energy (kcal/mol)	Phytochemicals in the active site of α -glucosidase	3D molecular amino acid interaction	2D molecular amino acid interaction
7	4',6-Dimethoxy kaempferol	-8.1			
8	3,5,5'-Trihydroxy-4'-methoxy flavone-7O- β -D-glucopyranoside	-9.6			

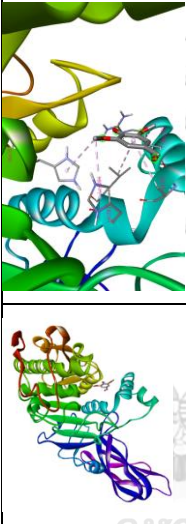
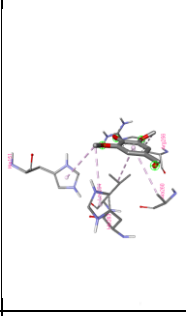
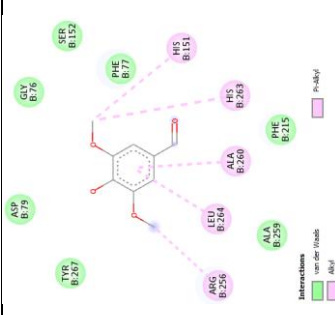
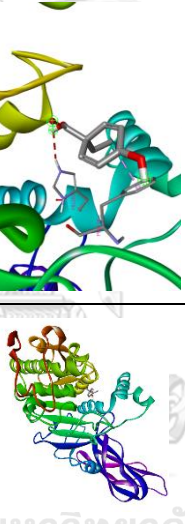
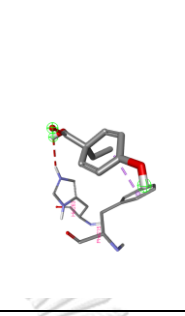
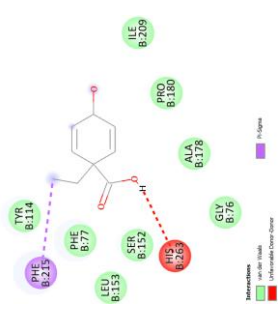
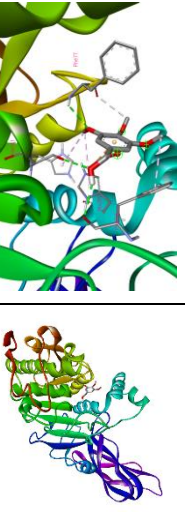
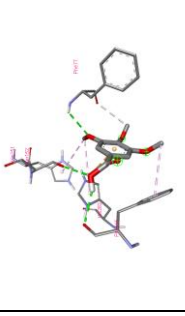
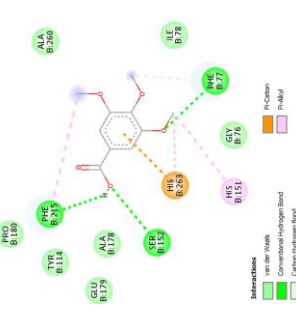
No	Phytochemical name	Binding energy (kcal/mol)	Phytochemicals in the active site of α -glucosidase	3D molecular amino acid interaction	2D molecular amino acid interaction
11	Quercetin-3-O- α -rhamnopyranosyl (1 \rightarrow 6)- β -glucopyranoside	-10.3			
12	Gossypetin-7-O- β -glucoside	-9.3			

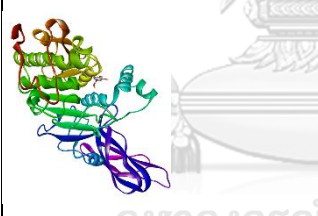
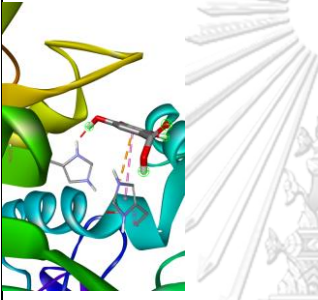
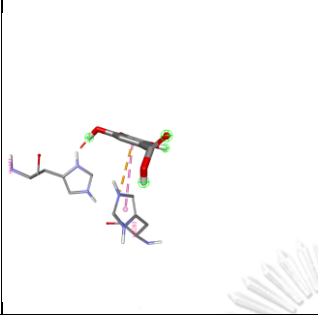
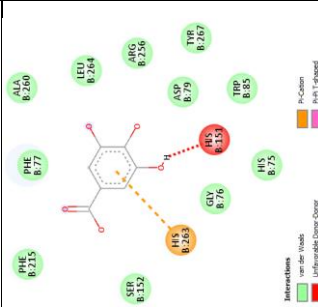
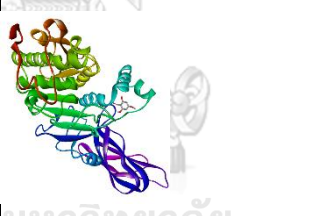
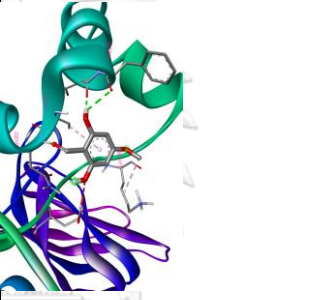
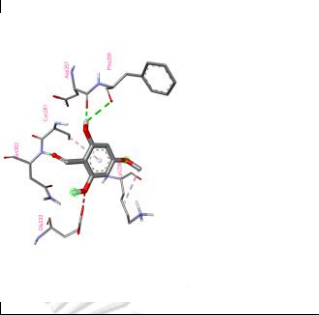
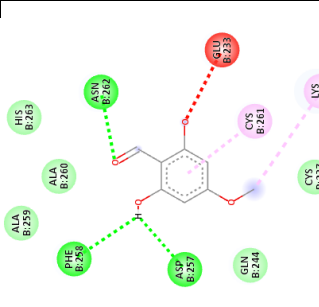
No	Phytochemical name	Binding energy (kcal/mol)	Phytochemicals in the active site of α -glucosidase	3D molecular amino acid interaction	2D molecular amino acid interaction
13	Gossypetin-8-O- β -glucoside	-9.1			
14	Luteolin	-9.5			
15	Luteolin-7-O- β -glupyranoside	-10.3			

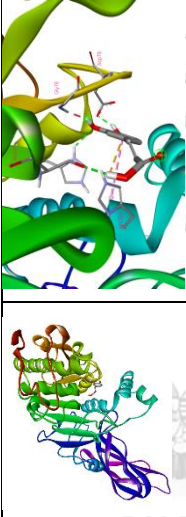
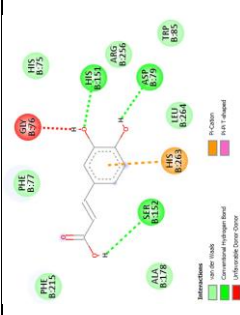
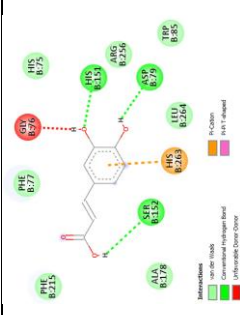
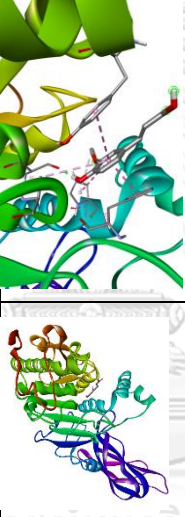
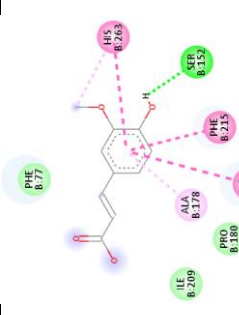
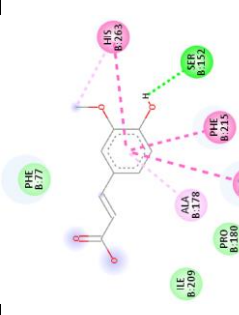
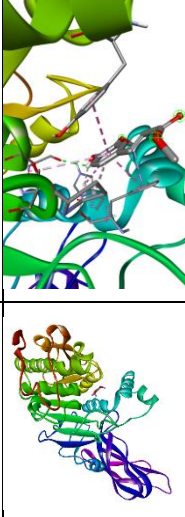
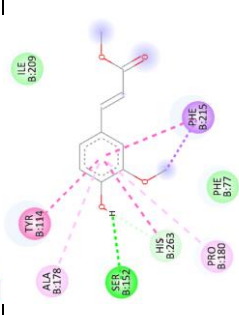
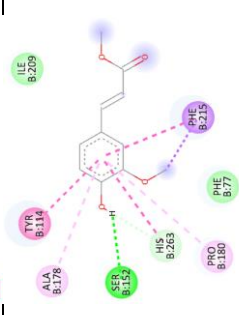
No	Phytochemical name	Binding energy (kcal/mol)	Phytochemicals in the active site of α -glucosidase		3D molecular amino acid interaction	2D molecular amino acid interaction
16	Chrysoeriol	-8.2				
17	Chrysoeriol-7-O- β -glupyranoside	-10.3				
18	Apigenin-7-O- β -glupyranoside	-9.1				

No	Phytochemical name	Binding energy (kcal/mol)	Phytochemicals in the active site of α -glucosidase		3D molecular amino acid interaction	2D molecular amino acid interaction
22	Vanillic acid	-5.7				
23	Glucovanilloylglucose	-7.4				

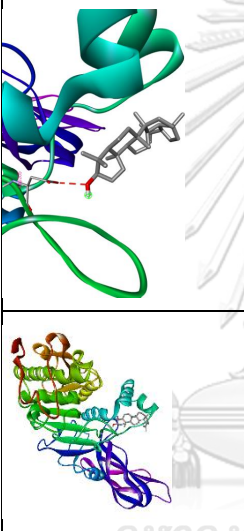
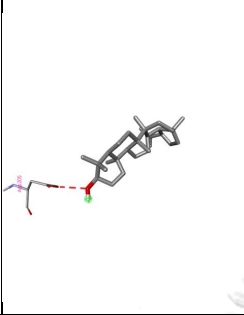
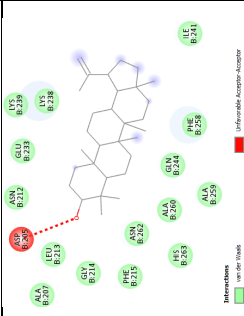
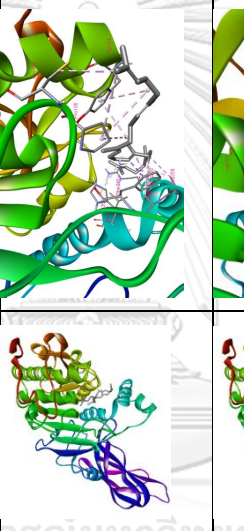
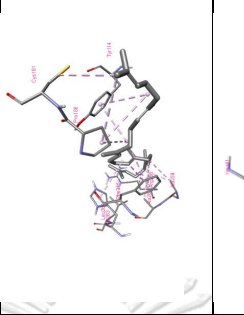
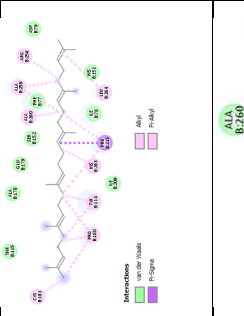
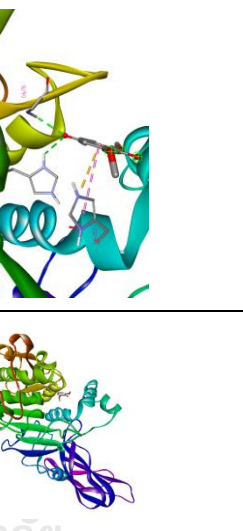
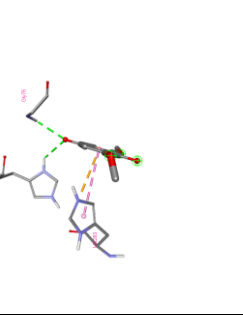
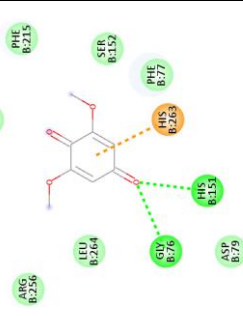
No	Phytochemical name	Binding energy (kcal/mol)	Phytochemicals in the active site of α -glucosidase	3D molecular amino acid interaction	2D molecular amino acid interaction
24	4-Hydroxyacetophenone	-5.8			
25	4-Hydroxybenzaldehyde	-5.4			
26	Vanillin	-5.3			

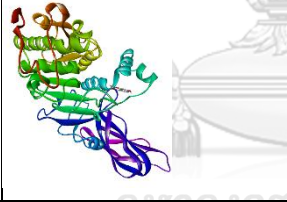
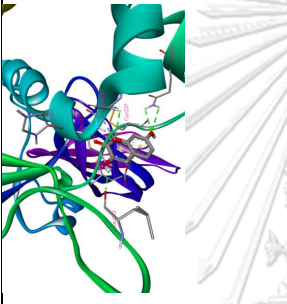
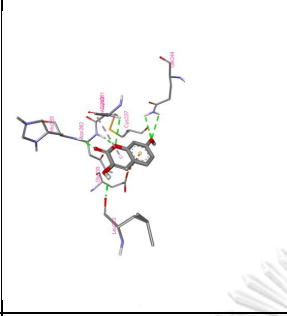
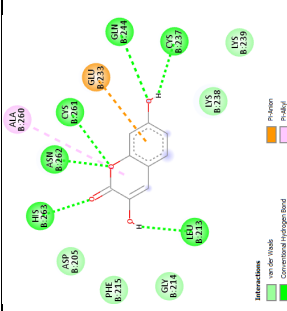
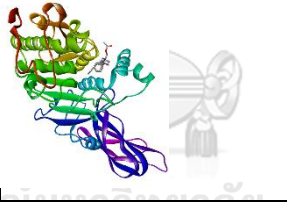

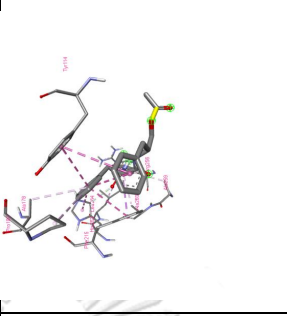
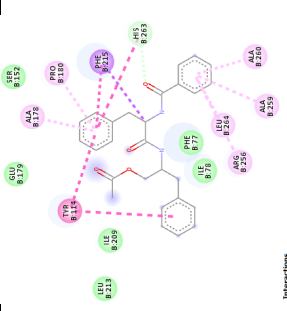
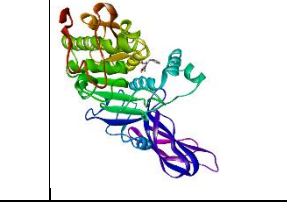
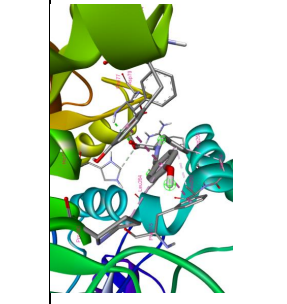
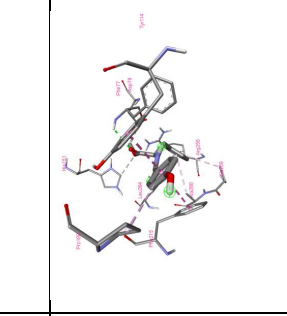
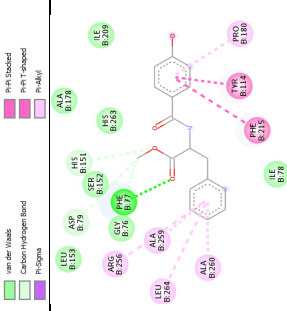
No	Phytochemical name	Binding energy (kcal/mol)	Phytochemicals in the active site of α -glucosidase	3D molecular amino acid interaction	2D molecular amino acid interaction
27	Syringaldehyde	-5.5			
28	Methyl-4-hydroxybenzoate	-5.8			
29	Eudesmic acid	-5.8			


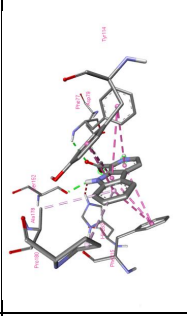
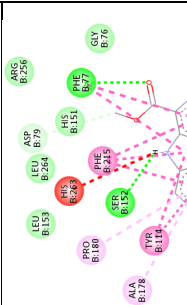
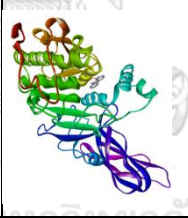
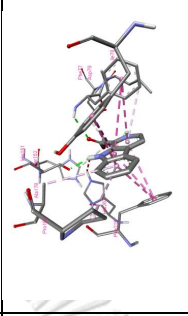
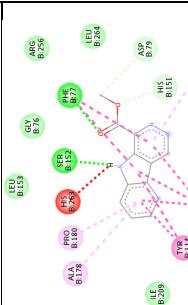
No	Phytochemical name	Binding energy (kcal/mol)	Phytochemicals in the active site of α -glucosidase		3D molecular amino acid interaction	2D molecular amino acid interaction
30	Gallic acid	-6.1				
31	2,6-Dihydroxy-4-methoxyacetophenone	-5.7				

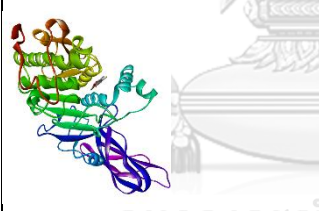
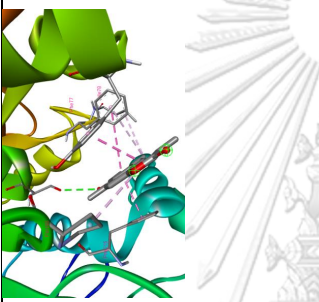
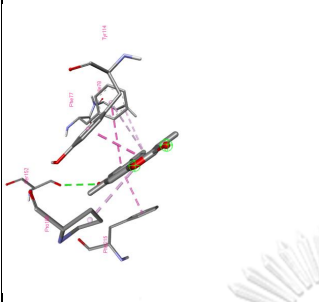
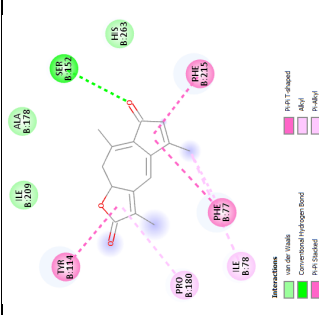
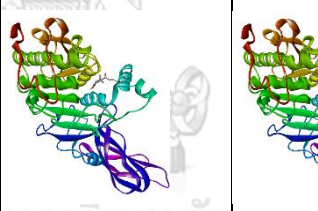
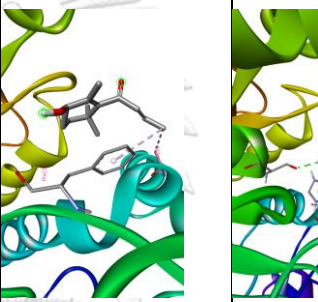
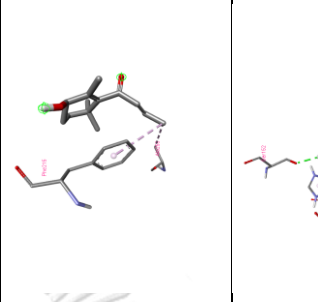
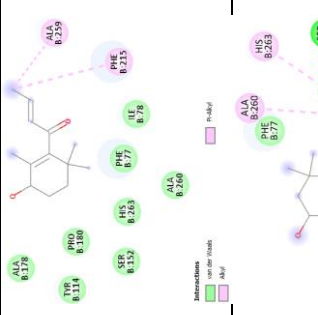

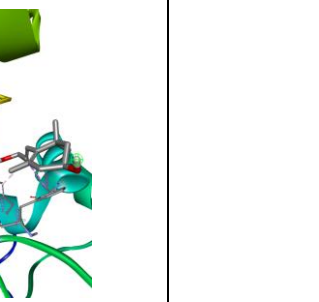
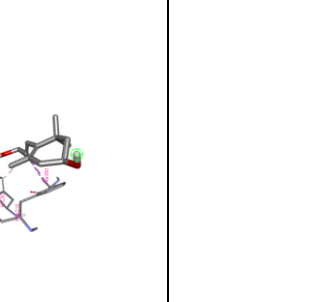
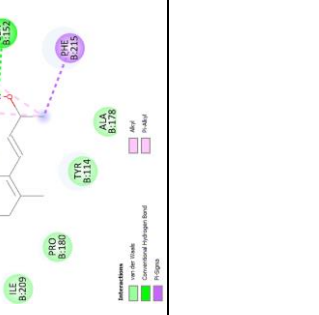
No	Phytochemical name	Binding energy (kcal/mol)	Phytochemicals in the active site of α -glucosidase	3D molecular amino acid interaction	2D molecular amino acid interaction
35	Caffeic acid	-6.6			
36	Ferulic acid	-6.1			
37	4-Hydroxy-3-methoxy-E-cinnamic acid methyl ester	-6.2			

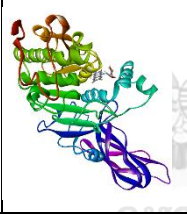
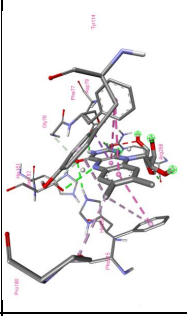
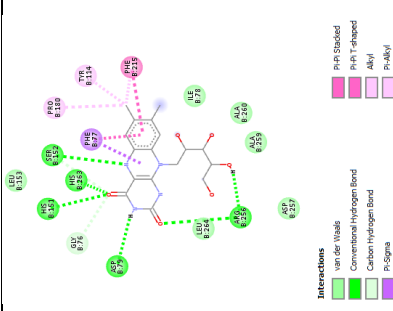
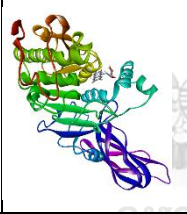
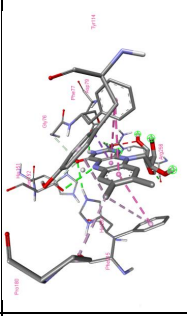
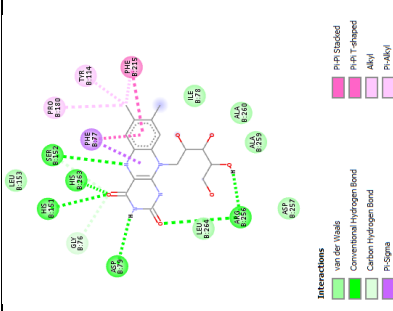
No	Phytochemical name	Binding energy (kcal/mol)	Phytochemicals in the active site of α -glucosidase	3D molecular amino acid interaction	2D molecular amino acid interaction
38	Methyl 4-hydroxyphenylacetate	-5.7			
39	Methylcoumarate	-6.3			
40	Abutilin A	-8.2			

No	Phytochemical name	Binding energy (kcal/mol)	Phytochemicals in the active site of α -glucosidase	3D molecular amino acid interaction	2D molecular amino acid interaction
45	Lupeol	-7.8			
46	Squalene	-8.0			
47	2,6-Dimethoxy-4-benzoquinone	-5.5			


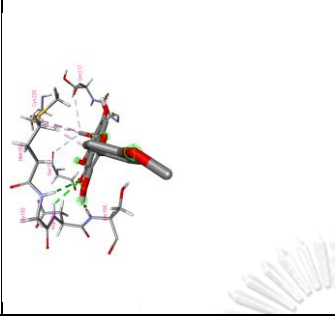
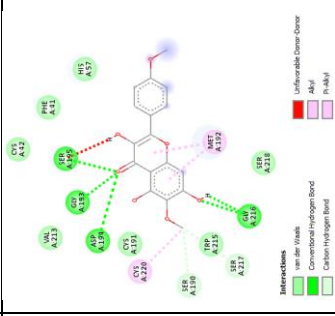
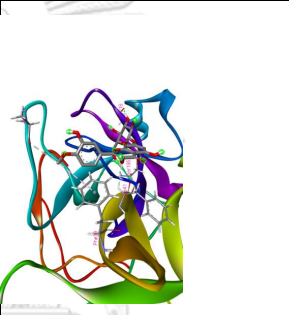
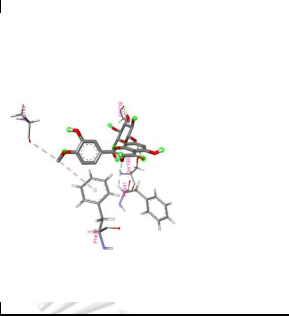
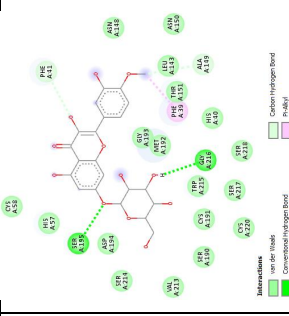
No	Phytochemical name	Binding energy (kcal/mol)	Phytochemicals in the active site of α -glucosidase		3D molecular amino acid interaction	2D molecular amino acid interaction
50	3,7-Dihydroxychromen-2-one	-7.1				
51	Aurantiamide acetate	-8.3				
52	(R)-N-(1'-Methoxycarbonyl-2'phenylethyl)-4-hydroxybenzamide	-8.7				


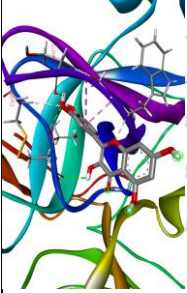
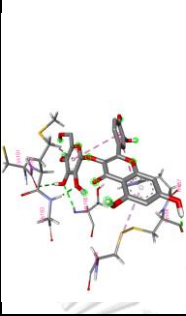

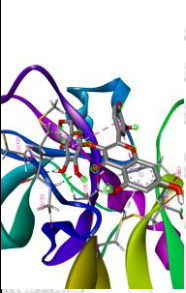
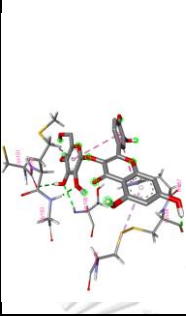
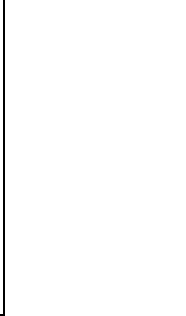
No	Phytochemical name	Binding energy (kcal/mol)	Phytochemicals in the active site of α -glucosidase	3D molecular amino acid interaction	2D molecular amino acid interaction
55	1-Methoxycarbonyl- β -carboline	-8.5			
56	Methyl indole-3-carboxylate	-8.5			

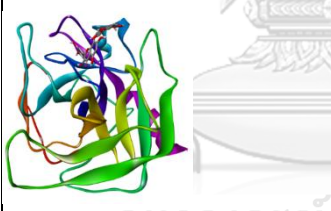
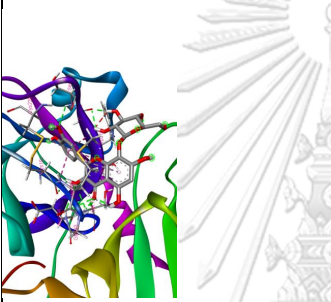
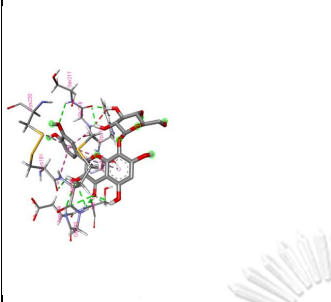
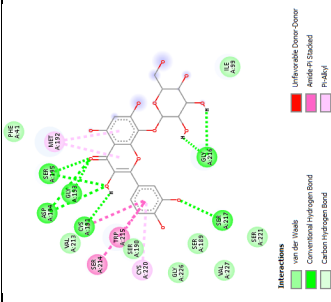


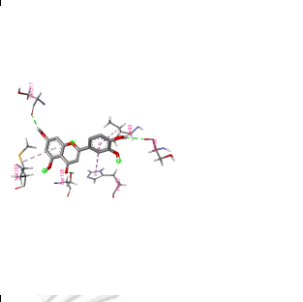
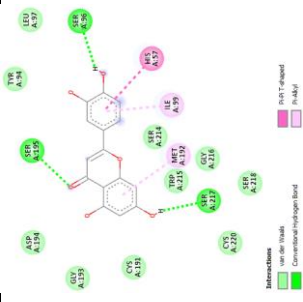


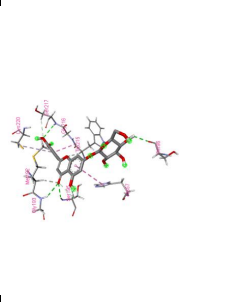
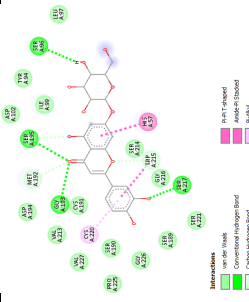
No	Phytochemical name	Binding energy (kcal/mol)	Phytochemicals in the active site of α -glucosidase		3D molecular amino acid interaction	2D molecular amino acid interaction
60	3-Hydroxy- β -damascone	-8.8				
61	3-Hydroxy- β -ionol	-6.0				
62	Riboflavin	-6.3				

No	Phytochemical name	Binding energy (kcal/mol)	Phytochemicals in the active site of α -glucosidase	3D molecular amino acid interaction	2D molecular amino acid interaction
63	Adenosine	-8.8			
64	Adenine	-7.3			

No	Phytochemical name	Binding energy (kcal/mol)	Phytochemicals in the active site of α -glucosidase	3D molecular amino acid interaction	2D molecular amino acid interaction
65	Thymine	-5.3			
66	Methyl triacontanoate	-5.7			
	Orlistat	-6.7			

No	Phytochemical name	Binding energy (kcal/mol)	Phytochemicals in the active site of α -glucosidase	3D molecular amino acid interaction	2D molecular amino acid interaction
7	4',6-Dimethoxy kaempferol	-7.1			
8	3,5,5'-Trihydroxy-4'-methoxy flavone-7-O- β -D-glucopyranoside	-8.5			

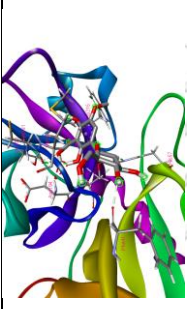

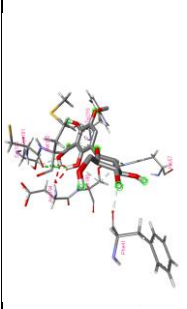
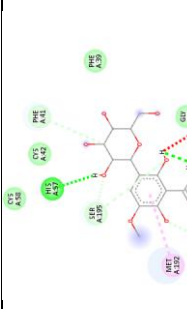
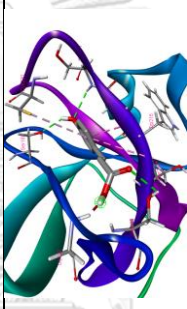
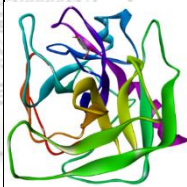
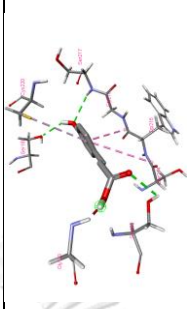
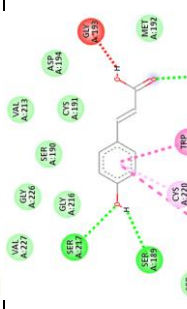
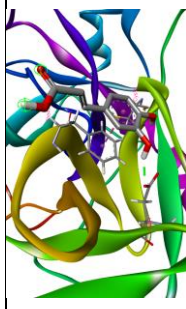
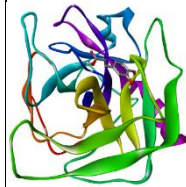
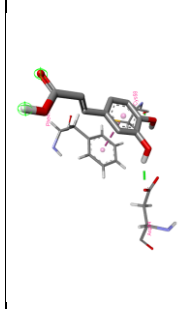
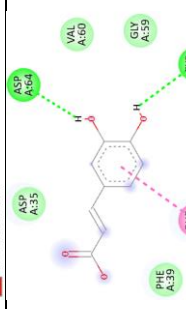
No	Phytochemical name	Binding energy (kcal/mol)	Phytochemicals in the active site of α -glucosidase		3D molecular amino acid interaction	2D molecular amino acid interaction
9	Quercetin	-7.7				
10	Quercetin-3-O- β -D-glucopyranoside	-7.7				

No	Phytochemical name	Binding energy (kcal/mol)	Phytochemicals in the active site of α -glucosidase		3D molecular amino acid interaction	2D molecular amino acid interaction
13	Gossypetin-8-O- β -glucoside	-8.5				
14	Luteolin	-7.0				
15	Luteolin-7-O- β -glupyranoside	-8.7				


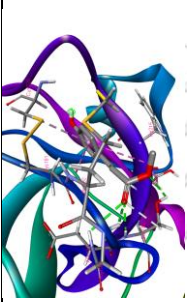
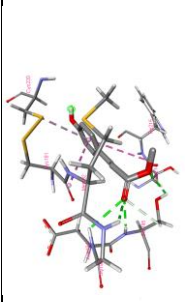
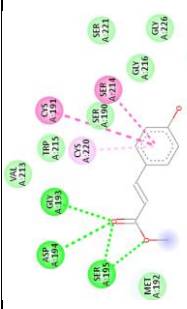
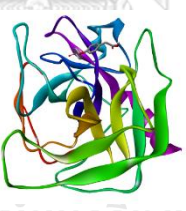
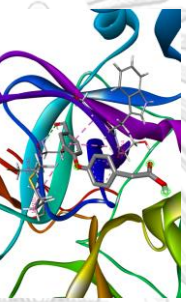
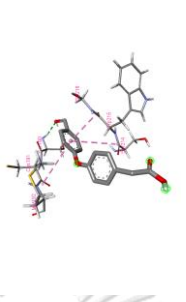
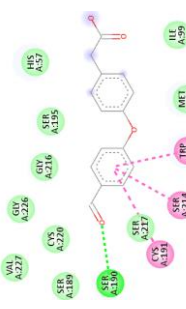
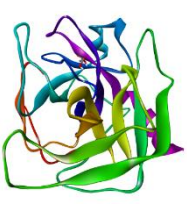
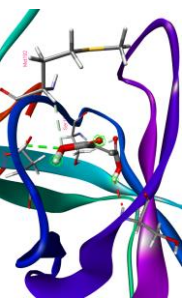
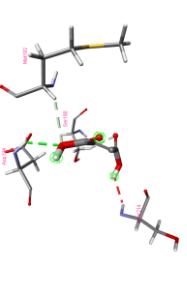
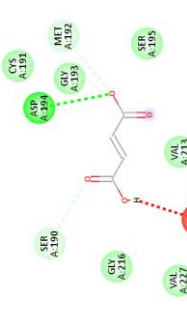
No	Phytochemical name	Binding energy (kcal/mol)	Phytochemicals in the active site of α -glucosidase	3D molecular amino acid interaction	2D molecular amino acid interaction
16	Chrysoeriol	-6.9			
17	Chrysoeriol-7-O- β -glupyranoside	-8.4			
18	Apigenin-7-O- β -glupyranoside	-8.6			

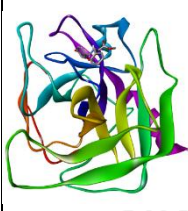
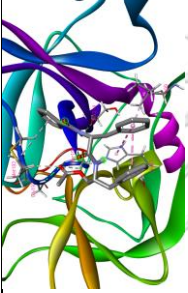
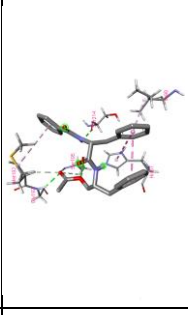
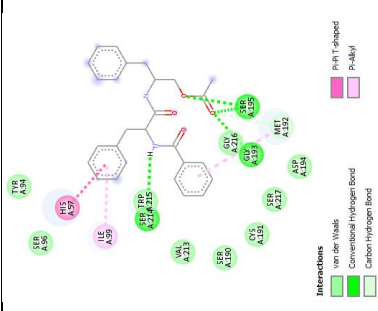
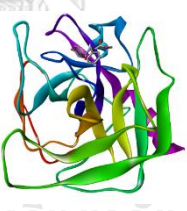
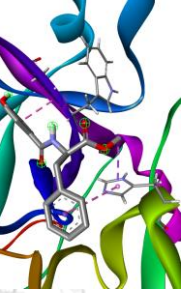
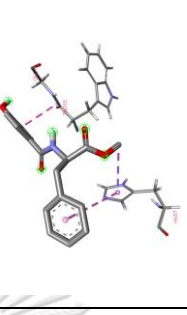
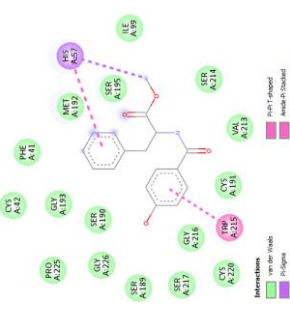
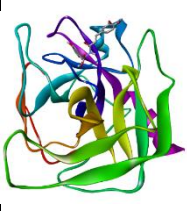
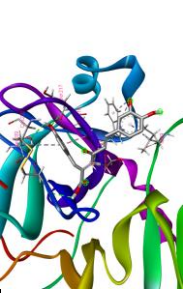
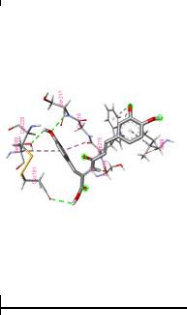
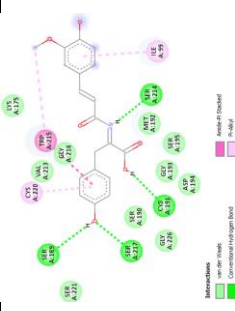
No	Phytochemical name	Binding energy (kcal/mol)	Phytochemicals in the active site of α -glucosidase	3D molecular amino acid interaction	2D molecular amino acid interaction
19	Cyanidin-3-O-rutinoside	-8.3			
20	Benzoic acid	-5.3			
21	<i>p</i> -Hydroxybenzoic acid	-5.8			

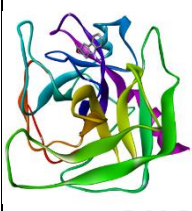
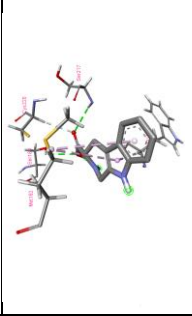
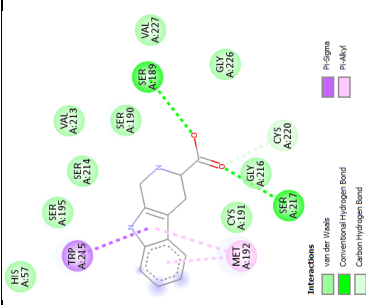

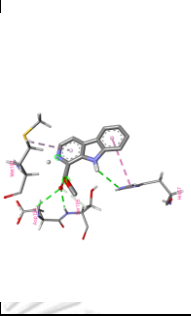
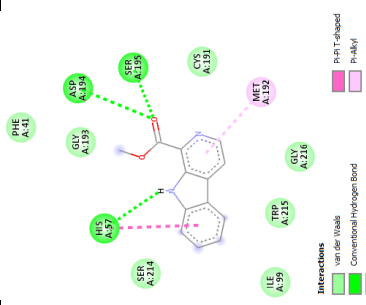
No	Phytochemical name	Binding energy (kcal/mol)	Phytochemicals in the active site of α -glucosidase		3D molecular amino acid interaction	2D molecular amino acid interaction
30	Gallic acid	-6.6				
31	2,6-Dihydroxy-4-methoxyacetophenone	-6.1				
32	4-O- β -Glucosylbenzoic acid	-7.2				

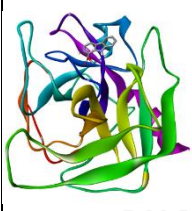
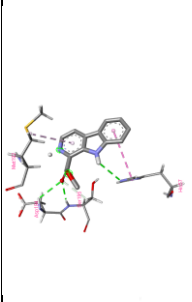
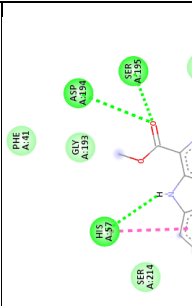

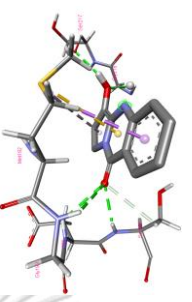
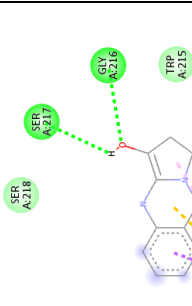
No	Phytochemical name	Binding energy (kcal/mol)	Phytochemicals in the active site of α -glucosidase	3D molecular amino acid interaction	2D molecular amino acid interaction
33	2,6-Dihydroxy-5-methoxy-(3-C-glucopyranosyl) benzoic acid	-6.5	 		
34	<i>p</i> -Coumaric acid	-6.3	 		
35	Caffeic acid	-5.1	 		



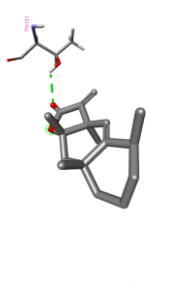
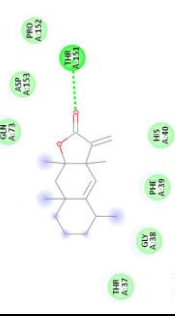

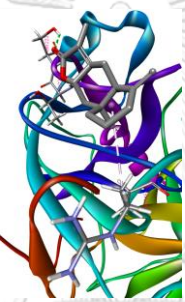
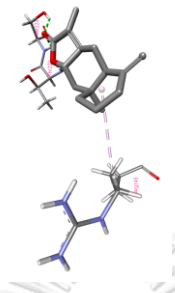
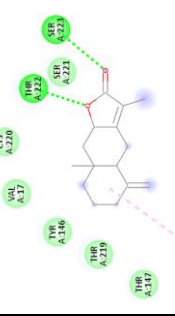


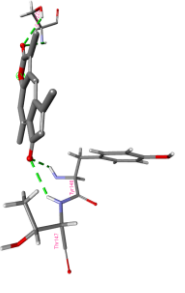
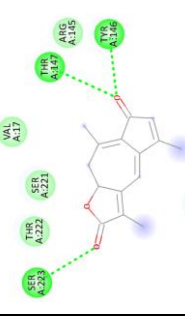
No	Phytochemical name	Binding energy (kcal/mol)	Phytochemicals in the active site of α -glucosidase		3D molecular amino acid interaction	2D molecular amino acid interaction
36	Ferulic acid	-5.3				
37	4-Hydroxy-3-methoxy-E-cinnamic acid methyl ester	-5.3				

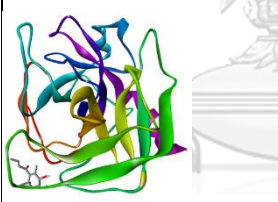
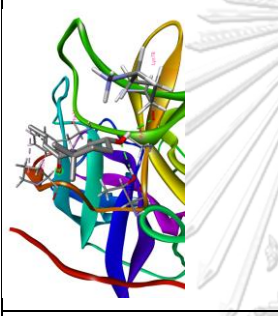
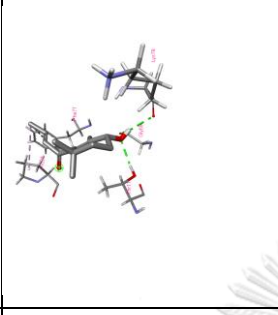
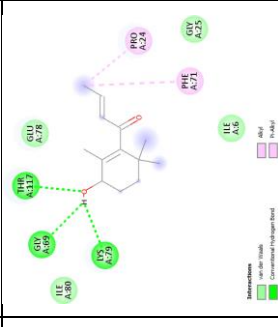

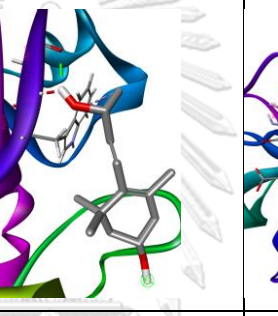
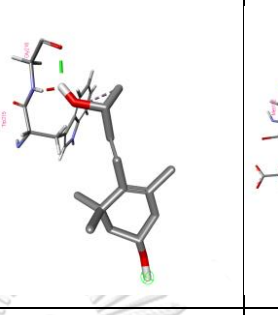
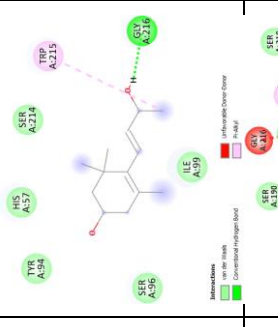
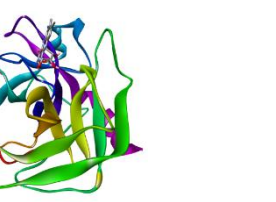
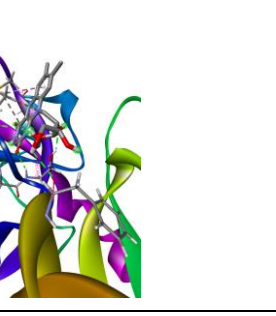
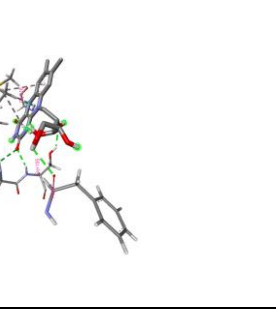
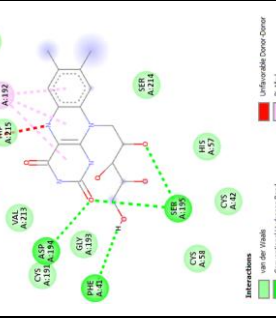
No	Phytochemical name	Binding energy (kcal/mol)	Phytochemicals in the active site of α -glucosidase		3D molecular amino acid interaction	2D molecular amino acid interaction
39	Methylcoumarate	-6.1				
40	Abutilin A	-6.1				
41	Fumaric acid	-4.8				

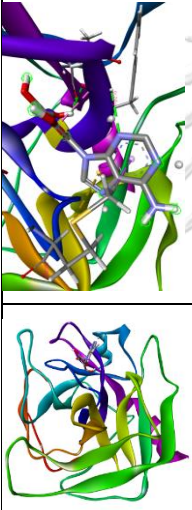
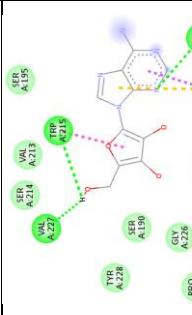
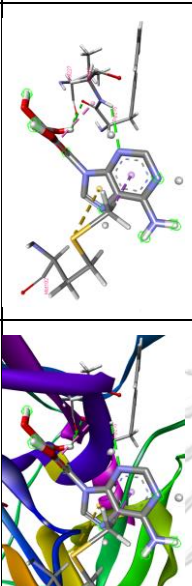
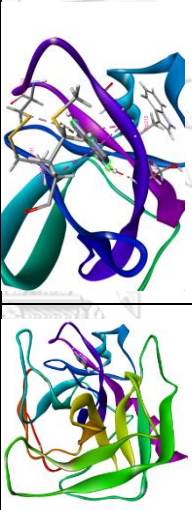
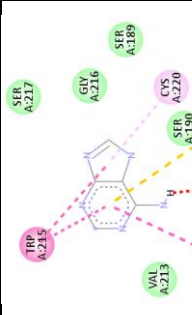
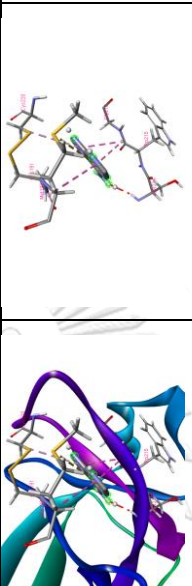


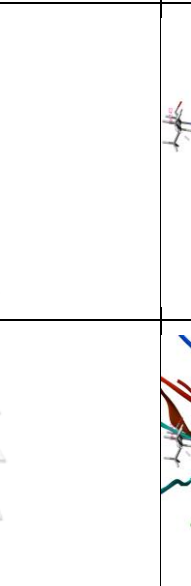
No	Phytochemical name	Binding energy (kcal/mol)	Phytochemicals in the active site of α -glucosidase		3D molecular amino acid interaction	2D molecular amino acid interaction
51	Aurantiamide acetate	-6.8				
52	(R)-N-(1'-Methoxycarbonyl-2'phenylethyl)-4-hydroxybenzamide	-7.0				
53	N-Feruloyl tyrosine	-7.5				

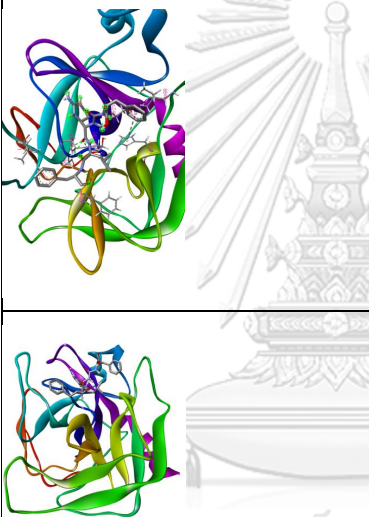
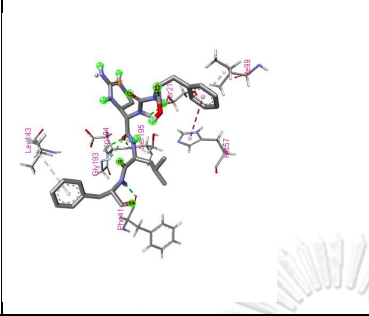
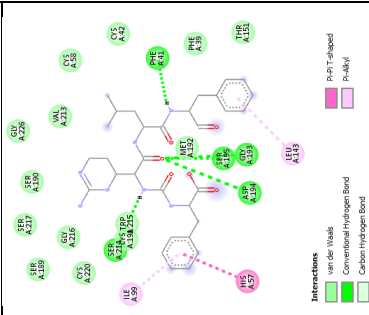
No	Phytochemical name	Binding energy (kcal/mol)	Phytochemicals in the active site of α -glucosidase	3D molecular amino acid interaction	2D molecular amino acid interaction
54	1-Lycoperodine	-6.9			
55	1-Methoxycarbonyl- β -carboline	-6.4			

No	Phytochemical name	Binding energy (kcal/mol)	Phytochemicals in the active site of α -glucosidase	3D molecular amino acid interaction	2D molecular amino acid interaction
56	Methyl indole-3-carboxylate	-6.4			
57	Vasicine	-6.7			

No	Phytochemical name	Binding energy (kcal/mol)	Phytochemicals in the active site of α -glucosidase		3D molecular amino acid interaction	2D molecular amino acid interaction
58	Alantolactone	-6.3				
59	Isoalantolactone	-6.8				
60	3-Hydroxy- β -damascone	-6.9				

No	Phytochemical name	Binding energy (kcal/mol)	Phytochemicals in the active site of α -glucosidase		3D molecular amino acid interaction	2D molecular amino acid interaction
61	3-Hydroxy- β -ionol	-5.3				
62	Riboflavin	-5.1				
63	Adenosine	-7.3				

No	Phytochemical name	Binding energy (kcal/mol)	Phytochemicals in the active site of α -glucosidase	3D molecular amino acid interaction	2D molecular amino acid interaction
64	Adenine	-7.4			
65	Thymine	-5.8			
66	Methyl triacontanoate	-4.3			

No	Phytochemical name	Binding energy (kcal/mol)	Phytochemicals in the active site of α -glucosidase	3D molecular amino acid interaction	2D molecular amino acid interaction
	Chymostatin	-9.1			 <p> Interactions van der Waals Conventional Hydrogen Bond Cation Hydrogen Bond Pi-Pi stacked Pi-Alkyl </p>



จุฬาลงกรณ์มหาวิทยาลัย
CHULALONGKORN UNIVERSITY

VITA

NAME Arum Restu Widyasti

DATE OF BIRTH 03 March 1996

PLACE OF BIRTH Kulon Progo, Special Region of Yogyakarta, Indonesia

INSTITUTIONS ATTENDED B.Ed. (Chemistry Education), Faculty of Mathematics and Natural Sciences, Universitas Negeri Yogyakarta (Yogyakarta State University), Indonesia

HOME ADDRESS Karanggede RT72/RW18, Jatimulyo (Village), Girimulyo (Sub-district), Kulon Progo (District), Special Region of Yogyakarta (Province), Indonesia 55674